Adsorption and reaction of cyanogen with copper oxide, chromium oxide and copper oxide-chromium oxide surfaces

Lockyer, D. M.

Award date:
1988

Awarding institution:
University of Bath

ADSORPTION AND REACTION OF CYANOGEN WITH COPPER OXIDE, CHROMIUM OXIDE AND COPPER OXIDE-CHROMIUM OXIDE SURFACES

Submitted by D.M. Lockyer for

the degree of Ph.D of the

University of Bath

1988

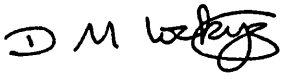

ProQuest LLC
789 East Eisenhower Parkway
P.O. Box 1346
Ann Arbor, MI 48106-1346

To my Parents and Penny

ACKNOWLEDGMENTS

The author would like to thank the following for their advice and assistance during the preparation of this thesis:

Professor F.S. Stone, my supervisor, for his help and encouragement throughout this work.

Mr Joe Stainer, Mr Mike Lock and Mr Mike Bailes for technical assistance.

The Ministry of Defence for the award of a Research Assistantship.

Sceptre Business Services for the typing and Penny Lockyer for proof reading the work.

Past Members of Laboratory 4W 0.5 for maintaining a congenial working atmosphere.

MEMORANDUM

The work described in this thesis was conducted in the Department of Physical Chemistry of the University of Bath during the period October 1982 and September 1985. The work has not been submitted for any other degree. All the work described is the original work of the author except where specially acknowledged.

SUMMARY

The interaction of cyanogen, C_2N_2, with silica-supported copper oxide, chromium oxide and copper oxide-chromium oxide samples has been studied by microgravimetry, mass spectrometry and infra-red spectroscopy. Interaction was found to be dependent on the surface pretreatment.

The key reaction at the CuO/SiO_2 surface was hydrolysis of adsorbed C_2N_2. This was enhanced by the presence of pre-adsorbed moisture. Surface-bound oxamide was formed at ambient temperature via a cyanoformamide-like intermediate. Oxamide was released on outgassing to 540 K. Formation of copper isocyanide occurred at ambient temperature, and infra-red spectroscopy showed that some isocyanate spilled over to the silica. Spectroscopic evidence for molecular adsorption of C_2N_2 and for the formation of a di-cyano copper species is provided. Oxidation of adsorbed cyanogen to CO_2, via a copper carboxylate intermediate was a minor reaction.

Oxidation and hydrolysis of adsorbed cyanogen were major reactions at the chromium surfaces. Chromium bicarbonate, bidentate carbonate and amide species formed at ambient temperature. At elevated temperatures, especially in the presence of Cr(VI) oxide carrying pre-adsorbed oxygen, CO_2 was produced. When pre-adsorbed moisture was present the amide species was hydrolysed to oxamide; in the absence of moisture mass spectrometry showed that dehydroxylation and decomposition occurred.

Isocyanate formation and spillover reactions were less pronounced than with the copper-containing samples.

The reaction of adsorbed cyanogen on the mixed oxide occurred largely by isocyanate intermediates over the copper sites and by amide species over the chromium sites. The overall reactivity was modified compared with the individual oxide systems and under certain circumstances the two oxides behaved synergistically, thus enhancing C_2N_2 uptake. The modified reactivity of the mixed oxide system is explained on the basis of cyanogen interacting with an intimately mixed layer of copper and chromium ions on the silica surface.

CONTENTS

CONTENTS continued

CONTENTS continued

CONTENTS continued

1. INTRODUCTION

The removal of noxious gases from the atmosphere by adsorption on solids has a long history, and activated charcoal has featured prominently as an adsorbent. In its application to the removal of hydrogen cyanide, it has long been known that the addition of metal salts, especially those of copper, chromium and silver, greatly enhance the effectiveness. Until about 20 years ago, little emphasis had been placed on the role which these added substances played. Since that time, however, there has been a growing scientific interest in the chemistry of the interaction of HCN with copper and chromium ions in particular.

The work to be described in this thesis developed out of studies initiated by Mellor (1) and Williams (2) on the adsorption and reaction of HCN on copper and its oxides. The research was later extended by Surman (3) to chromium(III) oxide and copper(II) oxide-chromium(III) oxide. The studies of HCN adsorption and conversion on mixed oxides of copper and chromium were developed further by Davies (4).

A consequence of this work was that cyanogen, C_2N_2, became recognised as a reaction product whose adsorption and removal deserved equally close investigation. Although several workers have studied the adsorption of C_2N_2 on surfaces, Davies (4) was the first to consider its adsorption and reactivity in the context of HCN

removal. The present thesis is concerned with the adsorption and reaction of C_2N_2 on silica-supported copper oxide-chromium oxide surfaces. The effect of the presence of pre-adsorbed oxygen and water vapour, the most chemically active components which would normally be expected to interfere with C_2N_2 reactions in environmental situations, has also been studied.

1.1 Adsorption of Gases on Solids

The adsorption of gases on solids is usually classified into two main types, physical adsorption and chemisorption, depending upon whether the forces involved are those of van der Waals interaction or of chemical bonding, respectively. The heat of adsorption is low for physical adsorption (typically less than 50 kJ mol^{-1}) and multilayers occur, whereas heats of chemisorption are typically much greater (50-500 kJ mol^{-1}) and the forces are of short range. Weak chemisorption and physical adsorption are sometimes difficult to distinguish, as when hydrogen-bonding is involved, e.g. in water adsorption on oxides. Investigations of physical and chemical adsorptive properties are often used to characterise the nature of catalyst surfaces.

The physical adsorption of inert gases on surfaces at low temperatures, e.g. N_2 at 77 K is used to determine the total surface area of finely divided solids. In spite of some theoretical shortcomings, the Brunauer, Emmett and Teller (BET) equation introduced in

1938 has become the standard method for determining the monolayer volume, V_m (5). Adsorption data (volume adsorbed, V at pressure p) are plotted according to the relationship;

$$\frac{p/p_o}{V(1-p/p_o)} = \frac{1}{V_m c} + \left[\frac{c-1}{V_m c}\right] \frac{p}{p_o}$$

In this equation p_o is the saturated vapour pressure of the adsorbate and c is a constant related to the relative lifetimes of molecules in the first and higher layers. The plot of $(p/p_o)/V[1-(p/p_o)]$ versus p/p_o is linear and V_m is given by 1/(slope + intercept). The surface area is obtained by converting V_m to molecules adsorbed and multiplying by the molecular area.

Chemisorption is used to characterise particular sites present on surfaces. This is made possible by the specific chemical nature of the adsorption bond. Chemisorption studies are frequently used to determine the surface areas of metals and metal oxides dispersed on high surface area supports, e.g. charcoal, silica and alumina. Selective determination of active sites in this way is normally carried out with small chemically active adsorbates. CO, O_2 and H_2 have been widely used, although other molecules, including N_2O, have specific applications. Bridge et al (6) have reported the adsorption of CO to measure the surface area of chromia supported on silica, whilst N_2O is frequently used to determine the area of supported copper (7). Below 373 K

N_2O decomposes to yield gaseous nitrogen and adsorbed oxygen without oxidation of sub-surface copper.

In addition to volumetric or gravimetric measurements of physical adsorption and chemisorption to determine surface areas many specialised physical techniques are available to study particular surface phenomena. One such technique is infra-red spectroscopy which has been extensively applied to the chemisorption of CO, NO, CO_2 and small hydrocarbon molecules. In the work described in this thesis, infra-red spectroscopy has been used to study the adsorption and subsequent reaction of cyanogen on various surfaces.

1.2 Infra-red Spectroscopy of Adsorbed Species

Since most metals and many metal oxide powders are opaque to infra-red radiation, i.r. transmission spectroscopy can only be applied when these materials are dispersed as thin layers on i.r. transparent supports. I.r spectroscopic studies of the surface reactions which occur on these materials are often carried out using silica or alumina as the supporting medium, since both are relatively inert and have high surface areas. Unfortunately this method is limited, due to the strong absorption of i.r. radiation by silica and alumina below 1300 cm^{-1}. The region normally studied is that between 4000 and 1300 cm^{-1}. The low wavenumber region can be overcome by using reflection-absorption infra-red spectroscopy (RAIRS), but this has been mainly restricted

to adsorption studies on single crystals. A number of important RAIRS studies have been made on copper single crystal surfaces, a review of recent studies is given by Pritchard and co-workers (8).

The interpretation of the i.r. spectra of chemisorbed species relies heavily on analogies because the surface complexes formed have no exact counterparts in conventional systems. Spectra are often explained by comparison with the spectra of known free molecules. This approach has been widely accepted by surface spectroscopists due to the self-consistency of the results obtained from a wide range of experimental systems.

I.r. spectroscopy is able to distinguish between physical and chemical adsorption. The vibrational spectra of physically adsorbed gases are similar to gas phase spectra. This is because molecular vibrations are largely unaffected by adsorption even though rotational freedom is restricted. However, non- dissociative chemisorption involves the formation of a chemical bond between the adsorbed molecule and the surface and thus new vibrational modes should in principle be observed. Chemisorption also causes a perturbation of the bonding within the molecule with the result that i.r. bonds are shifted relative to gas phase counterparts. In practice the vibrational modes involving bonds to surface atoms are usually at low wavenumber values and thus overlapped by vibrational modes of the bulk. Most

studies are therefore concerned with the spectral changes brought about by changes in the bonding within the adsorbed molecule. Dissociative chemisorption gives substantial spectral changes because bond rupture has major consequences for residual bonds in the fragments. The formation of new bonds when molecules react can also be studied.

1.3 Chemical Structure and Adsorption Studies on Chromium Oxides

Chromium oxide occurs mainly with chromium in the +3 or +6 oxidation state. Chromium(III) oxide, Cr_2O_3 (chromia) can be prepared in a high surface area form, although it is often studied when dispersed on high surface area silica or alumina (9-12). Conversely, $Cr(VI)O_3$ ('chromic acid'), cannot be prepared in a high surface area form, so surface studies in this case are usually only carried out when the oxide is dispersed on high surface area, inactive supports. Interestingly, by supporting chromic acid on silica an increase in thermal stability is observed. This effect is pronounced, since whereas pure CrO_3 is unstable above 473 K, silica-supported CrO_3 is stable up to 1273 K. Surface studies of Cr(VI) have therefore concentrated on the supported form, especially with SiO_2, Al_2O_3 and SiO_2-Al_2O_3 as supports.

Catalysts based on supported chromium oxide are commercially important in at least three key processes;

(a) polymerisation of olefins (the Phillips process (13)), (b) dehydrogenation of hydrocarbons (Houdry process (14)), (c) dehydrocyclisation of hydrocarbons. As a result, supported chromium oxides have attracted considerable scientific interest and there has been much speculation about the role of the support in stabilising different oxidation states of chromium.

One particular aspect of silica-supported chromium ions which has caused serious contradictions between different groups has been that of the active oxidation state for the polymerisation of ethylene. Merryfield (15) reported that every valence from Cr(II) to Cr(VI) has at some time been proposed as the active site. In fact the problem is complicated due to the simultaneous presence of several oxidation states. The following sections present a general overview of the preparation, characterisation and adsorption studies over the three most widely occurring supported chromium oxidation states, namely Cr(VI), Cr(III) and Cr(II).

1.3.1 Supported Chromium(VI) Oxide

Supported Cr(VI) oxide is best prepared by aqueously impregnating silica with chromic acid (CrO_3). The resultant slurry should be dried whilst maintaining agitation to prevent heterogeneity due to chromatographic effects. Finally, drying at 423-623 K results in anchorage of the chromium oxide to the silica surface by

esterification forming either surface chromate or dichromate as shown below:-

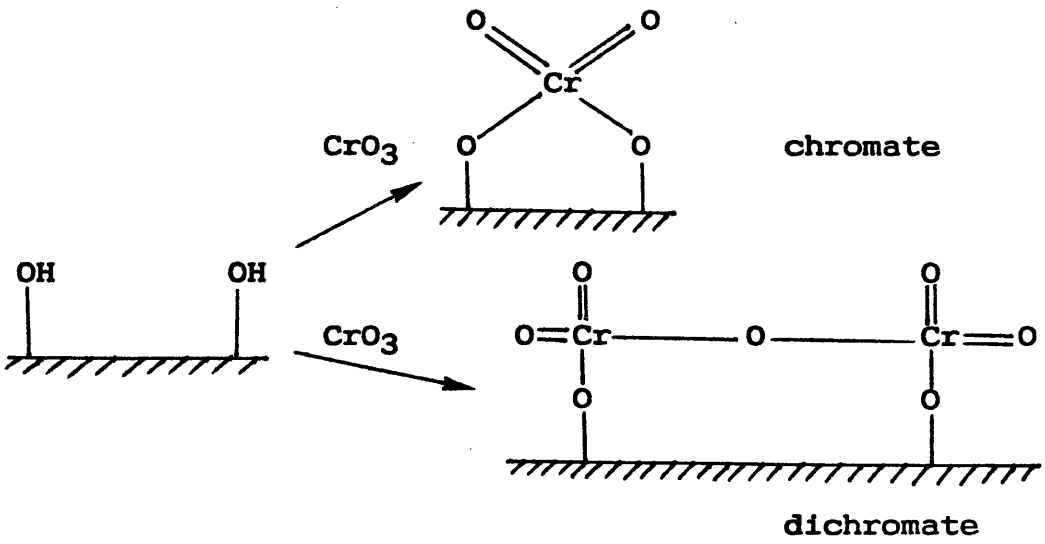

Zecchina et al (16) used i.r. spectroscopy to explain that since only one hydroxyl group is lost per surface chromium atom, chromium must exist as dichromate. The similarity of the UV-visible reflectance spectrum of the catalyst to that of potassium dichromate led others to a similar conclusion (17). Conversely, by measuring the weight increase caused by impregnation, Hogan (18) proposed that two hydroxyl groups were lost per chromium atom and thus he suggested that chromate was the surface species formed. McDaniel (19) recognised that these attempts to distinguish between the two possibilities by measuring the -OH content were not valid when aqueous impregnation was used. Instead by anhydrously impregnating the silica he found other OH/Cr ratios which favoured the chromate option. He strengthened his argument by reacting pre-calcined silica with chromyl chloride (CrO_2Cl_2)

whereupon he noted that two chlorine atoms were lost per surface chromium:-

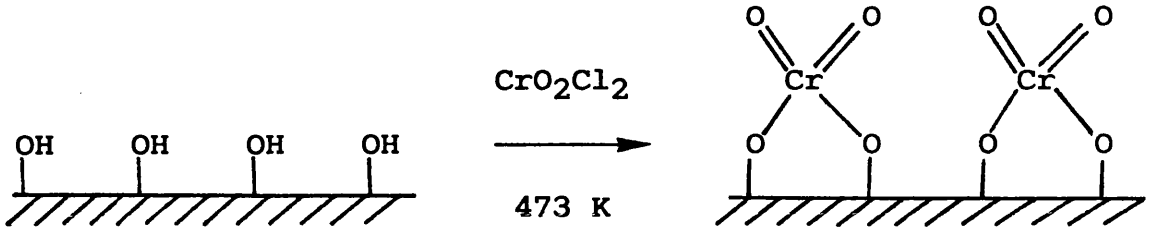

McDaniel re-affirmed his findings by reacting CrO_3/SiO_2 with hydrogen chloride gas (20), HCl stripped off the Cr(VI) in the form of CrO_2Cl_2 vapour leaving only one additional hydroxyl group for each point of attachment to the surface. The ratio between the increase in hydroxyl population and Cr atoms recovered could only be explained on the basis of a chromate structure.

Several papers have been written concerning the effect of chromium loading on the silica. When loadings are kept below 3% Cr by weight, it is possible to prepare catalysts with all of the chromium in the hexavalent state with no degradation when temperatures up to 873 K are used (19). However, when higher Cr loadings are used, surface stabilisation by esterification is accompanied by degradation of non-anchored CrO_3 to yield α-chromia-like particles in addition to surface stabilised low valence states of chromium (21). Using UV-visible reflectance spectroscopy, McDaniel (22) reported that the maximum amount of chromium which could be stabilised in the hexavalent state, an amount termed the saturation

coverage, declined at higher pretreatment temperatures (i.e. with decreased silanol concentration). Furthermore, above 773 K both moisture and lack of oxygen were found to destabilise Cr(VI). Studies using photoelectron spectroscopy (XPS) to characterise supported chromium oxide have been used to monitor the temperature-stimulated reduction of Cr(VI) to Cr(III) (23). This technique has also provided information on the stabilising influence of the support on Cr(VI) when low chromium loadings are present.

A second route to the silica supported Cr(VI) catalyst was that used by Merryfield (15). He prepared a 1.1 wt % chromium(VI) sample by impregnating microspheroidal silica with an aqueous solution of chromium(III) acetate, followed by calcination in dry oxygen. The presence of Cr(VI) in the bright orange catalyst was confirmed by titration with Fe(II).

The nature of the active sites involved in the Phillips process is still controversial. It is now widely accepted that the precursor of the polymerisation site is hexavalent chromium. Some have argued that the hexavalent chromium exists as dichromate (24) whereas others have suggested that surface chromate is the precursor (25). The active site itself is thought to be associated with Cr(II) ions which are generated by reduction of the hexavalent surface with ethylene or carbon monoxide (16,19,21,26). Reduction in the

presence of hydrogen-containing molecules leads to substantial amounts of chromium(III) (17).

Other reactions studied over supported Cr(VI) include the oxidation of ethanol (37) and the hydrogenation of olefins (28,29). The adsorption and reaction of cyano- compounds over $Cr(VI)/SiO_2$ is described later (Sec.1.6.4.2).

1.3.2 Supported Chromium(III) Oxide

Supported chromium(III) oxide can be prepared by aqueous impregnation of silica by Cr(III) nitrate, followed by thermal decomposition in vacuo at 623 K (9-12). An alternative route involves reduction of supported chromium(VI) oxide using CO, H_2 or C_2H_4, but the resultant surface contains some chromium also in the Cr(II) state (17,29,30,33). Both methods of impregnation lead to a dark material containing an excess of oxygen as evidenced by the formation of carbonate-like species on treating the sample in CO at 470 K. Excess oxygen can be removed by heating in CO at 673 K followed by evacuation at this temperature; this results in a green coloured sample. Beck et al (34) analysed the product using EPR spectroscopy and reported that Cr(III) ions existed in clusters (β-phase) (35) and as isolated ions in distorted octahedra (δ-phase). Even after CO reduction, diffusion of oxygen from the interior to the surface can still occur. Borello (9) and Groeneveld (36) reported that reduced catalysts

adsorb CO giving rise to several i.r. bands in the region 2210-2185 and 2150-2130 cm^{-1}. Groeneveld assigned these as follows: (a)2185 cm^{-1},CO adsorbed on Cr(III) ions (b) 2176 and 2195 cm^{-1}, symmetric and antisymmetric stretching of CO_2 adsorbed on Cr(III) respectively and (C) 2203 cm^{-1}, CO adsorbed on $(H\text{-}Cr)^{3+}$ sites. McDaniel (22) and Anderson (37) have reported that surface Cr(VI) can easily be reformed from silica-supported Cr(III) catalysts simply by heating in oxygen at 673 K.

The adsorption and reaction of a number of molecules on supported Cr(III) has been studied mainly using i.r. spectroscopy. Zecchina et al (10) studied CO_2 adsorption which resulted in a band at 2348 cm^{-1} together with five more bands between 1700 and 1350 cm^{-1}. The band at 2348 cm^{-1} was attributed to weakly adsorbed CO_2 due to localised physical adsorption, and bands near 1700, 1630, 1600, 1475 and 1350 cm^{-1} were assigned to a range of carboxylate species (e.g. CO_2^-, CO_3^-, CO_3^{2-}).

The adsorption of nitriles on silica-supported chromium (III) was also investigated using i.r. spectroscopy (12). By adsorbing propionitrile onto the reduced chromia catalyst, two distinct cyano-bands were recorded at 2257 and 2294 cm^{-1}. The first, which was lost by outgassing at room temperature, was assigned to CN stretching of the species

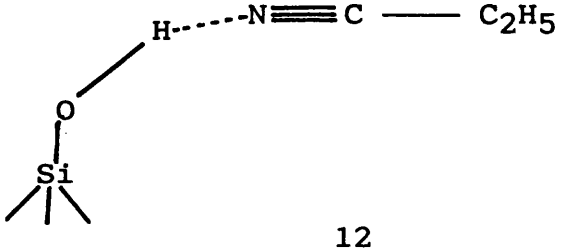

The band at 2294 cm^{-1} was removed only by outgassing at higher temperatures (being completely removed by 673 K), whereupon the i.r. spectrum indicated dehydrogenation and polymerisation of the adsorbed nitrile. It was suggested that the 2294 cm^{-1} band was due to CN stretching of the nitrile strongly interacting with the chromium through a σ- dative bond.

Nitric oxide adsorption on $Cr(III)/SiO_2$ (35,38,39) and on reduced $Cr(VI)/SiO_2$ (49) gave rise to two i.r. bands near 1875 and 1745 cm^{-1} on samples with high chromium loadings (i.e. ~10 wt. % Cr) with an additional band at $1800 \pm 10 cm^{-1}$ at lower loadings. Controversy exists over the explanation for the bands at 1875 and 1745 cm^{-1}. One group have assigned them to a cis-N_2O_2 dimer (34,35) whereas another (40) proposed formation of $Cr(II)(NO)_2$. The 1800 cm^{-1} band was assigned to monomeric NO adsorption on specific chromium sites [probably Cr(II)], whilst shoulders at 1880 and 1755 cm^{-1} were attributed to a $Cr(III)NO_2$ surface species.

At elevated temperatures, co-adsorption of CO and NO on Cr_2O_3/SiO_2 results in a band near 2210 cm^{-1} (41). The intensity of this band, assigned to isocyanate formation increased with time but the band could be removed by evacuation at 673 K. Surface isocyanate formation was proposed to occur by the following sequence:

$M + NO \longrightarrow M—NO$

$M—NO + M \longrightarrow M—N + M^{+}—O^{-}$

$M—N + CO \longrightarrow M—NCO$

(where M = surface Cr^{+2} ions)

A slow migration of -NCO from the chromium onto the silica was also observed.

Relevant evidence for -NCO formation on chromia also comes from studies of NO and CO adsorption on other surfaces. Rasko and Solymosi (42) dosed CO onto Al_2O_3/CrO_3 containing pre-adsorbed NO. The intensity of i.r. bands due to NO decreased, whilst a new band developed at 2262 - 2242 cm^{-1}. This was attributed to the formation of a surface isocyanate complex (43). The development of a band with a similar frequency was also observed when NO and CO were reacted over alumina-supported noble metals (44). In the case of the Al_2O_3/CrO_3 sample, the NCO species was therefore thought to be adsorbed on the alumina support and not on the active chromium sites. Solymosi and Rasko (45) verified this conclusion by studying the formation of isocyanate surface species over unsupported chromia. They found and assigned a band at 2210 cm^{-1} to the $\gtrless$Cr-NCO species and thus the 2262 - 2242 cm^{-1} band reported earlier was assigned to an alumina-NCO species. The absence of a band near 2210 cm^{-1} over Cr_2O_3/Al_2O_3 prompted the suggestion that NCO was first formed on the active Cr_2O_3 sites before rapidly migrating to the alumina. They

also reported similar experiments with Cr_2O_3/SiO_2 at 673 K. These resulted in a strong NCO band at 2210 cm^{-1} and a weak one at 2315 cm^{-1} (due to SiNCO). This showed that the migration of NCO from chromia to silica was a less favourable process than with alumina.

Examples of the application of i.r.-spectroscopy to studies of adsorbed species are given later in this chapter. A review of i.r. studies associated with the adsorption of cyano-compounds on unsupported and silica-supported Cr(III) is included in Sec.1.6.

1.3.3 Supported Cr(II) Oxide

Supported Cr(II) can be prepared by reduction of higher valence supported chromium oxide (15-17,21,26). Groeneveld (17) proposed that CrO_3-impregnated silica leads to adsorbed Cr(II) via surface Cr(III) ions as follows:-

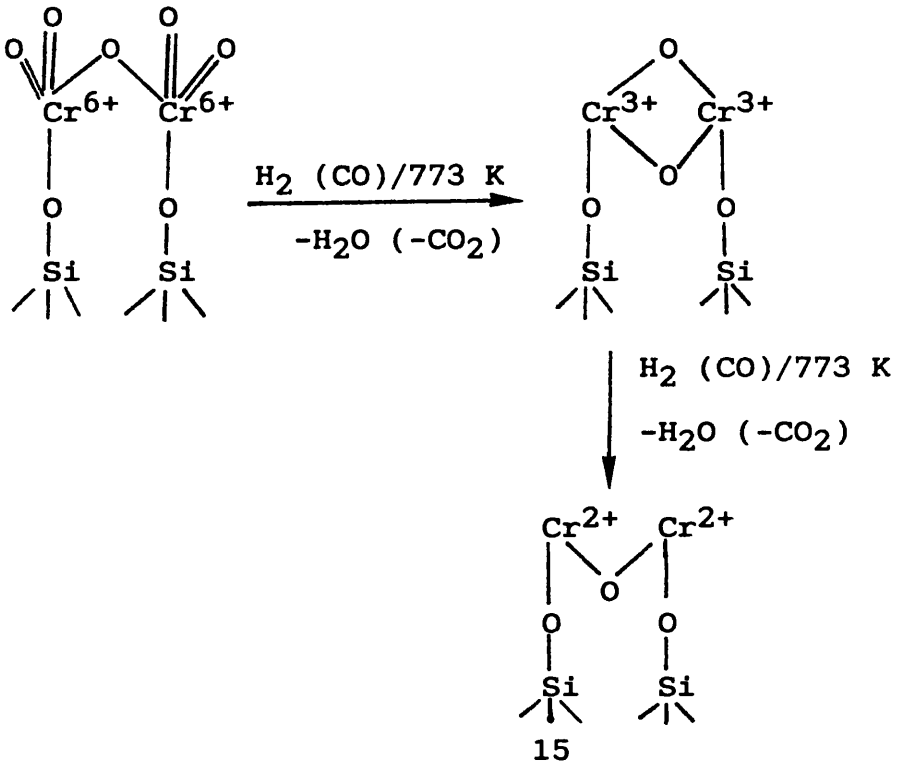

15

The nature of the supported Cr(II) surface and its adsorption characteristics has been widely investigated (15,21,29,32,40,46-54). The general conclusion reached is that Cr(II) is a highly co-ordinatively unsaturated species which seeks stabilisation by adding further ligands into its co-ordination sphere.

Four distinct types of surface Cr(II) ions have been identified (21). These have been designated Cr_A, Cr_B, Cr_{C1} and Cr_{C2}. A detailed insight into these species was carried out using NO adsorption (40,53). It was assumed that Cr_A, Cr_B and Cr_C ions were 2-, 3- and 4-co-ordinate to the surface. Fubini et al (21) concluded that Cr_A and Cr_B sites were exposed whereas the Cr_C type were not. Fubini and co-workers (21,53) have proposed that supported Cr(II) ions exist mainly in pairs.

The involvement of supported Cr(II) in the context of ethylene polymerisation has been widely studied. A direct correlation between surface Cr(II) and catalytic activity was found by Merryfield et al (15) and others (46-47). Fubini et al (21) have explained this reactivity in terms of the four types of chromium sites. The influence of the hydroxyl population on the activity of the sites has also been studied (55).

Finally, Eley et al (54) studied the adsorption of ammonia on Cr(II). I.r bands ascribed to adsorbed ammonia were observed at 3380 and 3300 cm^{-1}. On evacuation at 373 K spectral changes suggested that the ammonia had reacted on the surface.

1.4 Chemical Structure and Adsorption Studies on Copper Oxides

Copper forms two stable oxides, cupric oxide (CuO) and cuprous oxide (Cu_2O). Cuprous oxide can be converted into cupric oxide by heating in oxygen but at temperatures above 1050 K CuO becomes unstable and decomposes to Cu_2O. The pure oxides can be reduced to metallic copper by H_2 or CO at 450 K or above but with supported CuO, e.g. CuO/SiO_2, reduction is more difficult. It has been shown that, at low loadings (0.5 to 1.0 wt.% Cu), treatment in H_2 at 573 K results only in reduction to supported Cu_2O (56).

Amara et al (57) studied the preparation, spectroscopic characterisation and stability of silica-supported copper(I) species formed from Cu(II) precursors. At copper loadings above 2 wt.%, hyperdispersed CuO was reduced to Cu(0) by simply outgassing. Below a copper content of 1.0 wt.% supported on silica the copper existed as isolated Cu(II) ions, these were reduced directly to Cu(0) by outgassing to 673 K. The stability of supported Cu(I) species formed by reduction of cupric ions were stable up to 1073 K in vacuo.

De Jong et al (58) prepared CuO/SiO_2 at higher loadings (10-30 wt.% Cu) and investigated CO adsorption by i.r. spectroscopy. After calcination and adsorption, two types of adsorbed CO were identified showing absorption bands at 2136 and 2204 cm^{-1}. These bands

were ascribed to CO adsorbed on CuO clusters and on isolated Cu(II) ions on the silica surface respectively. They found that on reduction-reoxidation at 573 K the 2204 cm^{-1} band disappeared whilst the 2136 cm^{-1} band intensified. They concluded that the isolated copper ions had been mobilised and had formed copper oxide clusters.

Deen et al (59) have used EPR spectroscopy to study the chemistry of alumina-supported copper and copper oxide. They monitored changes in the relative amounts of isolated and clustered Cu(II) after passing gas mixtures containing oxidising constituents (O_2 and NO) and reducing gases (H_2 and CO) over the samples. They found that crystallites of CuO favoured oxidation of CO by O_2 whilst isolated copper ions played a part in the reduction of NO by H_2 and CO.

The nature of cupric oxide supported on activated carbon has been studied by Ehrburger et al (60). In freshly prepared samples, the copper was mainly present as amorphous CuO. However, during ageing in a humid atmosphere the amount of amorphous CuO decreases mainly due to crystallisation of CuO.

I.r. spectroscopy has been used to study CO_2, CO and NO adsorption and reaction on copper oxides (61-63). Weakly adsorbed CO_2 gives a band at 2350 cm^{-1} on CuO/SiO_2 (61), and unsupported CuO, CO_2 has been reported to produce bands between 1700 and 1300 cm^{-1} ascribed to carbonate, bicarbonate and carboxylate

species (62). Bands in this region were also observed by London and Bell (61) when they adsorbed CO onto CuO/SiO_2, they assigned these bands as follows; 1675 cm^{-1} (bicarbonate), 1585 cm^{-1} (carboxylate) and 1350 cm^{-1} (carbonate).

Current concern over exhaust emission control has led to widespread interest in the CO/NO reaction. This has included studies of the reaction over copper oxide by i.r. spectroscopy (64,65). Spectra recorded under reaction conditions showed the presence of adsorbed CO, CO_2, NO and N_2O, as well as CO_3^{2-} and NO_3^- structures. A band at 2200 cm^{-1} was ascribed to an isocyanate structure of the form Cu^+NCO^-. London and Bell (64) proposed that isocyanate formation occurred according to the following scheme:-

$$2Cu + NO(g) \longrightarrow CuN_{ads} + CuO_{ads}$$

$$CuN_{ads} + CO(g) \longrightarrow Cu(NCO)_{ads}$$

Conversely, Harrison and Thornton (65), who studied the CO/NO reaction on CuO/SnO_2, proposed that copper isocyanate formation occurs via CO dissociative adsorption followed by NO adsorption to yield an unstable fulminate which subsequently rearranges to isocyanate according to the scheme:-

$$2Cu + CO(g) \longrightarrow CuC_{ads} + CuO_{ads}$$

$$CuC_{ads} + NO(g) \longrightarrow Cu(CNO)_{ads} \longrightarrow Cu(NCO)_{ads}$$

isocyanate formation has since been reported when HCN was reacted with silica-supported copper oxides (2) (Sec.1.6.4.2) and following HCN (66), C_2N_2 (67) and HNCO

(68,69) adsorption on various unsupported clean and oxygen-dosed copper surfaces (Sec.1.6.2).

Other i.r. studies of unsupported and supported copper and copper oxides in the context of cyano-compounds are reviewed in Sec.1.6.

1.5 Studies with Copper Oxide - Chromium Oxide Mixtures

There is an extensive literature on mixtures of copper oxide and chromium oxide because of their long-standing interest as industrial catalysts. These mixtures, widely varied as regards phase composition and oxidation state, are often referred to collectively as 'copper chromite'. They are very effective catalysts in oxidation and hydrogenation reactions (70-77).

Copper chromite, strictly speaking, is either $Cu(I)_2Cr(III)_2O_4$ (cuprous chromite) or $Cu(II)Cr(III)_2O_4$ (cupric chromite), both of which are well-authenticated compounds, as is cupric chromate, $Cu(II)Cr(VI)O_4$. $CuCrO_4$ and $CuCr_2O_4$ can be formed by heating CuO with CrO_3 or Cr_2O_3, respectively, but above about 650 K the spinel $CuCr_2O_4$ (cupric chromite) is generally regarded as the stable phase. At temperatures above 1000 K, however, the spinel loses oxygen and cuprous chromite, $Cu_2Cr_2O_4$ (or $CuCrO_2$) is formed. These chromate and chromite phases and their interconversions have been studied by Charcosset et al (78-79) and by others (80-85).

Adsorption studies on well-characterized copper-chromium oxide have been relatively few. Rubene and Davydov (86) have applied i.r. spectroscopy to the adsorption of O_2, CO and D_2O, whilst Hertl and Ferrauto (73) have investigated adsorption of CO, NO and hydrocarbons in relation to the CO/NO reaction and hydrocarbon oxidation. Adsorption studies by Surman (3) and Davies (4) on copper-coated chromia, $CuO-Cr_2O_3/SiO_2$ and $CuO-CrO_3/SiO_2$ are described in Sec.1.6.

1.6. Adsorption of Cyano-Related Compounds

In this section a detailed account is given of previous work on the adsorption and reaction of C_2N_2, HCN and related compounds on carbon, metal and oxide surfaces. In recent years surface scientists exploiting ultra-high vacuum techniques have shown interest in C_2N_2 as a molecule amenable to study on single crystal metal surfaces, but previously much of the background to work with HCN and C_2N_2 was the need to develop adsorbents for protection from these gases as highly toxic substances. In the military context and also in the context of protection in industrial environments, where HCN and C_2N_2 are used in processes, the long term stability of adsorbents in bulk storage or in respirators also need to be assured and understood.

1.6.1. Adsorption of Cyano-Compounds on Activated Charcoal

The classic adsorbents for protection against HCN have been charcoal granules impregnated with active constituents, especially copper and chromium ions. Aged active charcoals, however, tend to release cyanogen when exposed to a stream of gas containing HCN.

The chemistry of HCN adsorption and C_2N_2 formation over copper surfaces is thought to occur as suggested by Williams (2) below;

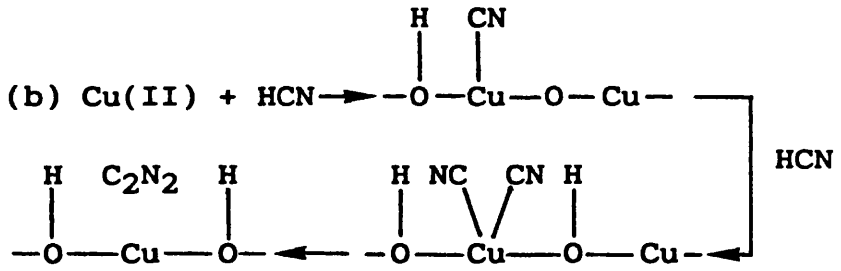

Adsorption studies of C_2N_2 on chromium-impregnated charcoals have shown that in the presence of Cr(VI) hydration occurs according to the reaction:

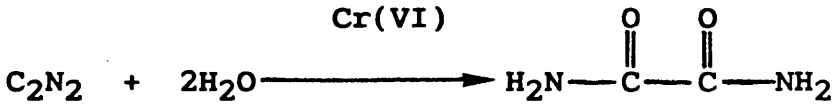

it has been proposed (87) that Cr(VI) is also able to oxidise low-valent copper to Cu(II) with simultaneous reduction of Cr(VI) to Cr(III). Combining these reaction steps it has been suggested that deterioration of copper-chromium systems may lead to premature C_2N_2

breakthrough by one or more of the following routes;

(a) Excess C_2N_2 formation and/or an enhanced rate of C_2N_2 formation, or

b) Suppressed C_2N_2 consumption and/or a slower rate of conversion to oxamide.

Gravimetric studies (4) discounted explanation (a), and therefore attention has been focused on the consumption of C_2N_2.

Since Cr(VI) was known to be reduced on contact with charcoal surfaces, it has been questioned whether Cr(III) is as active towards C_2N_2 conversion as Cr(VI). Davies (4) suggested that Cr(III) was incapable of hydrolysing C_2N_2, and therefore it was proposed that build-up of Cr(III) would decrease the ability of the surface to convert C_2N_2. This build-up of Cr(III) has been inferred from XPS measurements (87) which confirmed that Cr(VI) concentrations do indeed decrease when impregnated military charcoals are aged.

1.6.2. Adsorption on Metallic Surfaces

The earliest reports concerning the adsorption of HCN on metals were those of Anderson and Clark (88,89) who used evaporated metal films. By measuring the coverage of HCN as a function of time and by noting the amounts of hydrogen released during adsorption of HCN on Ni and W films containing pre-adsorbed hydrogen, they speculated on the mode of attachment of HCN to the surface. Four species were proposed as follows:

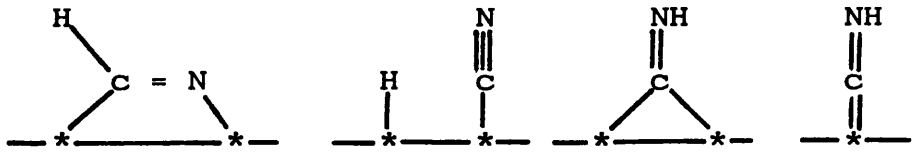

A B C D

(where *= surface metal atom)

At low coverages, HCN adsorbed onto paired sites either non-dissociatively (type A) or dissociatively (type B). A third species was also proposed (type C), formation which either involved dissociation followed by recombination, or H-migration. As the coverage increased these adsorption modes were converted to the one-site species (type D).

Anderson and Clark also studied the hydrogenation of adsorbed HCN on a range of metallic films and reported that four types of reaction occurred. These were; (a) hydrogenation to CH_3NH_2 (b) C-N bond rupture to give NH_3, CH_4 plus metal carbides and nitrides, (c) C-N bond formation to give $(CH_3)_2NH$ and $(CH_3)_3N$ and (d) C-C bond formation to produce C_2 and C_3 hydrocarbons (eg CH_3CN and $C_2H_5NH_2$). These processes are shown schematically in Fig. 1.1.

The thermal decomposition of HCN over Ti, Hf, Zr, Ta, Mo and W at 900-3000 K was reported

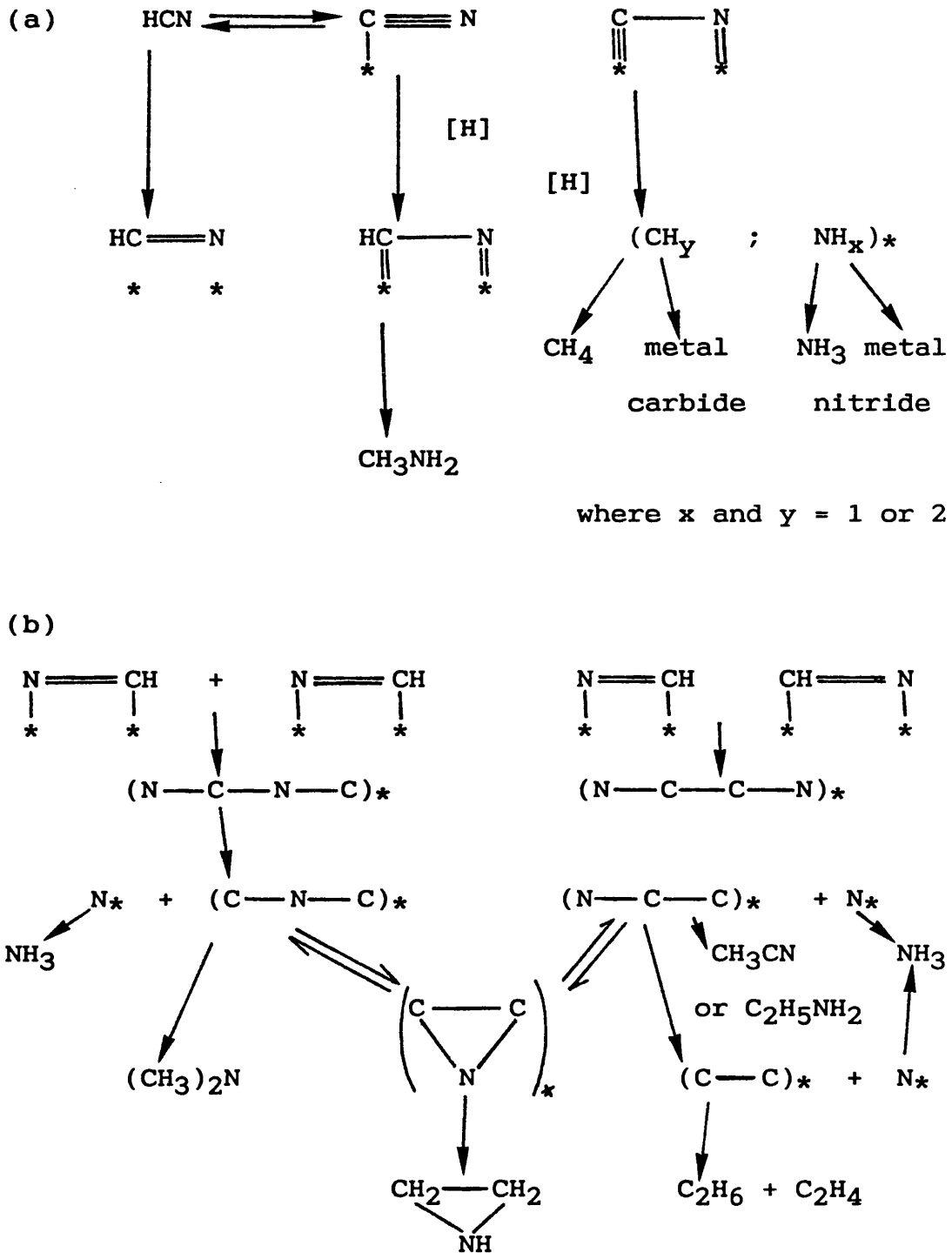

Fig 1.1. Schematic Representation of the Hydrogenation of HCN over Metal Films after Anderson and Clark (89).

by Fabbri et al (90). Under these conditions both H_2 and N_2 were released to the gaseous phase whilst some nitrogen and carbon was retained as surface nitride, carbonitride and carbide.

Cyanogen adsorption and reaction on metals has been studied on single crystal surfaces by UHV techniques, e.g. low energy electron diffraction (LEED), high resolution electron energy loss spectroscopy (HREELS) and thermal desorption spectroscopy (TDS).

Several groups have studied cyanogen adsorption on the Pt(110) surface (91 - 93). Two types of adsorption phase (α and β) were resolved by TDS. The α-phase is thought to consist of molecularly adsorbed, undissociated C_2N_2. Molecules in this state are molecularly desorbed by 413 K. The nature of the β-phase, which is desorbed above 673 K, remains a controversy. Some have suggested that it contains single CN units bonded to the metal whilst others have proposed that it also involves molecularly adsorbed C_2N_2. Netzer (92) favours a third explanation, namely that C_2N_2 molecules organise themselves into a polymeric, paracyanogen - like structure (Fig. 1.2.)

Fig. 1.2 The Structure of Paracyanogen

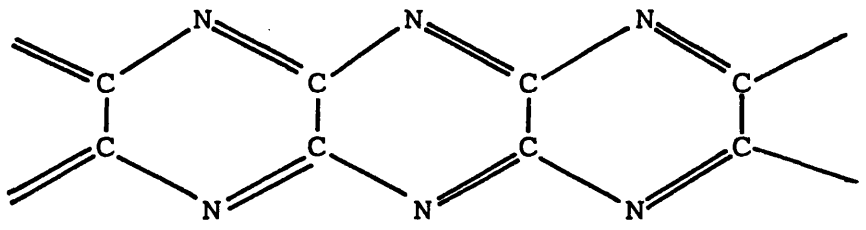

Bridge et al (94), who studied the adsorption of C_2N_2 on Pt(110) and Ag(110) surfaces, concluded that adsorption was out of registry with the underlying metal surface. A similar conclusion was reached by Netzer et al (95) using a stepped Pt(111) surface. Further insight into the nature of adsorbed C_2N_2 came from studies with HCN, also studied by Bridge et al (94). They found that HCN adsorbed dissociatively on Pt(110) with the release of H_2 at ~420 K and the release of cyanogen at 673-873 K. These results suggested that HCN adsorption led to a β-phase of adsorbed C_2N_2. HCN adsorbed molecularly onto the Ag(110) surface and on desorption HCN was the only product recovered. From these studies, Bridge et al concluded that the α-phase consisted of non-dissociatively adsorbed C_2N_2 whilst the β-phase contained adsorbed CN radicals. These workers also calculated the saturation coverage of C_2N_2 on Pt(110) which corresponded to approximately half a monolayer. This fact prompted the suggestion that C_2N_2 bonded multiply to the Pt surface, a conclusion reached theoretically by others (96).

Hemminger et al (97) studied C_2N_2 adsorption on a Ni(111) surface. The gas was strongly chemisorbed at 300 K and by 400 K the surface formed an ordered (6x6) structure which was stable to 800 K. At higher temperatures gaseous N_2 was released, a result in contrast with studies over Pt surfaces when the C-N group always desorbed intact. To account for these results,

Hemminger et al proposed that dissociative chemisorption initially occurred with the CN group parallel to the surface and bonded through both the carbon and nitrogen atoms. The ordering of the surface at 400 K was ascribed to polymerisation forming the trimeric form of cyanogen tricyanotriazine. Subsequent decomposition of this species above 800 K led to the desorption of gaseous nitrogen.

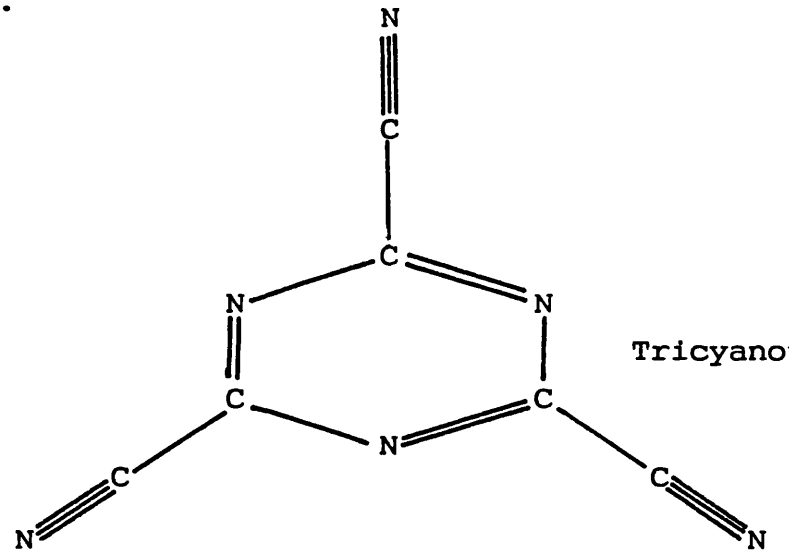

Tricyanotriazine

HREELS studies of C_2N_2 adsorption on Pd(100) (91, 98-101) showed that at monolayer and lower coverages at 100 K there was molecular adsorption but no stretching mode was observed. This result was explained by assuming that the molecular axis of the adsorbed cyanogen was parallel to the surface, thus the stretching modes were polarized parallel to the molecular axis. In addition the C-C bond of chemisorbed cyanogen seemed largely un-perturbed and π-bonding was suggested rather than a species bonded through the C or N atoms. Above 250 K dissociative chemisorption was observed, and the spectra suggested that the resultant

CN moieties were also π-bonded with the molecular axis parallel to the Pd surface.

The hydrogenation of adsorbed CN formed by dissociative adsorption of cyanogen was investigated on Pd(111) and Pd(110) by Kordesch et al using HREELS (99). The spectra suggested that C-C bond cleavage was a prerequisite step for hydrogenation and that the following reaction occurred:

$$H_{ads} + CN_{ads} \longrightarrow HC{=}N_{ads}$$

(H_{ads} was produced by adsorbing $H_2(g)$). They proposed that the chemisorbed HCN adopted a bent structure in which the C=N bond was parallel to the surface. Lloyd et al (102) disagreed with the C-C cleavage proposal. When they reacted C_2N_2 with H_2 on Pt(111) they provided HREELS and TDS evidence which suggested a partially-hydrogenated species in which one hydrogen was attached to each carbon and nitrogen atom of the C_2N_2. Two possible surface species were proposed (structure I and structure II), but the former was considered most likely. The di-imine species which formed at ~250 K decomposed to give back C_2N_2 and H_2 at ~430 K.

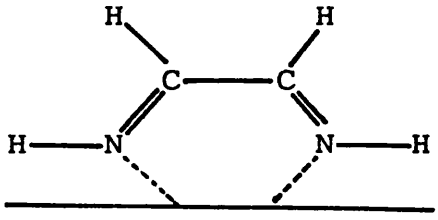

Structure I (a di-imine)

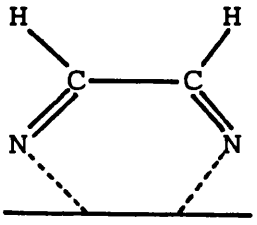

Structure II (a di-nitrene)

Ru(100) adsorbs C_2N_2 in three states; a molecular state, a dissociated state with Ru-C bonding and a dissociated state with Ru-C and Ru-N bonding (103). C_2N_2, N_2 and adsorbed carbon were produced during desorption.

The adsorption and reaction of cyanogen on copper surfaces has attracted the attention of several research groups. Outka (104) worked with a clean Cu(110) surface and showed that whereas C_2N_2 was molecularly adsorbed at 150 K, at higher temperature dissociation occurred to yield cyano groups which ultimately recombined and desorbed at 800-1000 K. Photoemission results indicated that these cyano groups bonded to the surface via a carbon atom, with their molecular axis perpendicular to the surface.

Dissociative adsorption of C_2N_2 was also reported over a clean Cu(111) surface (67). In contrast to C_2N_2, HCN (and HNCO) did not adsorb on this surface at 300 K (66). However, the presence of pre-adsorbed oxygen on the copper has a pronounced affect on C_2N_2 and HCN adsorption. The oxygen tends to suppress the uptake of cyanogen (67), whereas the dissociative uptake of HCN and HNCO was enhanced with concomitant release of water (66). Desorption spectra recorded following both C_2N_2 and HCN adsorption showed evolution of C_2N_2 above 700 K. This implied that CN radicals occur in pairs on the surface.

The different behaviours of C_2N_2 and HCN towards adsorption on clean and oxygen-dosed copper surfaces can be explained by a simple argument based on energetics. In the case of C_2N_2, two CN radicals form, these bond strongly with the copper, thus favouring dissociation of C_2N_2. With HCN, only one Cu-CN bond forms in addition to a weak Cu-H interaction. Therefore the dissociation of C_2N_2 is a more favourable process than that of HCN. However, in the presence of adsorbed oxygen, HCN adsorption is greatly enhanced due to the formation of strong O-H bonds as depicted by the scheme:

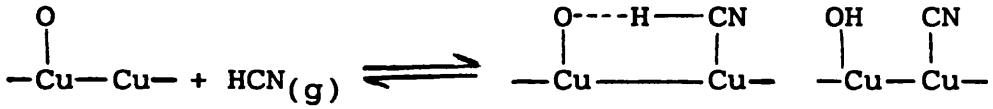

The release of water reported earlier is then explained since -OH groups are not stable on copper surfaces and dehydration readily occurs thus:

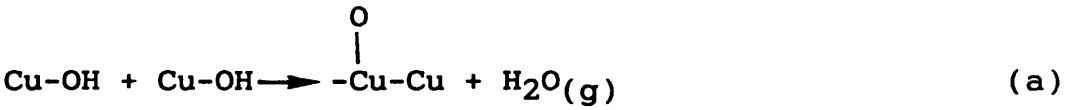

(a)

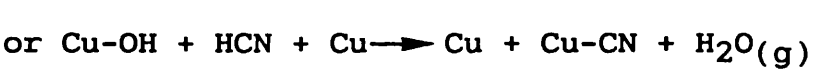

(b)

Both processes occur at 300 K, but whilst reaction (a) regenerates the oxygen coated surface, reaction (b) produces Cu-CN which prevents further uptake. Similar results were reported by Solymosi et al (68-69) for the

adsorption of HNCO on Cu(111) which contained pre-adsorbed oxygen.

Solymosi and Kiss (67) investigated the C_2N_2-O_2-Cu(111) reaction further after noticing that CO_2, N_2 and C_2N_2 were released stepwise at 400 K, 700 K and above 800 K, respectively. They formulated the following sequence of reactions to account for these observations.

$$C_2N_2 + 2Cu + CuO \xrightarrow{300\ K} 2Cu\text{-}CN + CuO$$

$$C_2N_2 + Cu + CuO \xrightarrow{300\ K} Cu\text{-}CN + Cu\text{-}NCO$$

$$Cu\text{-}CN + Cu\text{-}O \xrightarrow{300\ K} Cu\text{-}NCO + Cu$$

$$Cu\text{-}NCO + Cu\text{-}O \xrightarrow{400\ K} Cu\text{-}N + CO_{2(g)} + Cu$$

$$Cu\text{-}N + Cu\text{-}N \xrightarrow{700\ K} 2Cu + N_{2(g)}$$

$$Cu\text{-}CN + Cu\text{-}CN \xrightarrow{300\ K} 2Cu + C_2N_{2(g)}$$

Outka et al (104) studied the reaction of C_2N_2 with Cu(110) surfaces containing various amounts of pre-dosed oxygen. CO_2 and NO were produced on desorption up to 1000 K.

Studies of the adsorption of HCN on polycrystalline copper surfaces have been conducted in our laboratory by

Mellor (1) and by Williams (2). Mellor reported that reaction occurred to give a coverage approaching one HCN molecule per two surface copper sites and that H_2 was released to the gaseous phase. Williams found a limiting coverage closer to one HCN molecule per three surface copper sites. He proposed that adsorbed HCN molecules associated themselves via H-bonds in such a manner as to exclude one site for every HCN molecule adsorbed. The absence of a C≡N stretch in the i.r. spectrum of the adsorbed layer suggested that the HCN was adsorbed parallel to the copper surface and that the triple bond opened to form σ-bonds between the C and N atoms and the surface. This conclusion was consistent with Anderson and Clarks' Type A Model (Sec.1.6.2).

In a study of the nature and stability of isocyanates on metal surfaces, Gorte et al (105) investigated the adsorption of isocyanic acid on Pt(111). At 100 K, HNCO adsorbed molecularly, forming multilayers which were retained when the surface was heated to 150 K. On heating to 250 K, most of the HNCO decomposed to CO and nitrogen-containing fragments but no evidence of C-O bond cleavage was seen. They concluded that isocyanate was not a stable species on Pt surfaces at room temperature.

1.6.3. Adsorption of Cyano-Compounds on Oxides

1.6.3.1. Adsorption on Metallic Oxides

Most of the information available on the adsorption of HCN on unsupported transition metal oxides has arisen from our own laboratory (1-4). The majority of this work has concerned copper oxides, chromium oxides and mixtures of copper and chromium oxides, though some work has been carried out using nickel oxide, magnesia and alumina.

Mellor (1) was the first to study the interaction of HCN with unsupported transition metal oxides. He outgassed CuO above 700 K before adsorbing HCN at 297 K and noticed that C_2N_2 was the only product desorbed to the gas phase. This observation was explained by the heterolytic dissociation of HCN followed by the recombination of CN radicals. Release of cyanogen then left a cuprous hydroxide surface. The overall process is similar to that described schematically in Sec. 1.6.1.

Mellor also noticed that interaction of HCN with a less vigorously outgassed CuO surface resulted not only in the release of C_2N_2 but that CO_2 and H_2O were also formed. It was proved that interaction of HCN with residual surface hydroxyl groups and not with molecularly held water molecules led to the production of CO_2 and H_2O. Furthermore, only those hydroxyl groups attached to the Cu^{2+} ions or those formed by attachment of a proton to a lattice O^{2-} ion were thought to be reactive.

Williams (2) investigated the CuO + HCN system further using i.r. spectroscopy and concluded that at 323 K, recombination of the two CN moieties to form adsorbed cyanogen was a rapid reaction and that release to the gaseous phase was a much slower process. In contrast to Mellor he also reported that complete oxidation of HCN was possible on CuO, especially at elevated temperatures. Indeed, virtually all the carbon and nitrogen retained as HCN or CN groups at 323 K were removed as CO_2 and N_2 at 573 K (2,106), and a small amount of H_2O was also released It was proposed that CN groups were oxidised by the oxygen atoms from the CuO lattice and that H_2O was formed due to desorption from hydroxyl groups formed as a result of abstraction of hydrogen from HCN. An isocyanate species was identified as an intermediate in the oxidation reaction.

The adsorption of HCN on Cu_2O was also studied by Williams (2,106). This system was capable of decomposing adsorbed HCN even at 295 K to yield gaseous N_2 together with a mixture of gaseous CO_2 and surface carbonate.

The surface carbonate species decomposed to yield CO_2 on heating above 500 K. In the presence of moisture, hydroxyl groups interacted with the HCN to yield an isocyanate intermediate which then decomposed to CO_2 and a surface hydride species (a precursor to NH_3). Some C≡N bonds were returned without breakdown, presumably because the surface only had a limited

oxidation capability. At elevated temperatures (673-773 K) some HCN and C_2N_2 were released.

The adsorption of HCN on ∝-chromia was investigated using i.r. spectroscopy by Surman (3). Adsorption at room temperature occurred forming N_2 and several strongly bound surface species, these being dependent upon the surface pretreatment. One such species was considered to be adsorbed amide which gave rise to a band at 1680 cm^{-1}. It was proposed that this species could either reform HCN or it could decompose to CO_2 via formate and carboxylate intermediates. The following scheme illustrates the latter route;

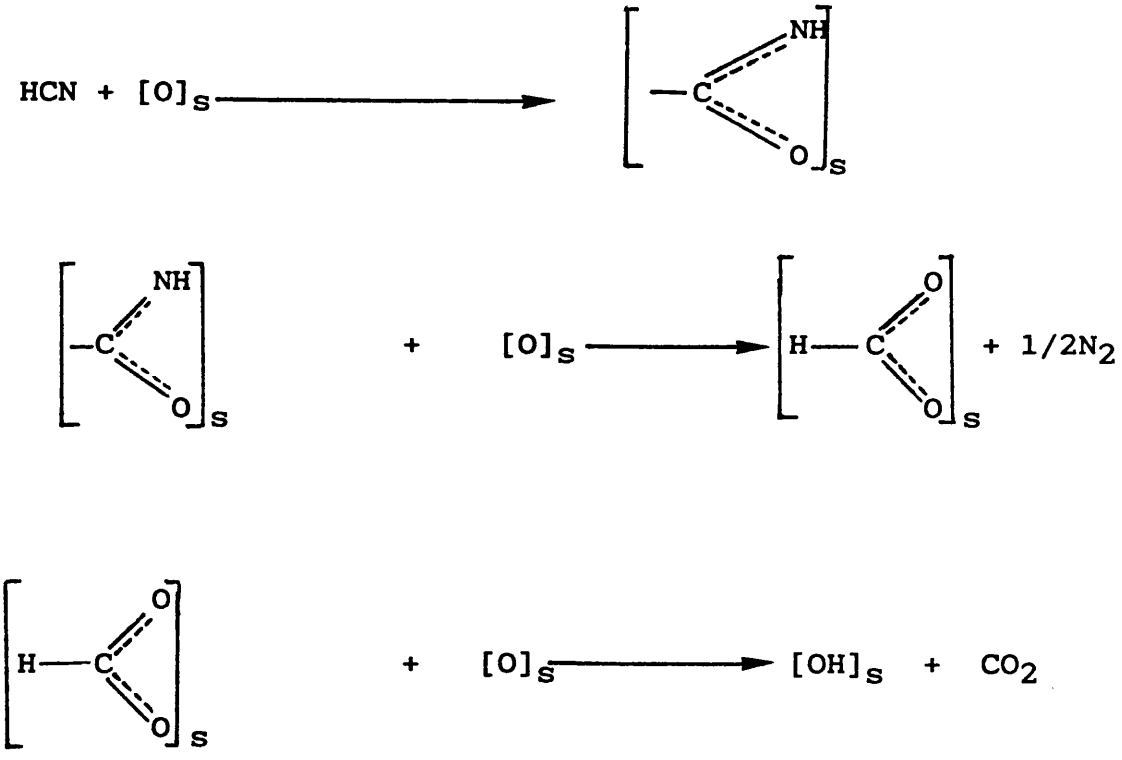

where $[O]_S$ represents lattice oxygen or pre-adsorbed oxygen.

The adsorption of HCN on copper-coated chromia has been studied by Surman (3) and Davies (4). Surman found that whilst CO_2, N_2 and H_2O were the only gaseous products recovered from pure chromia, C_2N_2 was also released when small amounts of cupric ions were present. Indeed, the amount of C_2N_2 formed was dependent upon the concentration of cupric ions. The formation and release of C_2N_2 from the mixed oxide system occurred via the same mechanism as over pure CuO, namely that adsorbed cyanogen was first formed by the recombination of cyanide groups associated with copper sites. Since no i.r. bands were identified corresponding to adsorbed C_2N_2, it was presumed that it was present as an i.r. inactive form, probably adsorbed parallel to the surface. At elevated temperatures residual adsorbed CN groups were converted to isocyanate species, a result explained in terms of surface mobility.

HCN contact with CuO/Cr_2O_3 at elevated temperatures caused a reaction with adsorbed water molecules associated with the copper sites. The reaction occurred via two routes, one of which led to NH_3 and CO_2 formation and the other to CH_4 and N_2. These reactions are represented by the following equations:-

$$HCN + 2OH^- \longrightarrow NH_3 + CO_2 + 2e$$

$$HCN + H_2O + OH^- \longrightarrow CH_4 + 1/2N_2 + 2[O] + e$$

Davies (4) confirmed that the main reaction of HCN when adsorbed on outgassed CuO/Cr_2O_3 was the formation

of C_2N_2 and reduction of copper to the monovalent state. On re-exposing a used sample to HCN he found that the ability to produce C_2N_2, was exhausted, a result consistent with the fact that the $Cu/\alpha Cr_2O_3$ surface is totally inactive for C_2N_2 formation. Instead HCN was converted according to the following reactions;

$$2HCN_{(g)} + 2OH^-_{(s)} \longrightarrow 2CN_{(ads)} + 2H_2O + 2e$$

On desorption the adsorbed cyanide decomposed to N_2 via $N_{(ads)}$ and to NH_3 and $NH_{x(ads)}$ via $NH_{2(ads)}$ according to the reactions;

$$CN_{(ads)} + 2O^{2-}_{(s)} \longrightarrow CO_{2(g)} + N_{(ads)} + 4e$$

$$CN_{(ads)} + H_2O_{(ads)} + O^{2-}_{(s)} \longrightarrow NH_{2(ads)} + CO_{2(g)} + 2e$$

Pre-hydration on CuO/ Cr_2O_3 did not significantly diminish the capabilities of the surface to form C_2N_2 but this surface also produced small amounts of isocyanic acid. This reaction was also thought to be linked with the copper oxide part of the surface.

Chromia (Cr_2O_3) was inactive for C_2N_2 formation from HCN. Instead, reversible adsorption and oxidation of HCN occurred.

The adsorption of HCN on Al_2O_3, CeO_2 and MgO surfaces results in polymerisation (107-108) and hydrolysis (109-110). CH_3CN also undergoes hydrolysis

on alumina, the acetamido group (CH_3CONH) being produced. On desorption this decomposes to surface carboxylate and $-NH_2$ groups according to the scheme;

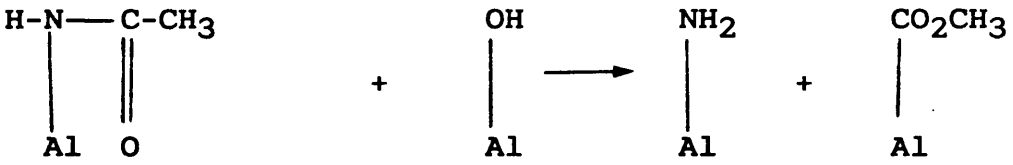

Conversely, the adsorption of acetonitrile on MgO was shown to be a reversible process, presumably because there were insufficient hydroxyl groups for hydrolysis to occur (111). Finally, Mellor (1) reported that the adsorption of HCN on NiO was an irreversible process and it was suggested that the gas was retained as a polymeric species.

1.6.3.2. The Adsorption of Cyano-related Compounds on Silica

Silica is extensively used as a support, so in order to understand the chemistry of the adsorption of cyano-compounds with silica-supported metals and transition metal oxides, it is first necessary to consider the interactions occurring with silica itself.

Ruttenberg and Low (112) used i.r. spectroscopy to investigate the adsorption of C_2N_2 on silica. Morrow and Cody (113) extended this work using isotopic labelling experiments and force constant calculations. The conclusions reached from these studies were that at 298 K

only a slight reaction occurred leading to silyl isocyanate (SiNCO, 2310 cm^{-1}). This reaction intensified at higher temperatures and other bands, due to this species, became visible at 2353, 1470 and 1505 cm^{-1}. These bands were near those observed for silicon isocyanate, $Si(NCO)_4$. The enhancement of the 2310 cm^{-1} bond was accompanied by a decrease in the intensity of the Si-OH band at 3747 cm^{-1}, and furthermore HCN was detected. The following reaction was proposed to account for these features:

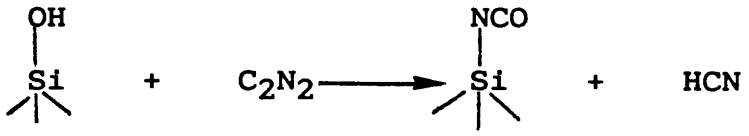

By 773 K silyl cyanide, SiCN (2212 cm^{-1}) and silyl isocyanide, SiNC (2100 cm^{-1}) were also produced. These species probably formed by reaction of C_2N_2 and HCN with siloxane bridges;

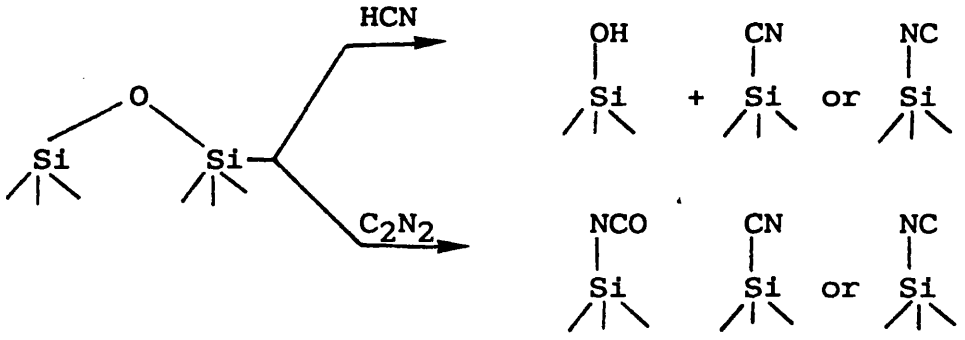

At higher temperatures the SiCN band shifted to 2218 cm^{-1} and a fourth band appeared at 2078-2075 cm^{-1}. This was ascribed to the vibration of the C-C≡N moiety of a precursor to a polymer. Further heating to 1073 K

completed the polymerisation process and new bands appeared at 2185 and 2165 cm^{-1}.

Williams (2) and Davies (4) investigated the adsorption of HCN on silica at 298 K. They assigned bands at 3520, 3330, 3265 and 2100 cm^{-1} to physically adsorbed HCN. Morrow and Cody (113) also studied HCN adsorption but they concluded that no reaction occurred until at least 773 K. After heating to 1073 K, the spectrum at ambient temperature contained bands due to SiNCO, SiCN and SiNC, a pair of bands at 2353 and 2150 cm^{-1} also appeared. They noted that unlike C_2N_2, reaction with HCN did not involve the Si-OH groups. Instead they proposed that reaction occurred with the strained unsymmetrical siloxane bridges. These Lewis acid sites formed during outgassing above 673 K and exhibited bands at 908 and 888 cm^{-1} (114). Heating at 1073 K also produced a series of bands at 3540, 3450 and 1550 cm^{-1}. These were ascribed to surface $SiNH_2$ (115). Williams (2) proposed that a similar feature at 3450cm^{-1} was due to a surface imide species, SiNH. Morrow and Cody (113) noted that SiCN and SiNC were resistant to oxygen treatment at 298 K but that on heating in oxygen at 473 K both species converted to Si-NCO. The resultant intensification of the 2313 cm^{-1} band was accompanied by the appearance of weak overtones at 3070 and 1470 cm^{-1}. If instead of oxygen treatment the SiO_2 was heated in HCN to 1273 K, then the 2313, 2218 and 2100 cm^{-1} bands intensified. When this sample was heated

in oxygen, not only were the SiCN and SiNC species converted to SiNCO but a broad doublet at 2200-2150 cm^{-1} was also observed. On continued heating the 2150 cm^{-1} band intensified and weak features between 3400-3300 and 1600-1370 cm^{-1} appeared. These changes were attributed to the production of a polymeric species containing $-NH_2$ and -C≡N moieties. Morrow and Cody (113) also studied the adsorption of acetonitrile (CH_3CN) on silica. They found that it behaved similarly to HCN except that CH_4 was the main gaseous product.

The adsorption of C_2N_2 on outgassed SiO_2 has also been studied using heat flow calorimetry, volumetry and mass spectrometry (116). At low temperatures, C_2N_2 was hydrogen bonded to the silanol groups and irreversibly adsorbed on the strained siloxane bridges. Reaction with silanol groups to form Si-NCO occurred above 473 K and was complete by 691 K. Above 773 K, C_2N_2 and HCN reacted with ordinary siloxane bridges but at higher temperatures SiNCO decomposed to CO_2, CO and N_2, a significant amount of N atoms being retained on the surface.

Eley et al (117) used i.r. spectroscopy to study the reaction between ethyl isocyanate (EtNCO) and silica surfaces. The products depended upon the temperature of reaction and the pretreatment of the silica. Evacuation of silica to 973 K followed by reaction at 306 K resulted in urethane formation by reaction with the silanol group;

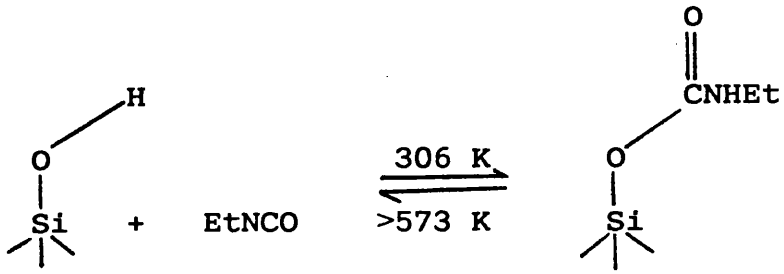

Molecular water adsorbed on silica reacted with ethyl isocyanate at 306 K to give ethylamine (reaction 1). This amine rapidly reacted with another ethyl isocyanate molecule to give 1,3-diethylurea (reaction 2). This product probably formed as a surface deposit.

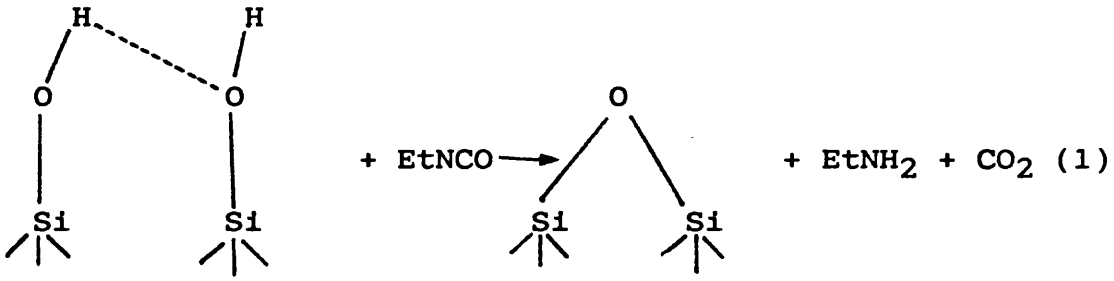

$EtNH_2$ + EtNCO ⟶ EtNH.CO.NHEt (2)

Although no evidence for chemisorptive interaction between diethylurea and the silica surface was found, it was proposed that hydrogen bonding occurred instead. At higher temperatures (673 K), ethyl isocyanate reacted with the siloxane bridges to form a range of products. The major reaction involved dissociative adsorption to yield an intense band at 2308 cm^{-1} due to silyl isocyanate which hydrolysed at 298 K to yield isocyanic acid HNCO.

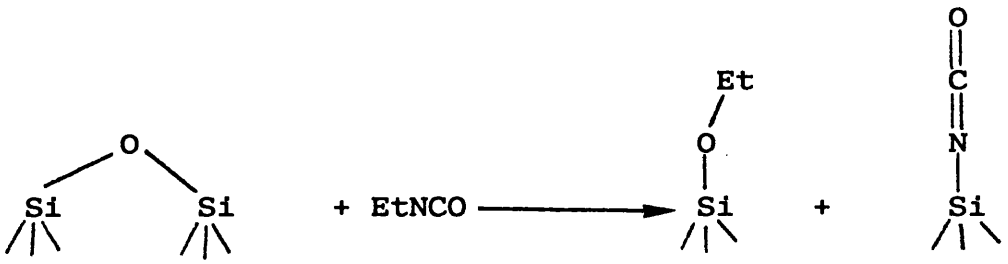

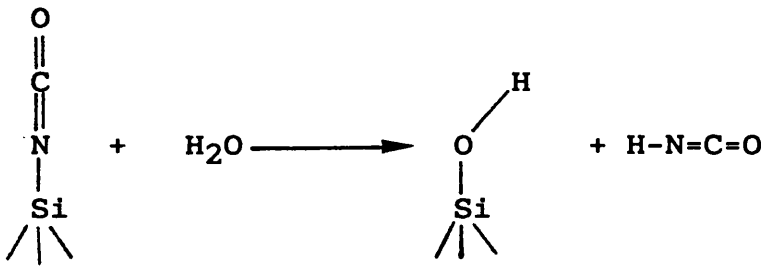

Solymosi et al (118-119) have studied the interaction of gaseous isocyanic acid with SiO_2. At 190 K it is only weakly adsorbed giving two bands at 3500-3400 cm^{-1} and 2265 cm^{-1}. The 2265 cm^{-1} band was assigned to the asymmetric ν_a(NCO) of weakly adsorbed HNCO whereas the 3500-3400 cm^{-1} band was ascribed to the ν(NH) vibration of HNCO. No residual bands were observed after outgassing at 190 K. Adsorption at 300 K gave rise to another band at 2310 cm^{-1} in addition to the bands associated with weakly adsorbed HNCO. This band was resistant to evacuation and was stable to at least 673 K. The intensity of this band, ascribed to SiNCO formation increased at higher adsorption temperatures.

1.6.4 Adsorption of Cyano-compounds on Silica-Supported Metals and Metallic Oxides

1.6.4.1 Adsorption on Silica-Supported Metals

In addition to the work on adsorption of HCN and C_2N_2 on metals reported in Sec.1.6.2, there has been much interest in the adsorption of polycrystalline dispersed metals supported on silica, since in this form they are amenable to study by i.r. spectroscopy.

Williams (2) studied the adsorption of HCN on silica-supported copper using i.r. spectroscopy and gravimetry. He found that although the HCN was desorbed intact at elevated temperatures, no chemisorbed HCN or CN bands were evident after evacuation at room temperature. He suggested that the molecule was adsorbed parallel to the surface as shown below and concluded that at room temperature adsorbed HCN molecules were H-bonded to one-another and to the silica surface.

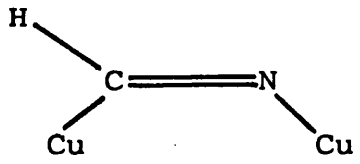

Mueller-Litz and Hobert (120) reported on the adsorption of HCN, C_2N_2 and BrCN on silica-supported Ni and Ir. All three gases were chemisorbed giving two types of adsorbed species, those associated with the silica support and those with the metal. The following i.r. bands were assigned:-

Wavenumber range	structure
2350 - 2250 cm^{-1}	Si- O-C≡N or M-O-C≡N
2250 - 2170 cm^{-1}	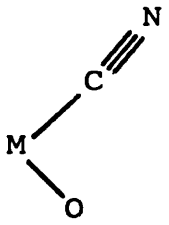 or 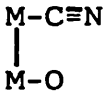
2170 - 2100 cm^{-1}	M-C≡N
2100 - 2000 cm^{-1}	$M^{\delta-}$—C≡N

(where M = Ni or Ir)

These results show that when the adsorbing site has a high electron density, then weaker C≡N bonds occur. This effect is caused by back donation of electrons from electron-dense sites to the CN antibonding orbitals.

The adsorption of HCN on silica-supported Rh, Pd and Ag was studied by Dunken and Hobert (121). They found that HCN adsorbed dissociatively giving rise to i.r. bands at 2160, 2080, 2175 and at 2170 cm^{-1} respectively.

Solymosi and Bánsági (118) and others (119) studied the interaction of HNCO with pure silica and with silica-supported platinum. This work formed part of a wider investigation into the chemistry of adsorbed isocyanates which, as already indicated, are intermediates in the catalytic conversion of NO and CO to NH_3 and HCN in

automobile exhaust catalysts. HNCO was found to be weakly adsorbed onto pure silica at 298 K but admission of HNCO to 5% Pt/SiO_2 gave rise to an intense i.r. band at 2180 cm^{-1}, even at 190 K. It was proposed that Pt promoted the dissociative chemisorption of HNCO into H_{ads} and NCO_{ads}, and the 2180 cm^{-1} band was ascribed to the Pt-NCO species. On raising the temperature to 223 K, a new band appeared at 2310 cm^{-1} whilst the Pt-NCO band diminished. This was explained by the formation of Si-NCO which occurred due to the migration of the isocyanate species from the Pt onto the silica support. At 323 K, in addition to the development of the Si-NCO band, a shoulder developed near 2030 cm^{-1}. This was ascribed to the formation of Pt-CO according to the reaction:-

$$Pt\text{-}NCO + Pt \rightleftharpoons Pt\text{-}N + Pt\text{-}CO$$

The presence of chemisorbed oxygen greatly enhanced the stability of NCO on Pt and the extent of migration onto the silica.

1.6.4.2 Adsorption onto Silica-Supported Metal Oxides

The adsorption of cyano-compounds onto silica-supported metal oxides has been investigated mainly by workers from this laboratory (2,4). As with the metals, by supporting transition metal oxides on silica, i.r. spectroscopic studies of otherwise poorly transmitting samples can be carried out.

Davies (4) studied the interaction of HCN with silica-supported Cr_2O_3 and CrO_3. On these surfaces HCN was converted at room temperature to a surface amide which exhibits an i.r. band at 1670 cm^{-1}. On desorption the band disappeared as the amide decomposed first to surface carbonate and NH_x species and then to CO_2 and N_2. Davies also adsorbed C_2N_2 onto a CrO_3/SiO_2 sample and recovered gaseous HCN, implying that C_2N_2 was dissociatively adsorbed. The conversion of C_2N_2 to a surface amide species also led Davies to conclude that silanol groups were active since there was no other source of hydrogen atoms. In addition to amide formation a desorbable diamide product was recovered from $Cr(VI)/SiO_2$ which had been contacted with either HCN or C_2N_2. The diamide can either be formed by hydrolysis of adsorbed C_2N_2 itself or by hydrolysis of adsorbed cyano species to yield surface amides which combine in pairs before being desorbed.

The adsorption of organic nitriles onto silica-supported chromia has already been discussed (section 1.3.2).

Williams (2) studied the interaction of HCN with silica-supported oxided copper and copper oxide. Three $\nu(C\equiv N)$ i.r. bands were observed with the oxided surface. One at 2100 cm^{-1} was ascribed to physically adsorbed HCN, which was removed by evacuation at room temperature. The other two bands at 2140 and 2180 cm^{-1} were assigned to the following chemisorbed species:-

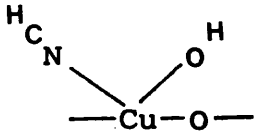

(I)

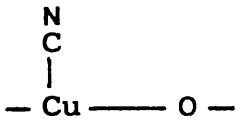

(II)

Williams noted that on heating the 2140 cm^{-1} band (due to species (I)) diminished whilst that at 2180 cm^{-1} increased in intensity. He explained this by suggesting that species (I) became dehydrated to species (II). Further heating caused two new bands to appear at 2300 and 2220 cm^{-1}. The 2300 cm^{-1} band was assigned to SiNCO whilst the band at 2220 cm^{-1} was attributed to both SiCN and CuNCO. Williams suggested that copper isocyanate was produced by the reaction of a type (II) species with an adjacent hydroxyl group or oxygen atom. At still higher outgassing temperatures surface hydrides were formed and NH_3 was released to the gas phase. Isocyanic acid was thought to be an intermediate in these latter reactions.

The adsorption of HCN onto silica-supported cupric oxide gave rise to two i.r. bands at 2100 and 2160 cm^{-1}. The former band was again attributed to physically adsorbed HCN whilst the 2160 cm^{-1} band was assigned to species (III) below:-

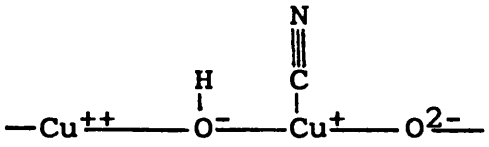

(III)

As expected from the work with CuO already reported, HCN adsorption on CuO/SiO_2 oxide resulted in the release of C_2N_2 to the gas phase. This was explained by the reaction of $(CN)_{ads}$ with gaseous HCN as described in Sec. 1.6.1. Reaction with HCN at higher temperatures produced isocyanate species giving bands at 2220 and 2300 cm^{-1}. Under these conditions, the appearance of a new band at 3450 cm^{-1} and the simultaneous decrease of the 2300 cm^{-1} band occurred. This was explained by the conversion silyl isocyanate to a surface imide. The reaction was accompanied by the release of CO_2:-

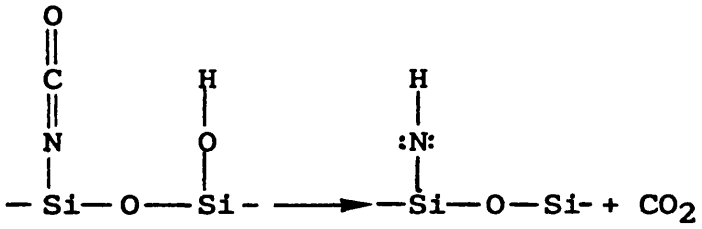

The interaction of HCN with Cu^{n+}/SiO_2 and Cr^{m+}/SiO_2 samples was compared with that of the mixed oxide Cu^{n+} - Cr^{m+}/SiO_2 system by Davies (4). He reported that the oxidation of HCN on $CuO\text{-}Cr_2O_3/SiO_2$ surface occurred separately on the two supported oxides. Reaction occurred via cyanide and isocyanide species on the copper sites and via surface amide intermediates on the chromium parts of the surface. He also identified some areas in which HCN reacted differently with the mixed oxide than with the separate oxides.

One difference concerned the appearance of a copper cyanide band at 2150 cm^{-1} over the reduced mixed oxide.

This result was in contrast to earlier work (2) which showed that the 2150 cm^{-1} band appeared when HCN was adsorbed onto outgassed CuO/SiO_2 but that it was not seen when the gas was contacted with a reduced CuO/SiO_2 sample. It was evident that in the case of the reduced mixed oxide the copper was either stabilised in the mono or divalent state or that it was reoxidised to one of the states prior to HCN contact. Davies explained this result by referring to the work of Borello et al (8) in which Cr_2O_3/SiO_2 sample produced by the decomposition of chromium nitrate took four reduction cycles to remove traces of excess oxygen. Davies suggested that it was the oxygen derived from the chromia part of the surface which was stabilising or re-oxidising the copper sites, enabling them to react with HCN to form a copper cyanide species.

Another difference with the silica-supported mixed oxide was revealed when the HCN-dosed sample was heated above 450 K. Under these conditions a species exhibiting a broad band centred near 2000 cm^{-1} developed on the mixed oxide. No such band was seen on chromia alone or on copper oxide. However, Surman (3) also saw a similar band on chromia-supported copper oxide. Davies postulated that this band was either due to the formation of a surface nitrosyl (-NO) species or less likely that a bridging cyanide was formed of the type:-

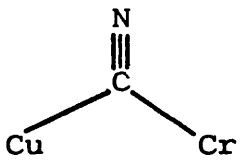

Finally, Davies noted a significant difference on adsorbing HCN onto silica-supported Cu(II)-Cr(VI) system as opposed to the separate oxides. This was that although the total absorptive capacity towards HCN was unchanged, the conversion to C_2N_2 was much less than one would have expected for a surface containing Cu^{2+} ions. He suggested that two mechanisms contributed towards this behaviour, namely; (1) C_2N_2 formation occurred on the copper sites, then instead of being desorbed it became re-adsorbed onto the Cr^{6+} ions and (2) unlike on unsupported $CuO-Cr_2O_3$ samples, in the case of the silica-supported sample CuO was not fully dispersed and hence was not all accessible to the HCN.

1.7 Aspects of the Chemistry of Cyanogen and Related Compounds

Cyanogen, N≡C-C≡N, is a colourless, volatile, poisonous compound which exists as a gas at ambient temperature (m.pt. 245 K, b.pt. 252 K). Like HCN it is a linear molecule, but the C-C bond has a much higher bond energy than the H-C bond of HCN. This influences its reactivity as an oxidative addition reagent in the sense that it only reacts with electronically dense metal centres yielding particularly strong metal(II)-cyanide bonds. The high dissociation energy of the C-C bond and short C-C bond distance (1.37± 0.02 Å , compared to 1.40 Å for a pure C-C single bond) suggests that the electronic structure usually only thought of in terms of structure I, actually has a contribution from the C-C double bonded species II.

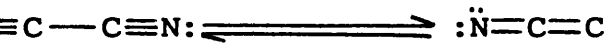

I II

Cyanogen can be obtained by direct oxidation of HCN in the gas phase by air over a silver catalyst, by chlorine over activated carbon or silica, or from the cyanide ion by aqueous oxidation using Cu^{2+}:-

$$Cu^{2+} + 2CN^- \longrightarrow CuCN + {}^1/_2C_2N_2$$

The preparation of dry C_2N_2 is best achieved by the reaction:-

$$Hg(CN)_2 + HgCl_2 \longrightarrow Hg_2Cl_2 + C_2N_2$$

Reimenschneider (122) reported that C_2N_2 can be produced by linking two HCN molecules by a simple oxidation

process involving gaseous oxygen. The reaction was homogeneously catalysed by a solution of copper nitrate in aqueous acetonitrile. Under suitable conditions the C_2N_2 produced could be hydrolysed through to oxamide:-

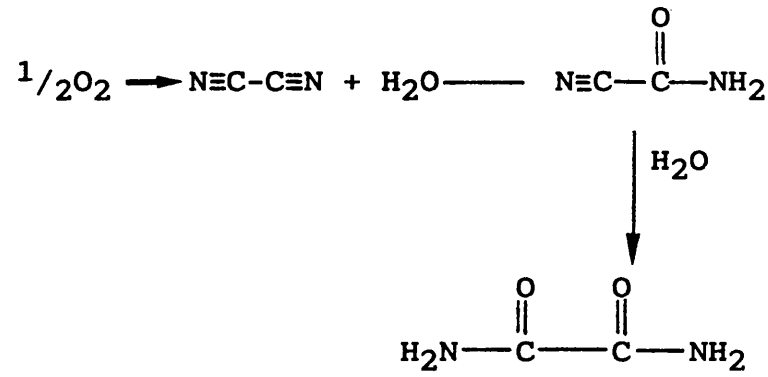

oxamide

Although only tentative comparisons can be made between the co-ordination chemistry and surface chemistry of cyanogen, it is interesting to consider some aspects of these studies in conjunction with the present work. Many co-ordination compounds of C_2N_2 have been reported in the literature (123). Spectroscopic studies have shown that C_2N_2 can act both as a terminally bonded ligand, preferably with end-on co-ordination, type (a), or as a bihapto, ligand types (b) and (c).

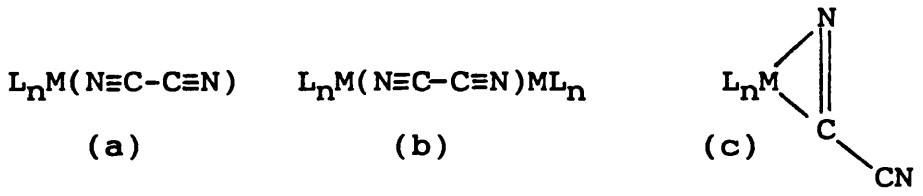

Type (a) compounds exhibit two $\nu_{C\equiv N}$ bands (e.g. $RhCl(PPh_3)_2(C_2N_2)$ has bands at 2240 and 2090 cm^{-1})(124),

whilst types (b) and (c) exhibit only one band (e.g. $[Cu(CN)(H_2O)(C_2N_2)]_n$, $\nu_{C\equiv N}$ = 2160 cm^{-1}) (125).

The spectrum of $[Cu(CN)_2(C_2N_2)]^-$ also exhibits two $\nu_{C\equiv N}$ bands even though it contains cyanogen only as a bridging ligand (126). This was explained since the structure also contained terminal cyanide linkages.

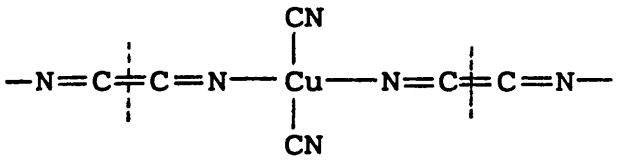

Although no "side-on" C_2N_2 co-ordination has been observed there is no reason why this mode of attachment should not exist.

Various products can be recovered from the hydrolysis of cyanogen-containing complexes in solution. Co-ordinated cyanogen in $[CuI(CN)(H_2O)(C_2N_2)]$ has been hydrolysed to yield glycine (125), a process best described by the following stoichiometry:

$$3NCCN + 6H_2O \longrightarrow H_2NCH_2COOH + 4HNCO + NH_3$$

Cyanogen in the complex $[RuII(NH_3)_5\text{-}C_2N_2\text{-}RuII(NH_3)_5]^{4+}$ has been hydrolysed to various amides, whilst the metal was irreversibly oxidised by water to ruthenium(III) (127). Other hydrolysis reactions of co-ordinated cyanogen have been reported (128). These have been described according to the equations:-

$$NCCN + 4H_2O \longrightarrow (COOH)_2 + 2NH_3$$

$$NCCN + H_2O \longrightarrow HCN + HNCO$$

It is evident from these examples that the hydrolysis pathway is influenced by the metal to which C_2N_2 is co-

ordinated. A range of reactions is also expected on hydrolysis of C_2N_2 over solid surfaces.

C_2N_2 can be regarded as a pseudo halogen. This is exemplified by its disproportionation in basic solution:

$$C_2N_2 + 2OH^- \longrightarrow CN^- + OCN^- + H_2O$$

Also whilst C_2N_2 can act as a ligand towards metal centres it can also dissociate into CN radicals allowing it to oxidatively add to lower valent metal atoms (e.g. Ni(0),Pd(0),Pt(0),Rh(I) giving dicyano complexes. This process has been reported with zerovalent nickel complexes of the type NiL_4 (129,130).

$$NCCN + NiL_4 \longrightarrow [NiL_3(CN)_2] + L$$

The mechanism of these reactions first involves an active "end-on" cyanogen intermediate complex ($L_3M{\leftarrow}N{\equiv}C{-}C{\equiv}N$), which then isomerises to a "side-on", π-bonded species

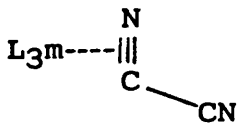

in which electron transfer to C_2N_2 occurs causing dissociation. The oxidative addition of C_2N_2 has also been illustrated in the reaction with biscyclopentadienyl compounds $(\eta\text{-}C_5H_5)_2Cr$ to yield $[(\eta\text{-}C_5H_5)_2Cr(CN)_2]$ (131).

Cyanogen also acts as an electrophile towards metal co-ordinated ligands; this process has significant catalytic implications. Thus for example C_2N_2 can react as follows (123):-

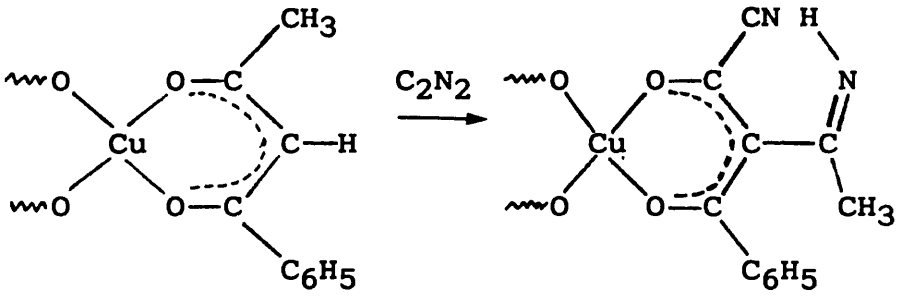

Since C_2N_2 is one of the most active nitriles, it usually undergoes reaction with transformation of both C≡N groups. It is not surprising that special moderating conditions are necessary to induce the reaction of only one cyano group. Welcher et al (132) reported conditions which limited the hydration of C_2N_2 to give a high yield of 1-cyanoformamide ($N{\equiv}CCO.NH_2$). Chemically, this product was very reactive undergoing either addition reactions across the CN bond or C-C bond cleavage reactions. Under acidic conditions it was quickly hydrated to oxamide. Addition reactions with alcohols and hydrogen sulphide have also been reported. Cleavage of the C-C bond occurred during hydrolysis in basic solution (a) and by reaction with amines (b).

(a) $NCCO.NH_2 + H_2O \longrightarrow HCN + CO_2 + NH_3$

(b) $NCCO.NH_2 + RNH_2 \longrightarrow H_2NCO.NHR + HCN$

Vibrational analyses of oxamide and of oxamido complexes have also been investigated (133-135). These have shown that oxamide usually acts as a bidentate ligand co-ordinating to the metal ion through both nitrogen atoms, both oxygen atoms or one nitrogen and one oxygen atom. The structure of the bis(oxamido) complexes of Cu(II) and Ni(II) was shown to be square planar:-

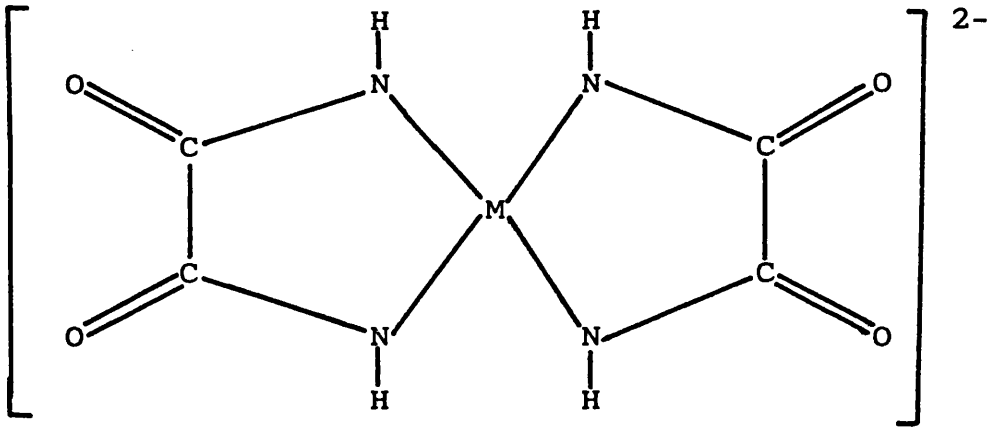

(where M=Cu or Ni)

The copper compound was hydrolysed in water and was less stable than the corresponding Ni(II) complex due to weaker metal-nitrogen linkages.

1.8 Aims of the Present Work

As already indicated, copper and chromium ions have long been known to be an active combination for the uptake and conversion of HCN to non-toxic products. Moreover, previous workers have shown that cyanogen is released when HCN is reacted over samples containing copper(II). However, very little work had been done on C_2N_2 surface chemistry on oxides. The main aim of this work was therefore to investigate further the reactions of cyanogen with oxide surfaces, particularly copper and chromium oxide. A second aim was to exploit i.r. spectroscopy, since it had already proved very valuable in previous HCN studies. Accordingly the oxides of copper and chromium have been studied in silica-supported form. It was considered particularly significant to examine the effect of the oxidation states of the metals

on the fate of the adsorbed C_2N_2 and to determine whether the presence of both metal ions influenced the reactivity relative to the pure oxides. Finally, by varying the pretreatment of the copper-chromium oxide, it was thought important to investigate the role of adsorbed moisture and oxygen on the reactivity of the oxides towards cyanogen.

2. EXPERIMENTAL

2.1. The Vacuum System

The results described in this Thesis were recorded on two purpose-built vacuum frames. One, described below, was designed for mass spectrometric and gravimetric studies, while the other was used for infra-red spectroscopic work (Sec. 2.4.2). Both frames were constructed from Pyrex glass and were capable of operating at pressures below 3×10^{-6} torr.

The gravimetric frame (Fig. 2.1) contained a gas preparation section which enabled evacuation, pressure measurement, gas storage and gas handling procedures to be carried out. This part of the frame contained conventional taps sealed with Apiezon N grease. The remainder of the frame consisted of an adsorption system. This comprised a vacuum microbalance and sample outlets for gas analysis. To prevent sample contamination by either mercury or grease, this portion of the frame was controlled with Young's greaseless taps sealed with Teflon or Viton O-rings.

The system was evacuated using a single-stage, water-cooled mercury diffusion pump backed by an oil-filled rotary pump. Exhaust gases were vented from the rotary pump to the laboratory extraction system via a charcoal bed which removed toxic waste gases. The hot mercury in the diffusion pump was protected from oxidising vapours by an in-line cold trap CT1. The low

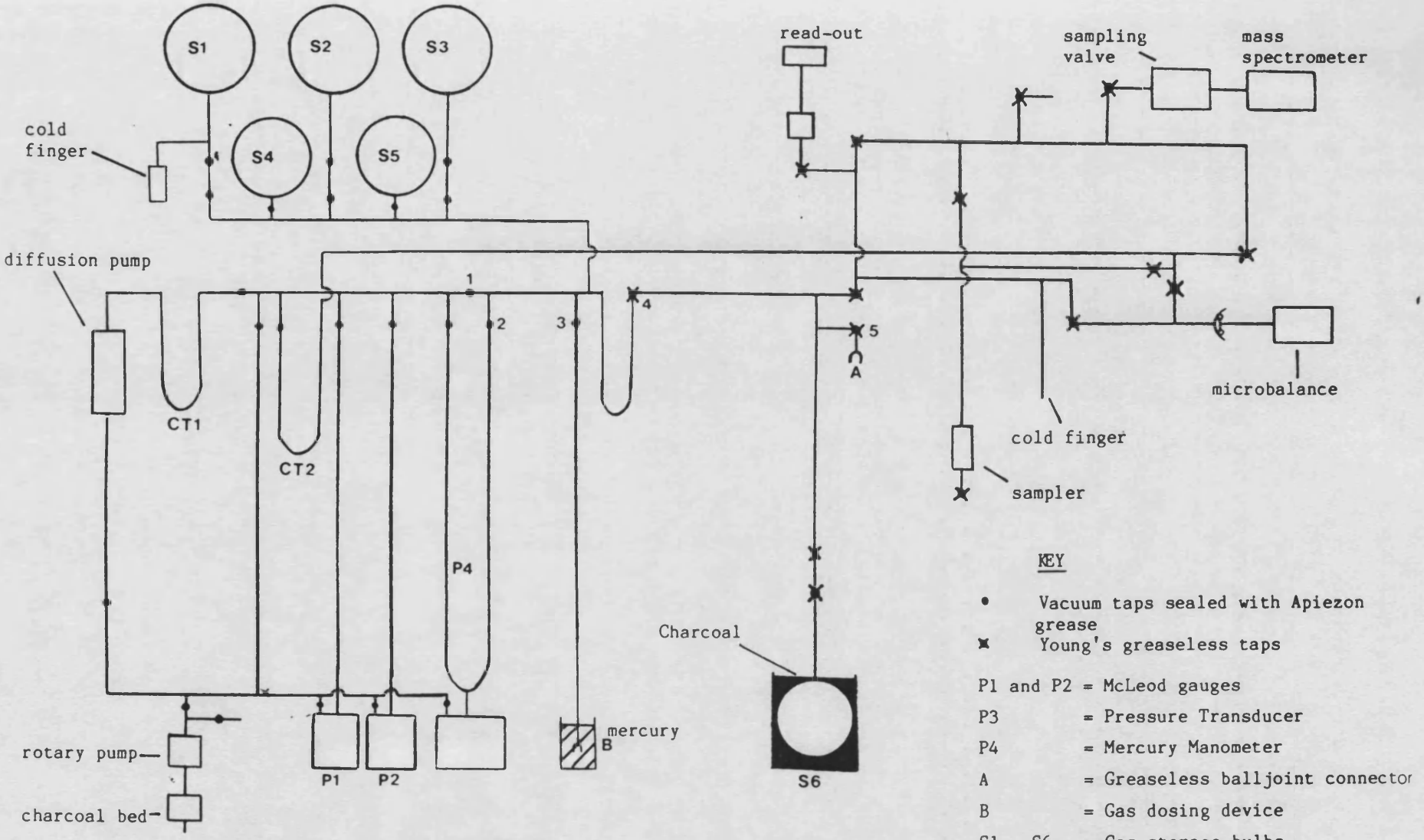

Fig. 2.1 The Vacuum Frame

pressures within the system, encountered during evacuation and sample outgassing, were measured using two McLeod gauges, P1 and P2. These had ranges from 10^{-1} to 10^{-4} and 10^{-3} to 10^{-6} torr, respectively. Higher pressures, met during adsorption studies, were measured using a low range pressure transducer, P3, (supplied by CEC Instrumentation Ltd, Type BHL 4104). This covered the pressure range 10^{-2} to 56 torr and a digital readout was given on a BHL-1420 transducer indicator. This instrument was calibrated with nitrogen gas against a mercury manometer P4 which was read using a cathetometer. The higher pressures encountered during BET surface area determinations were measured using the mercury manometer. A greaseless balljoint connector, A, was used for connecting the HCN generating apparatus (described in Sec. 2.6) to the frame. This joint was also used for dosing cyanogen and water vapour into the system. Other gases, for example N_2 and O_2, were admitted to the frame through an inverted inter funnel B. This was submerged in mercury to prevent air from entering the system. Gas from a high pressure cylinder was dosed with this gas admitter via a length of rubber hose fitted with a glass u-bend which was hooked under the funnel. These gases are stored in the 2000 cm^3 glass bulbs S1-S3 and in 250 cm^3 bulbs S4,S5. C_2N_2 or HCN were stored in a 1000 cm^3 bulb, S6. This was immersed in sufficient charcoal to adsorb the toxic gas in case of breakage.

Since adsorption was measured gravimetrically, it was not essential to know the volume of the adsorption system. However, it was necessary to quantify the amounts of gases released during desorption studies. This was done be relating the composition of the gas phase to its pressure and volume. The volume of certain parts of the adsorption system were measured by attaching a small glass bulb of known volume V_1 (ca 50 cm^3) to the balljoint connector, A. The bulb was filled with nitrogen to a recorded pressure P1 and sealed. The frame was then evacuated before expanding the contents of the bulb into the volume V_2 to be determined. By measuring the resultant pressure P_2 within the chosen section of the frame, the volume V_2 was calculated since ($V_2 = P_1V_1/p_2$). Using this method the volume enclosed between the taps 1,2,3 and 4 (with the storage vessels S1-S5 sealed off) was found to be 201.04 cm^3. The volume of the adsorption system, including the balance case, was about 870 cm^3.

The vacuum system was contained in a purpose-built cabinet described by Surman (3). The microbalance and the mass spectrometer sampling value are described later (Sec. 2.2 and 2.3.2 respectively).

2.2 The Microbalance

The microbalance (Fig. 2.2) was a standard C.I. Electronics Mk 11 balance contained in a Pyrex vacuum jacket. It was connected to the vacuum frame via a

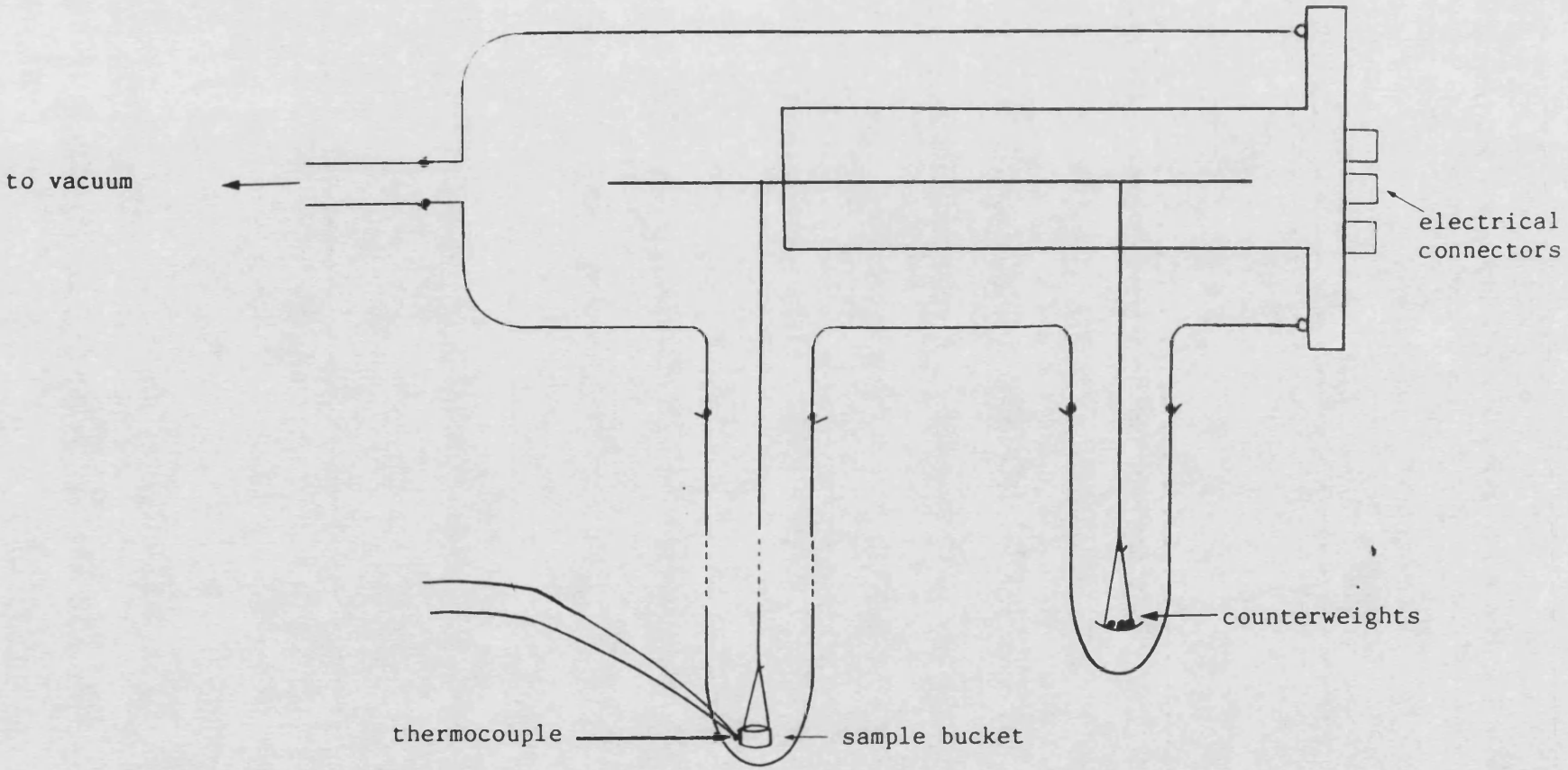

FIg. 2.2 The Microbalance

greaseless joint sealed with a Viton O-ring. Electrical connections were plugged into a metal end-plate which was sealed into the jacket with another O-ring. The head was protected from vibration, caused by the rotary pump, by supporting it in foam rubber-padded clamps.

The balance operated by generating a current directly proportioned to the weight of the sample. This provided an electrical output to a pen recorder. The current was generated when the microbalance arm moved, since it carried an aperture which permitted light from an internal source to impinge on a pair of photocells. Movement of the arm caused a change in the relative illumination of these cells causing an excess current to flow across an electrical bridge. When amplified this current restored the beam to its equilibrium position. The balance head was contained in a black cardboard sleeve; this protected the photocells from exposure to external light thus preventing signal interference. Furthermore, the balance head was protected from the excessive heat generated in the region of the sample by using a long (35 cm) suspension fibre, made of silica, for the sample bucket. Nevertheless, thermal effects were noticed during this work; however, the errors were minimised by applying small correction factors obtained from reference experiments.

The maximum load which could be supported by the microbalance was 1 gramme. The weight of the sample bucket plus the silica suspension fibre was therefore

kept to a minimum. This was done by making the bucket from silica and in this way the combined weight of the suspension and bucket was less than 400 mg. The sample bucket was contained in a silica hang-down tube connected to the microbalance case using a greaseless joint sealed with a Teflon O-ring. The temperature of the sample was measured using a chromel-alumel thermocouple whose junction was adjacent to the sample bucket. The thermocouple was held in place by securing it to the inner wall of the hang-down tube. To ensure that the balance operates with maximum sensitivity, counterweights were added to the opposite side of the balance arm. These weights were held in a light aluminium tray. This was supported by a short silica fibre and was contained in a Pyrex hang-down tube.

The microbalance was capable of measuring weight changes in the range 25 μg - 100 mg, over five sensitivity ranges. The output from the balance was plotted as a function of time on a Gould Bryans flat bed chart recorder (series 270). Calibration of the balance was a two-step process. The 1-100 mg range was set by adding known weights to the sample arm and adjusting the controls until an accurate readout was displayed. The 25 g to 1 mg ranges were set by using the balance controls to read a small weight on a previously calibrated scale. Then by switching to the next most sensitive range the electrical tare was adjusted to give the correct display. Counterweights were always chosen

to be as near to the weight of the sample as was possible. This ensured that the balance controls could be used to maintain positive readings when samples lost weight (e.g. during outgassing) or to back-off weight increases to keep the reading on the most sensitive scale possible.

2.3. Mass Spectrometry

Mass spectrometry is used to analyse gaseous, solid or liquid components by causing molecules to fragment into a set of ions. A mass spectrum shows the mass-to-charge (m/z) ratio of the ions formed versus their relative intensities. All mass spectrometers consist of three basic sections: (a) an ion source which converts the sample into gaseous ions and focuses them into an ion beam, (b) a mass filter which resolves these ions by differentiating between their different mass-to-charge ratios and (c) an ion collector which measures the intensity of each ion present.

The ion source operates by producing electrons from a heated filament by thermionic emission. These electrons are then accelerated across the ionisation chamber where they bombard neutral 'target' atoms or molecules. This causes ionisation and fragmentation, the extent of which depends on the energy of the incident electrons and on the structure of the molecule being analysed. Normally only one electron is removed from the 'target' species giving parent and fragment ions with

integral m/z values. It is also possible that two electrons are removed from the 'target', in this case doubly charged ions are formed. These give non-integral m/z values, a typical example being the HCN molecule which loses two electrons giving HCN^{2+} whose m/z value is 13.5. Complex molecules also undergo complex fragmentation processes which can involve internal molecular re-arrangements. The positive ions formed are focused into an ion beam using an electrical lens. The beam then passes into the mass filter.

Two common types of mass filter exist. The classical magnetic analyser, operates by applying a magnetic field perpendicular to the direction of travel of the ions. This causes the ion beam to bend and focus onto the detector. The other analyser, the quadrupole mass filter, consists of four stainless steel rods aligned parallel to one another. Opposite pairs of rods are joined electrically and each pair is supplied by a combination of rf and dc voltages. The phase of the rf potential and the sign of the dc potential is opposite for the two pairs of rods. When ions enter the changing electrical field, they oscillate and only those with particular m/z values are able to pass through the filter without becoming unstable and colliding with the rods or filter housing. The spectrum is produced by scanning the rf and dc voltages and recording the transmitted current as a function of these parameters. The ion collector is usually a Faraday cup which can be linked to an electron

multiplier to give a large measurable output current to feed a recorder.

The mass spectrum of a molecule (known as the cracking pattern) is reproducible when recorded under identical conditions. It is therefore possible to use this method to give qualitative results. Indeed, by comparison with standard reference tables (136) unknown compounds can be identified. Also, since the intensity of the cracking pattern is related to the amount of material being analysed, mass spectrometry can also be used as a quantitative tool.

Mass spectra of multi-component mixtures consist of a series of cracking patterns superimposed on one another. In the present, work mass spectrometry has been used to analyse the composition of gas mixtures both qualitatively and quantitatively. Details of the theoretical and practical considerations used to solve mass spectra are described in Chapter 3.

2.3.1. The Mass Spectrometers

The mass spectrometer used in the early part of this work was a magnetic analyser design (A.E.I. Ltd. type MS10). The instrument recorded spectra in the mass range 12-45 and 36-200 by varying the accelerating voltage from 40-200 V d.c. The following source parameters were used: trap current 50 μA, electron voltage 70 V, ion repeller voltage 1 V. The analyser chamber was evacuated to a pressure of 3×10^{-6} torr or less using a single stage oil

diffusion pump and a liquid nitrogen trap backed by an oil rotary pump. It was essential to maintain this low pressure during the operation of the spectrometer to prevent rapid deterioration of the electron source (a heated filament). Another reason for the high vacuum was to minimise the intensity of the background spectrum, thereby enabling accurate measurements of unknown spectra to be made. The background spectrum was reduced still further by baking the analyser chamber under high vacuum at 600 K for 12 hours. The intensity of the resultant background spectrum, which contained small peaks due to atmospheric contamination (mainly N_2, O_2 and H_2O) plus traces of diffusion pump oil, was less than 1% of the full scale deflection on the least sensitive of the seven amplification ranges. The MS10 allowed peak resolution up to m/z values of 70, which covered the whole range required in this research.

In the latter half of the work mass spectrometry studies were carried out using a Masstorr FX spectrometer (supplied by VG gas Analysis Ltd). The Masstorr was a small but powerful quadrupole mass spectrometer having both high sensitivity and good resolution over the entire 0-100 atomic mass unit (amu) range. The ion source contained an electrically heated thoriated iridium filament. The electrons produced were accelerated through a potential difference of 65 V and the ion repeller voltage on the source cage was set at 4 V.

The Masstorr chamber was pumped down to 10^{-8} torr using a two-stage rotary pump (Edwards High Vacuum, type BS 2208) and down to better than 10^{-8} torr using a turbomolecular pump (Leybold-Heraeus GmbH, model Turbovac 150). The pressure in the analyser chamber was monitored using a Penning gauge head (Edwards High Vacuum, type 1102 Penning Controller), which covered the range 10^{-2} to 10^{-8} torr. The Masstorr spectrometer was equipped with a digital readout which operated in three modes, namely PARTIAL PRESSURE, TOTAL PRESSURE and LEAK DETECT. The PARTIAL PRESSURE mode was used to measure the intensity of individual atomic mass units (amu). The TOTAL PRESSURE mode gave the total system pressure and the LEAK DETECT mode was used to detect amu 4 (i.e. for helium leak detection). The instrument had nine sensitivity ranges from 10^{-3} to 10^{-11} mbar. All spectra were recorded on at least three different ranges (usually 10^{-6}, 10^{-7} and 10^{-8}), thus enabling the intensities of weak peaks to be accurately determined. The output from the Masstorr was connected to a flat bed chart recorder (Gould Bryans series BS 270 yt recorder) set at 10 V F.S.D. Two scan speeds, 0.1 and 1.0 amu's per second were available when recording on this instrument. Faster scan speeds, upto 100 amu's per second, were possible when the Masstorr was connected to an oscilloscope. A typical background spectrum measured using the Masstorr spectrometer is shown in Fig.2.3; the notable difference between it and background spectra

recorded using the MS10 spectrometer was the reduced intensity of peaks due to oil contamination.

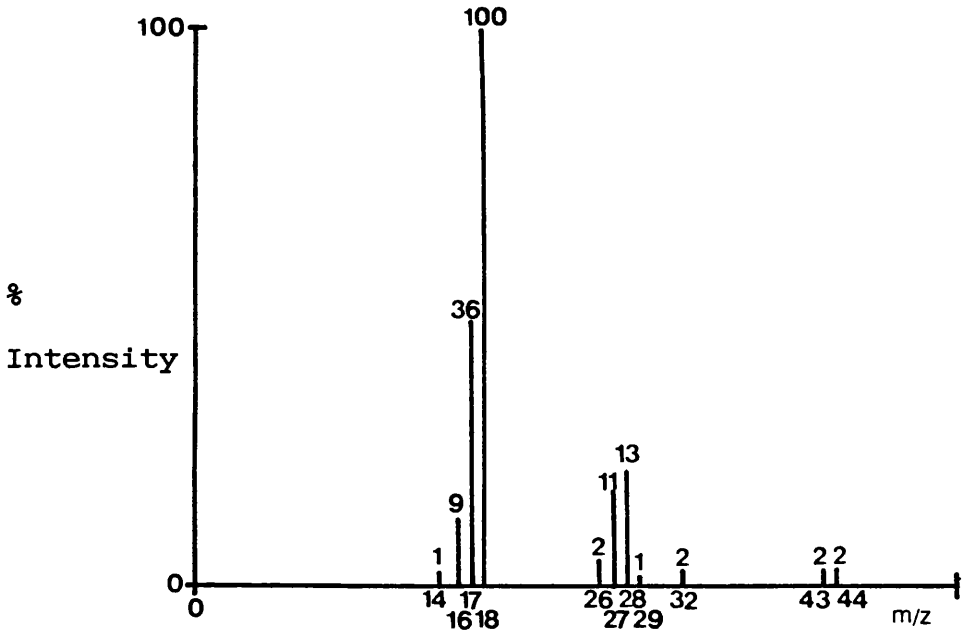

Fig.2.3. Typical Background Mass Spectrum Recorded on the Masstorr FX Spectrometer.

2.3.2. Sample Inlet Systems

To analyse the composition of gas mixtures contained in the vacuum frame using mass spectrometry, it was necessary to transfer sufficient of the sample into the analyser chamber to give a strong spectrum. Care was taken not to transfer too much sample since this could over-pressurise the chamber causing filament damage. Since the spectrometer was continuously pumped, it was necessary to have a continuous sample leak to give a steady dynamic state. Steady conditions were achieved by ensuring that the composition and pressure of the sample in the frame remained near constant and by

minimising the rate of transfer from the frame into the spectrometer.

Two sampling valves were used in this work; one was employed to admit gas into the MS10 spectrometer, the other to leak samples into the VG Masstorr instrument. The MS10 sampling valve, shown in Fig.2.4, consisted of a hairline fracture on the outer surface of a Pyrex tube. This fracture could be raised or lowered inside a second tube, using a Young's greaseless tap. A Viton O-ring seal was fixed into position within the outer tube such that when the fracture was raised completely above the seal the leakage of gas was prevented. On screwing the tap down, the fracture straddled the O-ring: this allowed a restricted amount of gas to flow past the ring. The leak valve was joined to the spectrometer via a 75 cm long stainless steel tube. Since sample mixtures often contained high boiling point compounds (e.g. H_2O and HCN), precautions were taken to prevent them from condensing or adsorbing onto the walls of this tube. Thus it was maintained at approximately 400 K by enclosing it in a heating tape.

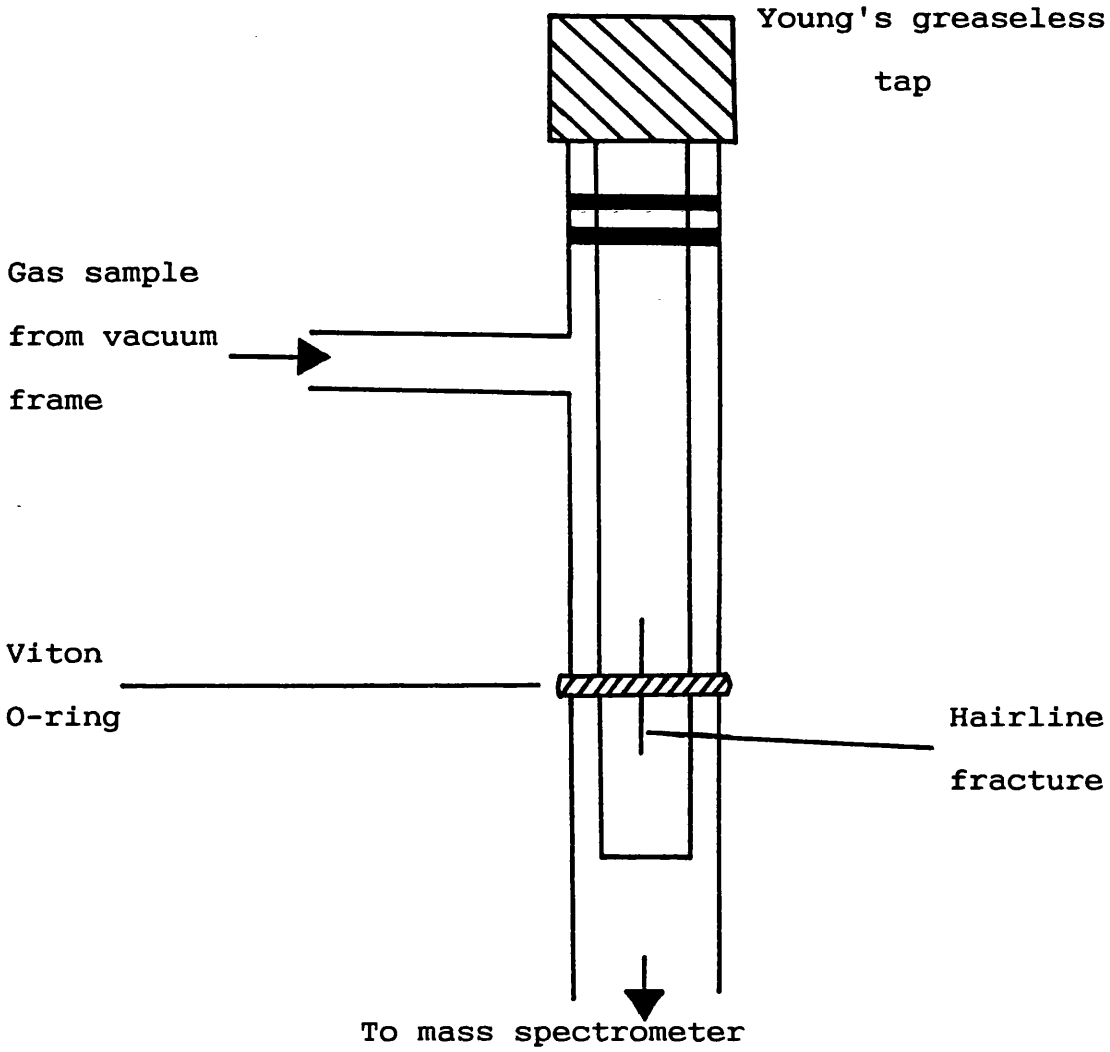

Fig.2.4. The MS10 Leak Valve

Sampling to the VG Masstorr spectrometer was via a high precision leak valve (VG Ltd., type MD7). The operating principle of this valve was that a gap between the edge of a stainless steel knife edge and a soft metal pad could be finely adjusted. The MD7 valve was chosen for its high sensitivity and reproducibity. Leak rates

were adjustable in the range 10^{-11} to 10^{-6} mbar ls^{-1}. Adjustments were made by turning a micrometer-type control knob until the desired leak rate was obtained, as shown by a Penning gauge mounted on the mass spectrometer. The leak rate was reproducible when the valve was opened to the same setting. Since the valve was constructed from stainless steels and oxidation resistant alloys, it was heated to prevent condensation or adsorption of high boiling point compounds.

2.3.3. Mass Spectra of Gas Phase Components

The mass spectrum of a multi-component mixture is assumed to be the summation of the cracking patterns of the individual components. To solve these spectra, it is necessary to measure the cracking pattern of each pure component and to record the background spectrum.

The background spectrum recorded with the VG Masstorr FX spectrometer contained peaks due to H_2O (m/z 18, 17 and 16), O_2 (m/z 32 and 16), N_2 (m/z 28 and 14), CO_2 (m/z 44) and pump oil (m/z 43, 27, 26) (see Fig.2.3). The intensity of these bands was decreased during gas mixture analysis since the higher analyser chamber pressures which occur during sampling tend to reduce desorption from the chamber walls.

The mass spectra of some compounds varied slightly with chamber pressure, and hence, all spectra (both of pure components and of gas mixtures) were measured at similar pressures. Mass spectra of pure samples of C_2N_2, HCN, HNCO, CO_2, O_2, H_2O, NH_3 and N_2 recorded using the

MS10 and Masstorr spectrometers are shown in Tables 2.1 and 2.2 respectively. These values were used to solve the spectra of gas mixtures using a method described later (Sec. 3.1.3). The mass spectral results of C_2N_2

Table 2.1. Mass Spectra Recorded Using the MS10 Spectrometer

m/z	Relative Intensities							
	C_2N_2	HCN	HNCO	CO_2	O_2	H_2O	NH_3	N_2
12	20.0	5.0	5.0	7.8				
13		2.2						
13.5		0.6						
14	4.25	1.8					2.0	7.0
15		0.3	14.0				7.0	
16				11.7	11.25	3.15	80.0	
17						25.8	100.0	
18						100.0		
24	10.0							
26	30.0	20.0	7.0					
27		100.0	5.0					
28		1.8	1.2	12.1				100.0
29			27.0					1.0
32					100.0			
38	4.15							
42			20.2					
43			100.0					
44			10.0	100.0				
52	100.0							

Table 2.2 Mass Spectra Recorded Using the VG Masstorr FX Spectrometer

m/z	Relative Intensities							
	C_2N_2	HCN	HNCO	CO_2	O_2	H_2O	NH_3	N_2
12	4.7	2.0	3.2	2.0				
13		1.0	2.3					
13.5		0.8						
14	1.0	0.7	4.8					3.9
15			8.3				38.4	
16			2.2	6.0	4.6	2.5	98.2	
17			1.7			25.1	100.0	
18			2.1			100.0		
19						2.0		
21.5			1.3					
22				1.5				
24	4.7							
26	14.6	17.2	8.7					
27		100.0	14.8					
28	18.0	16.4	17.2	5.7				100.0
29		0.3	17.9					
30			3.3					
32					100.0			
38	2.9							
42			54.3					
43			100.0					
44			1.5	100.0				
52	100.0							
53	3.0							

compare well with those of several other workers (4, 137-139) (Table 2.3). The mass spectra obtained for HNCO also agreed well with literature reports (140-143) (Table 2.4.).

Table 2.3 Mass Spectra of C_2N_2

m/z	Ion	Relative Peak Intensities		
		This work (MS10)	This work (VG Masstorr)	Previous Worker with MS10(4)
12	C^+	20.00	4.00	16.20
14	N^+	4.25	1.00	2.50
24	C_2^+	10.00	4.70	7.90
26	CN^+	30.00	14.60	22.50
28	N_2^+	-	18.00	-
38	C_2N^+	4.15	2.90	4.00
52	$C_2N_2^+$	100.00	100.00	100.00
53	-	-	3.00	-

2.3.4 Relative Sensitivities of Gases

Quantitative analysis of multi-component mixtures requires a knowledge of the relative sensitivity of the mass spectrometer towards each component (Sec. 3.1.2). Sensitivities for CO_2, C_2N_2, HCN, HNCO, O_2, H_2O and NH_3 were measured relative to that of N_2. This was done by dosing N_2 into the frame at a reproducible pressure P_N and setting the mass spectrometer leak valve to give a

Table 2.4. Mass Spectra of HNCO

m/z	Ion	Relative Intensities		
		This work (MS10)	This work (VG Masstorr)	Literature (143)
12	C^+	5.0	3.2	4.4
13	CH^+	-	2.3	0.3
13.5	HNC^{2+}	-	-	0.1
14	-	-	4.8	3.3
15	NH^+	14.0	8.3	13.5
16	-	-	2.2	0.9
17	-	-	1.7	0.1
18	-	-	2.1	-
21	NCO^{2+}	-	-	0.2
21.5	$HNCO^{2+}$	-	1.3	1.8
22	-	-	-	0.1
26	CN^+	7.0	8.7	3.5
27	HNC^+	5.0	14.8	3.5
28	CO^+	1.2	17.2	4.1
29	HCO^+	27.6	17.9	17.8
30	NO^+	-	3.3	2.0
42	NCO^+	20.2	54.3	22.8
43	$HNCO^+$	100.0	100.0	100.0
44	-	10.0	1.5	1.6
45	-	-	-	0.1

partial pressure of N_2 in the analyser chamber of about $3x10^{-6}$ torr. A spectrum of N_2 was recorded and the total ion intensity $\Sigma I_{i,N_2}$ was measured. With the leak valve in exactly the same position the next gas, CO_2, was dosed into the frame at the same pressure P_N. The gas was leaked into the mass spectrometer, the spectrum was recorded and the total ion intensity $\Sigma I_{i,CO_2}$ was measured. The relative sensitivity of the spectrometer to CO_2 relative to N_2 was given by :-

$$S_{CO_2} = \frac{\Sigma I_{i,CO_2}}{\Sigma I_{i,N_2}}$$

The relative sensitivity of the VG Masstorr spectrometer was found to be 410/513=0.80. The relative sensitivities for other gases were obtained in the same way, each time setting the position of the leak valve using nitrogen to give approximately $3x10^{-6}$ torr of N_2 in the analyser and then measuring the intensity of the nitrogen spectrum as a reference. The relative intensities for the gases analysed are tabulated in Table 2.5.

The effect on relative sensitivities of mixing components was assumed to be negligible. This assumption was based on the fact that all gases measured were of similar molecular weight and steric proportions. This assumption was verified by analysing an 85% N_2:15% CO_2 mixture supplied by BOC Ltd.

Table 2.5 Relative Sensitivities of Gases measured in the VG Masstorr Mass Spectrometer

Gas	Relative Sensitivity (Experimental)
N_2	1.00
CO_2	0.80
C_2N_2	1.54
HCN	0.65
HNCO	1.23
O_2	0.62
H_2O	1.10
NH_3	1.27

2.3.5 Solid State Mass Spectra

Solid state mass spectra of a white sublimate recovered from a hydroxylated $CuO\text{-}CrO_3/SiO_2$ sample (Sec. 4.5.3), of oxamide (BDH) and of cyanuric acid $(HNCO)_3$ (BDH) were measured on a VG 7070E Analytical Mass Spectrometer. Spectra were obtained at 70 ev and also on a lower energy range. Details of these spectra are shown in Appendix I.

2.4 Infra-Red Spectroscopy

2.4.1 The Infra-Red Spectrometer

Infra-red spectra were obtained on a Perkin-Elmer model 983 infra-red spectrometer interfaced with a Perkin-Elmer 3600 Data Station.[1] The spectrometer was used in the double beam mode to record spectra in the frequency range 5000-180 cm^{-1}. The frequency accuracy of this instrument was as follows:

±3 cm^{-1}	5000 to 4000 cm^{-1}
±2 cm^{-1}	4000 to 2000 cm^{-1}
±1 cm^{-1}	2000 to 180 cm^{-1}

The frequency reproducibility was 0.005 cm^{-1}, whilst resolution to 0.5 cm^{-1} was obtainable. Whenever possible spectra were recorded in triplicate and then averaged using the spectrometer memory, which reduced noise levels substantially. All spectra were stored on floppy discs using the data station; later they were subjected to a standardisation program (Sec. 3.2.2) before being reproduced in the most desirable way (Sec. 3.2.3).

2.4.2 The Infra-red Cell and Vacuum Frame

Infra-red spectra were recorded using a purpose-built vacuum frame and a cell design described by Surman (3). The frame, similar to the one used for gravimetric

---

[1] During the early part of this work, a few infra-red spectra were recorded on an Infrascan mark II H900 spectrometer manufactured by Hilger and Watts Ltd. The operation of this spectrometer has been described by Surman (3). Results obtained with this instrument are clearly marked as such in Chapter 4.

studies, was evacuated using a rotary pump and a water-cooled mercury diffusion pump protected by a liquid nitrogen trap. The frame incorporated pressure measurement devices, gas inlet connections, storage bulbs and a cold trap. To prevent sample contamination, greaseless taps were used throughout.

The infra-red cell (Fig. 2.5) was constructed so that the sample, in the form of a thin compressed disc, could be supported in the infra-red beam of the spectrometer whilst in vacuo. Since it was necessary to pretreat the sample at high temperatures, the cell was designed so that the disc could be moved between the i.r. beam and furnace without interrupting the vacuum. The sample holder consisted of a silica glass rod with a pair of silica hooks at one end, the opposite end of the rod being connected to a Pyrex tube. This tube was inserted into a precision bore tube, B. A vacuum seal was made between these tubes using a four O-rings. This made it possible to slide the inner tube up and down so that the attached sample could be moved into the furnace or the i.r. beam. The furnace consisted of a heating coil wound around a Pyrex tube which enabled sample temperatures up to 1073 K to be obtained. The heater was controlled by an 8 amp variac and the temperature of the sample was monitored using a chromel-alumel thermocouple whose junction was positioned alongside the sample disc. The cell was connected to the vacuum system via a glass side arm and a removable glass connecting tube. All

Fig. 2.5 The Infra-red Spectroscopy Cell

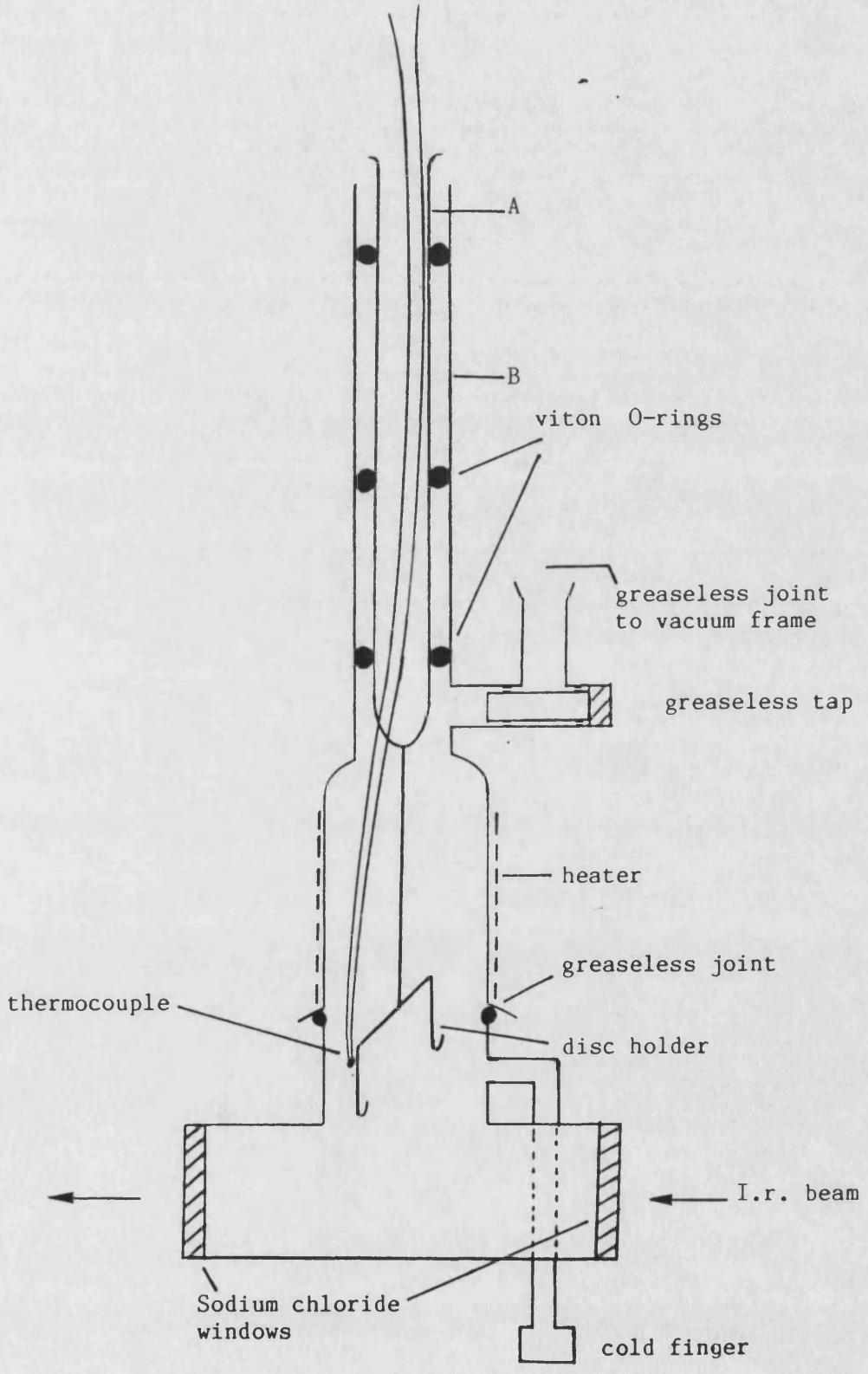

joints were sealed with Viton O-rings. A further greaseless tap enabled the cell to be isolated from the vacuum frame. A cold finger was incorporated into the cell (Fig. 2.5), enabling the gas phase to be condensed without re-connecting to the vacuum frame. The window section consisted of a 7.5 cm long Pyrex tube sealed at both ends with 2.5 cm diameter sodium chloride windows. The windows were fixed onto the glass tube using the high vacuum leak sealant 'Sprayseal' (supplied by Jencons Scientific Ltd.). The window section was attached to the remainder of the cell via a greaseless O-ring joint and was therefore fully removable. This allowed sample discs to be quickly installed and removed from the silica holder. The window section was stored in a desiccator when not in use to prevent atmospheric moisture from clouding the NaCl plates.

2.4.3 Preparation of Samples for Infra-Red Spectroscopy

Powdered samples of copper and chromium oxides supported on silica were prepared as described later (Sec. 2.7). For i.r. studies these powders were compressed into self-supporting discs. These were made as thin as possible to maximise their transparency towards the i.r. radiation. They were prepared by evenly sprinkling 100 mg of the sample over one face of a 28.5 mm diameter X-ray die (Beckmann RIIC Ltd) contained in a die holder. A second die was placed over the sample trapping the powder between the two mirror polished die

faces. A pressure of 3-5 tons per square inch was applied with a hydraulic press and maintained for several minutes. Before releasing the pressure, the space surrounding the dies was evacuated using a rotary pump to remove any traces of moisture. This prevented the sample discs from sticking to the die faces. The resultant discs were very fragile but when handled with care were sufficiently strong to resist the mechanical and thermal shocks encountered during the subsequent adsorption studies.

2.4.4 Automated Data Recording and Data Processing

Since the Perkin Elmer 983 spectrometer could be controlled from a computerised data station (Sec. 2.4.1), a program was written which enabled spectra to be recorded automatically as a function of time. The program, entitled 'DELAY. OY', was designed to record four spectra with time delays of 5 minutes, 5 hours, 10 hours and 15 hours. This was particularly useful when recording spectra overnight. The program, listed in Appendix II, employs a spectroscopy programming language developed by Perkin Elmer. It was written as an OBEY file which consisted of a series of CDS-II and OBEY specific commands. The spectra recorded were automatically stored on a floppy disc ready for data processing (Chapter 3).

2.4.5 Infra-red Spectra of Single Components

For reference purposes, infra-red spectra were recorded for pure gaseous cyanogen (Fig. 2.7 and 2.8) and HCN (Fig. 2.9). Other spectra of pure components were also measured but these are more appropriately cited in later sections.

The source and purification of cyanogen is described later (Sec. 2.7). It is one of few molecules of the general formula X_2Y_2 with $D_{\infty h}$ symmetry. The five fundamental vibrations possible with this structure are shown in Fig. 2.6, together with the corresponding wavenumber values for C_2N_2.

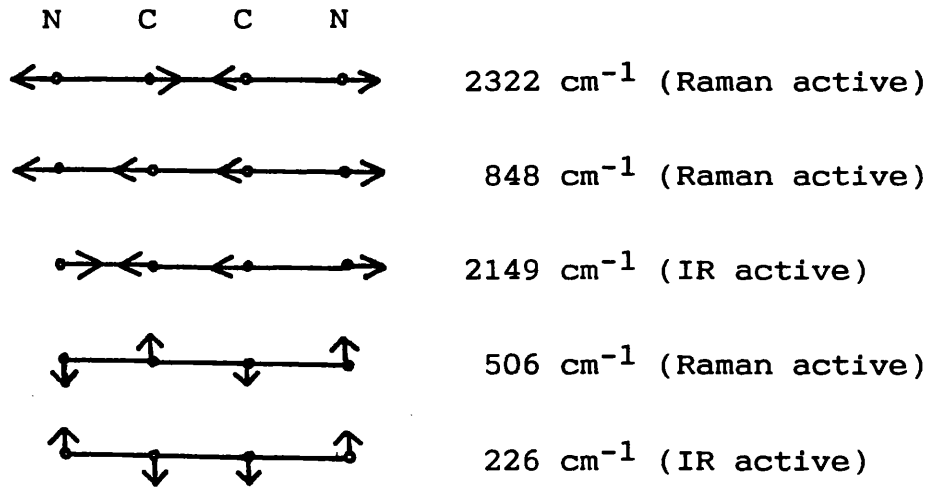

Fig.2.6. The Five Fundamental Vibrations of C_2N_2

The recorded spectrum for cyanogen is consistent with that reported in the literature (144) (Table 2.6).

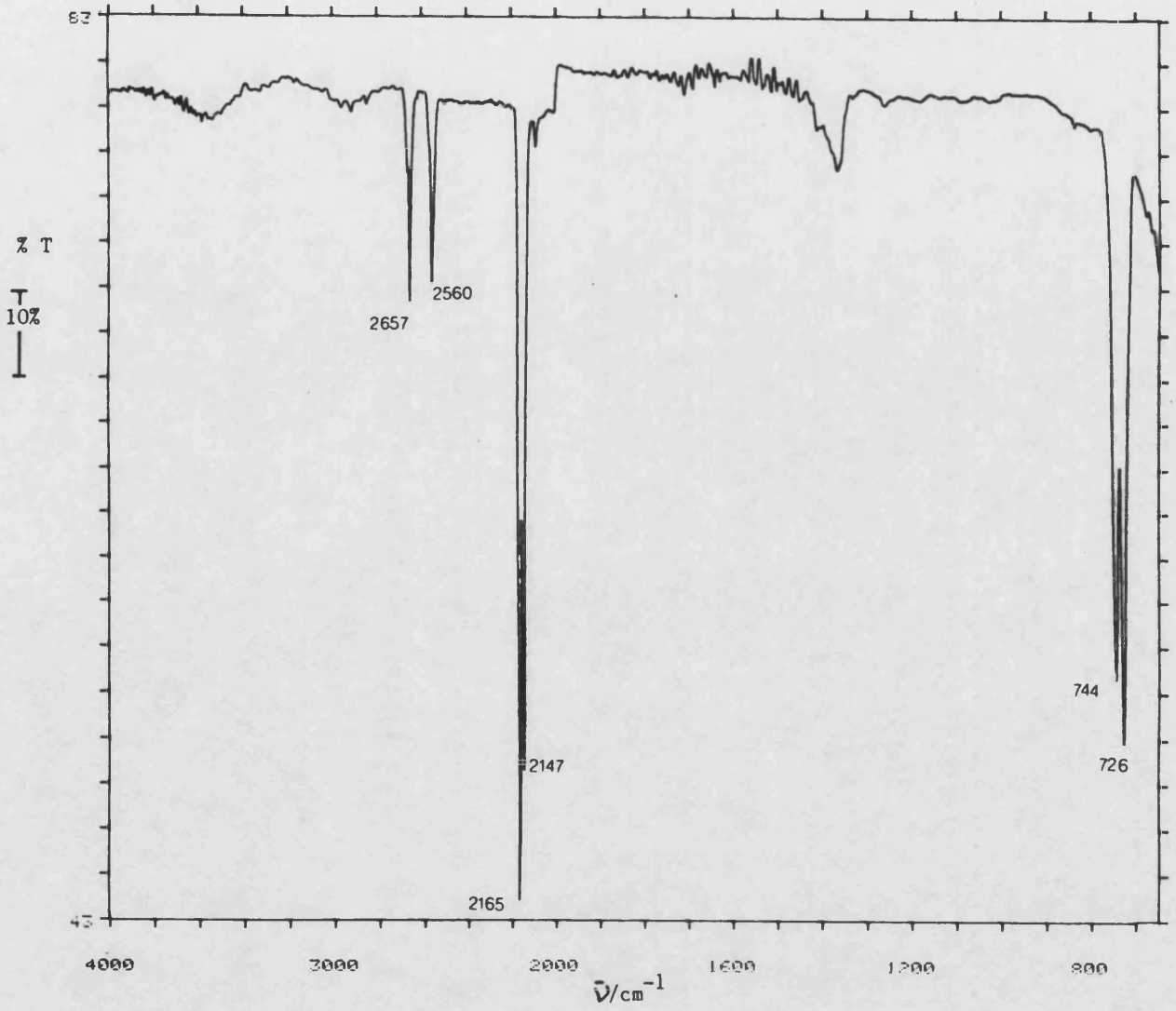

Fig. 2.7 Infra-red Spectrum of Cyanogen

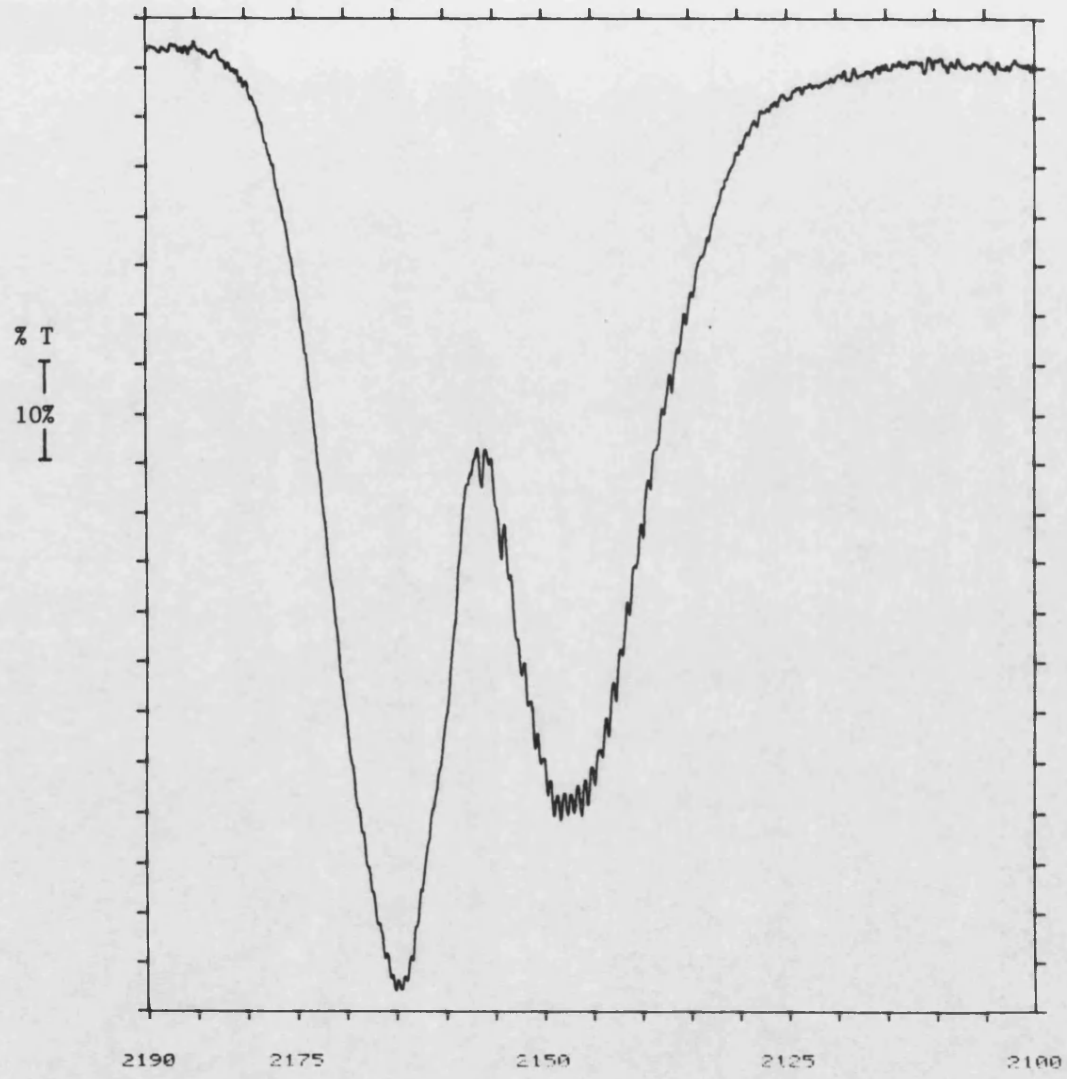

Fig 2.8. The ν_3 Infra-red Band of Cyanogen

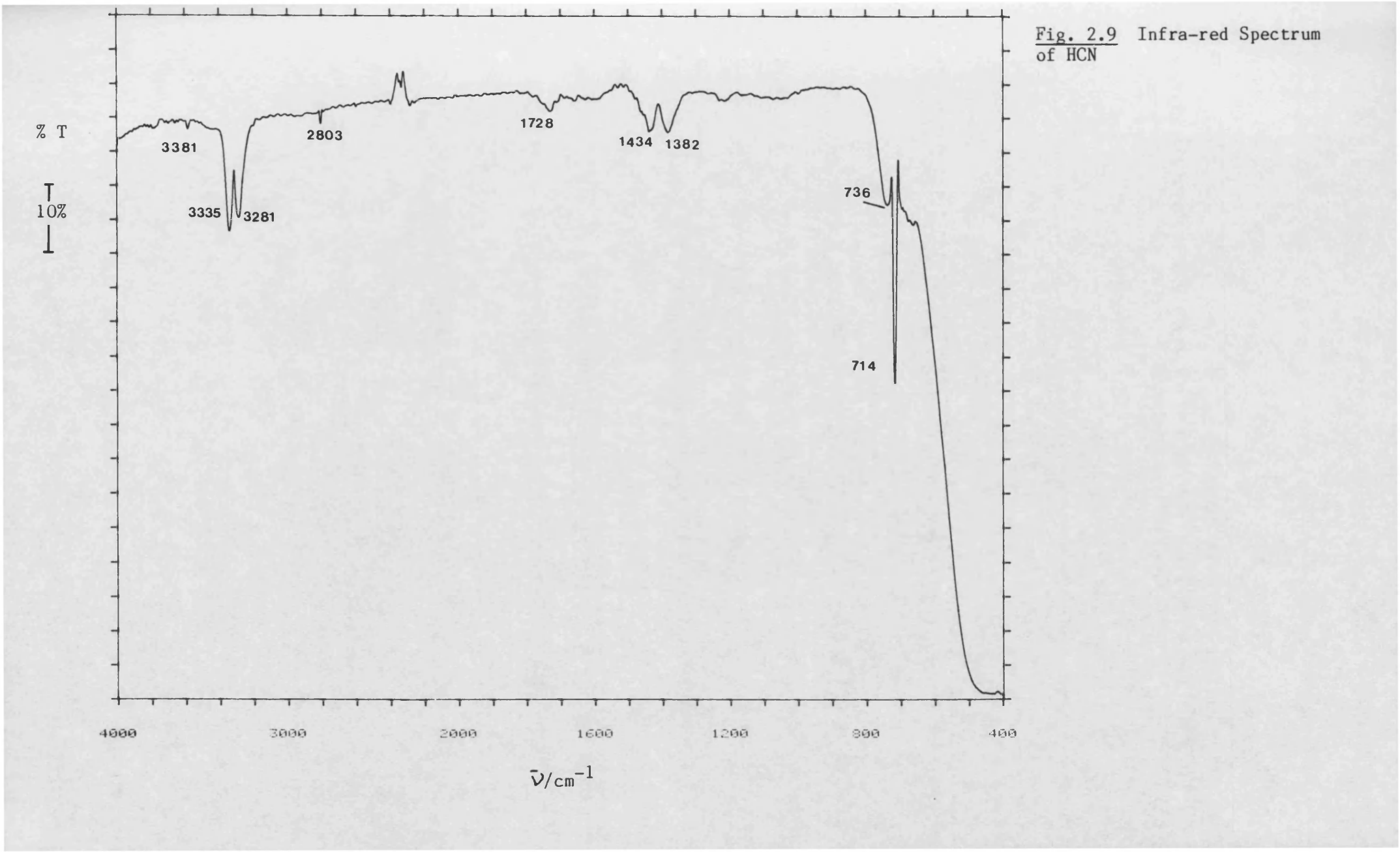

Fig. 2.9 Infra-red Spectrum of HCN

Table 2.6 Infra-red Absorption Bands of Gaseous Cyanogen

Absorption bands/cm^{-1}		
This work	Literature	Assignment
726 744	732	$\nu_4 + \nu_5$
2147 2165	2149	ν_3
2560	2562	$\nu_1 + \nu_5$
2657	2662	$\nu_3 + \nu_4$

The appearance of a doublet in the V_3 region was caused by the P and R branches of this fundamental. The observed rotational fine structure associated with this band, see Fig. 2.8, has been discussed by other workers (145-147). The noise at 3900-3500 cm^{-1} and near 1600 cm^{-1} was due to incomplete correction for moisture in the reference beam.

2.5 Surface Area Measurements

The surface areas of silica-supported chromium oxide, copper oxide and copper oxide-chromium oxide samples were determined gravimetrically on the microbalance by N_2 adsorption at 77 K. The BET equation was used in the form;

$$\frac{p/p_o}{X(1-p/p_o)} = \frac{p(c-1)}{p_o X_m c} + \frac{1}{X_m c}$$

where X is the weight of N_2 adsorbed at a pressure P, Po is the saturated vapour pressure, and X_m is the weight of N_2 required to form a monolayer on the sample surface. By plotting $(P/P_o/X(1-P/P_o)$ against P/P_o (when $0.05 \leq P_o \leq 0.35$) straight lines were obtained. The slope, S, and intercept, I, of the BET plots were given by $(c-1)/X_m c$ and $1/(S+I)$. From X_m, the number of moles and hence the number of atoms of N_2 required to form a monolayer was calculated. Taking the value 16.2×10^{-20} m^2 as the area of one N_2 molecule, the surface area of the samples was calculated.

2.6 Preparation and Handling of Cyano-Gases

Cyanogen was supplied in a lecture bottle by Argo International Ltd. It was 98.6% pure having listed impurity levels of 0.8% CNCl, 0.5% CO_2 and 0.1% HCN. The gas was transferred to the vacuum frame by connecting one end of a vacuum tight hose to the cylinder valve outlet, the other end had a glass balljoint connector which formed a greaseless seal with the gas inlet point, A (Fig. 2.1). The hose was evacuated then flushed with nitrogen gas before sealing a small section of the frame including the cold trap, CT3, under 100-200 torr N_2 gas. C_2N_2 was bled into the frame in a controlled manner, monitoring the amount using the mercury manometer, P4. Tap 5 was then closed. The cold trap was cooled in liquid nitrogen and the C_2N_2 condensed into it before the nitrogen gas was pumped away. The C_2N_2 was then

subjected to a sequence of freeze-pump-thaw operations until the mass spectrum of the residual gas contained no traces of CO_2, H_2O or O_2 impurities. The purified gas was stored as described in section 2.1. The mass spectrum of the purified gas has been reported in Table 2.3. Hydrogen cyanide was prepared from the reaction of aqueous sulphuric acid with potassium hexacyanoferrate according to the following equation:

$$K_4Fe(CN)_6 + 3H_2SO_4 \longrightarrow 2K_2SO_4 + FeSO_4 + 6HCN$$

The reaction was performed on the vacuum frame using a specially designed glass reaction vessel (Fig. 2.10). Finely ground potassium hexacyanoferrate was introduced into the glass bulb by removing the screw plug, X. The tap was then replaced and screwed down until the PTFE O-ring seated forming a water-tight seal. The small reservoir above the tap was filled with an appropriate amount of mixture containing four parts of concentrated sulphuric acid and six parts of water. The reaction vessel was then connected to the ball joint, A, on the vacuum frame (see Fig. 2.1) via a length of glass tubing containing a $CaCl_2$ drying tower. Since the reaction is sensitive to oxygen, all traces of it were removed by a series of evacuation and nitrogen purging operations before dosing 400-600 torr of nitrogen into the system. The cold trap, CT3, was cooled in liquid nitrogen before unscrewing the tap X allowing the sulphuric acid to drain onto the potassium ferricyanide. The reaction mixture was heated to boiling for several minutes until the green

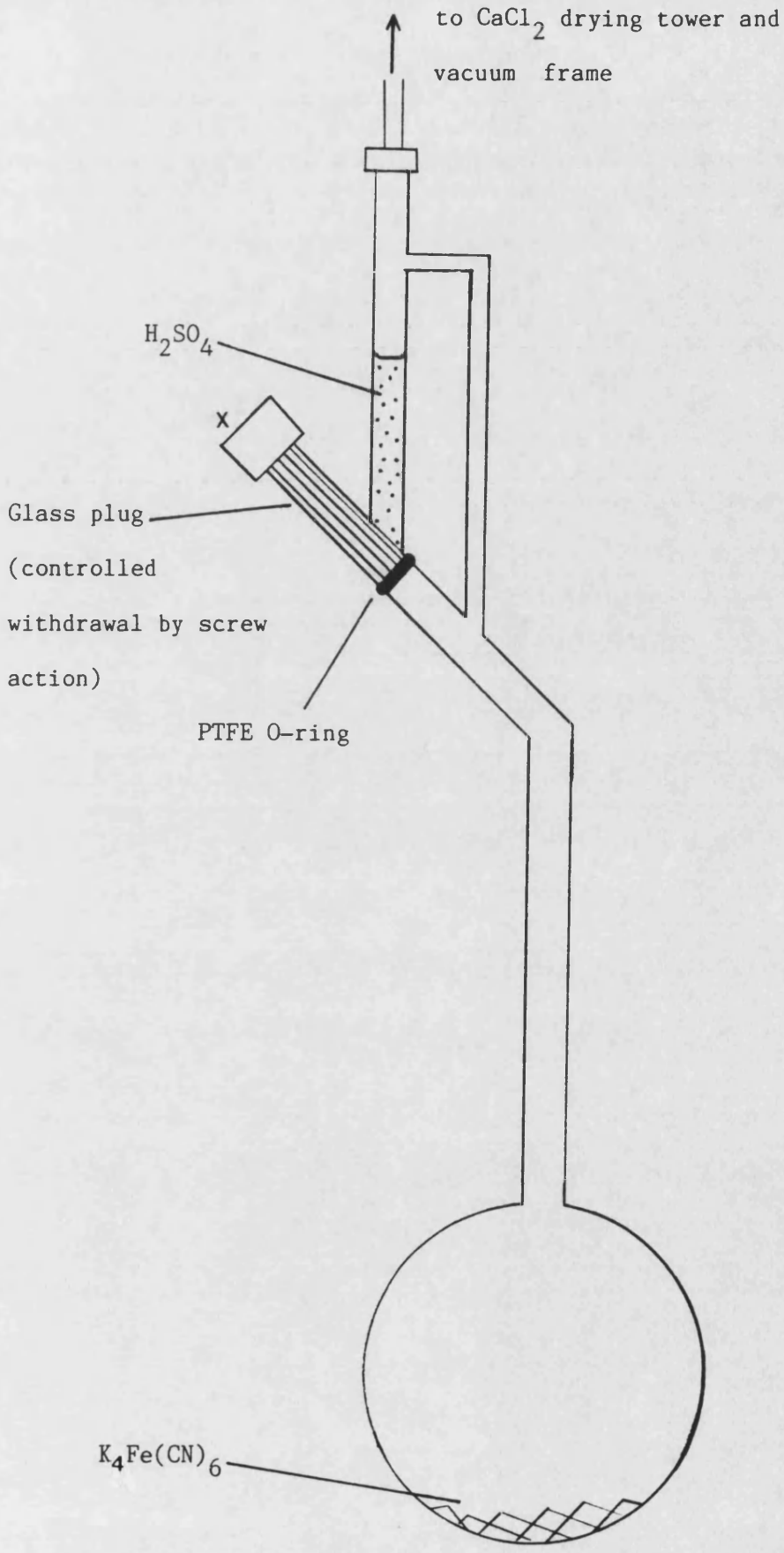

Fig. 2.10 Vessel for HCN Preparation

coloration of $FeSO_4$ became prominent. The reaction vessel was allowed to cool for several minutes before isolating it from the frame. The HCN produced had condensed into the cold trap together with some moisture and CO_2. The crude gas was purified by fractionation until mass spectral analysis showed no impurities. The HCN was stored as described in section 2.1. The mass spectrum of HCN is reported in Sec.2.3.3.

Isocyanic acid, HNCO was prepared by the thermal depolymerisation of cyanuric acid according to the equation:

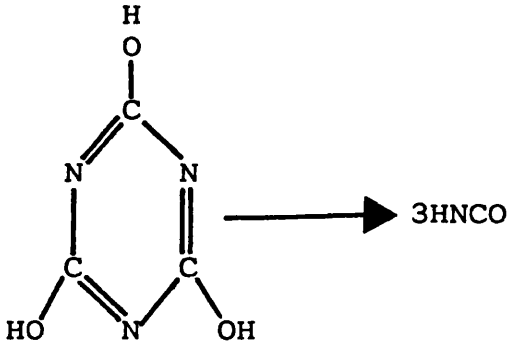

Since cyanuric acid tends to sublime without reaction, it was necessary to apply heat to vaporise it and then to heat the vapour further to effect the depolymerisation (148). The apparatus designed to do this is shown in Fig. 2.11. A silica glass reaction vessel containing several grammes of cyanuric acid (BDH) was connected to the vacuum frame via the balljoint connector, A, (Fig. 2.1). The bulb of the reaction vessel, with an attached chromel-alumel thermocouple, was supported in a furnace. A 30 cm length of silica tube extended from the bulb to a

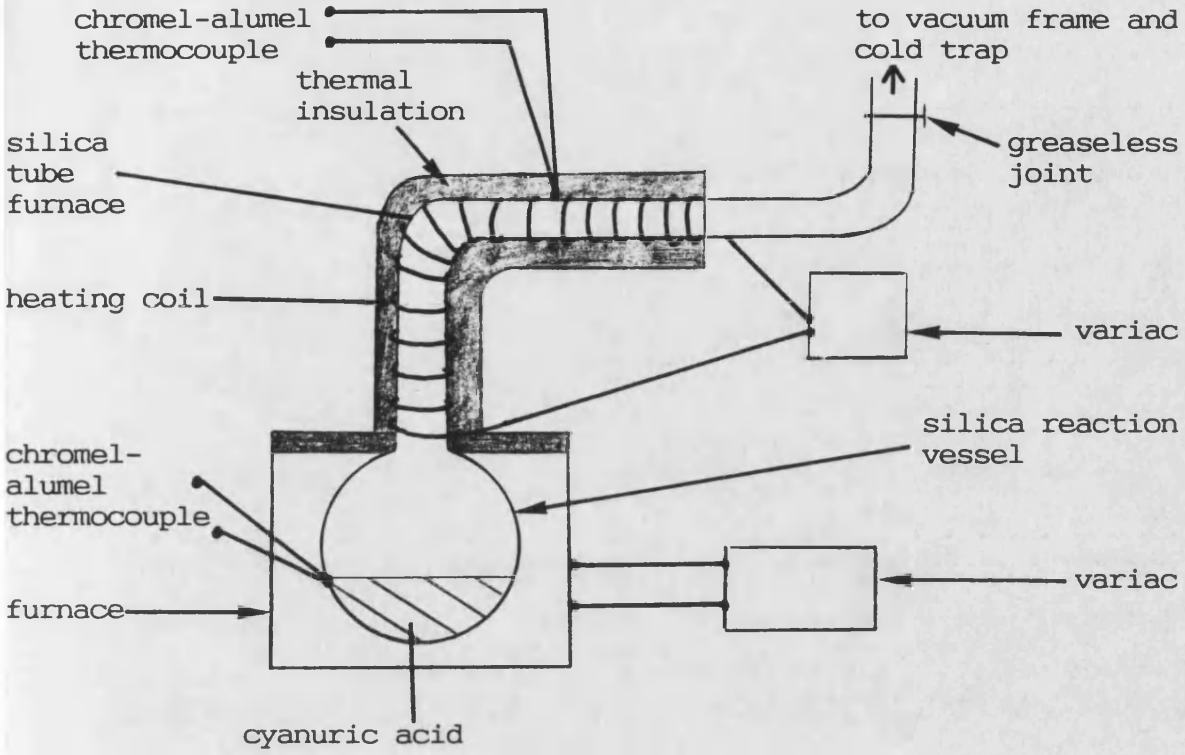

Fig. 2.11. Apparatus for Isocyanic Acid Preparation

greaseless joint, a 10 cm section of which was converted into a tube furnace by winding nichrome (4 Ωm^{-1}) tightly around it. a second thermocouple was positioned onto the centre of this furnace. The heated section of the tube was then lagged with insulating material to ensure that a uniform temperature could be maintained. The apparatus was evacuated and the reaction bulb was heated to 473 K for one hour to remove moisture. The tube furnace was then heated to 973 K and the cold trap. CT3 (Fig. 2.1), was cooled to 77 K. The cyanuric acid was then slowly volatilised in vacuo at 723 K and as the vapour passed through the tube furnace it depolymerised. The HNCO

produced was collected in the liquid nitrogen trap on the vacuum frame. Crude HNCO was purified by fractional distillation until mass spectral analysis showed that HCN and H_2O were absent. A mass spectrum of the gas was immediately recorded (Table 2.4) since it re-polymerised very rapidly. HNCO was stored below 243 K as suggested by Winnewisser (149). An i.r. spectrum of the HNCO was also recorded. The spectrum is reproduced in Fig. 2.12. The band positions fitted closely with literature values (Table 2.7) and the absence of bands characteristic of HCN confirmed the purity of the gas.

Table 2.7 I.r. Spectral Data for HNCO/cm^{-1}

Band	This work	Reid and Herzberg (150)	Morgan and Lawson (151)
ν_1	3525	3531	3520
ν_2	2264	2274	2271
ν_3	-	1327	1342
ν_4	786	797	572
ν_5	*	572	670
ν_6	*	670	(797)

* A series of bands were seen below 786 cm^{-1} with major maxima at 711, 685 and 660 cm^{-1}.

To ensure that HNCO was not re-polymerising to cyanuric acid an i.r. spectrum of the latter material was also measured. Spectra of the white powder were obtained by two methods. The first involved preparing a mull in nujol Fig. 2.13, spectrum B, where spectrum A shows the spectrum of pure nujol. The second method involved mixing cyanuric acid with NaCl and preparing a thin self

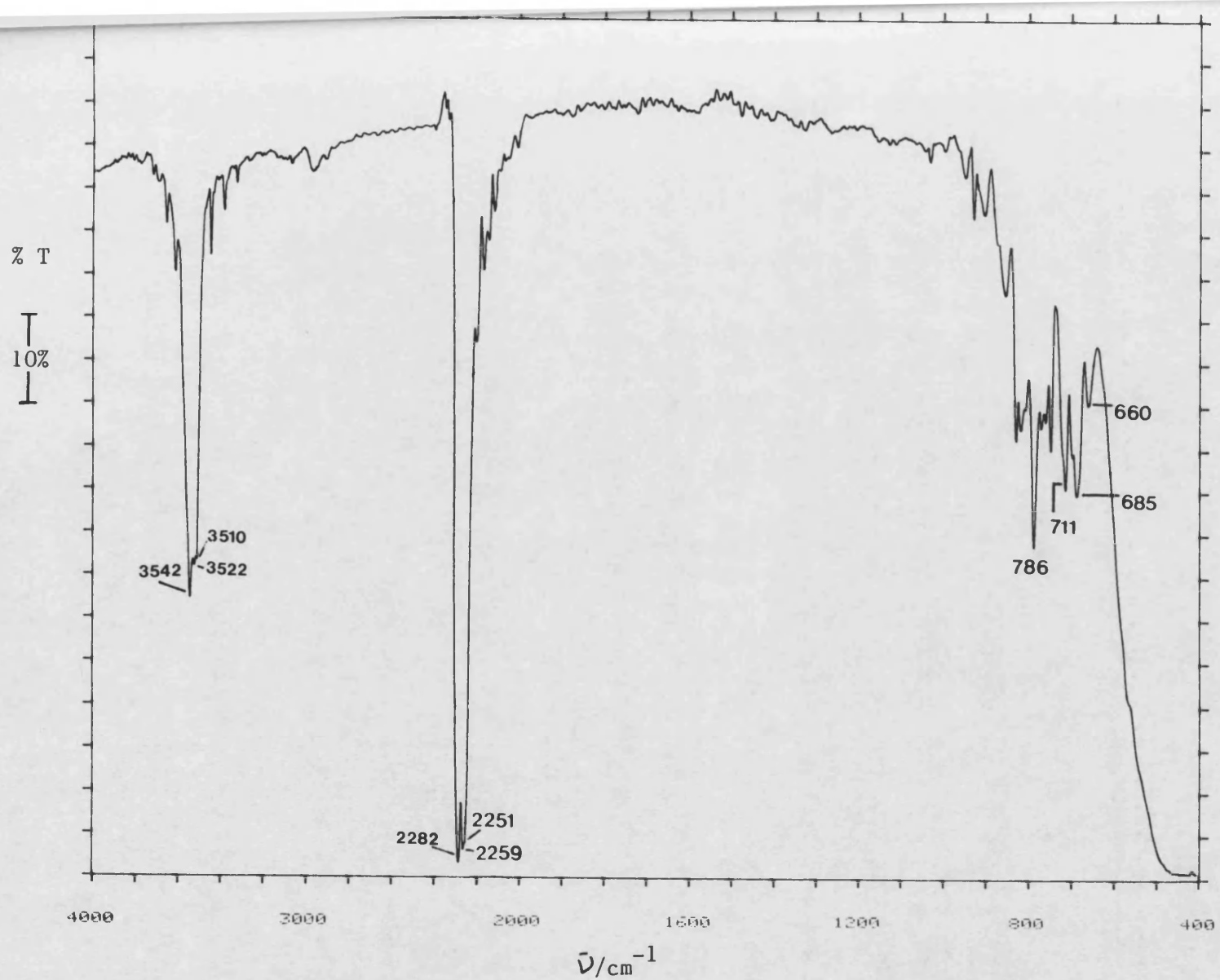

Fig. 2.12 I.r. Spectrum of Isocyanic Acid

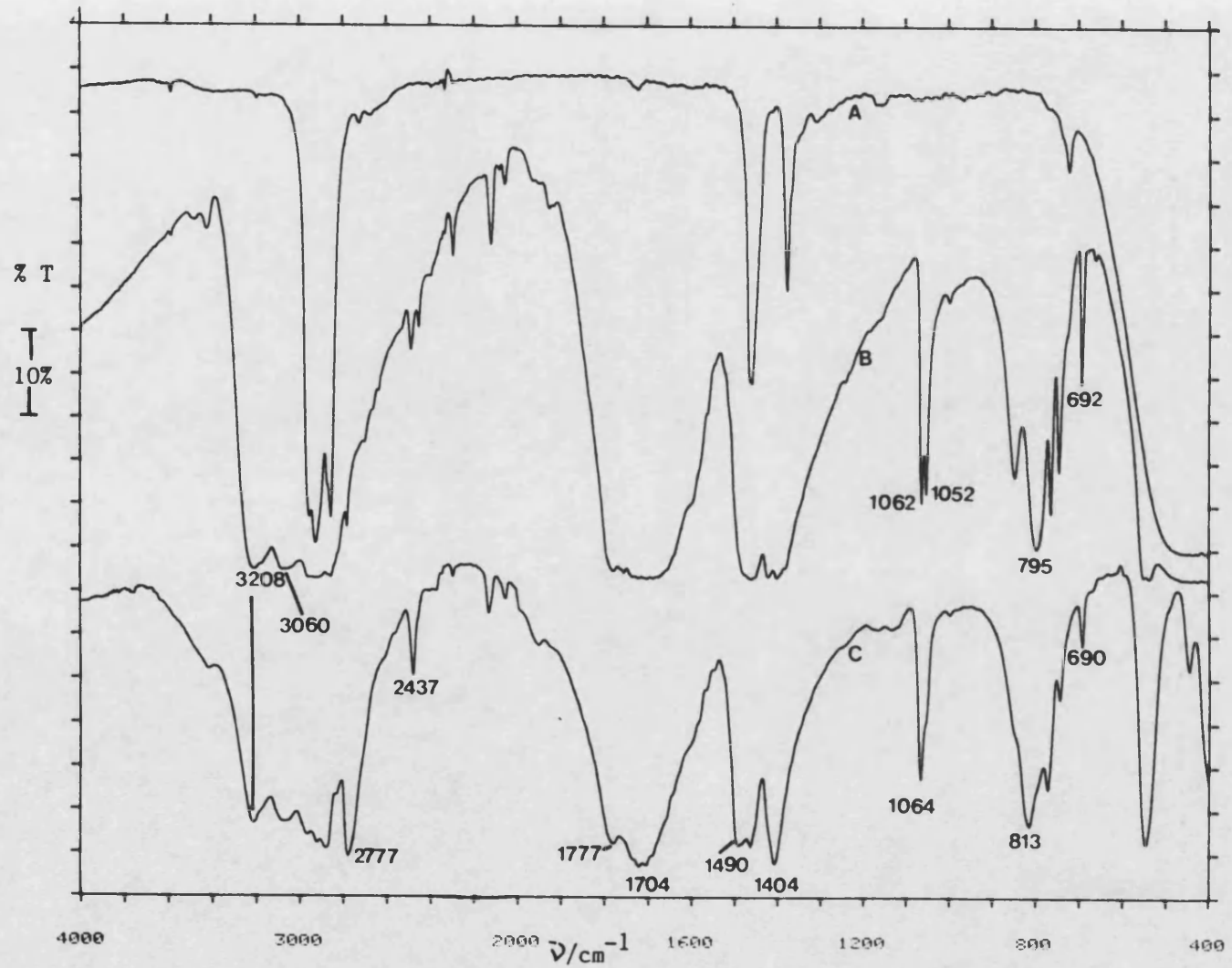

Fig. 2.13 I.r. Spectra of Cyanuric Acid $(HNCO)_3$

KEY

A = Nujol

B = Cyanuric Acid in Nujol Mull

C = Cyanuric acid/NaCl wafer

supporting disc. The spectrum produced is shown in Fig. 2.13, spectrum C. Comparison of spectra B and C of Fig. 2.13 with that of gaseous HNCO Fig. 2.12 shows that no polymerisation to cyanuric acid had occurred.

2.7 Preparation and Pretreatment of Silica-Supported Adsorbents

The silica used in this work was Aerosil 300, supplied by Bush Beach Segner and Bayley Ltd. It was a fine white powder having a surface area of 300 m^2g^{-1}. Samples of CrO_3/SiO_2, Cr_2O_3/SiO_2 and CuO/SiO_2 were prepared using chromium(VI) trioxide, chromium(III) nitrate and cupric nitrate, all supplied by BDH. The procedure involved making a solution of the metal salt, using distilled water, and mixing in a measured amount of Aerosil to give a 1.5% by weight loading of the metal ion, based on the weight of dry silica. The loading of 1.5 wt.% of metal ion on the sample was chosen since Cr (VI) is known to become unstable at higher loadings (see Sec. 1.3.1). This low level was also selected for the Cr(III) and Cu(II) impregnants to give well dispersed coverings of the ions on the silica surface with low levels of clustering, (see Sec.5.1). In the case of the $CuO\text{-}Cr_2O_3/SiO_2$ and $CuO\text{-}CrO_3/SiO_2$ samples, impregnation was carried out by mixing the silica into a solution of the mixed salts to give adsorbents containing 1.5 wt.% of each metal ion.

All Aerosil-metal salt slurries were stirred for 30 minutes to ensure an even distribution of the metal ions over the silica. The slurries were then dried at 313 K using a rotary evaporator. Dry powdered samples were stored in a vacuum desiccator until required.

For gravimetric studies, the samples were used in a powdered form. Approximately 100 mg of powder was placed into the sample bucket hanging on the microbalance. For infra-red spectroscopic studies a 100 mg sample was pressed into a thin self-supporting disc and placed into the i.r. cell. Each sample was then pretreated according to the following sequence of procedures:-

(1) The samples were evacuated at ambient temperature, until a vacuum of $1x10^{-5}$ torr or better was achieved (care was taken not to evacuate too quickly since powdered samples were prone to 'fluffing').

(2) The sample temperature was raised to 450-500 K at a rate of about 2 K per minute whilst maintaining the sample under high vacuum.

(3) The sample temperature was maintained at 450-500 K in vacuo for several hours to remove all physically held moisture. Gravimetric experiments confirmed that all samples reached constant weight after this treatment.

(4) The temperature was slowly raised to 673-698 K whilst maintaining a vacuum of 10^{-5} torr or better. These conditions were held for 10-15 hours.

At this stage several different sample preparation routes were followed depending on the desired pretreatment. Specimens hitherto referred to as outgassed 'OG' samples were cooled under vacuo and were then ready for adsorption studies. The loading of transition metals on these outgassed samples was confirmed by atomic absorption spectroscopy.

Hydroxylated ('HYDR'-) samples were prepared by exposing the outgassed sample to 18 torr of water vapour for 2 hours at ambient temperature. Excess water was removed by evacuating the sample at this temperature until it reached a constant weight. Hydroxylated-hydrated samples ('HYDR-PLUS') were prepared in a similar manner except that excess water was removed by condensing the gas phase into a liquid nitrogen trap.

Oxygenated ('OXY') samples were prepared by exposing an outgassed sample to approximately 100 torr oxygen at 673-698 K for 12 h. The sample was cooled to ambient temperature and evacuated until it reached constant weight.

The final pretreatment involved oxygenation followed by hydroxylation to give an oxygenated-hydroxylated ('OXY-HYDR-') sample.

2.8 Procedure for Adsorption Experiments

The interaction of C_2N_2 with silica-supported metal oxides was investigated using gravimetry/mass spectroscopy and i.r. spectroscopy. The two studies were performed independently and were carried out in separate purpose-built vacuum frames (Secs. 2.1 and 2.4.2). Gravimetric studies were conducted using 100 mg powdered samples placed in the sample bucket which in turn was suspended on the microbalance. I.r. studies were carried out by recording spectra through 100 mg self-supporting sample discs suspended in the i.r. cell (Sec. 2.4.2). Samples were pretreated by the methods described in Sec. 2.7.

Pretreated samples were exposed to 18-20 torr of pure cyanogen at ambient temperature and left to react for 10-25 h. During gravimetric studies, the composition of the gas phase was measured using the mass spectrometer at regular intervals. Condensable products were then concentrated by pumping them into a liquid nitrogen trap. The contents of the trap were thawed and analysed by mass spectrometry[1] and were then pumped to waste. Similar analyses were carried out on desorbates collected from the sample evacuated to a series of elevated temperatures (typically 298-473, 473-548, 548-623 and 623-698 K). Throughout these experiments the

---

1 Nitrogen was non-condensable thus it was not present in mass spectrometry samples.

microbalance was used to monitor the weight of the samples.

A similar procedure was used in the infra-red spectroscopic experiments, except that in this case the sample disc had to be lowered from the heating section of the i.r. cell into the i.r. beam to record spectra (Sec.2.4.2).

3. DATA-HANDLING TECHNIQUES

This section describes the background to the methods developed for handling the raw data from mass spectroscopic and infra-red spectroscopic measurements. By way of illustration, worked examples are included; the computer programmes written and used are given in Appendices.

3.1 Mass Spectral Analysis

3.1.1 Mass Spectra of Multi-Component Mixtures

The mass spectrum of a multi-component gas mixture is made up of the superimposed spectra of the various components. From a knowledge of the components present and of their respective cracking patterns, it is possible to assign the contribution to any given peak of each of the constituents. Additionally the intensity of the cracking pattern of each component is indicative of the partial pressure of that component.

The accuracy of quantitative determinations of the molar amounts of the components present in a gas phase mixture depends on the following assumptions: (152)

a) the mass spectrum of any component is unaffected by the presence of another compound and no intermolecular reactions occur within the analyser chamber;

b) when the spectral peaks superimpose at any mass

number then the intensities due to the various components are linearly additive;

c) the cracking patterns and sensitivities of the various components in a mixture do not differ from those of the pure component;

d) the ion beam intensity of any component (i.e. the sum of the intensities of the peak comprising the cracking pattern) is proportional to the partial pressure of that component;

e) each component exhibits at least one peak which differs markedly from the peaks of other components;

f) the transfer of sample into the mass spectrometer analyser chamber does not appreciably modify the composition of the residual sample;

g) Dalton's law of partial pressures applies to the gas mixture.

In the present work errors possibly present from the more important of these assumptions have been minimised in the following ways. By measuring mass spectra in a dynamic system, products resulting from intermolecular reactions were kept at low concentrations. Furthermore, by measuring spectra at low chamber pressures (typically 10^{-5} to 10^{-7} torr) interactions between ions were kept to a minimum. Maintaining low chamber pressures also helped to satisfy assumption (f) since by extracting only minute amounts of the gas mixture under examination the effect upon the composition of the residual mixture was lessened.

Having selected conditions such that the assumptions (a)-(g) were satisfactorily met, quantitative mass spectral analysis of multi-component mixtures could be addressed. Two methods are commonly used to resolve complex spectra. (153) The first method involves setting up and solving a set of linear simultaneous equations, whilst the second, used in this work, makes use of the subtraction (or 'artichoke') principle. There are many examples of quantitative analyses of mass spectra in the literature; see, for example, the treatments of Melpolder and Brown, (154) and of Millard. (155)

Although the accuracy of quantitative determinations by mass spectroscopy is typically in the order of 2-5%, (156) the determination of molar amounts of various components is also affected by factors outside the scope of the mass spectrometer itself. For example, the relationship between sample concentration within the chamber and the actual amount of each component contained in a sample reservoir (in the present case the adsorption system), is dependent upon the measurement of the pressure of the gas mixture in the reservoir. Although every possible precaution was taken to minimise such errors in the present work, it is likely that they contributed some additional inaccuracy.

3.1.2 Quantitative Mass Spectral Analysis

Most mixtures are too complicated to expect to find a single (analytical) peak unique to each given

component. Overlapping contributions to analytical peaks from different components in a mixture are often found in practice. In order to solve spectra it is then necessary to remove this overlapping. This can be done by using a stepwise calculation method known as the 'artichoke' method in which one 'peels out' the contributions of each compound from the spectrum of the mixture one at a time. This method is best described by a simple example taken from the present work. Consider a mixture containing four compounds A,B,C and D. Its mass spectrum and the known mass spectra of the pure compounds are shown in Table 3.1. It is required to determine the contribution to each m/z value in the mixture of each of the four compounds.

Table 3.1 Mass Spectrum of an Unknown Mixture and Mass Spectral Data for its Individual Pure Components

	Relative Peak Intensities				
m/z	Mixture	Pure A	Pure B	Pure C	Pure D
15	58.3	100.0	0.0	0.0	0.0
31	23.2	27.0	16.0	0.0	0.0
43	59.7	36.0	75.0	16.0	6.0
49	100.0	26.0	100.0	27.0	100.0
57	27.9	15.0	16.0	100.0	0.0

To solve this problem it is first necessary to choose an analytical peak which is unique to only one component. The peak at m/z 15 is unique to component A. The contribution of component A to the unknown spectrum can be deduced by multiplying the spectrum of pure A by the factor 58.3/100 = 0.583. Thus the contribution of component A to the total ion intensity of the mixture is that given in the second column below, and subtraction from the data for the mixture in Table 3.1 gives the B,C,D residue in the third column:

m/z	A	B,C,D residue
15	58.30	0
31	15.74	7.46
43	20.99	38.71
49	15.16	84.84
57	8.74	19.16

Of the three remaining components, B exhibits a unique peak at m/z 31 from which the contribution of B to the B,C,D residue can be deduced using the factor 7.46/16 = 0.446. Subsequent subtraction of the resultant spectrum of B leaves the C,D residual spectrum from which the contributions C and D can be similarly deduced, finally giving the solution shown in Table 3.2. The sum of the ion intensities ($\Sigma I_{i,j}$), (where i = ion i of component j) for each component is proportional to the partial pressure of that component (p_i). Assuming the validity

Table 3.2 Mass Spectrum of Unknown Mixture and Derived Contribution of Each Component

m/z	Peak Intensity in mixture	Derived Contribution to Intensity			
		I_A	I_B	I_C	I_D
15	58.3	58.30	0.00	0.00	0.00
31	23.2	15.74	7.46	0.00	0.00
43	59.7	20.99	34.95	1.85	2.11
49	100.0	15.16	46.60	3.11	35.03
57	27.9	8.74	7.46	11.54	0.00
	$\Sigma I_{i,j}$	118.93	96.47	16.50	37.14

of Dalton's law of partial pressures ($P_{total} = P_A + P_B + P_C + P_D$), and noting that the p_j's are in turn proportional to the number of moles x_j ($P_j = x_j.RT/V$), it follows that the mole percentages of A,B,C and D in the mixture are:

Component	$\Sigma I_{i,j}$	Molar composition (%)
A	118.93	44.21
B	96.47	35.86
C	16.50	6.13
D	37.14	13.80
	269.04	100.00

So far it has been assumed that the mass spectrometer is equally sensitive to each component present. In practice this is not so; instead the total ion intensity of a given compound ($\Sigma I_{i,j}$) is related to the abundance of that compound by a sensitivity factor S. Thus for a given partial pressure (P_j) of the jth compound in the ionization chamber, the following relationship applies: $\Sigma I_{i,j} = S_j P_j$, where S_j is the sensitivity of the mass spectrometer to the jth compound. Since the measurement of absolute values of S_j is susceptible to small changes in conditions within the ionization chamber, relative sensitivities are more commonly quoted. By relating the relative sensitivity of a compound to its total ion intensity, the relative partial pressure and consequently the mole fraction of that component can be determined.

The next section describes two complementary computer programs written especially to evaluate concentrations from the present work. This is followed by a section describing a worked example to show typically how mass spectral data from a mixture were analysed to derive the quantities of individual components.

3.1.3 Mass Spectral Analysis Programs

Two computer programs were written and used in this work. The first, entitled 'MS1', accepts raw data from the mass spectrometer in the form of line lengths (ion

intensities) and transforms them into a percentage contribution for each ion in relation to the total ion intensity in the spectrum ($\%\Sigma_i$). The second program, entitled 'MS ANALYSIS', accepts these revised ion intensities and solves the spectrum using the 'artichoke' method. However, no correction is applied at this stage for the different sensitivity of the mass spectrometer to each compound. Instead, sensitivity corrections and the calculation of partial pressures and mole fractions of each component present in the sample were performed manually afterwards (Sec. 3.1.4).

Computer Program 'MS1' This program, listed in Appendix III, accepts raw data in the form of ion intensities for the sample spectrum [AA(1)] and for the background spectrum [B(1)] for the integer m/z values between 12 and 60 plus m/z values at 13.5 and 21.5. It then subtracts the background spectrum to leave the corrected sample line lengths (P_i, designated Pcorr in the program) and stores the result as A9. $\%\Sigma_i$ values for all m/z values are then computed in line 150 from the relationship: $(P_i \times 100)/ P_i = \%\Sigma_i$. This program is also able to take account of relative amounts of each ion (Corr.%age) present throughout a series of spectra by allowing for the relative pressure of the sample (lines 140-166). Finally, raw input data and computed $\%\Sigma_i$ values are tabulated alongside corresponding m/z values (lines 175-

295). The total ion intensity and number of ions analysed is also printed out (Table 3.3).

Computer Program 'MS ANALYSIS' This program, listed in Appendix IV, accepts data from the previous program in the form of $\%\Sigma_i$, which are fed in as A(J) values in line 610. The 'artichoke' method which relies on a knowledge of the cracking patterns of each compound present in the mixture is then used to solve the spectrum. The cracking patterns for the gaseous components which regularly appeared in the work, namely C_2N_2, HNCO, CO_2, HCN, H_2O and NH_3, were therefore built into the program. Subtraction of each substance from the observed spectrum was performed in the above sequence since this was found to yield the unique analytical peaks necessary to calculate the relative contribution of each compound. The m/z 52 peak in the cracking pattern of cyanogen (Table 3.4) was used as the first analytical peak. The intensity of this peak, F(1), was used to compute the ion intensities of the other ions in the C_2N_2 spectrum [F(2)...F(8)] using the relationship below (lines 800-914).

F(n) = F(1) x Relative abundance of peak n.

These F(n) values were then subtracted from the sample spectrum and summed to give the total ion intensity of C_2N_2 (Σ_{i,C_2N_2}) which was stored as F(10) in line 920.

The ion intensities [G(1) ... G(16)] and total ion intensity [G(17)] for HNCO were next computed using m/z

Table 3.3 Example of the Printout from Computer Program 'MS 1'

MASS SPEC. REF NO.11/8 RUN AT 668 K

MASS NO	RESP	B.G.	P.CORR	MASS NO	%AGE	CORR.%AGE
12.0	34.0	.0	34.0	12.0	.73	1.68
14.0	5.0	.0	5.0	14.0	.10	.24
15.0	10.0	.0	10.0	15.0	.21	.49
16.0	157.0	.0	157.0	16.0	3.38	7.77
17.0	530.0	3.5	526.5	17.0	11.34	26.08
18.0	2170.0	14.2	2155.8	18.0	46.44	106.82
19.0	20.0	.0	20.0	19.0	.43	.99
20.0	4.0	.0	4.0	20.0	.08	.19
22.0	10.0	.0	10.0	22.0	.21	.49
24.0	5.0	.0	5.0	24.0	.10	.24
26.0	36.0	.2	35.8	26.0	.77	1.77
27.0	143.9	.8	142.2	27.0	3.06	7.04
28.0	128.0	2.4	125.6	28.0	2.70	6.22
29.0	3.0	.0	3.0	29.0	.06	.14
38.0	5.0	.0	5.0	38.0	.10	.24
39.0	5.0	.0	5.0	39.0	.10	.24
40.0	7.0	.0	7.0	40.0	.15	.34
41.0	15.0	.0	15.0	41.0	.32	.74
42.0	20.0	.0	20.0	42.0	.43	.99
43.0	40.0	.0	40.0	43.0	.86	1.98
44.0	1230.0	.4	1229.6	44.0	26.49	60.98
45.0	18.0	.0	18.0	45.0	.38	.89
46.0	6.0	.0	6.0	46.0	.12	.29
52.0	62.0	.0	62.0	52.0	1.33	3.07

TOTAL INTENSITY= 4641.5

PRESSURE FACTOR= 2.3

TOTAL %AGE = 100 TOTAL CORR. %AGE = 230

NUMBER OF LINES ANALYSED = 24

43 as the new analytical peak (lines 970-1155). Complete spectral interpretation was achieved by progressively working through each compound using the set of analytical peaks shown in Table 3.5.

Having computed $\Sigma I_{i,j}$ values for all seven compounds, these were then converted to percentage contributions to the total ion intensity in the spectrum (denoted $\%\Sigma_{i,j}$). This was done by multiplying by 100 and dividing by the total ion intensity (lines 2000-2060). The results obtained were printed out as in column 2 of Table 3.6.

In practice this program often accounted for more than 95% of the lines (peaks) arising from these seven compounds. However, a listing of residual (unanalysed) lines were found to be invaluable in characterising other minor gaseous compounds. The program computes these residual lines and prints them alongside the input (response) data for each m/z value (Table 3.6, lower part). The program also corrects the $\%\Sigma_{i,j}$ values for incomplete line analysis (lines 2177-2183), and it lists the corrected values in the third column of Table 3.6. Finally, since the pressure of the sample in the adsorption system is proportional to the $\%\Sigma_{i,j}$ values for each compound, a further set of results was derived by multiplying corrected $\%\Sigma_{i,j}$ values by an appropriate pressure factor (lines 2190-2197). These results shown in the fourth column of Table 3.6, enable the program operator to compare the relative amounts of each compound

Table 3.4 The Cracking Pattern of Cyanogen

m/z	Relative Abundance	Designation of the ion intensity in the program
52	1.000	F(1)
38	0.029	F(2)
28	0.180	F(3)
27	0.030	F(4)
26	0.146	F(5)
24	0.047	F(6)
14	0.010	F(7)
12	0.047	F(8)

Table 3.5 Analytical Peaks Chosen to Solve Mass Spectra of Mixtures Using the 'Artichoke' Method

Compound	Analytical Peak (m/z)
C_2N_2	52
HNCO	43
CO_2	44
O_2	32
HCN	27
H_2O	18
NH_3	15*

* The peak at m/z 15 was chosen for ammonia since this was found to minimize errors arising from incomplete subtraction of the moisture peaks at m/z 16 and 17.

Table 3.6 Example of Printout from Mass Spectral Analysis Program 'MS Analysis'

RESULTS OF ANALYSIS OF M/SPEC. REF NO.11/8 RUN AT 668 K

SAMPLE= DL17/6

EXPT DATE= 11-6-85

PROGRAM RUN ON= 05-9-85

% FRACTION OF LINES (12-60) ANALAYSED = 98.5048157

PRESSURE FACTOR= 2.3

COMPONENT	% FROM CRACKING PATTERN	CORRECTED % (SUM=100)	RELATIVE AMOUNT OF COMPONENT (CORR.%*PFACTOR)
C2N2	1.96	1.99	4.58
HNCO	2.09	2.12	4.89
CO2	30.51	30.98	71.25
O2	.00	.00	.00
HCN	4.04	4.11	9.45
H2O	59.02	59.91	137.80
NH3	.85	.86	1.99

MASS NO.	RESPONSE	RESIDUAL LINES
12.0	.73	.05
14.0	.10	.02
15.0	.21	.00
16.0	3.38	.26
17.0	11.34	.00
18.0	46.44	.00
19.0	.43	.43
20.0	.08	.08
22.0	.21	.00
24.0	.10	.03
26.0	.77	.00
27.0	3.06	.00
28.0	2.70	.32
29.0	.06	.00
38.0	.10	.06
39.0	.10	.10
40.0	.15	.15
41.0	.32	.32
42.0	.43	.00
43.0	.86	.00
44.0	26.49	.00
45.0	.38	.38
46.0	.12	.12
52.0	1.33	.00

present in the adsorption system. A printout of a typical set of results is shown in Table 3.6.

3.1.4 Mass Spectra : Worked Example

In the previous section a typical printout of the computer analysis for a gas phase mixture was shown (Table 3.6). This analysis did not take account of the differing sensitivities of the mass spectrometer towards various compounds, nor did it attempt to determine the actual amounts of each component present. This section will describe how these results can be converted into semi-quantitative data which can then be used to interpret the reactivity of cyanogen with silica-supported copper and/or chromium oxide surfaces.

First it was necessary to compensate for the sensitivity of the mass spectrometer towards each gaseous component. This was done by multiplying $\%\Sigma_{i,j}$ values for each compound by the corresponding relative sensitivity factor (S_j) which had previously been experimentally determined. These corrected relative ion intensities were then expressed in percentage terms (Table 3.7).

Since the sum of the ion intensities for a compound is directly proportional to its relative partial pressure (Sec. 3.1.2) a knowledge of the total pressure of the gas mixture enables one to calculate from the data in the final column of Table 3.7 the actual partial pressures of

Table 3.7 Correction of Mass Spectral Results using Sensitivity Factors

Compound	$\%\Sigma_{i,j}$ (from Table 3.6)	Relative Sensitivity Factor (S_j)	Relative $\Sigma_{i,j}$	$\%\Sigma_{i,j}$ (corrected for sensitivity)
C_2N_2	1.99	1.54	3.06	3.06
HNCO	2.12	1.23	2.61	2.61
CO_2	30.98	0.80	24.78	24.75
HCN	4.11	0.65	2.67	2.67
H_2O	59.91	1.10	65.90	65.82
NH_3	0.86	1.27	1.09	1.09
			100.11	100.00

each gaseous compound. In this example the total pressure was 0.545 torr, and the resulting partial pressures are shown in Table 3.8.

Knowing the volume of the system ($V = 201 \times 10^{-6}$ m^3) and the temperature ($T = 293$ K), the partial pressures could be converted to molar quantities ($p_j = n_j RT/V$),

Table 3.8 Partial Pressures, Molar Quantities and Weights of Gaseous Compounds Present in Sample DL 17/6

(Total pressure = 0.545 torr; volume of system = 201 x 10^{-6} m^3; Temperature = 293 K)

Compound (Molecular weight)	Relative Partial Pressure	Actual Partial Pressure (torr)	No. of µmoles present	Weight present (µg)
C_2N_2 (52)	0.031	0.017	0.187	9.72
HNCO (43)	0.026	0.014	0.154	6.62
CO_2 (44)	0.247	0.135	1.480	65.34
HCN (27)	0.027	0.015	0.165	4.45
H_2O (18)	0.658	0.358	3.938	70.88*
NH_3 (17)	0.011	0.006	0.066	1.12

* Analyses with proportions of water tended to introduce errors, since water molecules adhere to the glass walls of the adsorption system. However, when the partial pressure of water remained well below its saturation vapour pressure (ca 18 torr at 298 K) then these errors were ignored.

and thence, if required, to the respective weights. These data are also shown in Table 3.8.

In the following sections the results are normally presented in tabular form showing the relative weights of each component in the gas phase as a function of different reaction conditions. In view of the many possible sources of error, the results should be regarded as semi-quantitative only. However, when considered in conjunction with infra-red spectroscopic studies, the results derived from mass spectral analysis as described above have greatly assisted the complex task of elucidating the nature of the reactions occurring over the supported oxides studied in this work. Furthermore, the results have enabled some progress to be made on C and N mass balance analysis, in spite of the fact that it was not possible to measure the N_2 content of gaseous mixtures (owing to N_2 being non-condensable in the conditions employed).

3.2 Infra-red Spectral Analysis

3.2.1 The Need for Computer-Assisted Data Handling and Processing

In this work, i.r. spectra were recorded by passing the beam through thin compressed discs of each sample mounted in an adsorption cell (Sec. 2.4.2). To perform certain sample treatments, for example outgassing, it was necessary to remove the disc from the beam. It was not possible to replace the sample exactly into its original

position and therefore subsequent spectra were measured through a different section of the disc. Since the disc was not of uniform thickness, the intensity of these spectra were usually significantly different from before. Furthermore, it was difficult to align the disc so that the whole of the beam passed through it and in some cases a fraction of the beam missed the sample altogether, with the result that spectra appeared to be weakened. These errors made it very difficult to make quantitative statements about band intensities simply by comparing series of spectra.

These problems were overcome by writing a computer program which standardised spectra one-to-another. In the following section, the chemical basis for this program is described and its method explained. In a later section the use of these results to derive difference spectra is shown and finally the reasons for presenting them in particular sequences are given.

3.2.2 Infra-red Spectral Standardisation Program

Spectral standardisation is normally carried out by reference to an internal or external standard. The choice of a standard was based on the considerations that the standard should:

1) be present in all samples;
2) not be affected during the adsorption process or ensuing reactions;

3) give a strong signal, therefore minimising errors in its measurement;

4) not be masked by spectral changes occurring during the reaction.

An internal reference based on the intensity of the 1869 cm^{-1} band of silica was chosen, this being ascribed to internal lattice vibrations (157,158). This spectral feature satisfied all the above conditions. The basis for this program was to measure the intensity of this band in a reference spectrum, designated A1, and then to standardise all other spectra so that the intensity of this band was the same in all cases.

The program entitled 'STD.OY', listed in Appendix V employs a spectroscopy programming language developed by Perkin Elmer. It was written as an OBEY file which consisted of a sequence of CDS-II and OBEY specific commands which were automatically executed on the Perkin Elmer 3600 Data Station (Sec. 2.4.1). To run the program, the reference spectrum and the series of spectra to be standardised had to be copied onto a floppy disc which also held a copy of 'STD.OY'. The operation of the program may be summarised by the following sequence of routines.

a) The contribution of the blank cell was subtracted from the reference spectrum.

b) A baseline correction was applied to the reference spectrum by setting the transmission level at 1200 cm^{-1} to 0.2%. (1200 cm^{-1} was

chosen because at this wavenmumber silica is known to absorb all incident infra-red radiation).

c) The standard spectrum was converted to absorbance units and the intensity of the 1869 cm^{-1} band was measured. This was done by calculating the difference between the absorbance values of 1968 and 1869 cm^{-1}. These wavenumbers were selected to represent the band maximum and minimum, respectively.

d) The reference spectrum was then converted back into transmission units and stored on the floppy disc.

e) The first spectrum to be standardised to the reference spectrum was corrected as in (a).

f) The minimum transmission of this spectrum was corrected to equal 0.2% transmission as in (b).

g) The spectrum was converted into absorbance units and the intensity of the 1870 cm^{-1} bond was measured as in (c).

h) The intensity of the spectrum was expanded or contracted by a factor such that the new intensity of the 1870 cm^{-1} band was of equal intensity to that in the reference spectrum.

i) The spectrum was shifted such that the absorption value at 4000 cm^{-1} equalled that in the reference spectrum.

j) The spectrum was converted back into transmission units and stored on the floppy disc.

k) Routines (e) to (j) were repeated until all remaining spectra were standardised.

l) Finally a short routine was performed which enabled the user to confirm that the spectra were correctly standardised by ensuring that the percentage transmission values at 4000 and 1200 cm^{-1} were equal in all spectra.

These standardised spectra produced were used either for presentation purposes or for the calculation of derivative spectra as described in the next section.

3.2.3 Presentation of Infra-red Spectra

Infra-red spectra of samples were recorded at various stages of pretreatment, reaction and subsequent outgassing. These results are presented in two distinct ways, either as percentage transmission (%T) spectra and usually also as absorbance difference spectra. To highlight spectral changes occurring throughout each reaction, selected spectra from each reaction were plotted sequentially on the same chart. For clarity and to avoid overlapping, these spectra were offset by pre-determined amounts. The ordinate scales shown are, therefore, not absolute but are graduated so that relative band intensities can be seen.

Presentation of standardised %T in this way highlighted spectral changes and simplified interpretation. However, there were still features which could not clearly be seen due to the masking effect of strong bands in the spectrum of the silica support. To overcome this problem, the appropriate reference spectrum (usually of the outgassed oxide) was subtracted from each standardised spectrum in that series, thereby cancelling out the silica bands. This subtraction was performed when both spectra were in the absorbance mode since the Beer-Lambert Law states that the concentration of an absorbing species is proportioned to $\log_{10} (I_o/I)$;

Absorbance = $\log(I_o/I)$ = kcd

where I_o = the intensity of the incident beam, and

I = the intensity of the beam after passing through a sample of thickness d and where c is the concentration of the absorbing species whose molar extinction coefficient is k.

Subtraction of the reference spectrum in this way gave rise to absorbance difference spectra. Sequential presentation of these spectra enabled semi-quantitative measurement even of weak bonds which would otherwise have been masked by the spectrum of the silica support. For clarity these spectra were offset to avoid overlapping of bands. The intensity of bands can be measured by reference to the graduated absorbance scale.

Spectra were usually replotted after applying digital smoothing to reduce signal noise. In some

instances difference spectra were derived using spectra other than the outgassed oxide as a reference. In these cases, a clear statement is given defining how the spectrum presented was derived.

4. RESULTS

The results to be reported in this section relate to the interaction of cyanogen with six different adsorbents, each pretreated in a series of different ways. The first set of experiments was carried out using pure silica to investigate the nature of the reaction between C_2N_2 and the uncoated support. The subsequent experiments were undertaken to study the reaction of C_2N_2 with the individually supported metal oxide systems CuO/SiO_2, CrO_3/SiO_2 and Cr_2O_3/SiO_2. The final two sets of results relate to studies of C_2N_2 interaction with the mixed metal oxide systems $CuO\text{-}CrO_3/SiO_2$ and $CuO\text{-}Cr_2O_3/SiO_2$. These experiments were carried out to compare and contrast the reactivity of the mixed metal oxides to that of the single metal oxide systems.

4.1 Blank Experiments

All of the results reported in this Thesis were obtained by contacting C_2N_2 with various silica-supported oxide samples contained in a glass vacuum frame. It was therefore considered pertinent to study the interaction of C_2N_2 with the glass vacuum frame including the metal parts of the microbalance, the sample bucket and with an outgassed Aerosil sample.

The glass vacuum frame including the microbalance was outgassed to $<1x10^{-5}$ torr overnight before admitting

pure cyanogen (at ~20 torr) to the system. After 12 h the gas pressure fell to 18.8 torr but there was no measurable weight change recorded on the microbalance. Analysis of the residual gas pressure revealed that the vacuum frame contained pure cyanogen. The gas was frozen into a liquid nitrogen cold trap (CT3, Fig. 2.1) and the system was evacuated to $<1x10^{-5}$ torr for 30 minutes. A pressure of 20 torr was generated when the contents of the trap were thawed. Analysis of the gas confirmed that only pure C_2N_2 was present. These results were explained by proposing that a small amount of cyanogen adsorbed onto the interior surfaces of the system and any adsorption onto the microbalance itself did not unbalance the reading. The generation of 20 torr pressure on thawing the cold trap suggested that any C_2N_2 which adsorbed onto the interior surfaces of the system could easily be removed by evacuation. Since no conversion of C_2N_2 took place when C_2N_2 adsorbed onto the glassware and since it did not interfere with gravimetric measurements it was not considered necessary to investigate the blank system further.

Similar studies were carried out using N_2,CO_2,H_2O and HCN. No reaction or adsorption occurred with N_2 or CO_2 but H_2O and HCN reversibly adsorbed in a similar manner to C_2N_2. The vacuum frame was therefore considered to be inactive towards chemical conversion of C_2N_2 and other key reaction products.

The interaction C_2N_2 with Aerosil was given more attention since there is some controversy concerning whether C_2N_2 reacts with silica surfaces at ambient temperature (Sec. 1.6.3.2). It is pertinent to recall that some researchers reported that surface-bound HCN is produced during interaction of C_2N_2 at 298 K (112,113) whilst others reported that no gaseous products are released. The discrepancy between these reports probably arose due to differences in the exact pretreatment of the silica specimens used. It was considered necessary to perform a blank experiment to ensure that any reaction products could be accounted for in subsequent experiments using silica-supports.

An Aerosil sample, outgassed at 673 K for 12 h was exposed to C_2N_2 at 295 K for 12 h. The gas phase was evacuated through a cold trap and the contents were thawed and analysed using the mass spectrometer. No evidence for gaseous components other than pure C_2N_2 was found even after outgassing at 673 K. This study was consistent with that reported by Williams (2) who investigated the interaction of HCN with outgassed silica using mass spectrometry and gas chromatography. He concluded that no reaction yielding gaseous products occurred except at temperatures above 673 K.

Blank experiments to study the interaction of C_2N_2 with outgassed and hydroxylated silica were also carried out using i.r. spectroscopy (Sec. 4.8)

4.2 Mass Spectrometric and Gravimetric Studies of Cyanogen Interaction with CuO/SiO_2

The results of previous work with supported CuO have been reviewed in Chapter 1. It is relevant to recall that when HCN is contacted with a surface containing cupric ions, at 323 K, C_2N_2 is released. The following experiments were carried out to investigate the interaction between C_2N_2 and silica-supported CuO.

4.2.1 Outgassed CuO/SiO_2

A blue sample of $Cu(NO_3)_2$-SiO_2 was outgassed at 673 K and 10 h. The black CuO/SiO_2 produced weighed 93.6 mg and contained 1.5 wt.% of copper. The material was found to have a specific surface area of 224 m^2 g^{-1}. A total of 440 μg C_2N_2 was adsorbed onto this sample after exposure to cyanogen gas at 13 torr and 291 K for 22 h., conditions subsequently denoted more briefly as 13 torr/291 K/22 h. Residual gas was analysed by freezing it into a liquid nitrogen cold trap until the sample reached a constant weight. The condensate was thawed into an enclosed section of the vacuum frame which incorporated a manometer and a leak valve to the mass spectrometer. A pressure of 1.22 torr was measured in a volume of 49 cm^3. A mass spectrum of the gas mixture was recorded and the line lengths at each m/z value, corrected for background interference, are shown in Table 4.1.

Table 4.1. Mass Spectrum of Condensable Products Recovered at 291 K from Outgassed CuO/SiO_2 after Cyanogen Contact

m/z	Line Length (arb. units)
12	2.52
13	0.03
14	0.69
15	0.50
16	0.38
17	2.67
18	10.92
24	2.44
26	8.09
27	3.73
28	9.43
29	0.23
32	0.09
38	1.55
39	0.15
40	0.15
41	0.11
42	0.19
43	2.01
44	0.89
52	53.13

The percentage of the total ion intensity, $\%\Sigma_{i,j}$ for each component was computed using the 'MS 1' and 'MS ANALYSIS' programs described in Chapter 3. The partial pressures of each component were calculated and converted to molar amounts and finally to the actual weights of each component (Table 4.2). It can be seen that the desorbate contained a high proportion of unreacted C_2N_2 (138 μg), but isocyanic acid (6 μg), water (6 μg) and traces of hydrochloric acid, carbon dioxide and ammonia were also measured. A total of 290 μg C_2N_2 remained irreversibly adsorbed, equivalent to 13.8 μg m^{-2}.

The CuO/SiO_2 was then outgassed at 433 K/10^{-3} torr/2 h and condensable products were collected in the cold trap. The major desorbate was C_2N_2 (109 μg), but with appreciable quantities of HNCO (13 μg) and HCN (13 μg). The supported copper oxide sample was then outgassed up to 513 K/2 h, 598/2 h and finally 693 K/9 h. Mass spectral analyses of the desorbates collected after each stage are shown in Table 4.3.

The weak peaks at m/z=41,40 and 39 which were observed after room temperature cyanogen contact and which were present in the mass spectra of gaseous samples collected up to 673 K are best explained by the presence of methyl cyanide, CH_3CN, (see Appendix VI). The formation of this product is surprising. However, support for the assignment is provided by Williams who reported that the hydrogenation product CH_4 was formed when HCN was reacted with a silica surface (2).

Table 4.2. Gravimetric Results Derived from the Mass Spectrometric Analysis of the Condensable Products Removed at 291 K from Outgassed CuO/SiO_2 after Cyanogen Contact

Component	$\%\Sigma_{i,j}$	Partial Pressure (torr)	Amount (μmol)	Mass (μg)
C_2N_2	74.61	0.9992	2.66	138.3
HNCO	4.62	0.049	0.13	5.6
CO_2	0.93	0.006	0.02	0.7
HCN	4.50	0.025	0.07	1.8
H_2O	13.30	0.126	0.34	6.1
NH_3	1.93	0.021	0.06	1.0

The weak peaks observed at m/z = 58,57,55,53 could have been due to $CH_3\overset{O}{\overset{\|}{C}}-NH_2$ or less probably due to $H_2N-\overset{O}{\overset{\|}{C}}-NH_2$. These species would be expected to exhibit peaks at m/z=44,43,28,16 and 15. In the current work peaks due to CO_2, HNCO and NH_3 would have obscured these bands.

4.2.2 Hydroxylated CuO/SiO_2

133.6 mg of blue $Cu(NO_3)_2/SiO_2$ was outgassed (673 K/12 h). The 118.93 mg of black CuO/SiO_2 produced was then exposed to water vapour for 0.5 h whereupon it assumed a purple coloration. Gaseous phase and physically adsorbed water were removed by freezing it into a cold trap until the sample maintained a constant weight. The irreversible uptake of water was 520 μg,

Table 4.3 Condensable Products Released from Outgassed CuO/SiO_2 after Cyanogen Contact at 291 K

Outgassing Temperature (K)	Mass (μg)						
	C_2N_2	HNCO	CO_2	HCN	NH_3	H_2O	Other
291	138.3	5.6	0.7	1.8	1.0	6.1	*1
433	109.2	13.0	1.8	12.7	1.0	7.8	*1
513	41.4	9.2	1.4	7.0	0.8	4.1	*1
598	31.4	15.2	1.9	5.0	1.0	6.6	*2
693	8.0	7.7	1.5	1.2	0.9	6.5	*3
μg product released above 291 K	190.0	45.1	6.6	25.9	3.7	25.0	-
μg m^{-2} released above 291 K	9.06	2.15	0.31	1.24	0.18	1.19	-

*1 weak peaks at m/z 41,40,39

*2 weak peaks at m/z 41,40,39,31

*3 weak peaks at m/z 58,57,55,53,41,40,39,31

equivalent to 19.5 μg m^{-2}. C_2N_2 was then dosed at 10 torr/18 h and the sample was again allowed to reach a constant weight (121.32 mg). The residual gaseous phase was analysed and found to contain pure C_2N_2; this was frozen into a cold trap and discarded. The sample was then evacuated until it reached a constant weight (120.73 g). Analysis of the condensate showed that H_2O and C_2N_2 were the main desorbates (Table 4.4). Computer analysis of the mass spectrum revealed residual peaks at m/z 31, 30 and 29. These are best explained by the presence of CH_3NH_2 which has the following ions in its cracking pattern: $[CH_3NH_2]^+$, m/z = 31; $[CH_2NH_2]^+$, m/z = 30; $[CH_3N]^+$, m/z = 29. Other peaks expected in the mass spectrum of CH_3NH_2, e.g. 28, 27, 26, 16 and 15, were so weak as to be unresolved from the more intense spectrum of C_2N_2. The sample was 1280 μg heavier after cyanogen contact than after the hydroxylation step; however, since some moisture was released when the cyanogen-exposed sample was evacuated, it was evident that the irreversible uptake of C_2N_2 was greater than the 1280 μg (equivalent to at least 48.1 μg m^{-2}).

The sample was again evacuated and heated to 425 K/2h with condensable products being collected in the cold trap. These conditions caused several milligrams of a white powder to sublime onto the inside of the glass walls of the microbalance hang down tube. A sample of the white sublimate was recovered at the end of this experiment and analysed using a VG 7070E Analytical

equivalent to 19.5 μg m^{-2}. C_2N_2 was then dosed at 10 torr/18 h and the sample was again allowed to reach a constant weight (121.32 mg). The residual gaseous phase was analysed and found to contain pure C_2N_2; this was frozen into a cold trap and discarded. The sample was then evacuated until it reached a constant weight (120.73 g). Analysis of the condensate showed that H_2O and C_2N_2 were the main desorbates (Table 4.4). Computer analysis of the mass spectrum revealed residual peaks at m/z 31, 30 and 29. These are best explained by the presence of CH_3NH_2 which has the following ions in its cracking pattern: $[CH_3NH_2]^+$, m/z = 31; $[CH_2NH_2]^+$, m/z = 30; $[CH_3N]^+$, m/z = 29. Other peaks expected in the mass spectrum of CH_3NH_2, e.g. 28, 27, 26, 16 and 15, were so weak as to be unresolved from the more intense spectrum of C_2N_2. The sample was 1280 μg heavier after cyanogen contact than after the hydroxylation step; however, since some moisture was released when the cyanogen-exposed sample was evacuated, it was evident that the irreversible uptake of C_2N_2 was greater than the 1280 μg (equivalent to at least 48.1 μg m^{-2}).

The sample was again evacuated and heated to 425 K/2h with condensable products being collected in the cold trap. These conditions caused several milligrams of a white powder to sublime onto the inside of the glass walls of the microbalance hand down tube. A sample of the white sublimate was recovered at the end of this experiment and analysed using a VG 7070E Analytical

Table 4.4 Condensable Products Released from Hydroxylated CuO/SiO_2 after Cyanogen Contact at 291 K

Outgas Temp.	Mass of Product Released (μg)							
(K)	C_2N_2	HNCO	CO_2	HCN	NH_3	H_2O	CH_3NH_2	Other
291	7.5	0.2	0.2	0.2	0.8	9.9	0.9	0
425	3.2	17.4	0.7	2.8	1.0	11.4	1.3	0.6*[1] plus oxamide
523	2.2	2.9	0.5	1.8	0.7	12.8	1.0	*[2]
602	0.9	2.3	1.1	1.9	0.8	23.5	1.3	*[2]
673/1 h	0.4	0.8	3.3	1.3	0.2	3.8	0.4	0.3*[3]
673/15 h	0.9	0.9	4.5	0.1	1.1	31.5	1.5	0.2*[4]
Total released above 291 K (μg)	7.6	24.3	10.1	7.9	3.8	83.0	5.5	1.1
(μg m^{-2})	0.29	0.91	0.38	0.30	0.14	3.12	0.21	0.04

*[1] 0.6 g of organic species characterised by peaks at m/z = 60, 59, 58, 56, 55, 54, 53, 45, and 41

*[2] weak peaks as in *[1]

*[3] mainly due to m/z = 45

*[4] peaks as in *[1] plus additional ones at m/z 51, 50, 46, 40, 39, 38.

Mass Spectrometer. A sample of oxamide (BDH) was also analysed. Mass spectral data for the white sublimate and for oxamide are presented in Table 4.5. Comparison of the spectra confirmed that the white sublimate contained a high proportion of oxamide.

Mass spectrometric analysis of the thawed contents of the cold trap showed that HNCO was the major product (17 μg), whilst H_2O (11 μg) and C_2N_2 (3 μg) were also released. Assuming a sensitivity factor of 1 for organic compounds, then approximately 1 μg of CH_3HN_2 and 0.6 μg of other organic species were also present. The peaks at m/z = 60 down to 54 could have been caused by NH_2CO_2H and H_2N-CO-NH_2 whilst the one at m/z 45 was probably due to formamide ($HCONH_2$, or the M-1 ion of formic acid (HCO_2H). Water was the major product released on outgassing to 523, 602 and 673 K, but it is likely that some of this was due to moisture released from the glassware. For this reason the masses shown in Table 4.4 were treated with suspicion. 8 μg of CO_2 were also released when the sample was heated above 602 K.

By calculating the amount of carbon in each of the gaseous products released between 425 and 673 K, the total weight of carbon released was found to be 19.3 μg. Since a total of 590.8 μg carbon was irreversibly adsorbed as C_2N_2 (i.e. 1280 μg C_2N_2 uptake), then 590.8 - 19.3 = 571.5 μg carbon was either converted to a sublimate, or was held on the surface at 673 K, or was

Table 4.5 The Mass Spectrum of the Sublimate Released from Cyanogen - Contacted Hydroxylated CuO/SiO_2 and of Oxamide

m/z	Relative Peak Height (%) White Sublimate	Oxamide
27	2.5	2.3
28	7.5	27.1
29	4.3	3.3
41	5.8	1.0
42	2.5	1.8
43	18.8	8.8
44	100.0	100.0
45	52.1	65.5
60	26.9	38.0
88	32.9	35.2
89	-	1.7
100	0.5	-
107	0.6	-

lost in non-condensable products. Assuming that the entire 571.5 µg was converted to oxamide, then 2.09 mg of oxamide was produced. This was equivalent to forming 78.6 µg oxamide per m^2 surface. However, i.r. studies (Sec. 4.9.2) revealed that some carbon was retained on the surface as Si-CN and Cu-CN species.

4.2.3 Hydroxylated CuO/SiO_2 Containing Excess Adsorbed Water Vapour

A 124.83 mg sample of CuO/SiO_2 was prepared by outgassing $Cu(NO_3)_2$-SiO_2 at 673 K/12 h. The sample was exposed to water vapour for 0.5 h, and excess vapour was then removed by pumping through a cold trap until 3.1 mg of water was retained on the surface (equivalent to 110.9 $\mu g\ m^{-2}$ surface). The bright yellow sample was exposed to 15 torr C_2N_2 at ambient temperature for 15 h; it increased in weight by a further 3.2 mg. The residual gaseous phase was frozen into a cold trap until no further weight change could be detected; a total of 2.02 mg of material desorbed from the CuO/SiO_2. The cold trap contained 86 µg of H_2O with considerable amounts of HCN, HNCO, CO_2 and NH_3 in addition to about 6.6 mg C_2N_2 (Table 4.6). Evacuation of the powder at 291 K/10^{-3} torr caused a further weight loss of about 200 µg, the desorbate being mainly H_2O and C_2N_2. 4.08 mg of adsorbed material resisted evacuation. From the weight of water irreversibly adsorbed and measurement of the amount desorbed after evacuation of the cyanogen-exposed sample, it was calculated that at least 980 µg (equivalent to 35 $\mu g\ m^{-2}$) of the irreversibly held material was derived from the irreversibly held C_2N_2. The actual amount of C_2N_2 probably exceeded this but any additional weight increase was offset by the simultaneous release of moisture.

Outgassing from 288 to 412 K caused the sublimation of a large quantity of white product, presumably oxamide. 181 μg of HNCO was collected in the cold trap together with 120 μg H_2O, 50 g HCN and lesser amounts of CO_2, C_2N_2 and NH_3. Water was the dominant product released when the sample was outgassed at temperatures up to 678 K. A significant feature of this experiment was that relatively large quantities of C_2N_2, HNCO, CO_2, HCN and NH_3 were released above ambient temperature. A complete analysis of the gaseous products collected at each stage of this experiment is shown in Table 4.6.

Using a similar approach to that described in Section 4.2.2, the maximum amount of oxamide produced was calculated as 1.10 mg, equivalent to 39.4 μg of oxamide produced per m^2 surface.

4.3 Mass Spectrometric and Gravimetric Studies of Cyanogen Interaction with CrO_3/SiO_2

Davies (4) reported that when HCN or C_2N_2 were reacted with CrO_3/SiO_2 surfaces, amides were key products. He provided evidence which showed that at elevated temperatures surface amides reacted in two distinct ways: (a) Loss of nitrogen to produce surface carbonate and ultimately CO_2; (b) desorption of amide products containing C-C bonds.

Starting from HCN, reaction (b) was possible only after combination of two $CONH_2$ moieties to form a

Table 4.6 Condensable Products Released from Hydroxylated CuO/SiO_2 Containing Excess Adsorbed Water Vapour after Cyanogen Contact at 288 K

Outgas Temp. (K)	Mass of Product Released (μg)						
	C_2N_2	HNCO	CO_2	HCN	H_2O	NH_3	Other*2
*1	6586.5	14.2	10.2	29.9	85.6	8.5	
291	76.1	1.5	1.3	1.4	142.2	2.9	
412	12.8	180.3	22.3	50.2	121.8	4.2	oxamide
508	6.1	27.2	6.5	6.4	120.6	7.2	
572	10.1	34.3	13.8	18.6	95.3	2.8	
678	4.5	21.2	36.0	17.4	205.4	3.3	
Total μg released above 291 K	33.5	263.5	78.6	92.6	548.1	12.5	
(μg m^{-2})	1.20	9.43	2.81	3.31	19.61	0.45	

*1 Condensable products of residual gas phase in contact with CuO/SiO_2 after C_2N_2 contact

*2 Weak peaks at m/z 45,31,30,29 were seen in all spectra.

diamide or combination of a $CONH_2$ and a CN moiety to yield a cyanoamide product.

It was decided to investigate the effect of adsorbed water on the uptake and conversion of C_2N_2, over CrO_3/SiO_2 samples since this would be expected to

influence the hydrolysis reactions. To draw comparative conclusions between hydroxylated, oxygenated and outgassed surfaces and to link the findings into the studies of C_2N_2 adsorption over other surfaces in the present work, it was considered necessary to repeat some experiments reported by Davies (4).

Mass spectrometer studies on CrO_3/SiO_2 samples were carried out using an A.E.I. MS10 spectrometer. These results were less detailed than ones obtained using the VG Masstorr FX spectrometer which was used in all other work presented in this thesis. For this reason less importance is assigned to these results.

4.3.1 Outgassed CrO_3/SiO_2

A 52.7 mg sample of CrO_3/SiO_2 was prepared by outgassing a dried slurry of chromium trioxide and silica at 698 K/12 h. (Sec. 2.7). The specific surface area of a similar sample was found by nitrogen adsorption at 77 K to be 273 $m^2\ g^{-1}$. Exposure of the cooled yellow-brown powder to C_2N_2/18 torr resulted in an increase in weight which became steady when 0.94 mg C_2N_2 had adsorbed. When this sample was evacuated to below $1x10^{-3}$ torr, the weight of the sample reduced to 53.34 mg. The amount of C_2N_2 irreversibly held was 0.67 mg, equivalent to 47.0 µg m^{-2} (Davies reported a figure of 57.0 µg m^{-2} (4). Analysis of the gas phase which had been condensed into the cold trap after adsorption at room temperature confirmed that no decomposition of C_2N_2 had occurred.

This was in contrast to Davies' work which showed that small amounts of HCN and H_2O were returned to the gas phase at 293 K.

The results of outgassing the cyanogen contacted sample at a series of elevated temperatures have been presented in Table 4.7. The main observations are listed below.

1) Desorption between 298-698 K showed that HNCO and C_2N_2 were the most abundant products and that considerable amounts of HCN, H_2O and CO_2 were also formed. Davies did not mention the presence of HNCO in his results over Cr(VI) surfaces, this was probably due to his incomplete interpretation of his mass spectral data since he commented on the presence of 'significant peaks' at m/z 43 and 42 which are ascribed to HNCO in this work.

2) In agreement with the results obtained by Davies, a peak at m/z 31 was present in the mass spectra of condensates collected by desorbing above 298 K. Further peaks at m/z 45,41,40,39 and 38 were observed when analysing desorbates collected at higher temperatures. These are best explained by the presence of $HCOCH_3$ and CH_3CN.

3) In agreement with Davies, very little HCN or C_2N_2 was desorbed above 567 K and small amounts of NH_3 were recorded during the experiment.

4) A mass balance revealed that 670 μg of C_2N_2 was irreversibly absorbed. This contained 309 μg of

Table 4.7 Condensable Products Released from Outgassed CrO_3/SiO_2 after Cyanogen Interaction at 298 K

Outgassing Temp. (K)	Mass of Product Released (μg)						
	C_2N_2	HNCO	CO_2	HCN	NH_3	H_2O	Other
298-448	85.6	64.9	12.0	34.9	0.3	13.0	*1
567	15.6	43.7	18.9	19.9	0.6	23.7	*2
638	0.5	3.3	1.2	0.8	0.1	2.9	*2
698	0.5	2.7	1.4	0.7	0.1	3.4	*3
Total released above 298 K (μg)	102.2	114.6	33.5	56.3	1.1	43.0	
μg m^{-2} released	7.1	8.0	2.3	3.9	0.1	3.0	

*1 Peaks at m/z 45, 31 and 30
*2 Peaks at m/z 45, 41, 40, 39, 38 and 31
*3 Peaks at m/z 41, 40, 39, 38, 31 and 30

carbon, yet only 113 μg of carbon were recovered as condensable gases. Davies also reported a considerable inbalance between irreversibly adsorbed C_2N_2 and desorbed product, he explained this with reference to the loss of non-condensable products.

4.3.2 Oxygenated CrO_3/SiO_2

A 37.0 mg sample of CrO_3/SiO_2 was prepared as described earlier (Sec. 4.3.1). The brown-green powder was oxygenated by heating in oxygen (100 torr/673 K/12 h - see Sec. 2.7). This produced a yellow powder in which the surface chromium was all expected to be in the hexavalent state. The yellow powder was cooled to room temperature and C_2N_2 was dosed at 20 torr/12h. Initial uptake of C_2N_2 was slow but the rate of weight increase became faster. This result was consistent with the findings of Davies who studied the effect of increasing the C_2N_2 pressure in a stepwise manner. He concluded that oxidation blocked sites available for cyanogen uptake but as the reaction progressed some surface oxygen was consumed creating more sites available for C_2N_2 uptake (4). Gas phase C_2N_2 was removed by pumping through a cold trap and a total of 404 μg C_2N_2 irreversibly adsorbed, equivalent to 40 μg m^{-2}. The results of outgassing this sample were not clear due to oxidation of the filament in the mass spectrometer. The only positive result relating to the gas phase analysis was that large quantities of CO_2 were evolved and a small amount of C_2N_2 was also recovered. On heating the sample to 673 K the sample colour changed to green suggesting that the chromium was reduced to the trivalent state and a small amount of white sublimate, presumably oxamide, was observed.

In a second experiment CrO_3/SiO_2 was oxygenated at 673 K as before and exposed to C_2N_2 at 295 K in the presence of residual oxygen. The sample was then heated to 423 K in the oxygen-cyanogen atmosphere before being cooled to 295 K and evacuated. The results of mass spectrometric analysis of the gas phase collected at 298 K and of condensable product released at a series of higher outgassing temperatures are shown in Table 4.8.

The key results of the experiment were that H_2O and other hydrogen containing species were desorbed by 423 K. Relatively little C_2N_2 was desorbed above 298 K and indeed the prominent gaseous product released was CO_2. The peak at m/z=30 detected in the spectra of all desorbates collected above 298 K is best explained by the presence of the oxidation product NO. On heating above 703 K a trace of white sublimate was deposited onto the glass walls of the microbalance hang-down tubes. Finally, the colour of the sample changed from yellow to green on evacuating from 658-703 K.

4.3.3 Hydroxylated CrO_3/SiO_2

A 64.35 mg sample of outgassed CrO_3/SiO_2 with a surface area of 17.6 m^2 was exposed to water vapour at 18 torr/2 h. Residual water vapour was evacuated, leaving 2.1 mg of water irreversibly adsorbed, equivalent to 120 $\mu g\ m^{-2}$. Cyanogen was dosed at 20 torr until equilibrium was reached, the sample was then evacuated to remove residual gas. The irreversible cyanogen uptake was

Table 4.8 Relative Amounts of Condensable Products Released from Oxygenated CrO_3/SiO_2 after Heating in C_2N_2-O_2 at 423 K.

Outgassing Temp. (K)	Mass of Product Released (μg)						
	C_2N_2	HNCO	CO_2	O_2	HCN	H_2O	Other
298	70.1	0.1	1.5	27.5	0.3	0.3	-
423	9.3	0.8	1.2	14.3	0.7	18.6	*1
508	1.0	0.05	0.9	1.2	0.2	1.6	*1
578	0.1	0.1	4.4	1.5	0.6	3.2	*1
688	0.1	0.1	8.7	0.0	0.0	4.2	*1
733	0.0	0.1	5.7	0.0	0.0	2.7	*1,*2
Relative amount released above 298 K	10.5	1.15	20.9	17.0	1.5	30.3	

*1 Large peak at m/z = 30

*2 Trace of white sublimate

0.05 mg, equivalent to 2.8 μg m^{-2}. This was a surprisingly low amount which was probably due to blockage of active adsorption sites by adsorbed water molecules. The relative amounts of condensable gases released from the C_2N_2-exposed hydroxylated CrO_3/SiO_2 sample at a series of outgassing temperatures are presented in Table 4.9.

Table 4.9 Relative Amounts of Condensable Products Released from Hydroxylated CrO_3/SiO_2 after C_2N_2 Contact at 298 K

Outgassing Temp. (K)	Relative Amounts of Condesable Product						
	C_2N_2	HNCO	CO_2	HCN	H_2O	NH_3	Other
298	12.2	0.4	0.1	0.2	79.5	0.5	-
493	1.7	1.2	3.9	0.3	66.2	0.6	-
563	28.4	1.1	67.4	3.3	0.0	7.2	*1
633	0.0	0.0	0.0	0.0	156.0	0.0	*1
693	1.0	0.6	11.8	0.0	8.2	0.1	*1
Total released above 298 K	31.1	2.9	83.1	3.6	230.4	7.9	

*1 significant peak at m/z 30

The important results in this study were that with the exception of water, carbon dioxide was the main condensable desorbate. Furthermore a considerable amount of C_2N_2 was desorbed below 563 K. The only hydrolysis product released was HNCO but this was only in relatively small quantities. No white sublimate was observed despite the high level of surface hydroxylation.

4.3.4 Oxygenated-Hydroxylated CrO_3/SiO_2

A CrO_3/SiO_2 sample was pretreated with oxygen and

water vapour as described in Section 2.7. The sample was exposed to cyanogen 20 torr/12 h. The main features recorded when the sample was outgassed at a series of temperatures were as follows:

1) HNCO and CO_2 were released below 473 K,
2) On outgassing to 643 K a faint white smear formed on the cooler parts of the microbalance case above the specimen,
3) The sample changed colour from yellow/brown to green during the sublimation process.

Detailed spectroscopic data were lost during this experiment due to instrument breakdown.

4.4 Mass Spectrometric and Gravimetric Studies of Cyanogen Interaction with Cr_2O_3/SiO_2

No studies of the interaction of C_2N_2 with Cr_2O_3/SiO_2 have previously been reported. It was decided to investigate this subject to identify how C_2N_2 and supported Cr(III) ions react and to compare the results to studies of HCN interaction with unsupported α-chromia (3) and silica-supported chromia (4).

Surman (3) found that HCN reacted with α-chromia even at room temperature to produce CO and N_2. I.r. spectroscopic studies revealed that reaction occurred via the formation of surface amides. These were thought to occur by some form of condensation reaction with surface hydroxyl groups.

Using Cr_2O_3/SiO_2, containing 5 wt % Cr, Davies (4) also reported oxidation of HCN to CO_2 and N_2. Surface amides were again cited as the intermediates, but unlike Cr(VI) no amide species were desorbed.

The results presented in the following section using Cr_2O_3/SiO_2 and C_2N_2 complement the studies using HCN.

4.4.1 Outgassed Cr_2O_3/SiO_2

A 96.4 mg sample of Cr_2O_3/SiO_2 was prepared by outgassing $Cr(NO_3)_3$-SiO_2 at 698 K/15 h. The specific surface area was found by nitrogen adsorption to be 227 $m^2\ g^{-1}$. Exposure of the brown-green sample to C_2N_2/30 torr/12 h resulted in an uptake of 1.737 mg C_2N_2. Residual gas phase cyanogen was removed by freezing it into a cold trap leaving 710 µg C_2N_2 still adsorbed. On evacuation to below 10^{-3} torr, the sample weight reduced by a further 80 µg. This desorbate was collected and found to be mainly C_2N_2 with a trace of HCN and H_2O. The remaining 630 µg of irreversibly held C_2N_2 was equivalent to 28.8 µg m^{-2} of sample or 3.34×10^{17} C_2N_2 molecules per m^2.

The result of outgassing the cyanogen-contacted sample at a series of elevated temperature is shown in Table 4.10. The main observations were that approximately 50% of the irreversibly held C_2N_2 was released unchanged and that in agreement with previous

studies of HCN interaction with Cr_2O_3/SiO_2 there were no hydrolysis products released.

Table 4.10 Condensable Products Released from Outgassed Cr_2O_3/SiO_2 after Cyanogen Exposure at 289 K

Outgassing Temperature (K)	Mass of Product Released (μg)				
	C_2N_2	CO_2	HCN	NH_3	H_2O
*1	157.1	-	0.06	-	0.1
289-417	151.9	13.4	14.7	0.2	-
417-504	48.7	17.7	15.5	0.3	-
504-604	28.4	39.8	17.8	2.9	-
504-673/1 h	13.0	40.1	10.6	6.7	0.1
504-673/12 h	71.5	87.4	15.9	18.4	0.9
μg released above 289 K	313.5	198.4	74.5	28.5	1.0
μg m^{-2} released above 298 K	14.3	9.1	3.4	1.3	0.5

*1 Analysis of condensate evacuated from sample at 298 K after condensing residual gas phase

4.4.2 Hydroxylated Cr_2O_3/SiO_2

A 102.9 mg sample of $Cr(NO_3)_3/SiO_2$ was outgassed at 673 K/12 h. The resultant brown-green Cr_2O_3/SiO_2 weighed 89.9 mg. The surface area found by nitrogen adsorption was 20.4 m^2, corresponding to a specific surface area of 227 $m^2\ g^{-1}$. 1.02 mg (equivalent to 50.0 $\mu g\ m^{-2}$) of water was irreversibly held after hydroxylation/evacuation at room temperature. The hydroxylated pale brown sample adsorbed 2.02 mg C_2N_2 when exposed to C_2N_2 at 20 torr /18 h. After evacuation at 293 K, the sample was 1.17 mg heavier than the hydroxylated sample; however, the actual irreversible uptake of C_2N_2 was higher than this since the condensate recovered from the sample contained some water vapour and traces of CO_2, NH_3, HNCO and HCN. Thus it was concluded that at least 1.17 mg (equivalent to 57.32 $\mu g\ m^{-2}$) was irreversibly adsorbed.

Analysis of the desorbates collected by outgassing at higher temperatures is shown in Table 4.11. The major product desorbed on outgassing to 418 K was HNCO, although large amounts of C_2N_2, HCN and water were also released. By 523 K, water was the main desorbate, but the level CO_2 desorption had also increased. Carbon dioxide was the major product released at 523-590 K but in the range 590-673 K release of this gas declined and water again became the prominent desorbate. A total of 269.7 $\mu g\ H_2O$ was released above 670 K (a significant proportion of this was thought to be due to dehydration from the silica-glass vacuum frame).

Table 4.11 Condensable Products Released from Hydroxylated Cr_2O_3/SiO_2 after Cyanogen Exposure at 293 K

Outgassing Temperature (K)	Mass of Product Released (μg)					
	C_2N_2	HNCO	CO_2	HCN	H_2O	NH_3
Evac. at 293 K	135.6	2.4	1.1	1.0	64.3	-
293-418	89.0	148.7	8.3	61.7	56.3	4.7
418-523	19.5	11.4	41.6	6.8	213.1	4.0
523-590	11.1	6.9	90.4	6.4	46.3	2.1
590-670	11.2	6.9	66.7	4.5	72.7	1.1
670-673/12 h	12.3	7.3	47.6	0.9	269.7	6.9
μg released above 293 K	143.1	181.2	254.6	80.3	658.1	18.8
μg m^{-2} released above 293 K	7.0	8.9	12.5	3.9	32.2	0.9

The 1170 μg C_2N_2 irreversibly held at 293 K contained 540 μg carbon. Only 41.1% of this was recovered in the form of condensable gases. The remainder was either lost as non-condensable products or was retained by the surface after outgassing to 673 K /12 h.

4.4.3 Hydroxylated Cr_2O_3/SiO_2 Containing Excess Adsorbed Water Vapour

A 141 mg sample of $Cr(NO_3)_3/SiO_2$ was outgassed at 673 K/15 h. The resultant Cr_2O_3/SiO_2 sample weighed 121.7 mg and had a surface area of 27.6 m^2. Water vapour was adsorbed onto this material, and residual gas phase H_2O was then frozen into a cold trap leaving 2-3 mg (equivalent to 83.2 μg m^{-2}) of adsorbed water. On exposure to 20 torr C_2N_2/12 h the sample weight increased by a further 640 μg. The entire gas phase was frozen into a cold trap, and analysis of the condensate revealed traces of HNCO and NH_3 in addition to HCN, CO_2 and H_2O (Table 4.12, top line). The adsorption system was then evacuated at 293 K to remove unreacted H_2O and C_2N_2 from the surface. The cyanogen-challenged evacuated sample was lighter than after the hydroxylation treatment, so that the weight of C_2N_2 adsorbed was less than the weight of H_2O desorbed. The amount of C_2N_2 irreversibly adsorbed was therefore not measurable from these micro-balance results.

A white product sublimed when the sample was evacuated up to 403 K, and the amount of this sublimate increased on raising the temperature to 501 K. Analysis of the gases released at a series of increasing temperatures is shown in Table 4.12.

The general features noticed during outgassing above 293 K were as follows:

1) release of 818 μg moisture;

2) release of 63 μg cyanogen;

3) sublimation of oxamide below 403 K, accompanied by release of HNCO;

4) desorption of CO_2, notably above 501 K.

From the amounts of water released on outgassing to 668 K an estimation of the irreversible uptake of cyanogen by outgassed Cr_2O_3/SiO_2 was possible using the following data:

Weight of outgassed Cr_2O_3/SiO_2..... 121.70 mg

Weight of sample after hydroxylation and irreversible C_2N_2 uptake.....122.93 mg

Weight of irreversibly held H_2O and C_2N_2.....1230 μg

Weight of H_2O desorbed up to 668 K.....818 μg

Assuming that all of the irreversibly adsorbed water was desorbed unchanged, then the weight of irreversibly adsorbed C_2N_2 was 1230 - 818 = 412 μg. Since some of the adsorbed water did react, it can be stated that the irreversible C_2N_2 uptake was less than 412 μg, equivalent to <14.9 μg m^{-2} surface.

Knowledge of the amount of cyanogen irreversibly adsorbed also made it possible to estimate the amount of oxamide produced. This calculation was based on the following data:-

Irreversible uptake of cyanogen.....>412 μg

Irreversible uptake of carbon atoms in the form of cyanogen.....>190 μg

Weight of carbon contained in condensable products.....125 μg

From these results the amount of carbon available for oxamide formation was at least 65 μg. Assuming that all of this carbon was converted to oxamide then the amount of oxamide produced was at least 238 μg [i.e. > (88/24) x 65 μg], equivalent to 8.62 μg m^{-2}.

Table 4.12 Products Released from Hydroxylated-Hydrated Cr_2O_3/SiO_2 after C_2N_2 Contact at 293 K

Outgassing Temperature (K)	Mass of Product Released (μg)						
	C_2N_2	HNCO	CO_2	HCN	NH_3	H_2O	Other
Condensate at 293 K	91.8	2.1	1.0	1.6	2.2	178.0	-
293-403	36.4	16.7	13.1	6.8	3.5	235.0	oxamide
403-501	15.5	20.7	53.2	3.1	2.3	257.7	oxamide
501-573	8.3	16.1	163.7	0.9	1.0	125.9	-
573-668	3.2	15.3	34.0	-	0.6	199.1	-
μg released above 293 K	63.4	68.8	264.0	10.8	7.4	817.7	
μg m^{-2} released above 293 K	2.3	2.5	9.6	0.4	0.3	29.6	

4.5 Mass Spectrometric and Gravimetric Studies of Cyanogen Interaction with $CuO-CrO_3/SiO_2$

The interaction of HCN with the $CuO-CrO_3/SiO_2$ system has been studied by Davies (4) who found that surprisingly little C_2N_2 was released when compared to

Cu^{2+}/SiO_2 or Cu^{2+}-Cr^{3+}/SiO_2 samples. Furthermore, the two metal ions did not react independently as in the case of Cu^{2+}-Cr^{3+}/SiO_2 surfaces. Indeed, the combination of Cu^{2+}-Cr^{3+} was more oxidising than a CrO_3/SiO_2 sample. Davies studied the effect of various pretreatments and concluded that hydration further suppressed C_2N_2 desorption. As there had been no investigation of the interaction of C_2N_2 with the Cu^{2+}-Cr^{6+} system and since this combination provided unexpected results in HCN adsorption studies, it was decided to investigate this system in some detail.

4.5.1 Outgassed CuO-CrO_3/SiO_2

A mixture of $Cu(NO_3)_2$-CrO_3/SiO_2 was prepared as described in Section 2.7. After outgassing at 698 K/12 h, 84.83 mg of dark brown powder, CuO-CrO_3/SiO_2, containing 1.5 wt. % of Cr and 1.5 wt. % of Cu was obtained. The material was found to have a specific surface area of 193.0 m^2g^{-1}. The powder was exposed to C_2N_2 at 20 torr until a constant weight (86.00 mg) was reached. Evacuation of the residual gaseous phase at 298 K revealed that 570 µg C_2N_2, equivalent to 35 μgm^{-2} was irreversibly adsorbed. The condensed gas contained 599 µg of C_2N_2 and 1 µg of HCN. The lack of any desorbed reaction products was consistent with the work carried out by Davies (4) who reported that pure HCN was desorbed from an identical sample which had been interacted with HCN.

Analysis of the condensates collected when the sample was evacuated at a series of higher temperatures upto 703 K are shown in Table 4.13. The results show that the outgassed sample is active in converting C_2N_2 to oxidation and hydrolysis products below 468 K. Examination of the mass spectrum after subtracting the contributions of C_2N_2, HNCO, CO_2, HCN and H_2O from corresponding m/z values a series of peaks were evident at m/z 45,41,40,39,31 and 30. Formamide, methylamine and ethylamine are the most likely species responsible for these observations (see Appendix VI). After taking into account relative peak heights and allowing for the fact that some peaks were masked by other species present in the mixture the compounds which best fitted the results were CH_3CN and CH_3NH_2. At higher temperatures the amounts of HNCO, CO_2, HCN and organic species which desorbed were much higher than below 468 K. The most abundant condensable reaction product released throughout the experiment was HNCO, closely followed by CO_2.

Comparison between the amount of C_2N_2 irreversibly adsorbed and the masses of carbon and nitrogen recovered as condensable gases revealed that only 52% of the irreversibly held carbon and 40% of the nitrogen was measured. The sample was green-black at the end of the experiment.

Table 4.13 Condensable Products Released from Outgassed CuO-CrO_3/SiO_2 After Cyanogen Challenge at 298 K

Outgas Temp (K)	Mass of Product Released (μg)						
	C_2N_2	HNCO	CO_2	HCN	H_2O	Organics	Comments
*1	6935.7	0.0	0.0	10.9	0.0	0.0	-
468	86.8	12.7	7.4	3.3	0.9	1.0	*2
586	41.3	29.3	27.1	15.6	1.1	7.1	*3
703	27.9	29.5	33.6	33.6	8.9	0.9	*3
Total released above 302 K (μg)	156.0	71.5	68.2	27.7	2.9	19.4	
μg m^{-2} released above 302 K	9.5	4.4	4.2	1.7	0.2	1.2	

*1 Analysis of residual gas phase after C_2N_2 contact at 302 K

*2 Residual peaks at m/z 45,41,40,39,31 and 30

*3 Peaks as *2 plus ones at m/z 16,15, and 14

4.5.2 Oxygenated $CuO-CrO_3/SiO_2$

The adsorption and reaction of C_2N_2 on oxygenated $CuO-CrO_3/SiO_2$ was studied using a 75.4 mg outgassed sample. Oxygenation at 673 K/12 h caused the colour of this material to change from dark-brown to brown-yellow. 560 µg of oxygen, equivalent to 38.5 µg m^{-2} was irreversibly held. This value was much higher than the 8.8 µg m^{-2} obtained by Davies (4). This discrepancy arised from his incomplete oxidation procedure.

Cyanogen was dosed at 20 torr/298 K until an equilibrium was reached. Analysis of the residual gas phase showed that reaction had taken place already at room temperature. The residual gas contained 1617 µg C_2N_2, 10 µg HNCO, 4 µg HCN, 5 µg H_2O plus traces of oxygen and ammonia. After evacuating the gas phase via a liquid nitrogen cold trap, a total of 470 µg, equivalent to 32 µg m^{-2} of cyanogen was retained at 295 K. This compares with an uptake of 51.5 µg m^{-2} reported for HCN adsorption (4).

The condensable gases desorbed when the sample was heated to a series of higher temperatures upto 686 K were analysed using the mass spectrometer. The results are shown in Table 4.14.

Carbon dioxide was the major reaction products, but large amounts of HNCO and H_2O were also desorbed. Mass spectral analysis revealed that all of the irreversibly adsorbed carbon was desorbed by 683 K, 48% of which was desorbed as C_2N_2. 72% of the irreversibly adsorbed

Table 4.14 Condensable Products Released from Oxygenated CuO-CrO_3/SiO_2 after Cyanogen Contact at 295 K

Outgas Temp. (K)	Mass of Product Released (μg)									
	C_2N_2	HNCO	CO_2	O_2	HCN	H_2O	NH_3	Organics	CH_4	Other
*1	1616.9	9.8	0.0	0.0	3.9	5.2	0.1	-	-	*2
445	175.8	51.5	19.7	2.0	19.5	9.1	0.4	2.4	0.4	*3
543	24.3	41.0	51.3	2.2	3.7	24.7	0.6	5.4	3.6	*4
618	14.1	27.3	67.4	1.4	1.2	21.9	1.0	5.0	1.5	*3
683	10.9	21.0	26.3	3.7	0.8	20.0	0.5	3.0	0.4	*5
Total released above 298 K	225.1	140.8	163.7	9.3	25.3	75.7	2.4	15.9	6.0	
μg m^{-2} released above 298 K	15.5	9.7	11.3	0.6	1.7	5.2	0.2	1.1	0.4	

1 Condensable products after C_2N_2 exposure at 298 K

2 Weak peaks at m/z 41, 40 and 39

3 Weak peaks as in *2 plus m/z 45, 31 and 30

4 Weak peaks at m/z 61, 46 plus those in *3

5 Weak peaks at m/z 45, 40, 31 and 30.

nitrogen was recovered as condensable desorbates. A total of 15.9 μg of organic compounds were released during outgassing. Comparison of the mass spectral results to those shown in Appendix VI suggested that CH_3CN was released during room temperature adsorption and that a mixture of methylamine and ethylamine was desorbed by 445 K. Methane was also desorbed during this experiment. The gas was characterised by residual lines in the mass spectrum at m/z=16,15 and 14. Williams also assigned these bonds to CH_4 when he studied HCN interaction with silica (2).

4.5.3 Hydroxylated $CuO-CrO_3/SiO_2$

81.0 mg of outgassed $CuO-CrO_3/SiO_2$ was exposed to water vapour at room temperature and evacuated to leave a hydroxylated surface. The irreversible uptake of water was equivalent to 154 μg m^{-2}. This sample was highly active towards cyanogen, irreversibly adsorbing 115 μg m^{-2} of cyanogen at 298 K. Some reaction occurred at ambient temperature which resulted in desorption of H_2O and HNCO. Analysis of the condensable gases released when the sample was evacuated at 488 and 606 K are presented in Table 4.15.

Heating the sample to 488 K in vacuo yielded several milligrammes of a white sublimate. This was analysed using a VG 7070E analytical organic mass spectrometer and comparison with a pure sample of oxamide confirmed that the sublimate was the diamide. A carbon and nitrogen

Table 4.15 Condensable Products Released from Hydroxylated $CuO-CrO_3/SiO_2$ after Cyanogen Contact at 298 K

Outgassing Temp. (K)	Mass of Product Released (μg)						
	C_2N_2	HNCO	CO_2	HCN	H_2O	NH_3	Other
*1	1264.5	47.5	4.1	5.3	541.3	7.8	
488	108.7	371.1	84.2	206.0	357.3	8.1	white sublimate
606	19.3	22.4	255.9	2.7	119.2	3.6	
Total Released above 302 K (μg)	128.0	393.5	340.1	208.7	476.5	11.6	
Total Released above 302 K ($\mu g\ m^{-2}$)	8.2	25.2	21.7	13.3	30.5	0.7	

*1 Gas phase in contact with sample after Cyanogen contact at 298 K.

mass balance was carried out to estimate the amount of oxamide which sublimed. The balance showed that 32% of the irreversibly held carbon and only 21% of the nitrogen was desorbed in condensable products. Assuming that the remaining 68% of the carbon was converted to oxamide then 4.14 mg of oxamide was produced, equivalent to 265 $\mu g\ m^{-2}$. This approximation compared favourably with

microbalance results, which indicated a weight loss of 4.12 mg on outgassing the sample.

Examination of the condensable gases released above 302 K showed that only 7% of the irreversibly adsorbed cyanogen was released unchanged. The condensate desorbed below 488 K was rich in HNCO and HCN whilst the desorbate released upto 606 K consisted mainly of CO_2.

4.5.4 Oxygenated-Hydroxylated $CuO-CrO_3/SiO_2$

92.3 mg of outgassed $CuO-CrO_3/SiO_2$ was oxygenated at 673 K/15 h in 20 torr of oxygen, whereupon 1.5 mg, equivalent to 84.22 μg m^{-2} oxygen was adsorbed. The cooled sample was exposed to water vapour for 20 minutes, then excess water vapour and oxygen were evacuated prior to C_2N_2 dosage.

Approximately 150 μg m^{-2} of H_2O was irreversibly adsorbed. The uptake of C_2N_2 was accompanied by the desorbtion of some H_2O and O_2, therefore it was difficult to calculate the exact amount of C_2N_2 irreversibly adsorbed. However, an approximation of the C_2N_2 uptake was made since the cyanogen contacted sample was 1.76 mg heavier than the oxygenated-hydroxylated sample, thus at least 1.76 mg, equivalent to 100 μg m^{-2} of C_2N_2 was irreversibly held.

The condensable gases released when the sample was heated to a series of elevated temperatures upto 723 K are shown in Table 4.16. The dominant product released was CO_2, indeed 64% of the carbon adsorbed as C_2N_2 was

released in the form of CO_2. Only 8% of the nitrogen present in the adsorbed C_2N_2 was measured in the desorbed condensable products. Since a high degree of oxidation to CO_2 occurs here it is likely that the unaccounted nitrogen was lost as N_2. Less than 1% of the irreversibly held C_2N_2 was desorbed intact on heating to 723 K; this confirmed that the sample was very active for C_2N_2 conversion. Smaller amounts of C_2N_2 were also converted to HNCO, HCN and NH_3 and a trace of white sublimate was also seen.

4.6 Mass Spectrometric and Gravimetric Studies of Cyanogen Interaction with $CuO-Cr_2O_3/SiO_2$

The interaction of HCN with Cu^{2+}-Cr^{3+} systems was described earlier (Secs. 1.6.3 and 1.6.4). The main findings were that in addition to oxidation, C_2N_2 formation occurred. The following experiments were carried out to investigate the interaction of C_2N_2 with this mixed oxide system. In order to compare the results to the interaction of C_2N_2 with the individual oxide surfaces, a loading of 1.5 wt. % of each metal ion was used. This was in contrast to the 4.6 wt. % loading used by Davies (4).

The results of C_2N_2 interaction with outgassed and hydroxylated surfaces containing varying amounts of adsorbed moisture are presented in the following pages. An investigation of the interaction of C_2N_2 with an oxygenated Cu^{2+}-Cr^{3+} sample was not carried out since it

Table 4.16 Condensable Products Released from Oxygenated-Hydroxylated $CuO-CrO_3/SiO_2$ after Cyanogen Interaction at 298K

Outgassing Temp. (K)	Mass of Product Released (μg)							
	C_2N_2	HNCO	CO_2	O_2	HCN	H_2O	NH_3	Other
*1	17.8	2.3	0.0	0.9	0.4	39.8	0.5	-
511	0.0	62.2	738.9	0.0	1.3	527.3	10.7	-
593	15.3	2.3	519.0	8.6	0.0	258.7	0.5	-
665	0.0	39.5	308.8	0.0	4.6	190.5	1.3	-
723	0.0	61.8	348.2	4.3	2.9	206.5	6.2	trace of white sublimate
Total Released above 301 K (μg)	15.3	165.8	1914.9	13.4	8.8	1183.0	18.7	
Total Released above 301 K ($\mu g\ m^{-2}$)	0.9	9.3	107.5	0.8	0.5	66.4	1.1	

*1 Gas phase in contact with sample after Cyanogen Contact at 298 K.

was considered to be a reasonable assumption that such a pretreatment would yield a surface similar to the oxygenated Cu^{2+}-Cr^{6+} sample studied in Sec. 4.5.

4.6.1 Outgassed $CuO-Cr_2O_3/SiO_2$

108.2 mg of $Cu(NO_3)_2 + Cr(NO_3)_3.9H_2O/SiO_2$ was outgassed at 703 K/12. The resultant black powder, $CuO-Cr_2O_3/SiO_2$, weighed 90.8 mg and had a specific surface area of 225 m^2 g^{-1}. The sample was exposed to cyanogen at 11 torr/291 K for 21 h before condensing the residual gas phase into a liquid nitrogen trap. The sample chamber was then evacuated through a clean cold trap to less than 1 x 10^{-3} torr. The condensate collected contained 115 µg C_2N_2 and less that 2 µg of other products. The actual uptake of C_2N_2 in the current work was 1.08 mg, equivalent to 52.9 µg m^{-2}.

Analyses of the condensates collected when the sample was evacuated to a series of higher temperatures up to 698 K is shown in Table 4.17. Examination of these results revealed that 17% of the carbon atoms which had been irreversibly held at 291 K were released as gaseous C_2N_2 by 698 K. A further 18% was released as gaseous carbon dioxide and 3% was desorbed as a mixture of HCN, HNCO, NH_3, H_2O and traces of organic products. The remaining 62% of irreversibly held C_2N_2 was either lost as non-condensable products or was retained by the surface at 698 K. The only evidence for hydrolysis of adsorbed C_2N_2 was the desorption of HNCO above 298 K.

Comparison of the condensable products recovered above 295 K from the CuO/SiO_2 and Cr_2O_3/SiO_2 samples to that liberated from the mixed oxide (Table 4.18) allows some of the products desorbed from the mixed oxide to be

Table 4.17 Condensable Products Released from Outgassed $CuO-Cr_2O_3/SiO_2$ after Cyanogen Interaction at 291 K

Outgassing Temperature (K)	Mass of Product Released (μg)						
	C_2N_2	HNCO	CO_2	HCN	NH_3	H_2O	Other
298	114.6	0.2	0.6	0.8	-	-	-
423	108.4	10.0	39.3	31.3	0.4	-	*1
523	46.0	9.0	39.5	24.8	1.8	1.2	*2
603	16.0	3.3	45.5	20.8	11.1	1.5	*2
698	12.0	2.9	70.4	26.2	9.0	1.2	*2
μg released above 298 K	182.4	25.2	194.7	97.1	3.9	22.3	
μg m^{-2} released above 298 K	8.9	1.2	9.5	4.8	0.2	1.1	

*1 Trace peaks at m/z 58, 53, 46 and 45

*2 Minor peaks at m/z 41, 40; trace peks at 58, 53, 46, 45, 39, 38

attributed to either the copper or chromium sites. It was evident that HNCO formation over the mixed oxide was associated with copper sites. The amount of CO_2 and HCN formed seemed to be the sum of the amounts formed on the individual metal ions. Conversely the amount of C_2N_2

Table 4.18 Comparison of Products Desorbed when Outgassed Silica-Supported Copper and Chromium Oxides were Heated above 295 K after Cyanogen Contact

	Mass of Product Released ($\mu g\ m^{-2}$)						
Sample	C_2N_2	HNCO	CO_2	HCN	NH_3	H_2O	Other
CuO/SiO_2	9.1	2.1	0.3	1.2	0.2	1.2	Organics
Cr_2O_3/SiO_2	14.3	-	9.1	3.4	1.3	0.5	none
$CuO\text{-}Cr_2O_3/SiO_2$	8.9	1.2	9.5	4.8	0.2	1.1	Organics

desorbed from the mixed oxide was lower than that released from either of the individual oxide samples.

4.6.2 Hydroxylated $CuO\text{-}Cr_2O_3/SiO_2$

A 91.0 mg sample of $CuO\text{-}Cr_2O_3/SiO_2$ was hydroxylated and residual moisture was frozen into a cold trap. 580 µg of water, equivalent to 28.33 µg m^{-2}, was irreversibly held by the solid. Exposure to gaseous cyanogen at 18 torr/295 K/15 h resulted in at least 2.06 mg of adsorbed cyanogen, equivalent to 100.6 µg m^{-2} surface. The actual uptake of C_2N_2 was probably higher than this because an unknown amount of moisture desorbed when the sample was exposed to the cyanogen gas. After evacuation of the sample chamber to below 1 x 10^{-3} torr, at least 1.48 mg

of adsorbed cyanogen, equivalent to 72.3 μg m^{-2} surface, was irreversibly held. Analysis of the condensate revealed that it contained high proportions of C_2N_2 and H_2O and only small amounts of decomposition products.

Mass spectrometric analyses of the condensates collected when the sample was outgassed at a series of higher temperatures upto 673 K are shown in Table 4.19.

The main feature of this experiment was the desorption of large amounts of carbon dioxide, mainly above 414 K. Indeed the conversion of cyanogen to CO_2 was more pronounced on this mixed oxide than on either of the individual oxides, a total of 19.0 μg m^{-2} was released above 288 K. In comparison to the individual oxides (Table 4.20), large amounts of HNCO and HCN were also produced, most of this was liberated below 497 K. Only 17% of the original irreversibly adsorbed carbon was released as C_2N_2 and only 46% of the adsorbed carbon was measured as gaseous products. This latter result was explained by the release of a small amount of oxamide between 414 and 497 K.

The peak at m/z=45 which was apparent in the mass spectrum of the condensate collected between 288-414 K is best explained by the presence of formamide $HCONH_2$. This peak was also observed in earlier studies when C_2N_2 was interacted with hydroxylated CuO/SiO_2 (Sec. 4.2.2). With the exception of the weak bond at m/z=46, the other weak bands in the mass spectra of samples desorbed above 414 K, namely those at m/z 41,40,39 and 38, were best

Table 4.19 Condensable Products Released from Hydroxylated $CuO-Cr_2O_3/SiO_2$ after Cyanogen Contact at 295 K

Outgassing Temperature (K)	Mass of Product Released (μg)						
	C_2N_2	HNCO	CO_2	HCN	NH_3	H_2O	Other
288	137.3	2.1	1.3	3.8	0.6	53.1	-
414	52.3	183.0	29.5	107.6	0.7	52.7	*1
497	48.3	39.4	83.4	51.8	0.9	123.1	*2
598	9.9	12.0	143.8	28.8	2.0	43.6	*3
673	4.9	11.5	131.9	12.8	11.2	90.3	*3
Total Released above 288 K (μg)	115.4	245.9	388.6	201.0	14.8	309.7	
Total Released above 288 K ($\mu g\ m^{-2}$)	5.6	12.0	19.0	9.8	0.7	15.1	

*1 Weak peak at m/z 45

*2 Weak peaks at m/z 46, 45, 41, 40, 39 and 38 plus oxamide

*3 as *2 but no oxamide

Table 4.20 Comparison of Products Desorbed from Hydroxylated Silica-Supported Copper and Chromium Oxide Surfaces

	Irreversible Uptake ($\mu g\ m^{-2}$)		Mass of Product Released between 288 - 295 K ($\mu g\ m^{-2}$)						
	H_2O	C_2N_2	C_2N_2	HNCO	CO_2	HCN	NH_3	H_2O	Other
CuO/SiO_2	19.5	>48.1	0.3	0.9	0.4	0.3	0.1	3.1	*1
Cr_2O_3/SiO_2	50.0	>57.3	13.7	8.9	12.5	3.9	0.9	32.2	-
$CuO-Cr_2O_3/SiO_2$	28.3	72.3	5.6	12.0	19.0	9.8	0.7	15.1	organics incl. oxamide

*1 Up to 78.6 $\mu g\ m^{-2}$ of oxamide plus other organics

explained by the existence of methyl cyanide formed from the CuO surface (see earlier 4.2.2).

4.6.3 Hydroxylated $CuO-Cr_2O_3/SiO_2$ Containing Excess Adsorbed Water Vapour

A 96.0 mg sample of $CuO-Cr_2O_3/SiO_2$ was found to have a surface area of 21.6 m^2 (by nitrogen adsorption). The black powder was exposed to water vapour until 4.0 µg had condensed on it. Residual water vapour was carefully removed so that some physically adsorbed water remained on the surface. The sample was left to reach a steady weight. A total of 2.0 mg H_2O was retained, equivalent to 92.6 $\mu g\ m^{-2}$ surface. Davies (4) studied HCN

adsorption on hydrated $CuO-Cr_2O_3/SiO_2$ containing a similar level, 90 μg m^{-2}, of adsorbed H_2O. By comparison with Section 4.6.2, where 580 μg H_2O was irreversibly adsorbed onto an identical sample weighing 91.0 mg, the amount of physically adsorbed water was calculated to be about 1.4 mg. The sample weight increased by 9.87 mg and reached equilibrium after exposure to C_2N_2/17 torr/12 h. The actual uptake of cyanogen probably exceeded this amount due to the loss of physically adsorbed H_2O into the surrounding cyanogen atmosphere.

During outgassing at 288 K, the sample weight only decreased by 600 μg. 253 μg of this was attributed to desorbed water vapour. The irreversible uptake of cyanogen was therefore calculated to be at least 9.52 mg (i.e. 440.9 μg m^{-2} surface).

On outgassing this sample to 419 K, the sample weight decreased by 8.6 mg and a large amount of white sublimate was deposited on the glass walls of the sample chamber. The weight of the condensate collected in the cold trap was 739 μg (see Table 4.21). A large proportion of the remaining 7.86 mg was probably oxamide. The condensates collected when the sample was outgassed at temperatures up to 692 K are shown in Table 4.21. Only 10.2% of the carbon irreversibly held in the form of C_2N_2 at 288 K was returned to the gaseous phase as condensable products.

The above results clearly show that a high conversion of cyanogen to the white sublimate had

Table 4.21 Condensable Products Released from Hydroxylated-Hydrated $CuO-Cr_2O_3/SiO_2$ after Cyanogen Contact at 288 K

Outgassing Temperature (K)	Mass of Product Released (μg)						
	C_2N_2	HNCO	CO_2	HCN	NH_3	H_2O	Other
288	317.1	3.6	1.8	3.9	4.6	252.6	-
419	44.2	139.1	20.1	92.7	25.0	417.7	white sublimate approx. 7.9 mg
512	21.9	186.6	247.3	9.9	17.7	118.0	
592	5.6	222.2	261.4	0.0	84.2	96.9	
692	2.3	141.8	104.0	0.0	21.1	9.6	
μg released above 288 K	74.0	689.7	632.8	102.6	148.0	642.2	
μg m^{-2} released above 288 K	3.4	31.9	29.3	4.8	6.9	29.7	357.0

occurred. Analyses of the condensable products collected when the sample was outgassed from 288 to 692 K showed that 633 μg CO_2 and 690 μg HNCO were desorbed whilst only 74 μg of C_2N_2 was recovered. 102.6 μg HCN and 148.0 μg NH_3 were also released.

4.7 Effect of Thermal Treatment on Oxamide

Since oxamide was produced in several of the reactions involving C_2N_2 with silica-supported copper and

chromium oxides it was considered prudent to investigate the effect of heating this material in the vacuum frame and recording a mass spectrum of any condensable products recovered.

A 6.6 mg sample of oxamide (BDH Chemicals) was placed in the sample bucket of the microbalance and evacuated to $<10^{-3}$ torr at 293 K. The sample was heated to 398 K and any condensable gases were collected in a cold trap. The weight decreased to 0.43 mg and was still falling when it was decided to stop heating and analyse the contents of the cold trap. A mass spectrum of the condensate is shown in Table 4.22. The liquid nitrogen cold trap was evacuated and the outgassing temperature was then raised to 573 K whereupon the remaining oxamide sublimed/decomposed. Analysis of the contents in the cold trap from the second stage of heating is also shown in Table 4.23. At the end of this experiment a large quantity of white sublimate was observed on the walls of the microbalance hang-down tube. Analysis of the condensate collected showed that the major product was H_2O whilst a series of weak peaks notably m/z 44 and 27 were also present. The results confirmed that the major reaction which occurred when oxamide was heated was loss of water and sublimation.

Davies (4) had previously conducted a short study which gave similar results to those presented here. The peak at m/z 43 was more intense in his work; this was explained by the presence of HNCO which also enhanced the

Table 4.22 Mass Spectral Results of Thermal Treatment of Oxamide

	$\%\Sigma_{i,j}$ at Outgassing Temperature (K)	
m/z	398	573
17	20.2	22.0
18	75.8	68.3
19	1.9	1.7
20	0.2	0.2
26	0.1	0.6
27	0.1	2.3
28	0.5	0.7
29	0.1	0.2
30	0.1	0.1
31	0.3	0.3
41	0.1	0.1
42	0.0	0.2
43	0.1	0.6
44	0.2	1.9
45	0.1	0.1

intensities of the peaks at m/z 42,29 and 15. The amounts of HNCO in the current work was considered to be very low in comparison to the amount of H_2O produced. It was therefore decided that the isocyanic acid reported during adsorption studies was not produced from decomposition of free oxamide. However, it is worthy to comment that adsorbed oxamide may react differently from free oxamide. Indeed, surface-bound oxamide may well

thermally decompose to yield a range of products which could include HNCO.

4.8 Infra-red Spectroscopic Studies of Cyanogen Interaction with Silica

In the work reported in subsequent sections, infra-red spectroscopy was used to investigate the interaction of C_2N_2 with silica-supported copper and chromium oxides. In order to simplify the interpretation of the results, it was considered necessary to carry out a series of blank experiments in which cyanogen was interacted with outgassed and hydroxylated samples of uncoated silica.

Previous i.r. studies of cyanogen interaction with silica were discussed in Section 1.6.3.2. Ruttenberg and Low (112) reported that interaction at 298 K caused a weak i.r. band to develop at 2310 cm^{-1}. Other changes also occurred on heating. Since the silica used in their work was outgassed at 1273 K it was decided to investigate the interaction of C_2N_2 with silica outgassed at 673 K, the outgassing temperature used throughout this work. It was also decided to investigate the effect of pre-adsorbed moisture to see whether any reaction with the adsorbed cyanogen could be induced.

4.8.1 Outgassed Silica

A 100 mg Aerosil disc was prepared as described in Sec. 2.4.3. This was mounted in the infra-red cell and evacuated at 673 K/12 h. The sample was cooled in vacuo

and an i.r. transmission spectrum was recorded of the outgassed (i.e. dehydroxylated) silica (Fig. 4.1 A). The spectrum contained a sharp band at 3744 cm^{-1}, two broad bands centred around 1864 and 1641 cm^{-1} plus a shoulder near 2000 cm^{-1}. Peri (159) assigned these bands as follows; The sharp band at 3744 cm^{-1} was ascribed to 'isolated' (i.e. not hydrogen-bonded) surface silanol groups. The tail in the 3750-3500 cm^{-1} region was attributed to strongly H-bonded silanol groups. The features at 2000,1864 and 1641 cm^{-1} have been attributed to combinations and/or overtones of lattice vibrations (157, 158). This spectrum was used as a reference spectrum from which to compare subsequent spectra and to derive difference spectra.

The outgassed silica disc was contacted with cyanogen at 20 torr at 295 K for 70 h (20 torr/295 K/ 70 h) and then evacuated at room temperature. I.r. transmission spectra recorded after 10 minutes and 70 hours are shown in Fig. 4.1. Absorbance difference spectra obtained by subtraction (Sec. 3.2.3) are shown in Fig. 4.2. The use of difference spectra makes it easier to observe spectral changes especially in regions where absorption was already high. The spectra revealed that a series of bands were apparent after C_2N_2 contact. The bands at 2657, 2560, 2165 and 2147 cm^{-1} were due to gaseous phase C_2N_2. The intensification of the broad absorption around 3500 cm^{-1}, and the appearance of a band at 1617 cm^{-1} was due to adsorbed water molecules whilst

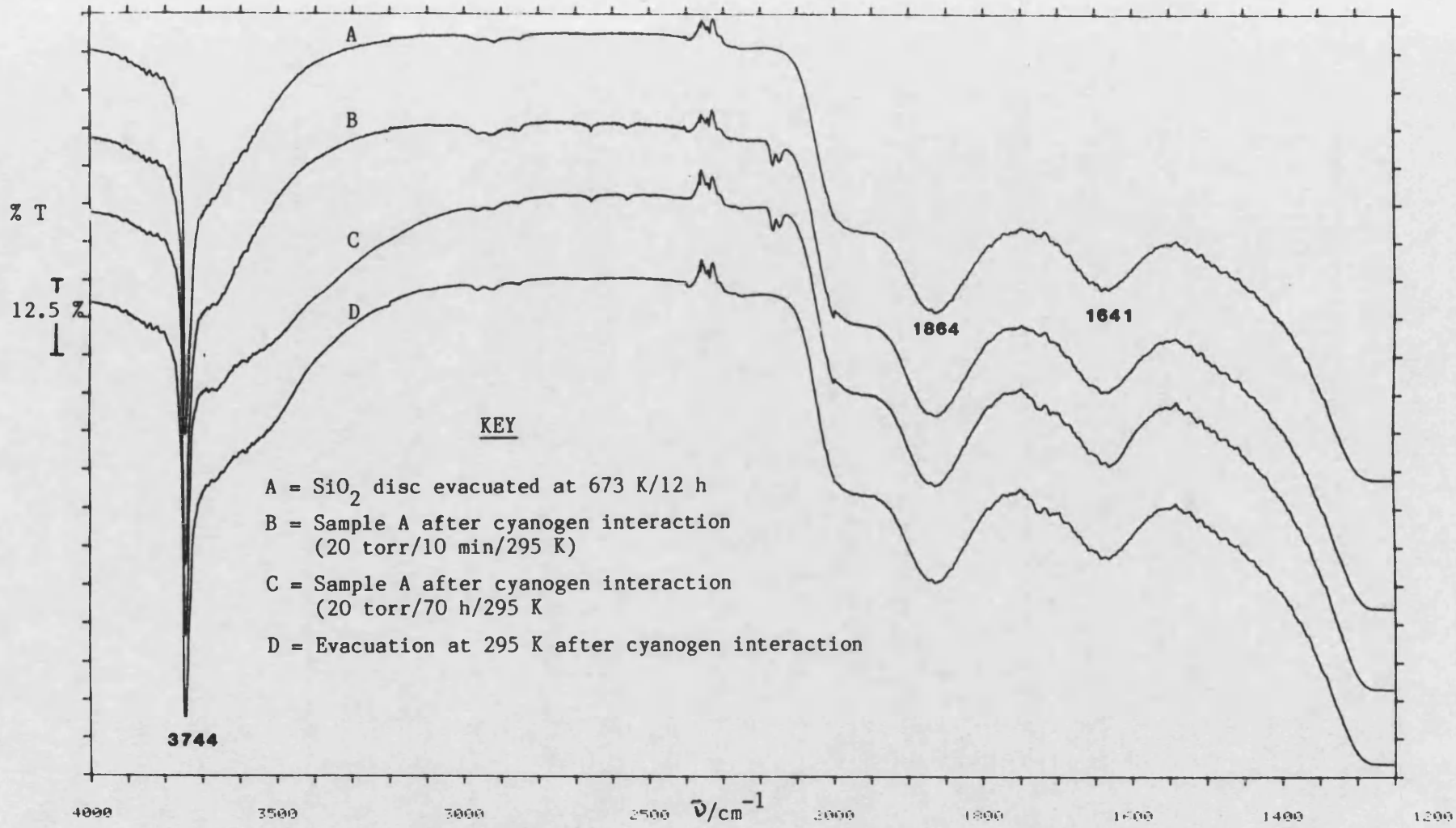

Fig. 4.1 I.r. Transmission Spectra of Cyanogen Contact with Silica at Ambient Temperature *

(* The i.r. beam raises the sample temperature to approximately 313 K)

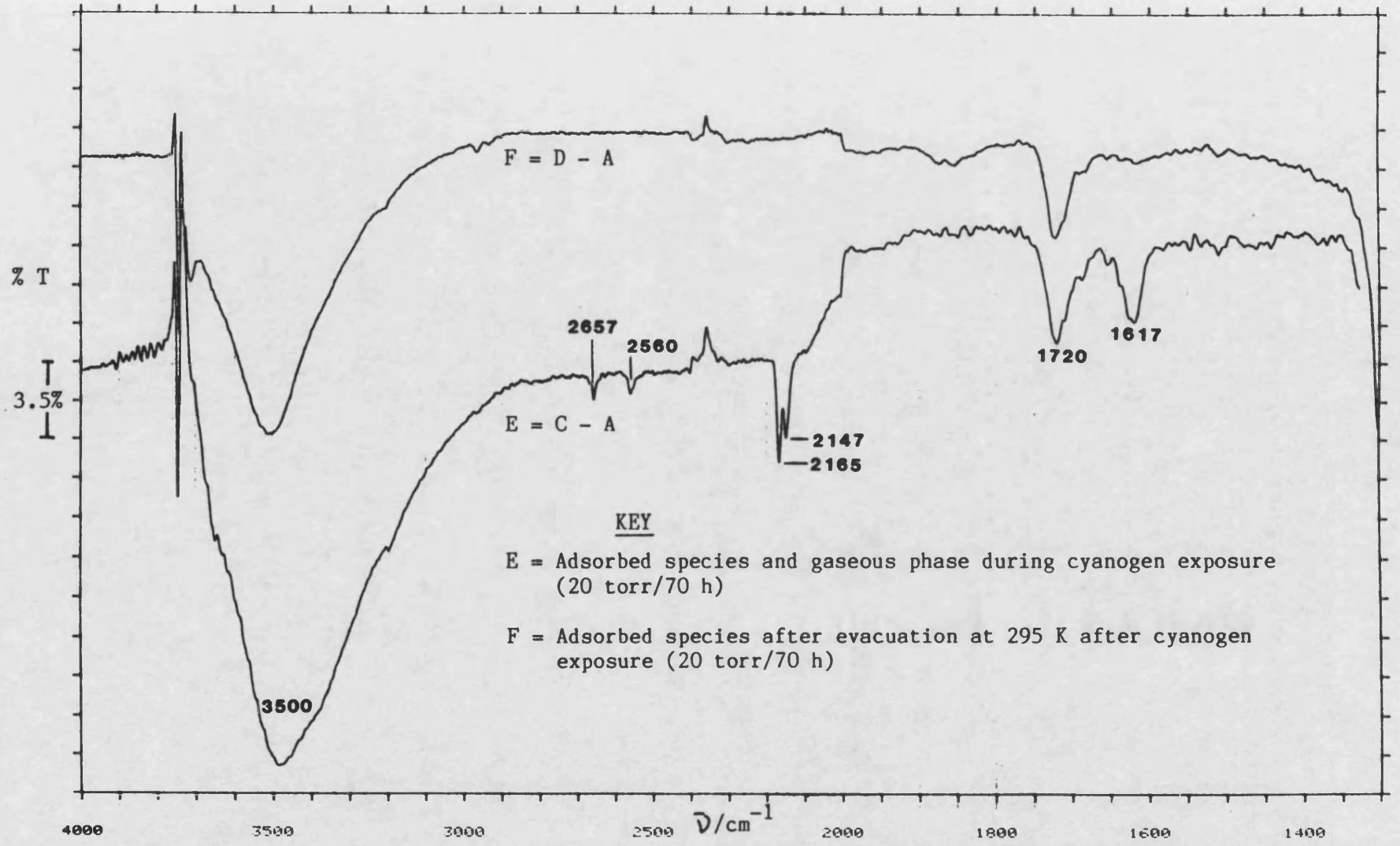

Fig. 4.2 Infra-red Transmission Difference Spectra of Cyanogen Exposure with Silica at Ambient Temperature

the perturbation of the band near 3744 cm^{-1} was due to interference with isolated silanol groups. A strong band also appeared at 1720 cm^{-1}. Removal of the adsorbed water during evacuation at 293 K explained the loss of the band at 1617 cm^{-1} and reduction in the intensity of the broad band at 3500 cm^{-1}. The band at 1720 cm^{-1} was unaffected by evacuation at ambient temperature but was lost by 673 K. The position of this bond is typical of the C=O stretch. This bond could arise due to partial hydrolysis of C_2N_2. The spectrum recorded after outgassing to 673 K (not shown) was identical to pure outgassed silica.

4.8.2 Hydroxylated Silica

A disc prepared from Aerosil 300 silica was outgassed at 673 K for 10 h prior to being cooled to 298 K. An i.r. transmission spectrum of the disc was recorded (Fig. 4.3 Spectrum A). This spectrum was identical to the one presented in the case of outgassed silica. This spectrum was used as a reference spectrum from which to compare subsequent spectra and to derive difference spectra. The disc was then exposed to water vapour from a water reservoir, the contents of which had been purified by a series of freeze-thaw cycles. Excess adsorbed and gaseous phase moisture was removed by freezing into a cold finger immersed in liquid nitrogen. The new spectrum was measured (Fig. 4.3 spectrum B). An i.r. difference spectrum derived by subtracting the

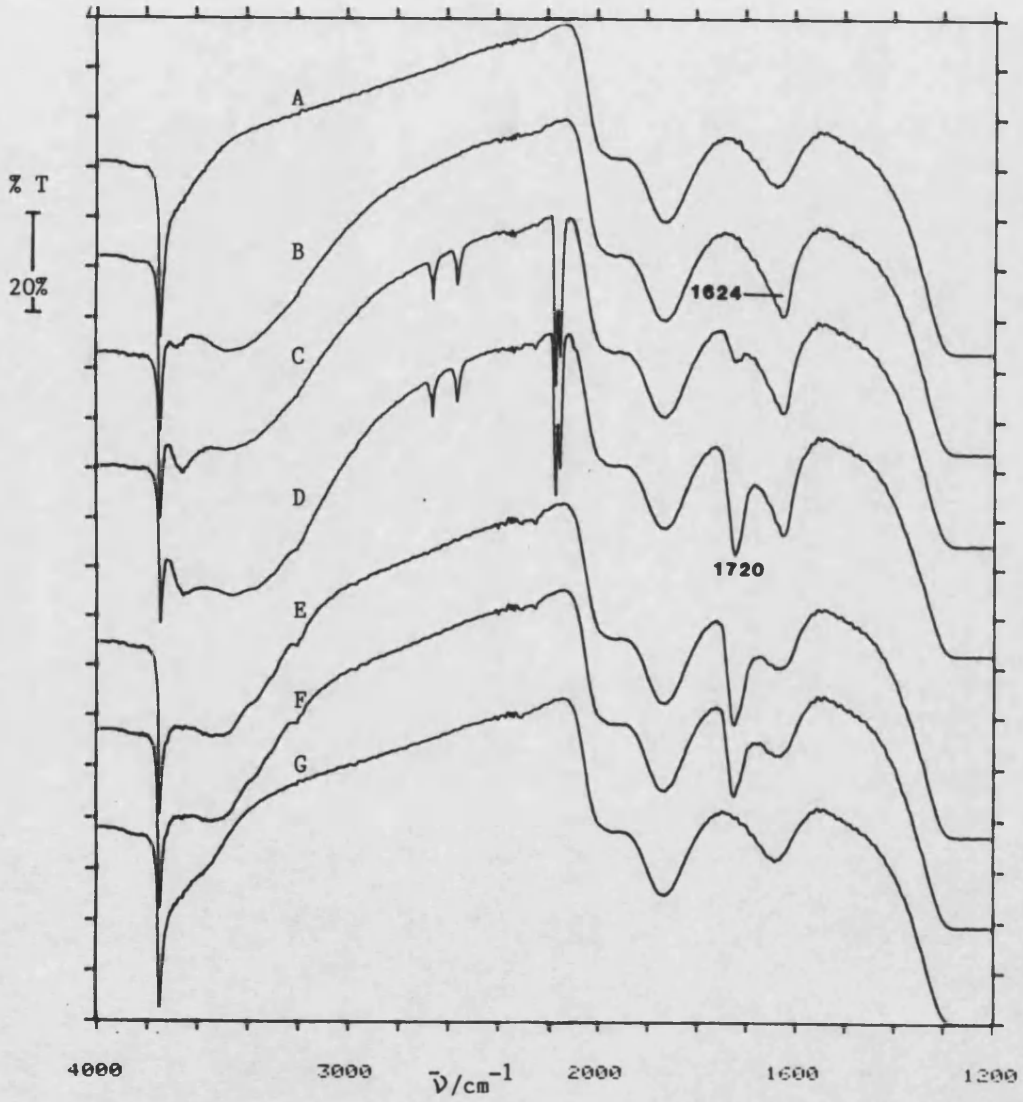

Fig. 4.3 I.r. Transmission Spectra of Cyanogen Interaction with re-hydroxylated Silica.

A = SiO_2 outgassed at 693 K/10 h

B = Sample in A cooled to 298 K, then exposed to H_2O vapour, excess H_2O being frozen into liquid nitrogen cold finger.

C = Sample in B exposed to C_2N_2/40 torr/10 min

D = Sample in B exposed to C_2N_2/40 torr/12 h

E = Sample in B exposed to C_2N_2/40 torr/14 h., then opened to cold trap

F = Sample in E evacuated 298 K/30 min

G = Sample in F outgassed 472 K/2 h

spectrum of the outgassed silica from that of the hydroxylated disc is shown in Fig. 4.4, spectrum A, presented in the absorbance mode. This reveals bands at 3432 (broad), 1619 and 920 cm^{-1}, whilst a negative band appeared near 3740 cm^{-1}.

Cyanogen also purified by the freeze-thaw procedure, was next admitted to the adsorption chamber at a pressure of 40 torr. A sequence of transmission spectra and of corresponding difference spectra are shown in Figs. 4.3 and 4.4, respectively. I.r. spectra recorded after 10 minutes and then 12 h exposure showed that reaction occurred rapidly at first giving rise to a new band at 1716 cm^{-1}, whilst continued exposure revealed weak bands between 3500-3000 and at 2330, 2247, 2091 and 1368 cm^{-1}, accompanied by enhancement of all the features which had developed since the initial exposure to moisture and cyanogen. After 14 h exposure, the adsorption system was opened to the cold finger at 77 K. This caused the intensity of the broad absorption at 3744-3500 cm^{-1} to decrease, whereas the band previously at 1619 cm^{-1} shifted to 1607 cm^{-1} and reduced in intensity. The weak bands near 2330 and 2091 cm^{-1} disappeared, and only the 1720 cm^{-1} band was unaffected. Evacuation at 293 K had no further effect, but after an outgas at 472 K the spectrum of the sample reverted to that of the outgassed unchallenged silica with the exception of a weak band at 907 cm^{-1} and a slightly intensified feature near 3550 cm^{-1}.

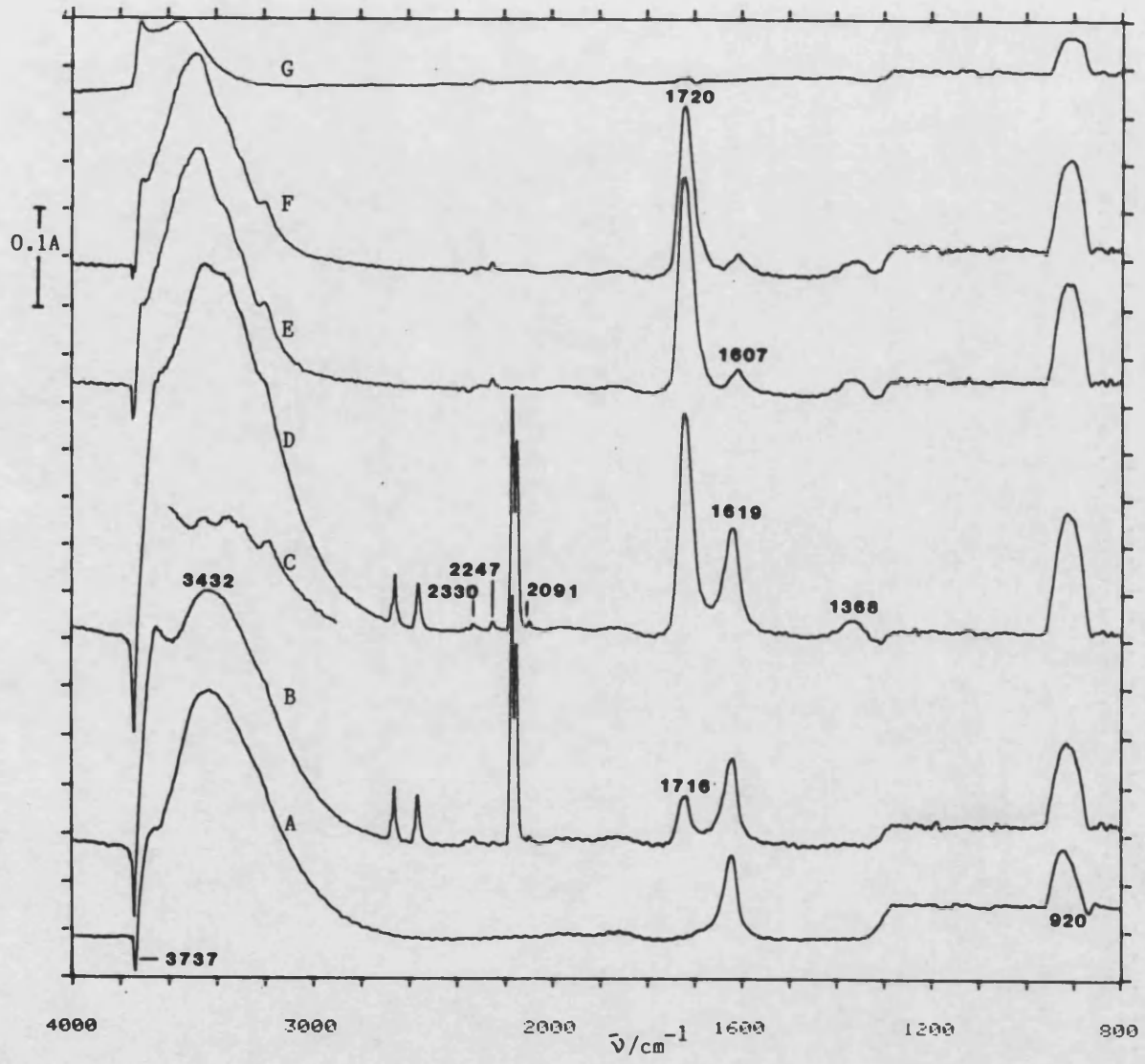

Fig. 4.4 I.r. Absorbance Difference Spectra of Cyanogen Interaction with Hydroxylated silica.

A = Adsorbed species resulting from hydroxylation of outgassed SiO_2

B = Adsorbed and gaseous species after exposure to C_2N_2/40 torr/10 min

C = After C_2N_2 for 12 h (Fig. 4.3 D-B)

D = Adsorbed species and gas phase after C_2N_2/12 h

E = Adsorbed species after C_2N_2 at 293 K for 14 h

F = Irreversibly adsorbed species in E.

G = Adsorbed species after outgassing for 2 h at 472 K.

4.9 Infra-red Spectroscopic Studies of Cyanogen Interaction with CuO/SiO_2

Although the interaction of cyano compounds with supported and unsupported CuO is well documented (Sec. 1.6), the interaction of C_2N_2 with these surfaces has not yet been reported. Williams studied the interaction of HCN with cupric oxide, silica-supported cupric oxide and silica-supported copper (2). His studies revealed that although HCN interaction resulted in C_2N_2 formation, no i.r. bonds due to adsorbed C_2N_2 were observed. Williams used i.r. spectroscopic results to develop mechanisms for C_2N_2 formation and for HCN decomposition. It was hoped that the current study would supplement Williams' findings which in turn would help to explain the involvement of CuO in the reactions over mixed oxide samples.

4.9.1 Outgassed CuO/SiO_2

A 100 mg sample of CuO/SiO_2 containing 1.5 wt.% Cu was compressed into a self-supporting disc (Sec. 2.4.3). The disc was evacuated at 1 x 10^{-5} torr for 2 h before outgassing at 688 K. The disc was cooled and an i.r. spectrum was recorded, Fig. 4.5 spectrum A. The spectrum had bands at 3740,1863 and 1640 cm^{-1} which are all due to the silica support (Sec. 4.8). There was no perturbation of the spectrum due to the presence of cupric oxide.

Infra-red spectroscopic results of the interaction of this sample with C_2N_2 at 293 K and of the subsequent

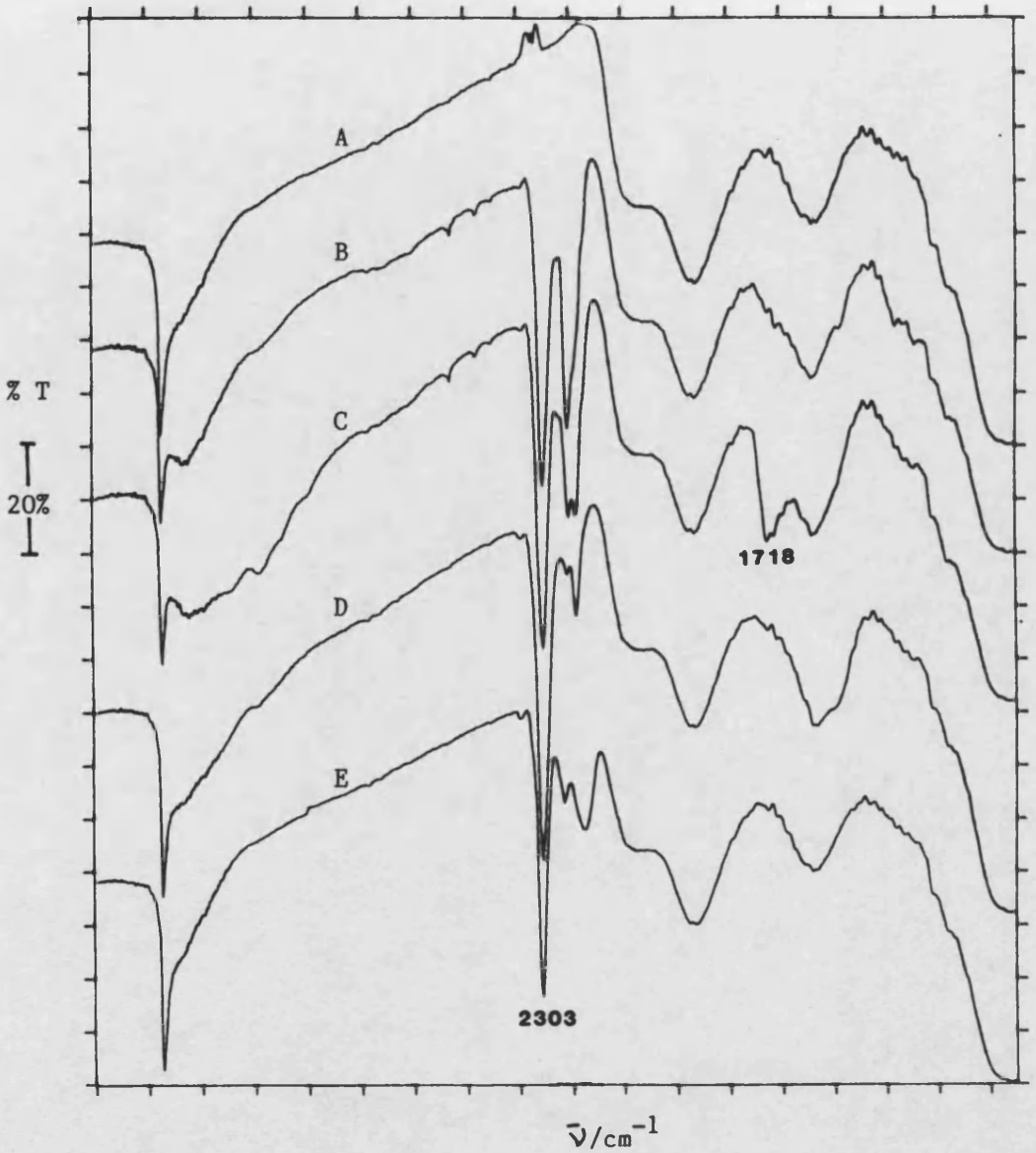

Fig. 4.5 I.r. Transmission Spectra of Cyanogen Interaction with Outgassed CuO/SiO_2

A = Outgassed CuO/SiO_2

B = Sample A, exposed to C_2N_2 at 293 K/2 h

C = " " " " " 293 K/21 h

D = Sample as C, outgassed to 423 K/2.5 h

E = " " " " " 688 K/3 h

outgassing upto 688 K are shown sequentially as transmission spectra in Fig. 4.5. Spectra expanded between 2400-1900 cm^{-1} (the C-N multiple bond stretching region) are shown in Fig. 4.6. To clearly reveal spectral bonds notably in the 3500-3200 and 1750-1450 cm^{-1} regions, which would otherwise have been obscured by strong silica absorptions, absorbance difference spectra were derived by subtracting the spectrum of outgassed CuO/SiO_2 (Fig. 4.5 spectrum A) from the appropriate spectra. The results are shown in Fig. 4.7. For clarity the spectra are described by dividing them into two sections, namely, changes in the region 2400-1900 cm^{-1} and those occurring in the remainder of the spectrum.

Two bands, at 2303 and 2209 cm^{-1}, developed rapidly (within 20 minutes) during C_2N_2 exposure at 293 K. These bands are characteristic of C-N multiple bonds. A notable feature of the 2303 cm^{-1} band was that it developed gradually over a period of 20 h (Fig. 4.8) but its' intensity was unaffected by evacuation or outgassing upto 688 K. The position of this band and the thermal stability of the species causing it were characteristic of a surface silyl isocyanate (Si-NCO) species. The i.r. band was due to the antisymetric stretch of the NCO group. (Sec.1.6.3.2). It is relevant to recall that no such band occurred when pure SiO_2 was contacted with C_2N_2 at room temperature (Sec.4.8). The second strong band which appeared rapidly at room temperature (2209 cm^{-1})

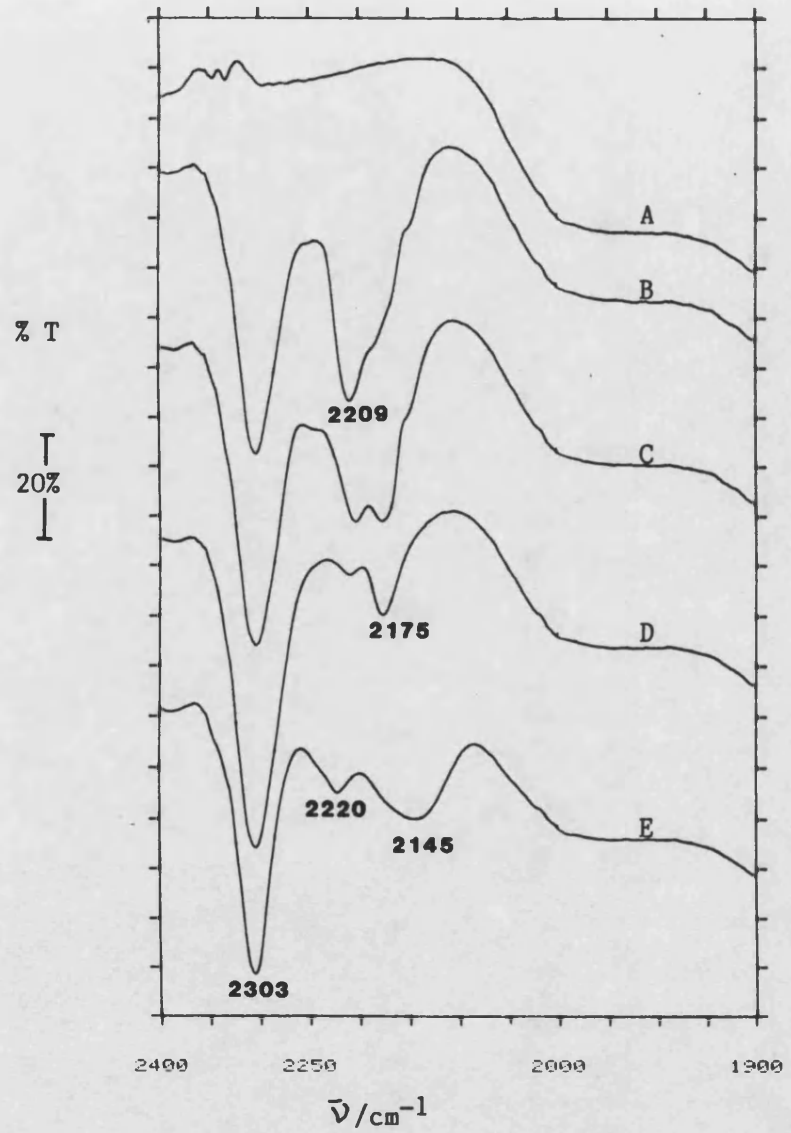

Fig. 4.6 I.r. Transmission Spectra of C_2N_2 Interaction with Outgassed CuO/SiO_2

A = Outgassed CuO/SiO_2

B = Sample A exposed to C_2N_2 at 293 K/2 h

C = Sample A exposed to C_2N_2 at 293 K/21 h

D = Sample as C then outgassed to 423 K/2.5 h

E = Sample as C then outgassed to 688 K/3 h

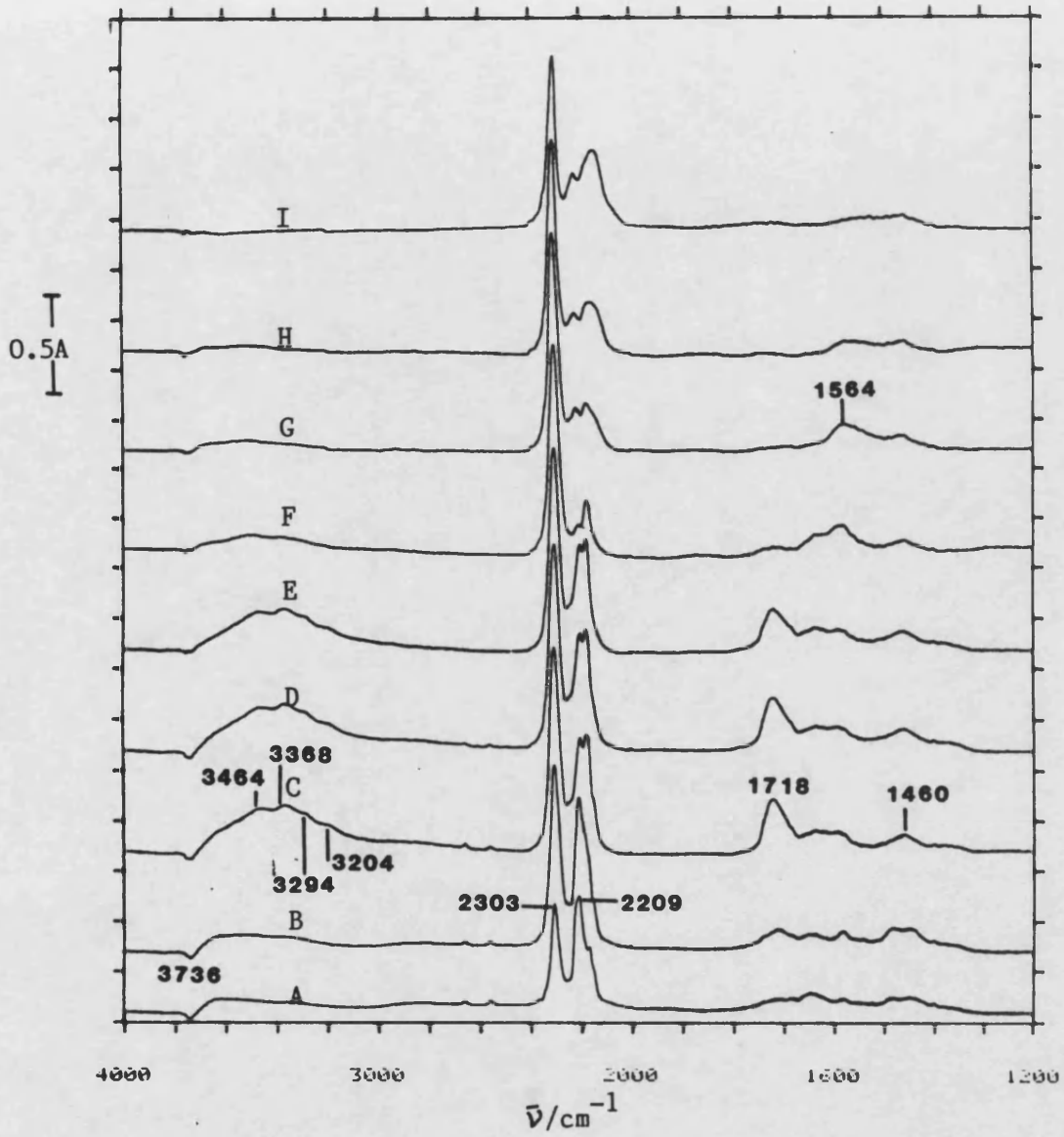

Fig. 4.7 Absorbance Difference Spectra: Cyanogen Interaction with Outgassed CuO/SiO_2

A = Adsorbed species on CuO/SiO_2 plus gaseous phase after C_2N_2 exposure for 20 minutes.

B = As A except 2 h C_2N_2 exposure

C = " " " 21 h " "

D = Adsorbed species after C_2N_2 exposure for 21 h., followed by condensing gas phase in a liquid nitrogen trap.

E = As D plus evacuation at 293 K

F = Adsorbed species after outgassing 423 K/2.5 h

G = " " " " 548 K/2 h

H = " " " " 623 K/2 h

I = " " " " 688 K/3 h

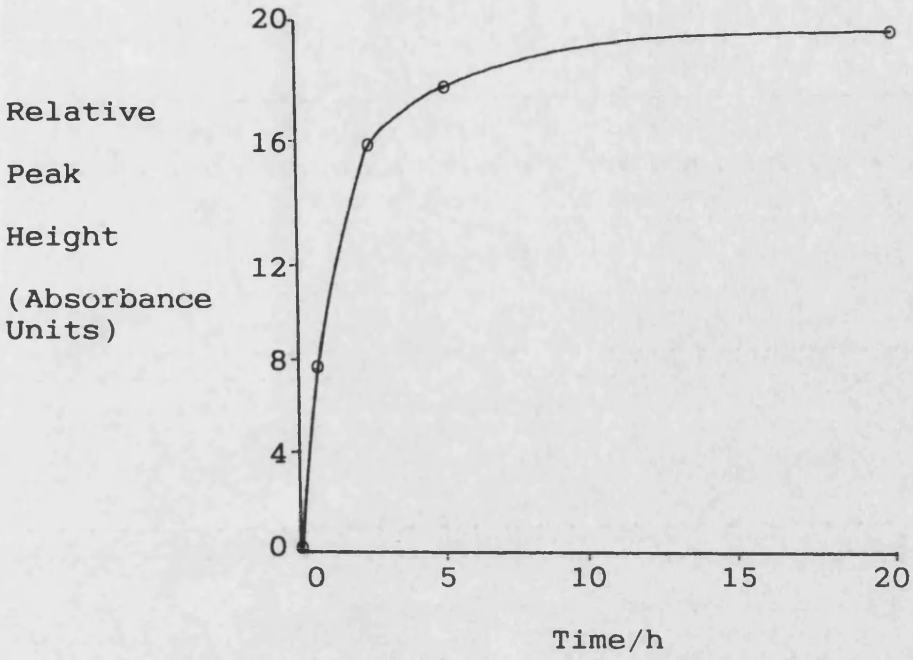

Fig.4.8 Development of the 2302 cm^{-1} band on C_2N_2 exposed, outgassed CuO/SiO_2.

gradually gave way to a band at 2175 cm^{-1}. After extended exposure at room temperature equilibrium was reached and the bonds at 2209 and 2176 cm^{-1} were of equal intensity (Fig. 4.6.C). On heating to 423 K the intensity of the band at 2209 cm^{-1} decreased and it began to shift to higher wavenumbers. By 548 K this band was seen at 2220 cm^{-1}. The position and intensity of this band did not change further on outgassing upto 688 K. This band was due to copper isocyanate and the shift from 2209 to 2220 cm^{-1} was due to changes in the surface environment. This assignment is in good agreement with the literature since London and Bell (64) reported a band due to CuNCO at 2200 cm^{-1} when NO and CO were interacted

over a CuO surface. Surman (3) also assigned a band at 2220 cm^{-1} to this species when he adsorbed HCN onto a CuO/SiO_2 sample.

On heating above 423 K the peak at 2175 cm^{-1} shifted to a lower wavenumber and slowly intensified at the expense of the CuNCO bond. By 688 K the band was observed as a broad absorption centred at 2145 cm^{-1} (Fig. 4.6.E).

Other changes which occurred during C_2N_2 exposure at 293 K included the slow development of a band at 1718 cm^{-1}. This was lost on evacuating to 423 K. A similar feature with identical characteristics was observed over outgassed and hydroxylated silica and was thought to be due to the C=O stretch of adsorbed, partially hydroxylated C_2N_2 (Sec. 4.8).

Room temperature C_2N_2 exposure also caused a slight decrease in the intensity of the hydroxyl band around 3736 cm^{-1} but intensity was restored during evacuation to 423 K. A series of weak bands developed at 293 K in the N-H stretching region with peaks at 3464, 3368, 3294 and 3204 cm^{-1}. These peaks supported the supposition that partial hydrolysis had occurred. These bands were lost on outgassing to 423 K. Finally during adsorption at 293 K a series of weak bands developed between 1710-1447 cm^{-1}. Major features included a broad absorption between 1640-1590 cm^{-1} and a peak at 1460 cm^{-1}. These features were lost on outgassing above 423 K.

4.9.2 Hydroxylated CuO/SiO_2

The experiments to be reported in this section were designed to investigate the role of pre-adsorbed moisture on the uptake and conversion reactions of cyanogen over CuO/SiO_2. The results are presented as follows: (i) offset transmission spectra (Fig. 4.9), (ii) transmission spectra expanded in the 2400-2000 cm^{-1} (Fig.4.10) region and (iii) difference spectra plotted in the absorbance mode (Fig. 4.11). The difference spectra were produced by subtracting a spectrum of outgassed CuO/SiO_2 from appropriate spectra.

Treatment of the outgassed disc with water vapour caused enhancement of broad bands near 3488 and 1621 cm^{-1} due to adsorbed water molecules whilst the intensity of the sharp band due to isolated silanol groups at 3739 cm^{-1} decreased. Exposure of this hydroxylated disc to cyanogen at 30 torr for 5 minutes produced new bands near 2303 (SiNCO), 2203 (CuNCO) and 1719 cm^{-1} (C=O) (see Fig. 4.11B). The two isocyanate bands intensified after 2.5 h exposure and thereafter reacted in a similar way as in the case of outgassed CuO/SiO_2. The 2164, 2147 cm^{-1} doublet due to gaseous cyanogen also intensified and moved slightly to 2168, 2151 cm^{-1}. A series of new bands near 1687, 1587, 1464 and 1369 cm^{-1} also developed. Furthermore the broad absorption above 3000 cm^{-1} now revealed a shoulder near 3383 cm^{-1}. After 6 h exposure, a new shoulder appeared at 3199 cm^{-1} whilst the first shoulder intensified. The bands near 1719 and more so at

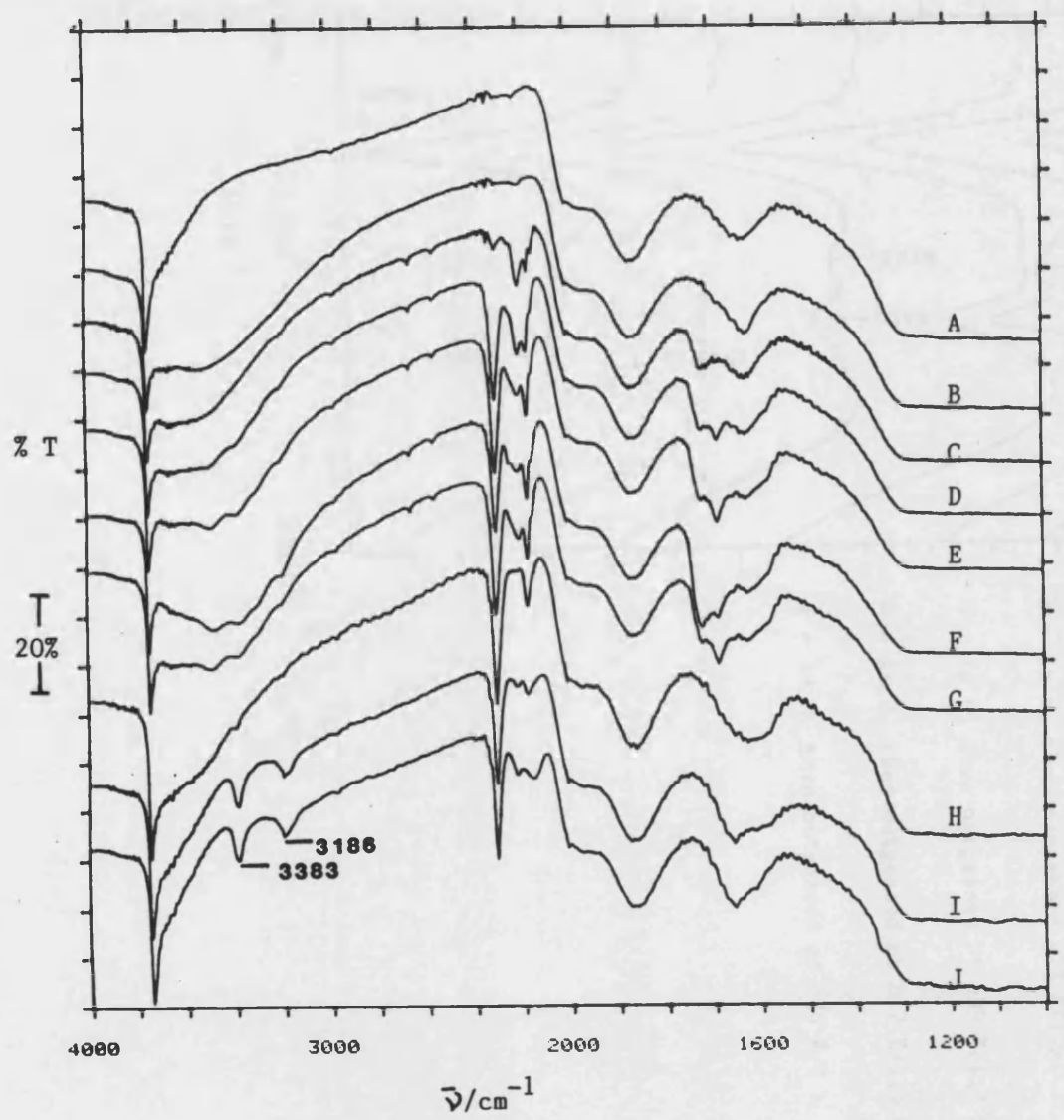

Fig. 4.9 I.r. Transmission Spectra of Cyanogen Interacted with Hydroxylated CuO/SiO_2

A = CuO/SiO_2 outgassed at 673 K/15 h

B = As A, then exposed to H_2O vapout/15 mins. (excess moisture removed by evacuation through cold trap/25 mins.)

C = Sample in B exposed to C_2N_2/30 torr/5 mins.

D = Sample in C exposed to C_2N_2/2.5 h.

E = Sample in D exposed to C_2N_2/6 h.

F = Sample in E exposed to C_2N_2/17 h.

G = Sample in F at 291 K evacuated through cold trap at 291 K.

H = Sample in G outgassed at 423 K/1 h.

I = Sample in H outgassed at 539 K/1.3 h.

J = Sample in I outgassed at 674 K/1 h.

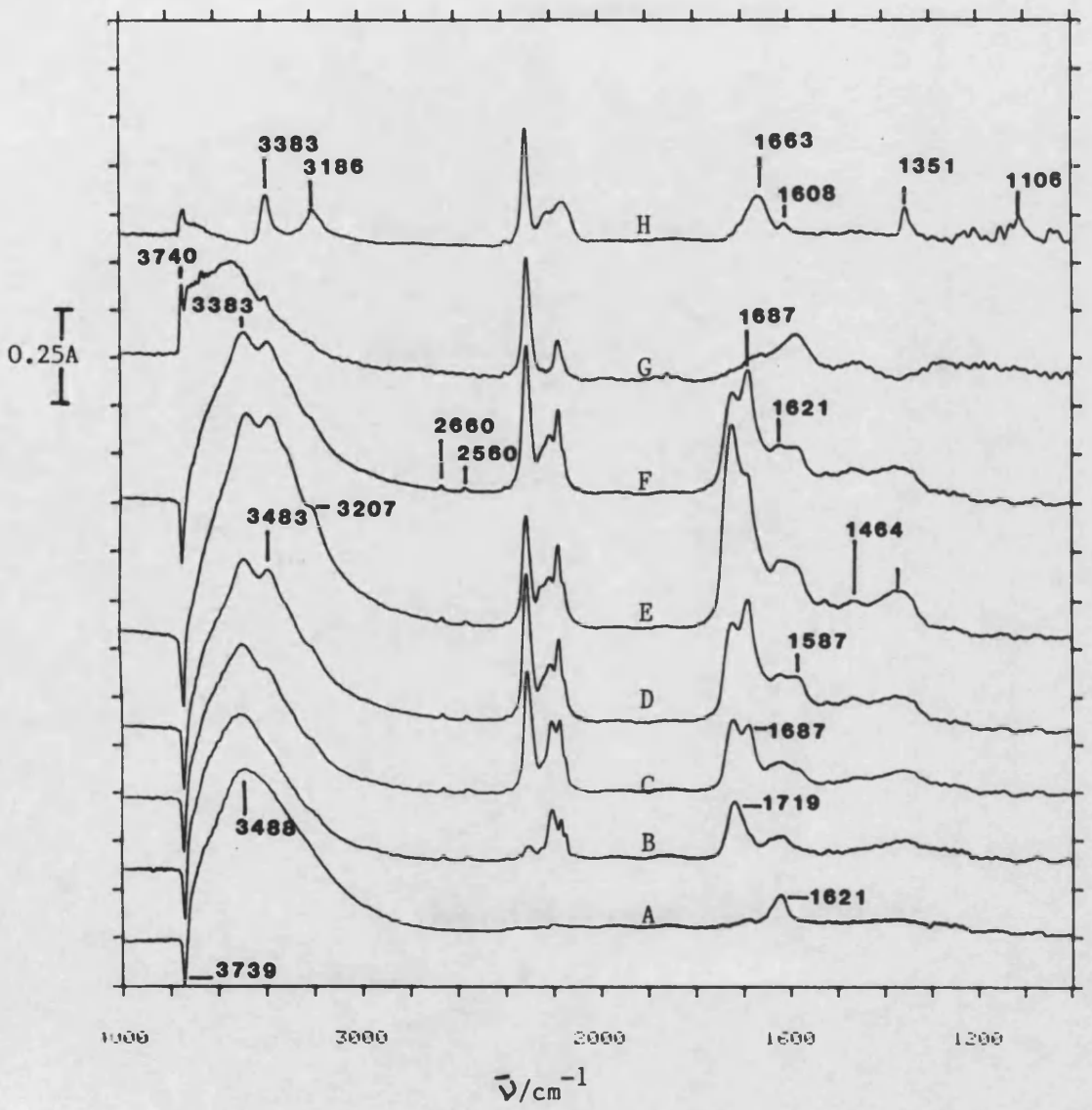

Fig. 4.11 I.r. Absorbance Difference Spectra of Cyanogen Interaction with Hydroxylated CuO/SiO_2

A = Adsorbed species on CuO/SiO_2 after outgassing at 673 K/15 h., then exposure to H_2O/15 min/ and evacuation through cold trap/25 min.

B = Adsorbed species and gaseous phase after exposing A to C_2N_2/30 torr/5 min.

C = As B, but C_2N_2/2.5 h.

D = As B, but C_2N_2/6 h

E = As B, but C N /17 h

F = Adsorbed species after evacuation at 291 K/1 h

G = As F, then outgassed at 423 K/1 h

H = As G, then outgassed at 539 K/1.3 h, 617 K/1.5 h and 674 K/1 h.

1687 cm^{-1} were also enhanced. After 17 h exposure a distinct band was now apparent at 3383 cm^{-1} and the shoulder shifted to 3207 cm^{-1}. The 1719 cm^{-1} band continued to grow and a new absorption at 2240 cm^{-1} appeared. The only notable effects caused by evacuation at 291 K was to reduce the intensity of the bands near 3383, 3200, 2240 and 1719 cm^{-1}. It is significant to report that the absorptions at 2660, 2560, 2168 and 2151 cm^{-1} were unaffected. Outgassing to 423 K greatly reduced the intensity of the broad absorption above 3000 cm^{-1} and only a weak feature at 3383 cm^{-1} remained on it. Furthermore, the negative band at 3740 cm^{-1} in the difference spectrum F (Fig. 4.11) now became a positive one (spectrum G). The bands at 2203, 2168,2151, 1719,1687, 1621 and 1369 cm^{-1} all disappeared but a new band, characteristic of CuCN appeared at 2175 cm^{-1}. Outgassing at 539 K caused a decrease in the intensity of this band and the development of a new band at 2216 cm^{-1} (Fig. 4.11). Bands at 3383, 3186, 1663, 1351 and 1106 cm^{-1} also appeared. Further heating to 617 K caused the disappearance of the 2175 cm^{-1} band but that at 2216 cm^{-1} intensified and a new band appeared at 2147 cm^{-1}.

Outgassing to higher temperatures (674 K/1 h) resulted in the sublimation of a white product onto the i.r. cell plates. A spectrum recorded through the windows alone contained bands at 3383,3186,1663,1351 and 1106 cm^{-1}. Comparison to literature values confirmed that the sublimate was oxamide (Table 4.23).

The only bands due to surface species were those due to SiNCO (2303 cm^{-1}), CuNCO (2216 cm^{-1}) and to a band at 2150 cm^{-1}.

Table 4.23 I.r. Spectrum of Oxamide and of the Sublimate Released from Cyanogen Exposed-Hydroxylated CuO/SiO_2

Peak Postions/cm^{-1}	
Present Work	Solid Oxamide [Assignment] Desseyn et al (160)
3383	3380 vs [$\nu_{as}(NH_2)$]
3186	3190 m [ν_s (NH_2)]
1663	1656 vs [$\nu(CO)$]
-	1600 vw [$\delta(NH_2)$]
1351	1343 m [$\nu(CN)$]
-	1162 vw [-]
-	1145 w [-]
1106	1104 m [$\rho(NH_2)$]
-	793 w [$\omega(NH_2)$]
-	678 s [$\tau(NH_2)$]
-	638 s [$\delta(NCO)$]
-	617 [$\pi(NCO)$]

4.10 Infra-red Spectroscopic Studies of Cyanogen Interaction with CrO_3/SiO_2

I.r. spectroscopic studies of the interaction of cyano compounds with silica-supported CrO_3 was mentioned in Sec. 1.6.4.2. The results supplement the work presented in Sec. 4.3 and work by Davies (4) who used

mass spectrometry and gravimetry to study HCN and C_2N_2 interaction with outgassed and oxygenated CrO_3/SiO_2. Davies concluded that hydrolysis of adsorbed C_2N_2 and HCN was a key reaction over these surfaces.

The current work represents the first i.r. studies relating to C_2N_2 interaction with silica-supported chromium(VI) oxide. The studies were carried out to further investigate the conversion of C_2N_2 especially via the hydrolysis route. I.r. studies are reported using outgassed, oxidised and hydroxylated surfaces. To assist interpretation, spectra were also obtained from an oxidised sample containing adsorbed D_2O.

4.10.1 Outgassed CrO_3/SiO_2

A 100 mg sample of CrO_3/SiO_2 was outgassed below $1x10^{-4}$ torr at 683 K/13 h. The green disc was cooled to room temperature and lowered into the i.r. beam. A spectrum of the outgassed sample is reproduced in Fig. 4.12 A. Spectra recorded through this disc during exposure to C_2N_2 at 291 K and subsequently as the disc was outgassed at a series of elevated temperatures are shown sequentially in Fig. 4.12 as transmission spectra and as absorbance difference spectra in Fig. 4.13. The latter spectra were obtained by subtracting a spectrum of outgassed CrO_3/SiO_2 from appropriate spectra (Sec. 3.2.3).

Dosing cyanogen to the outgassed disc caused several rapid spectral changes. The sharp -OH bond at 3741 cm^{-1}

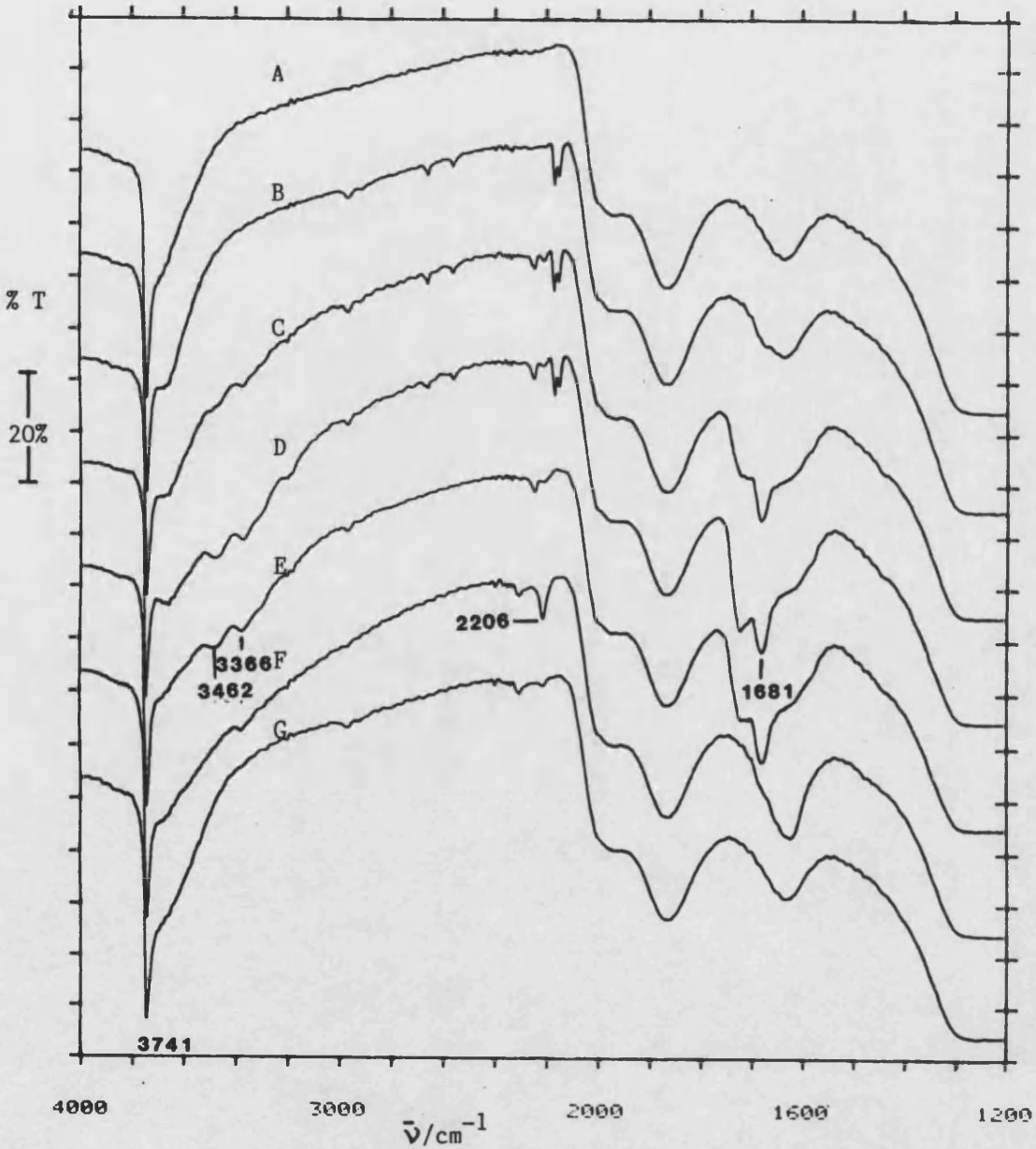

Fig. 4.12 I.r. Transmission Spectra of Cyanogen Interaction with Outgassed CrO_3/SiO_2

A = CrO_3/SiO_2 outgassed at 683 K/ 13 h

B = As A, then exposed to C_2N_2 20 torr/291 K/20 min

C = " " " 20 torr/291 K/15 h

D = " " " 20 torr/291 K/25 h

E = As D, then evacuated to $<10^{-3}$ torr

F = As E, then evacuated at 473 K/3 h

G = As F, then evacuated at 573 K/2.5 h

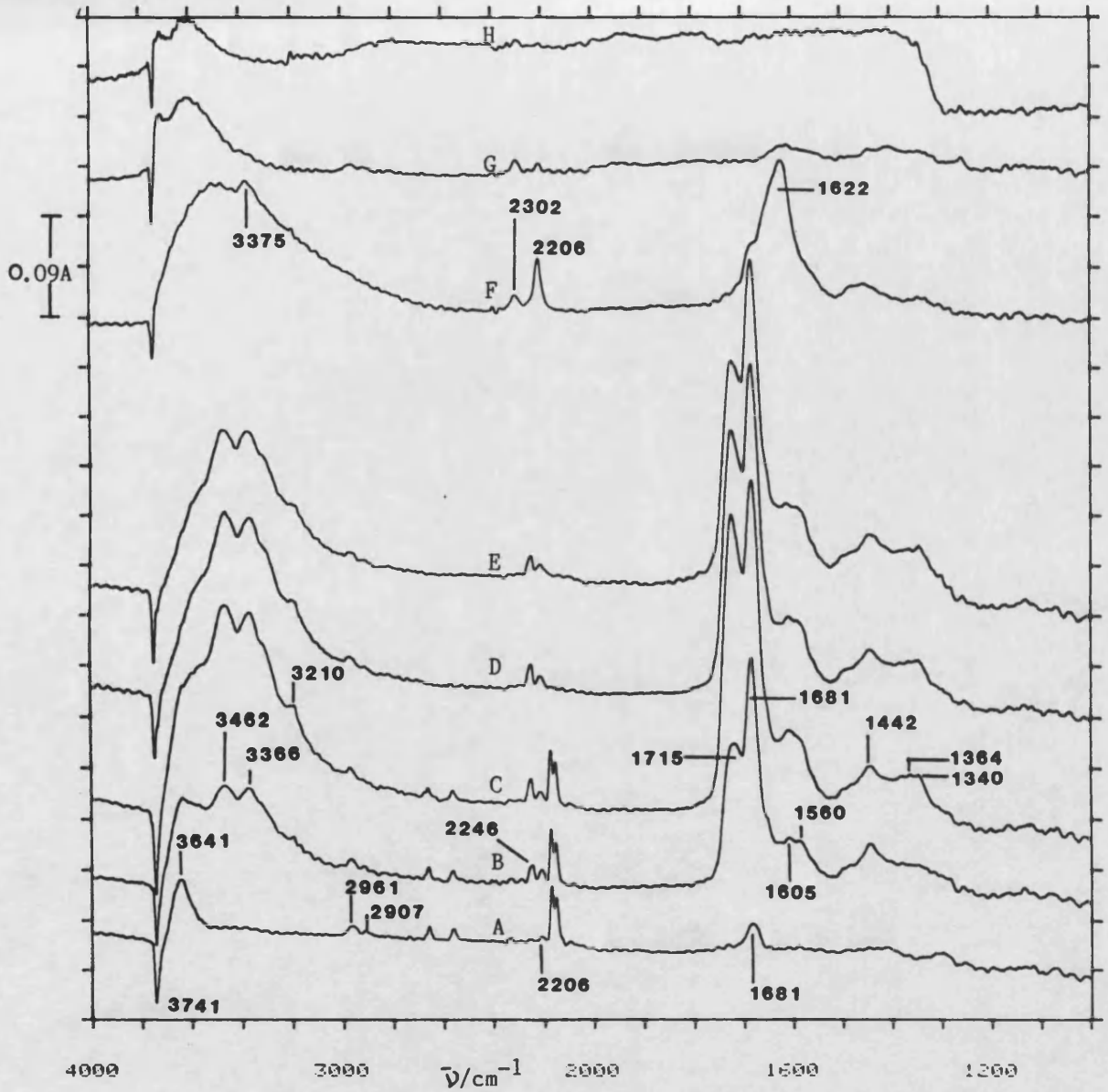

Fig. 4.13 I.r. Absorbance Difference Spectra of Cyanogen Interaction with Outgassed CrO_3/SiO_2

A = Adsorbed species plus gaseous phase after exposure of outgassed CrO_3/SiO_2 to C_2N_2 at 20 torr/291 K/20 min

B = As A but after 15 h

C = As B but after 25 h

D = Adsorbed species in spectrum C. (After removal of condensable products)

E = Adsorbed species in spectrum C (After evacuation at 291 K)

F = Adsorbed species after 10^{-3} torr/473 K/3 h

G = " " " " /573 K/2.5 h

H = " " " " /683 K/2 h

was diminished, this was accompanied by the appearance of an equally intense band at 3641 cm^{-1} also characteristic of isolated hydroxyl groups. It was evident that C_2N_2 exposure had caused a re-arrangment of surface -OH groups. Initial contact of the disc with C_2N_2 also caused a series of weak bands to appear at 2246,2206 (characteristic of isocyanate associated with chromium sites, and 1681 cm^{-1} (Fig. 4.13 A). The band at 1681 cm^{-1} was in a similar position to a band ascribed to an amide species when HCN was reacted with a chromia surface (4). The band is therefore assigned to a chromium-amide species.

After C_2N_2 exposure for 15 h more changes were apparent (Fig. 4.13 spectrum B). The band at 3641 cm^{-1} was masked by a broad absorption between 3650-3100 cm^{-1}. This underlying spectral intensity was due to O-H vibrations of H-bonded hydroxyl groups. The region contained maxima at 3462 and 3366 cm^{-1} which are due to N-H stretching. These two bands intensified during extended exposure and shoulders appeared at 3315 and 3193 cm^{-1}. The faint bands between 2300-2200 cm^{-1} also intensified during extended exposure but they remained weak. The spectrum between 1750-1300 cm^{-1} slowly underwent considerable change. Both of the weak features at 1681 and 1721 cm^{-1} intensified during extended exposure. The one at 1721 cm^{-1} was near one previously observed at 1720 cm^{-1} when C_2N_2 was interacted with hydroxylated silica (Sec. 4.8.2). Weak features also

appeared with maxima or shoulders at 1605,1560,1442,1364 and 1340 cm^{-1}. The band at 1442 cm^{-1} was possibly due to surface carboxylate on the chromium ions (10) or to surface chromium carbonate (161-162). An alternative explanation could be the formation of the species:-

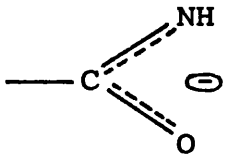

Such a species formed when HCN was adsorbed on alumina and i.r. bands were ascribed at 1600, 1440 and 1375 cm^{-1}. Features at 1560 and 1340 cm^{-1} coincide well with bands assigned to bidentate carbonate on chromia (163). There was no change to the spectrum on evacuation, this confirmed that all bands were due to adsorbed species (Fig. 4.13 spectrum E).

Spectra of the adsorbed species after evacuation between 291 and 683 K revealed the following changes (Fig. 4.13 F-H). The ν(N-H) bands at 3462 and 3366 cm^{-1} plus associated shoulders were lost by 473 K, only a weak peak at 3375 cm^{-1} remained visible on a broad band centred around 3450 cm^{-1}. The weak feature at 2241 cm^{-1} was replaced by another at 2302 cm^{-1} due to SiNCO (Sec. 4.9.1) whilst the 2206 cm^{-1} band intensified. The strong band at 1715 cm^{-1} disappeared and the one at 1681 cm^{-1} diminished to a weak shoulder at 1675 cm^{-1} on a new band seen at 1622 cm^{-1}. The series of features below this wavenumber were lost by 473 K. By 573 K all the bands present in the previous spectrum weakened except the one

at 3375 cm^{-1} which vanished. The hydroxyl band previously centred around 3450 cm^{-1} shifted to 3600 cm^{-1}. Evacuation at 683 K gave rise to a difference spectrum which only contained a negative peak at 3741 cm^{-1} a small band around 3600 cm^{-1} and a reduction in spectral intensity below the absorption edge at 1320 cm^{-1}.

4.10.2 Outgassed CrO_3/SiO_2 Heated in Cyanogen

A 100 mg disc, identical to that in the last section was exposed to C_2N_2 at room temperature as before. Spectra of C_2N_2 interaction with the outgassed CrO_3/SiO_2 disc are presented as transmission spectra and as absorbance difference spectra in Figs. 4.14 and 4.15, respectively. The spectrum recorded after cyanogen exposure for 291 K/20 h, was, as expected, identical to one recorded using similar conditions in the previous section.

The sample was then heated in residual C_2N_2 to 423 K/2 h. A spectrum of the adsorbed species plus gaseous phase (Fig. 4.15E) revealed that the only significant change was the reduction of the intensity of the band at 1721 cm^{-1}, (Sec. 4.8). After 20 hours at 423 K, the intensity of the band at 1681 cm^{-1}, previously assigned to a surface chromium-amide species was enhanced. Spectral intensity between 3500-3200 cm^{-1} and 1680-1300 cm^{-1} also increased, this supported the proposal that several features in these regions were due to surface amide.

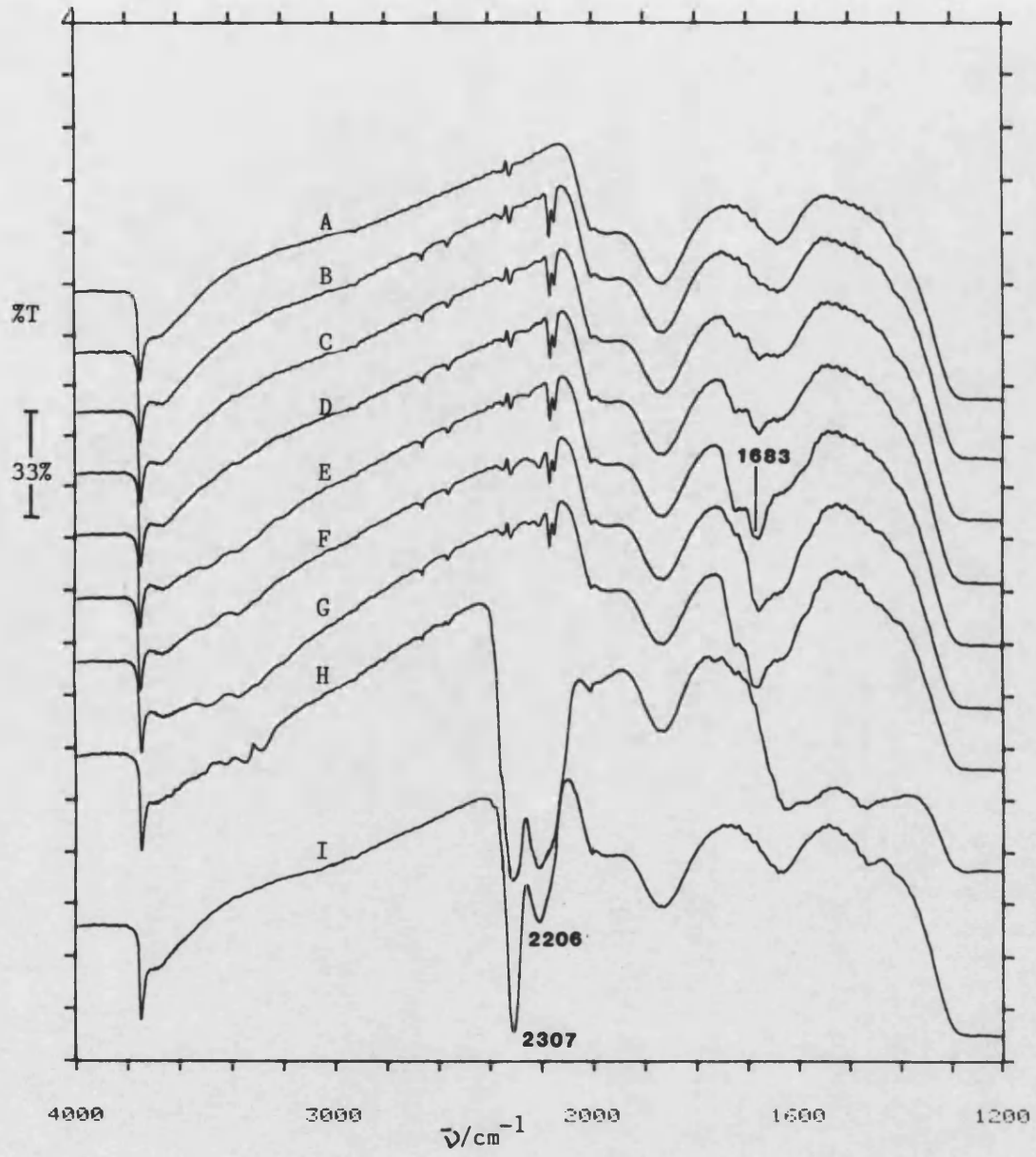

Fig. 4.14 I.r. Transmission Spectra of Cyanogen Interaction with Outgassed CrO_3/SiO_2

A = CrO_3/SiO_2 outgassed at 673 K/12 h

B = Sample A, in C_2N_2/24 torr/291 K/15 min

C = " " " /1 h

D = " " " /3 h

E " " " /20 h

F = Sample E, heated in C_2N_2/423 K/2 h

G = " F " " /423 K/18 h

H = " G " " /673 K/2 h

I = " H " " /673 K/12 h

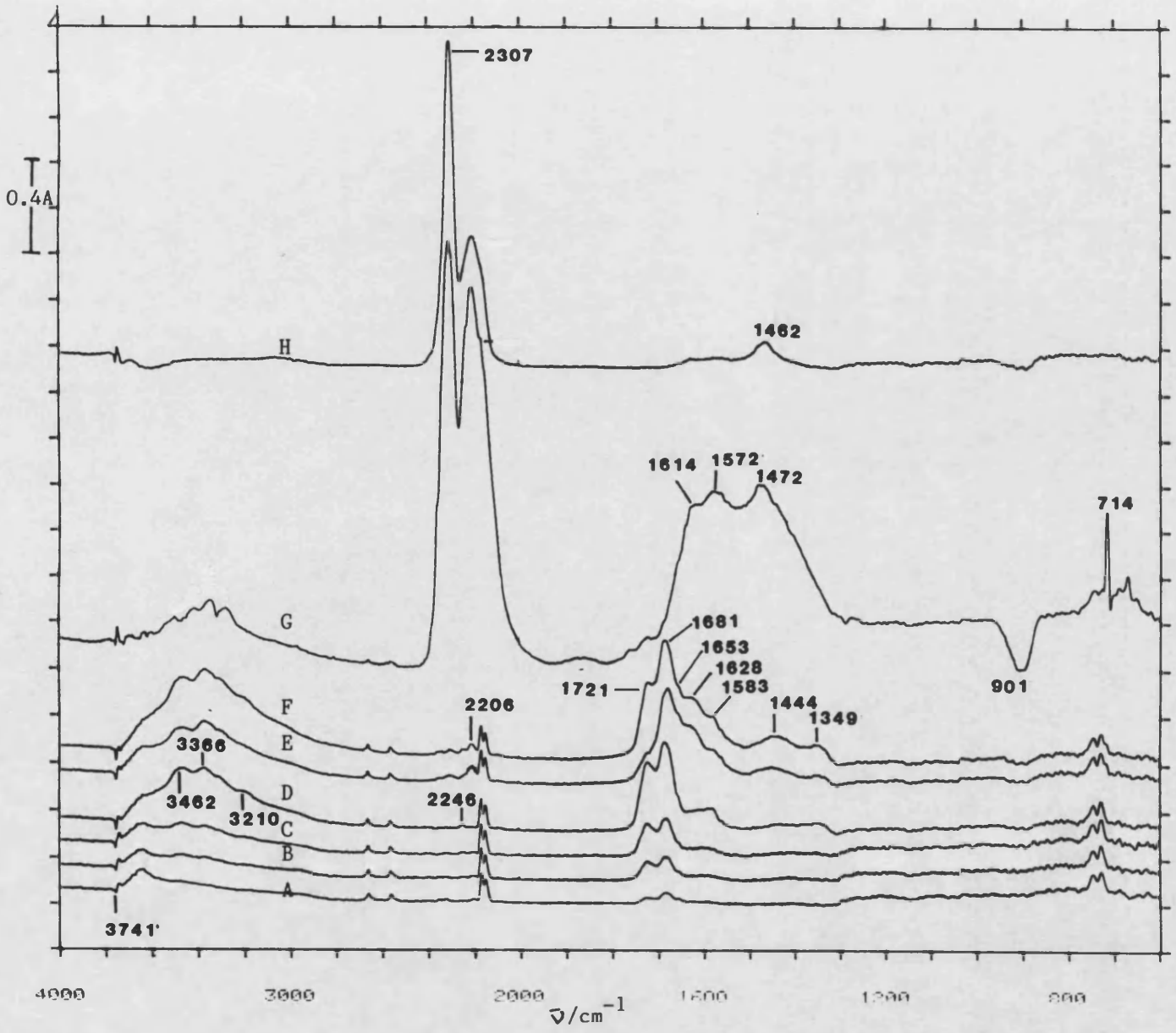

Fig. 4.15 Absorbance DIfference Spectra. Cyanogen Interaction with Outgassed CrO_3/SiO_2

A = Adsorbed species and gaseous phase after C_2N_2 interaction with outgassed CrO_3/SiO_2 at 291 K/15 min

B = Sample A in C_2N_2/1 h

C = " " /3 h

D = " " /20 h

E = Sample D then heated in C_2N_2/423 K/2 h (including gaseous phase)

F = Sample E heated in C_2N_2/423 K/20 h (including gaseous phase)

G = Sample F heated in C_2N_2/673 K/2 h (including gaseous phase)

H = Sample G outgassed 673 K/12 h

* All spectra referenced to spectrum of outgassed CrO_3/SiO_2

Heating the sample in C_2N_2 from 291 K to 673 K/2h. caused dramatic changes to the spectrum of the adsorbed species plus gaseous phase (compare Fig. 4.15F with 4.15G). The changes are described below.

(1) Bands ascribed to SiNCO at 2307 cm^{-1} and to CrNCO at 2206 cm^{-1} became very intense.

(2) A strong broad absorption developed between 1700-1400 cm^{-1} with peaks at 1614, 1572 and 1472 cm^{-1}. There are several possible explanations for these bands including symmetric stretching of isocyanate species and formation of precursors to carbon dioxide.

(3) Bands due to gaseous HCN were apparent at 3340 and 3273 cm^{-1} together with a sharp one at 714 cm^{-1} (compare to spectrum of gaseous HCN, Fig. 2.9).

(4) The negative peak observed at 3741 cm^{-1} reversed to a positive peak suggesting an increase in population of free hydroxyl groups.

(5) A negative band developed at 901 cm^{-1}. A band at 870 cm^{-1} has been assigned to SiOH bending (157). If SiOH is the cause of this feature, it is peculiar that spectral intensity decreased when the band at 3741 cm^{-1} due to isolated silanols increased. One explanation is that a certain degree of rehydration of silica occurred. Boccuzzi et al reported that bands between 908-888 cm^{-1} immediately disappeared when a small amount of moisture was chemisorbed onto outgassed silica at elevated temperatures (164). If

this latter explanation was true we would have expected to see evidence for gaseous H_2O in the spectrum since the i.r. cell was isolated from the vacuum frame. A band at 1614 cm^{-1} may well be caused by gaseous moisture.

The sample was maintained at 673 K in C_2N_2 for a further 10 h and was then evacuated. Only three spectral features relating to adsorbed species remained (Fig. 4.15H). The SiNCO band at 2307 cm^{-1} was unchanged but the 2206 cm^{-1} band ascribed to CrNCO was slightly weaker than before. Finally a weak band was observed at 1462 cm^{-1}. This latter band was due to the symmetric stretch of surface NCO groups (112-113).

4.10.3 Oxygenated CrO_3/SiO_2

The results of C_2N_2 interaction with oxygenated CrO_3/SiO_2 are shown as transmission spectra (Fig. 4.16) and as absorbance difference spectra (Fig. 4.17). Oxygenation caused several changes to the spectrum of outgassed CrO_3/SiO_2 (Fig. 4.17 spectrum A). The band intensity of the sharp band at 3734 cm^{-1} and of the broad band centred at 3609 cm^{-1} due to isolated and H-bonded silanol groups respectively were reduced in intensity whilst there was a slight intensification of the silica lattice vibrations near 2003, 1978 and 1870 cm^{-1}. These observations suggest that oxygenation caused surface dehydroxylation.

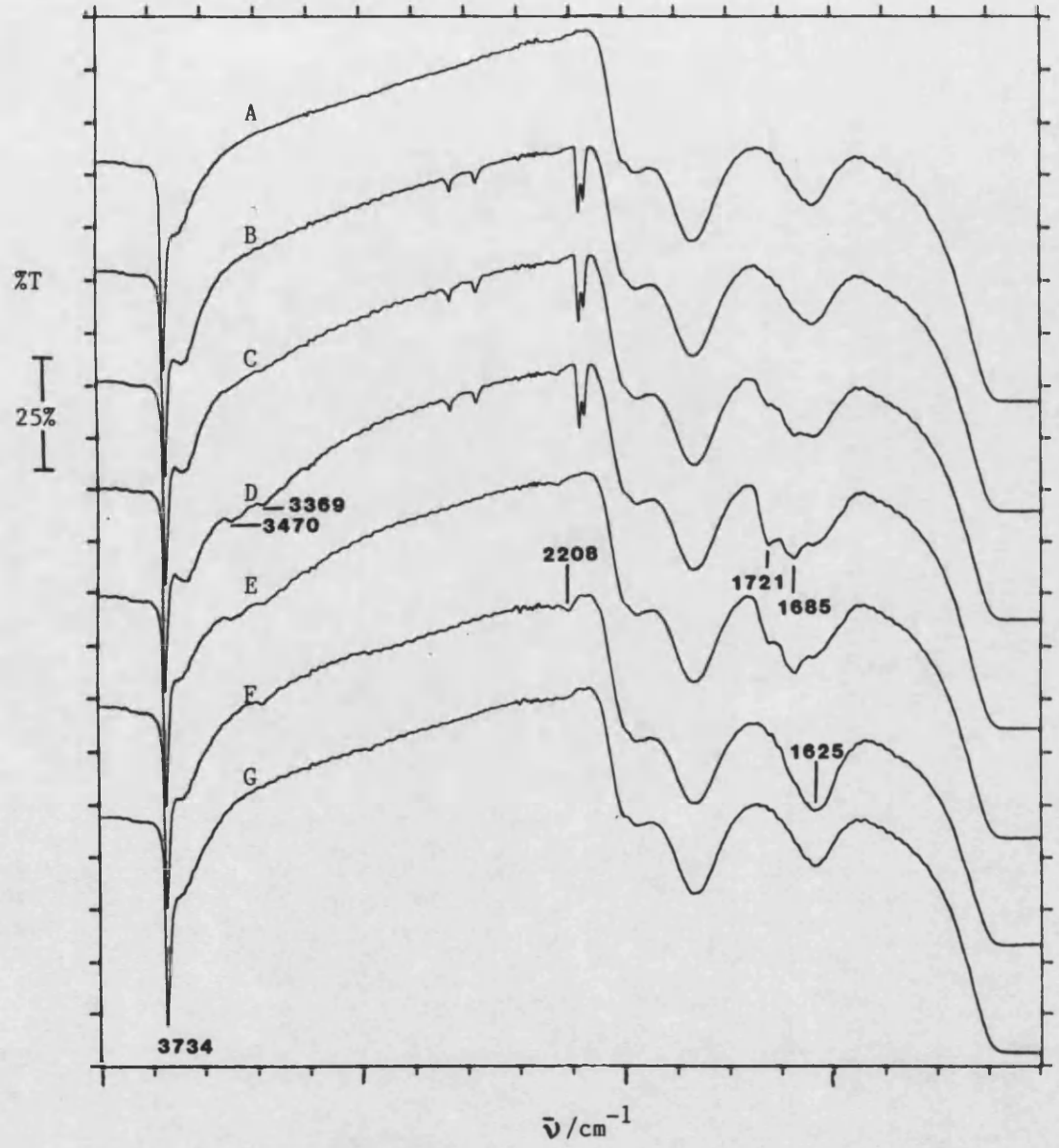

Fig 4.16 I.r. Transmission Spectra of Cyanogen Interaction with oxygenated CrO_3/SiO_2

A = Oxygenated CrO_3/SiO_2

B = Sample A exposed to C_2N_2/291 K/15 min

C = Sample B exposed to C_2N_2/291 K/6 h

D = " C " " /15 h

E = Sample D exposed to Liquid nitrogen trap

F = Sample E evacuated at 293 K/2 h

G = Sample F " " 473 K/2 h

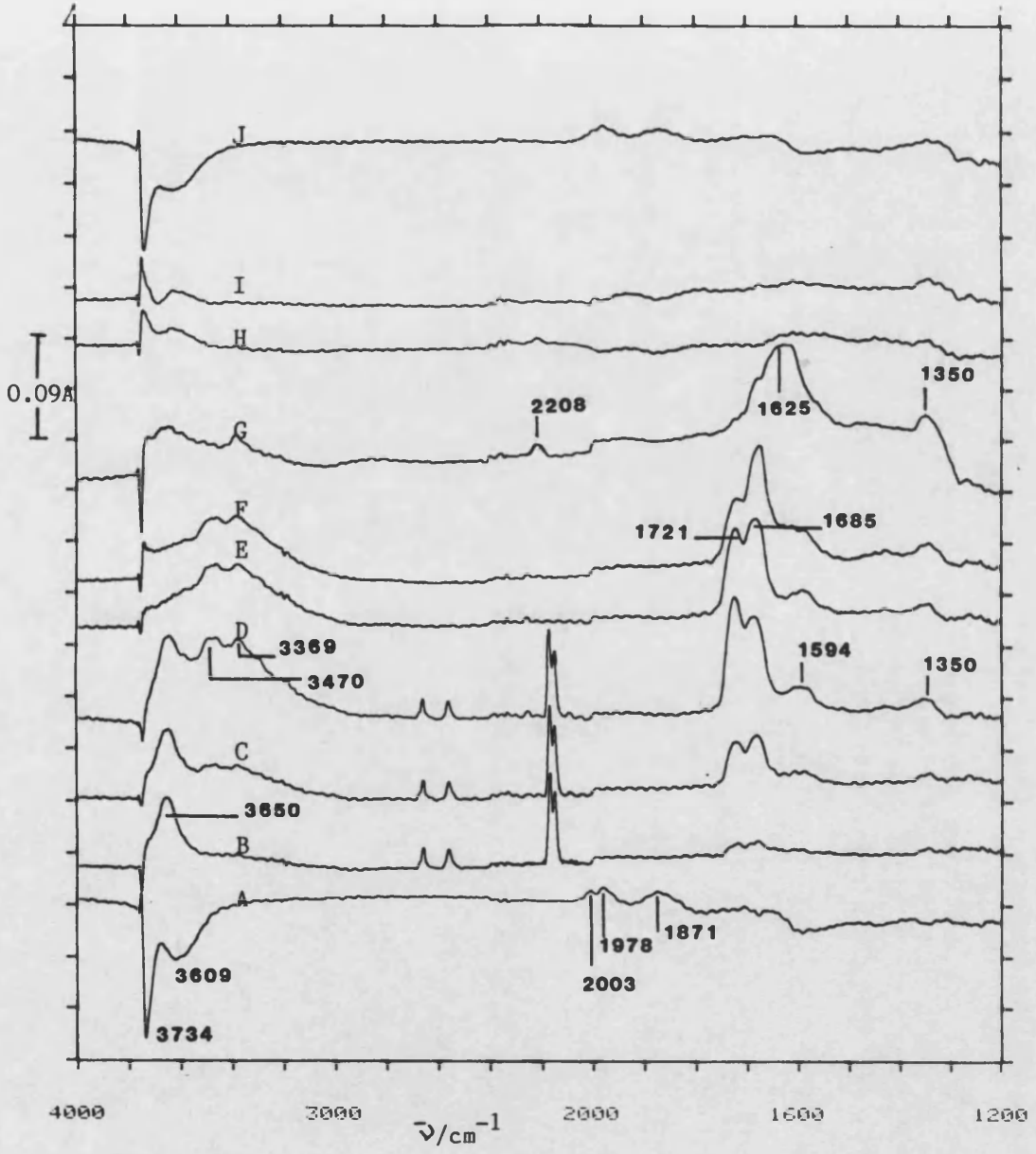

Fig. 4.17 I.r. Absorbance Difference Spectra of Cyanogen Interaction with Oxygenated CrO_3/SiO_2

A = Difference spectrum produced by oxygenation of outgassed CrO_3/SiO_2

B = Adsorbed species plus gaseous phase after C_2N_2 interaction with oxygenated CrO_3/SiO_2 at 291 K/15 min

C = Sample B, in C_2N_2/6 h

D = Sample B, in C_2N_2/18 h

E = Sample D exposed to liquid nitrogen trap

F = Sample E evacuated at 293 K/1 h

G = Sample F evacuated at 473 K/2 h

H = Sample G evacuated at 573 K/3 h

I = Sample H evacuated at 683 K/3 h

J = Sample I referenced to outgassed CrO_3/SiO_2

* All spectra except A and J are referenced to oxygenated CrO_3/SiO_2

Several spectral changes were evident when C_2N_2 was interacted with the oxygenated sample at 291 K (Fig. 4.17 B-D). The changes were as follows:

(1) Absorption around 3650 cm^{-1} was enhanced and the sharp peak at 3734 cm^{-1} intensified.

(2) A general intensification of the absorption between 3600-3000 cm^{-1} slowly occurred and peaks developed near 3470 and 3369 cm^{-1}. These peaks were probably due to N-H stretching but they were considerably weaker than similar bands observed on outgassed CrO_3/SiO_2, presumably due to the reduced availability of hydrogen caused by the lower number of hydroxyl groups.

(3) Strong bands slowly developed at 1721 and 1685 cm^{-1}. These were previously assigned to an adsorbed species on silica containing the C=O moiety and to an amide species associated with the chromium ions. Both bands were weaker than those observed on outgassed CrO_3/SiO_2.

(4) Weak bands developed near 1594 and 1350 cm^{-1}. These features are near those at 1560 and 1340 cm^{-1} seen in the case of C_2N_2 adsorption on outgassed CrO_3/SiO_2 (Sec. 4.10.1) and are assigned to bidentate carbonate present on the chromium ions (163).

When the gas phase surrounding the C_2N_2 - exposed oxygenated CrO_3/SiO_2 was condensed into a cold finger immersed in liquid nitrogen the intensity of the 1721

cm^{-1} band diminished and the 3650 cm^{-1} band vanished. Evacuation at 293 K further reduced the height of the peak at 1721 cm^{-1} (Fig. 4.17F).

On outgassing to 473 K, the bands at 3470 and 1721 cm^{-1} disappeared due to the removal of moisture and hydrolysis species associated with silica. New bands appeared at 2208 and 1625 cm^{-1} whilst the band near 1350 cm^{-1} strengthened. These features were identical to those observed over outgassed CrO_3/SiO_2 (Sec. 4.10.1). The 2208 cm^{-1} band was ascribed to the Cr-NCO species. The increase in intensity of the 1350 cm^{-1} band is attributed to the build-up of bidentate carbonate associated with the chromium sites. A sister band expected around 1590 cm^{-1} was not visible due to the tail associated with the 1625 cm^{-1} band.

On outgassing to 573 K all bands due to adsorbed species disappeared and by 683 K the spectrum was identical to the oxygenated disc prior to C_2N_2 exposure (compare spectra A and J of Fig. 4.17).

4.10.4 Hydroxylated CrO_3/SiO_2

Results of infra-red spectroscopic studies relating to C_2N_2 contact with hydroxylated CrO_3/SiO_2 are shown as transmission spectra in Fig. 4.18 and as absorbance difference spectra in Fig. 4.19. The effect of hydroxylation was clearly seen by the reduced intensity of the sharp band at 3746 cm^{-1} and the development of two strong broad bands at 3415 and 1624 cm^{-1} (Fig. 4.19A).

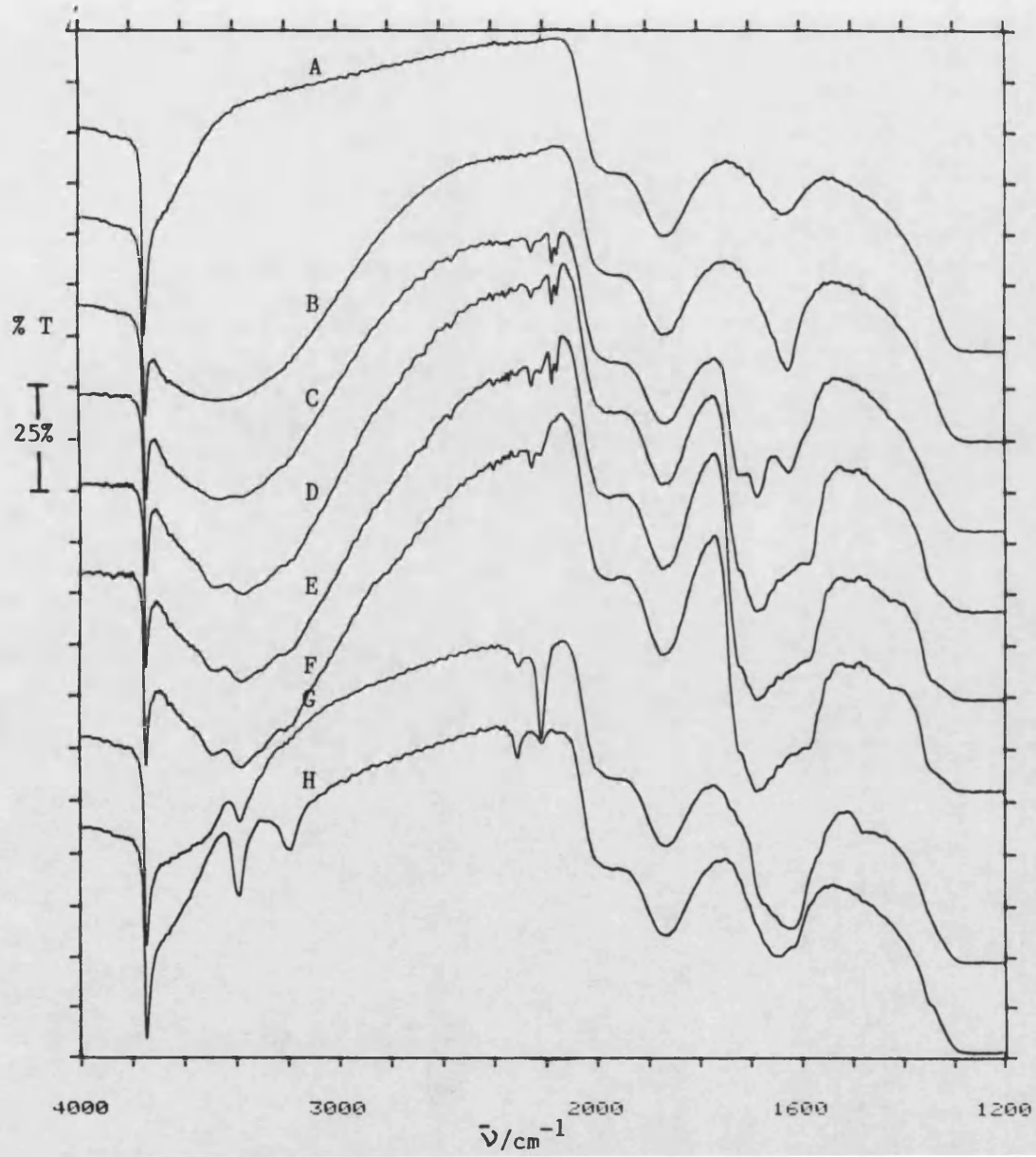

Fig. 4.18 I.r. Transmission Spectra of Cyanogen Interaction with Hydroxylated CrO_3/SiO_2

A = CrO_3/SiO_2 outgassed at 673 K/7 h

B = Hydroxylated sample from A.

C = Sample B exposed to C_2N_2/291 K/15 min

D = " " " " " /5 h

E = " " " " " /14 h

F = Sample E exposed to liquid nitrogen trap

G = Sample F evacuated at 471 K/2 h

H = Sample G evacuated at 573 K/2 h

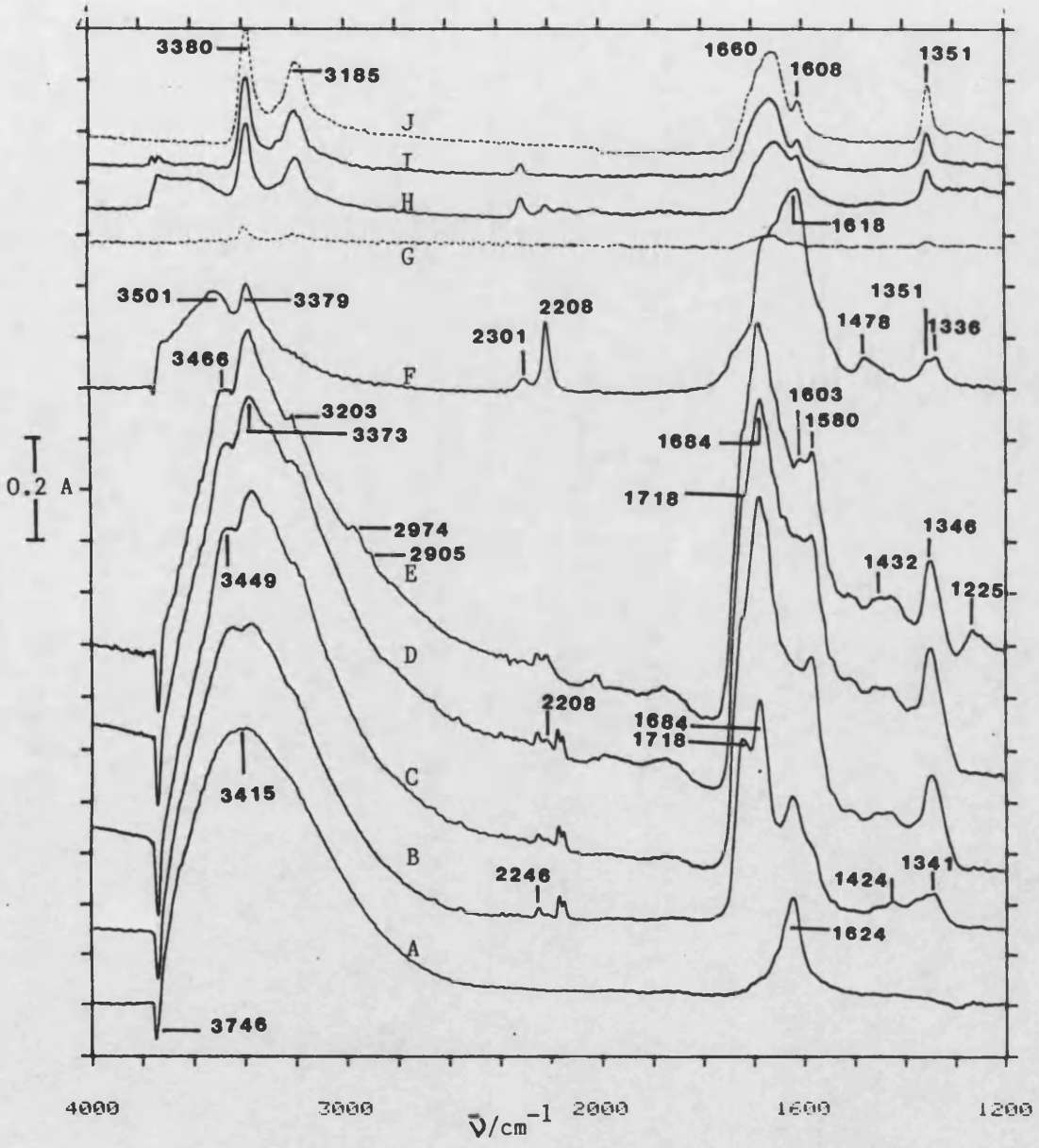

Fig. 4.19 I.r. Absorbance Difference Spectra: Cyanogen Interaction with Hydroxylated CrO_3/SiO_2

A = Adsorbed species caused by hydroxylation

B = Adsorbed species plus gaseous phase after cyanogen interaction with hydroxylated CrO_3/SiO_2 at 291 K/15 min

C = As in B except C_2N_2 contact 291 K/5 h

D = " " contact 291 K/14 h

E = Irreversibly adsorbed species after C_2N_2 contact 291 K/14 h

F = Adsorbed species after evacuation at 471 K/2 h

G = Spectrum of white sublimate on cell windows after evacuation at 471 K/2 h

H = Adsorbed species after evacuation at 573 K/2 h

I = " " " " 683 K/2 h

J = Spectrum of sublimate deposited on cell windows in I.

These changes were attributed to interaction of H_2O with the silica support (see Sec. 4.8.2). The hydroxylated disc reacted rapidly with cyanogen, the main spectral changes which were apparent after C_2N_2 contact were as follows; (1) Development of two strong bands at 1718 and 1684 cm^{-1} ascribed to surface amide species on the silica and chromium surfaces respectively. As one would predict, these bands were much more intense than those observed over outgassed CrO_3/SiO_2. (2) Evidence for N-H bond formation was provided by the appearance of peaks at 3449 and 3373 cm^{-1} on the broad band centred at 3415 cm^{-1} and (3) the formation of weak bands at 2246, 1424 and 1341 cm^{-1}, similar to those seen on outgassed CrO_3/SiO_2 after C_2N_2 interaction.

After 14 h exposure to C_2N_2 the band at 1684 cm^{-1} had intensified suggesting that the formation of surface amide over chromium sites was a slow prosess (Fig. 4.19D). Furthermore a series of bands developed at 1603, 1580,1508,1432,1346 and 1225 cm^{-1} plus a shoulder at 1618 cm^{-1}. By comparison with studies of CO_2 adsorption onto α-Cr_2O_3 by Zecchina et al (163), several of these bands were ascribed to surface bicarbonate and bidentate carbonate species (Table 4.24). Zecchina assigned three pairs of bands to bidentate carbonates due to surface and ligand heterogeneity (163). The appearance of only one pair of bands in the current work was due to the presence of a definite surface phase containing chromium ions in only one type of co-ordination site. Other changes which

were apparent after 14 h C_2N_2 contact were the intensification of the N-H bond at 3373 cm^{-1} and the appearance of a weak peak at 2208 cm^{-1} due to CrNCO.

Table 4.24 Assignment of Surface Carbonate-Like Species

Frequencies/cm^{-1}		
Present work	Zecchina et al (163)	Assignment
1620-1432-1225	1620-1430-1225	strongly chemisorbed bicarbonate
1580-1346	1560-1340	strongly chemisorbed bidentate carbonate
1580-1346	1590-1305	strongly chemisorbed bidentate carbonate
1580-1346	1635-1285	strongly chemisorbed bidentate carbonate

All spectral features were retained on evacuation at 291 K. The only change was that the broad band due to H-bonded hydroxyl groups centred around 3415 cm^{-1} was reduced in intensity and fine structure above 3000 cm^{-1} was revealed. A series of peaks and shoulders became visible at 3466,3373,3203,2974 and 2905 cm^{-1} (Fig. 4.19E). The bands above 3000 cm^{-1} were observed over outgassed CrO_3/SiO_2 after C_2N_2 contact and were attributed to N-H vibrations. The two bands below 3000 cm^{-1} were also similar to those observed in the case of outgassed CrO_3/SiO_2.

Evacuation at 471 K had a marked effect on the spectrum above 3000 cm^{-1} (Fig. 4.19F). The intensity of the peak at 3746 cm^{-1} was restored to the level present in the outgassed surface and most of the physically held moisture, which gave rise to the broad band around 3415 cm^{-1}, was removed. Bands ascribed to N-H and CH_3 moieties were removed with the exception of one at 3379 cm^{-1}. Heating to 471 K also intensified spectral features at 2301 (SiNCO) and 2208 cm^{-1} (CrNCO). Below 1700 cm^{-1} marked changes were observed. The intense absorption at 1684 cm^{-1}, due to surface amide associated with chromium sites was greatly reduced and was now seen as a weak shoulder on a broad, intense band centred at 1618 cm^{-1}. The bicarbonate absorptions at 1432 and 1225 cm^{-1} were lost, as were bands previously observed at 1603 and 1508 cm^{-1}. A new band appeared at 1478 cm^{-1} and a second one appeared near 1350 cm^{-1}, these band positions were near those at 1490 and 1365 cm^{-1} attributed to monodentate carbonate on chromium (163). This assignment of the peak at 1350 cm^{-1} to monodentate carbonate was dubious because a small amount of white material sublimed onto the i.r. cell windows during outgassing at 491 K and this exhibited a band at 1351 cm^{-1}. The spectrum of the sublimate also contained features at 3380 and 3185 cm^{-1} characteristic of oxamide (Fig. 4.19G).

Evacuation upto 573 K caused more oxamide to sublime onto the cell windows and the intensity of the characteristic bands at 3380,3185,1664,1603 and 1351 cm^{-1}

increased (Fig. 4.19H). (Other bands also characteristic of oxamide at 1106,797 and 637 cm^{-1} also appeared but are not shown here). The only bands due to surface species were those at 2301 cm^{-1} (SiNCO), 2208 cm^{-1} (CrNCO) and 2150 cm^{-1}. The features characteristic of strongly chemisorbed carbonate disappeared by 573 K. Only the SiNCO band at 2301 cm^{-1} resisted evacuation at 683 K/2h (Fig. 4.19I).

4.10.5 Oxygenated and Hydroxylated CrO_3/SiO_2

A CrO_3/SiO_2 disc was oxygenated as in Sec. 4.10.3 and then exposed to water vapour at 18 torr for 10 minutes. Excess water vapour was removed by evacuation through a liquid nitrogen cold trap for 3 minutes. An i.r. transmission spectrum of the pretreated disc is shown in Fig. 4.20B. The differences between this and a spectrum of the outgassed disc is presented in absorbance units in Fig. 4.21A. The difference spectrum revealed that oxygenation and hydroxylation caused three changes to the spectrum. These were (1) A decrease in the concentration of free silanol groups resulting in a negative peak at 3751 cm^{-1}. (2) Development of a very strong broad band between 3600-3000 cm^{-1} with a peak at 3500 cm^{-1} due to hydrogen-bonded silanols and physically adsorbed water and (3) a weak feature at 1617 cm^{-1} due to H_2O associated with the silica.

The results of cyanogen interaction with the oxygenated and hydroxylated sample are presented as

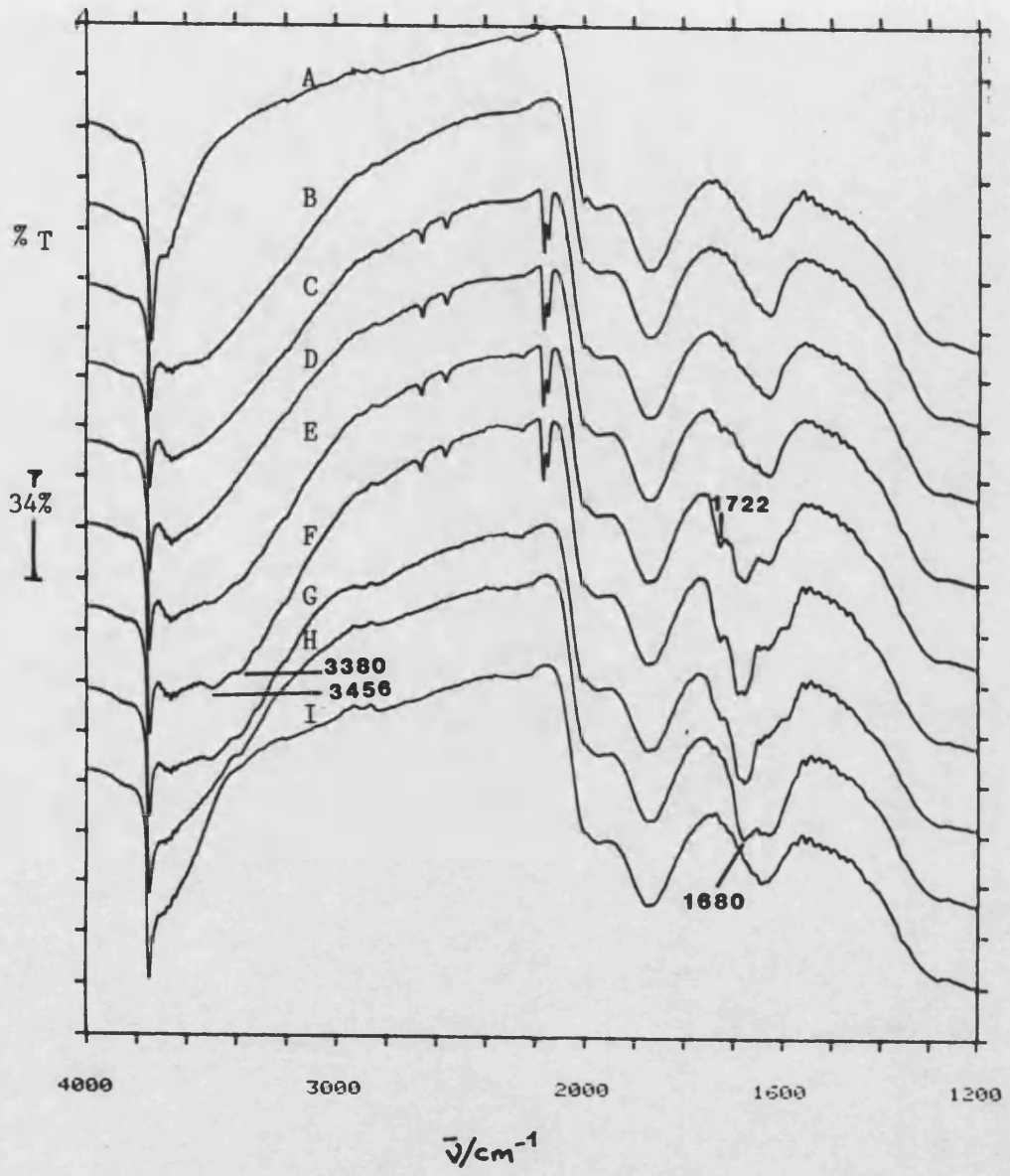

Fig. 4.20 I.r. Transmission Spectra of Cyanogen Interaction with Oxygenated -Hydroxylated CrO_3/SiO_2

A = CrO_3/SiO_2 outgassed at 673 K/14 h

B = Oxygenated and hydroxylated CrO_3/SiO_2

C = Sample B exposed to C_2N_2 at 18 torr/291 K/5 min

D = " " " " /30 min

E = " " " " /5.5 h

F = " " " " /14 h

G = Sample F evacuated at 298 K

H = As G then outgassed at 411 K/2 h

I = As H then outgassed at 575 K/2 h

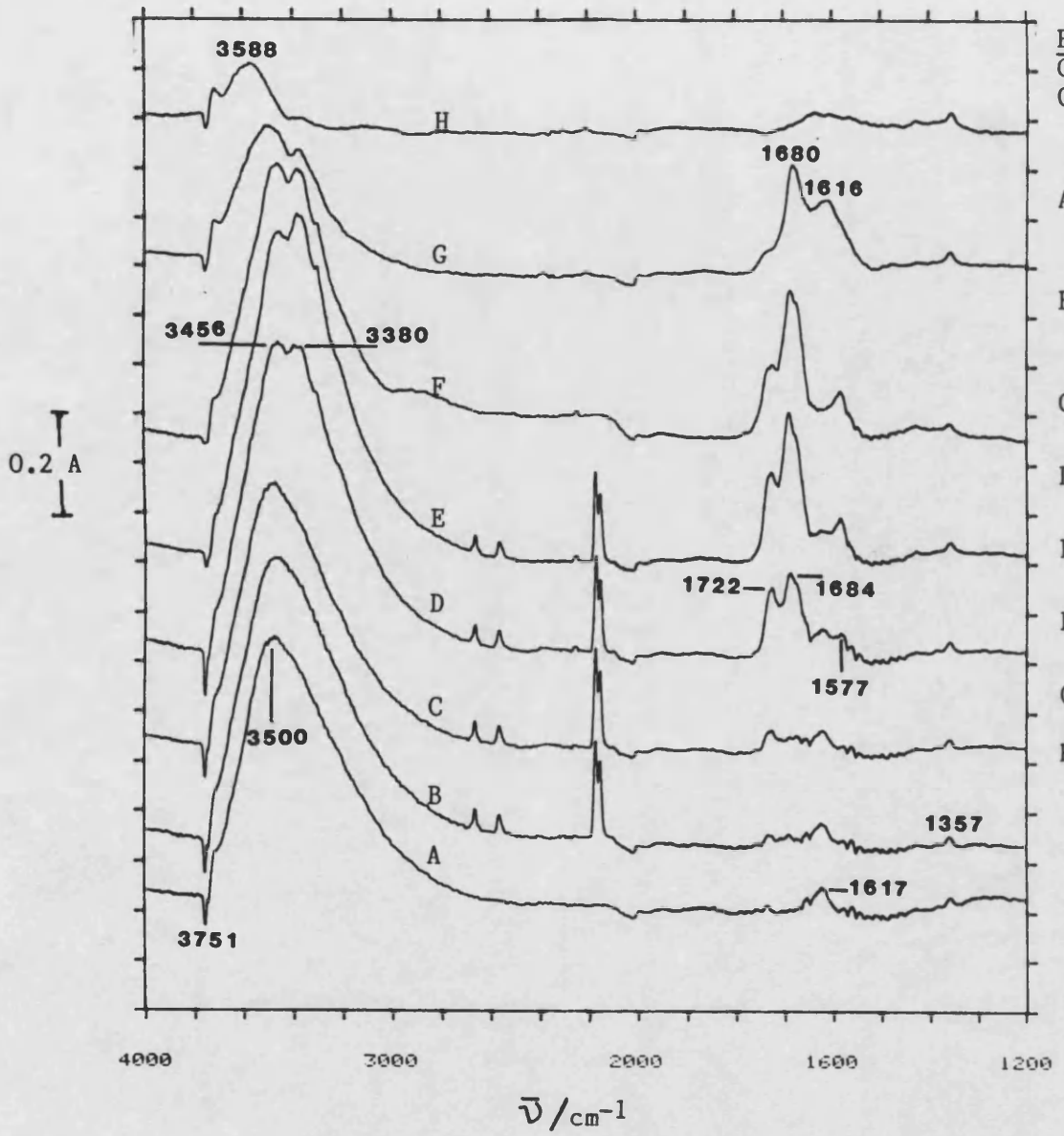

Fig. 4.21 I.r. Absorbance Difference Spectra of Cyanogen Interaction with Oxygenated-Hydroxylated CrO_3/SiO_2

A = Changes caused by oxygenation and hydroxylation of CrO_3/SiO_2

B = Adsorbed species plus gaseous phase after C_2N_2 18 torr/291 K/5 min

C = As B except C_2N_2/20 min

D = " " /5.5 h

E = " " /14 h

F = Adsorbed species after evacuation at 298 K

G = " " " outgassing at 411 K/2 h

H = " " " " " 575 K/2 h

transmission spectra in Fig. 4.20 and as absorbance difference spectra in Fig. 4.21. I.r. bands developed very slowly when the sample was contacted with C_2N_2/20 torr/291 K. Indeed little reaction was observed until 5.5 h exposure whereupon the following changes were apparent; first, two peaks at 3456 and 3380 cm^{-1} developed, which were ascribed to N-H stretching vibrations, and secondly, a series of new bands at 1722,1684,1577 and 1357 cm^{-1} appeared. The peaks at 1722 and 1684 cm^{-1} are asigned to amide-like species on the silica and chromium sites whilst the bands at 1577 and 1357 cm^{-1} are due to surface chromium carbonate. The peaks near 1430 and 1225 cm^{-1} which were assigned to surface carbonate over hydroxylated CrO_3/SiO_2 were not present in this study. After 14 h exposure to C_2N_2 the bands at 3380,1684 and 1577 cm^{-1} developed further; no spectral changes were apparent when the i.r. cell was evacuated at 298 K.

On outgassing at 411 K/2 h absorptions due to moisture associated with the silica (i.e. 3600-3000 and at 1618 cm^{-1}) diminished, but a new band at 1616 cm^{-1}, ascribed to H_2O deformation of adsorbed water molecules did appear. Evacuation at 575 K/2 h resulted in a spectrum which only contained features associated with hydroxylated silica. No absorptions due to C-N bonds were observed in this study.

4.10.6 Oxygenated and Deuterated CrO_3/SiO_2

A CrO_3/SiO_2 disc was outgassed at 673 K/13 h and then heated in 30 torr oxygen at 688 K for a further 18 h. The yellow disc was cooled to ambient temperature and D_2O which had been purified by a series of freeze-pump-thaw cycles was dosed at 10 torr/1 h. Excess D_2O was removed by freezing it into a liquid nitrogen trap. I.r. transmission spectra recorded before and after D_2O treatment are shown in Fig. 4.22 spectra A and B, respectively. The appearance of sharp bands at 3738 and 2761 cm^{-1} confirmed that both free O-H and O-D groups were present on the surface. A difference spectrum showing the effect of deuteration is shown in the absorbance mode in Fig. 4.23A. This spectrum contained a sharp band at 2761 cm^{-1} (O-D stretching) plus a tail from 2750-2000 cm^{-1} due to D-bonded OD groups. Due to the exchange of H for D, the OH band was observed as an inverted peak at 3738 cm^{-1}.

The results of C_2N_2 interaction with the disc are presented as a series of transmission spectra in Fig. 4.22 and as absorbance difference spectra in Fig. 4.23. To enable the changes caused by C_2N_2 contact to be clearly visible difference spectra were derived by subtracting a spectrum of the oxygenated-deuterated disc from appropriate spectra. After C_2N_2 exposure for 5 minutes no changes were apparent but after 6 h a peak appeared at 2441 cm^{-1} and a broad absorption at 1730-1620 cm^{-1} with peaks at 1716,1688 and 1653 cm^{-1} was observed. The peak at 2441 cm^{-1} is typical of an N-D stretch whilst

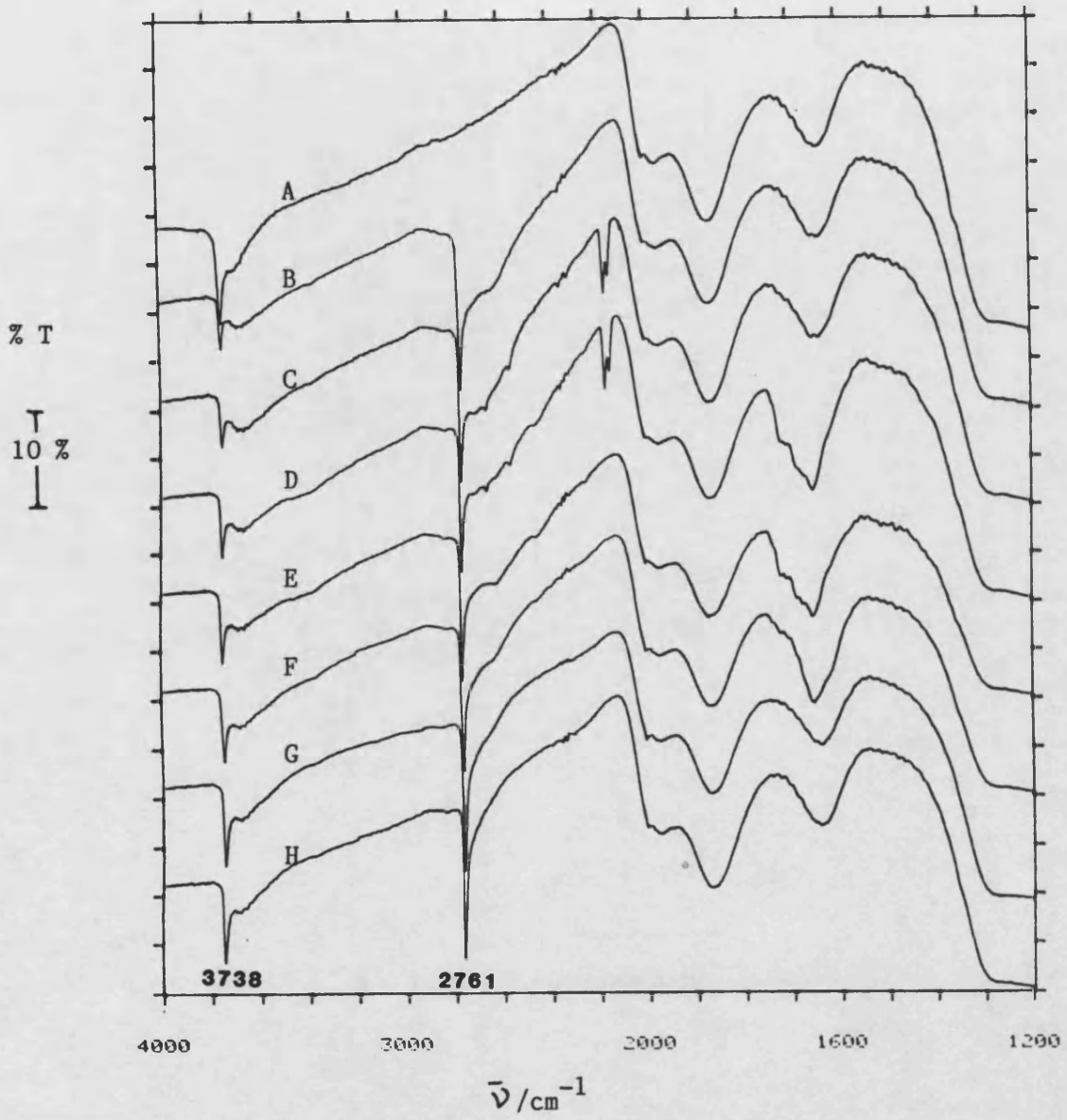

Fig. 4.22 I.r. Transmission Spectrum of Cyanogen Interaction with Oxygenated-Deuterated CrO_3/SiO_2

A = Oxygenated CrO_3/SiO_2

B = Sample A treated with D_2O

C = Oxygenated and deuterated CrO_3/SiO_2 exposed to C_2N_2 at 22 torr/5 min

D = Oxygenated and deuterated CrO_3/SiO_2 exposed to C_2N_2 at 22 torr/16 h

E = Sample in D evacuated at 298 K

F = Sample in E outgassed at 410 K/2 h

G = " F " " 560 K/2 h

H = " G " " 683 K/15 h

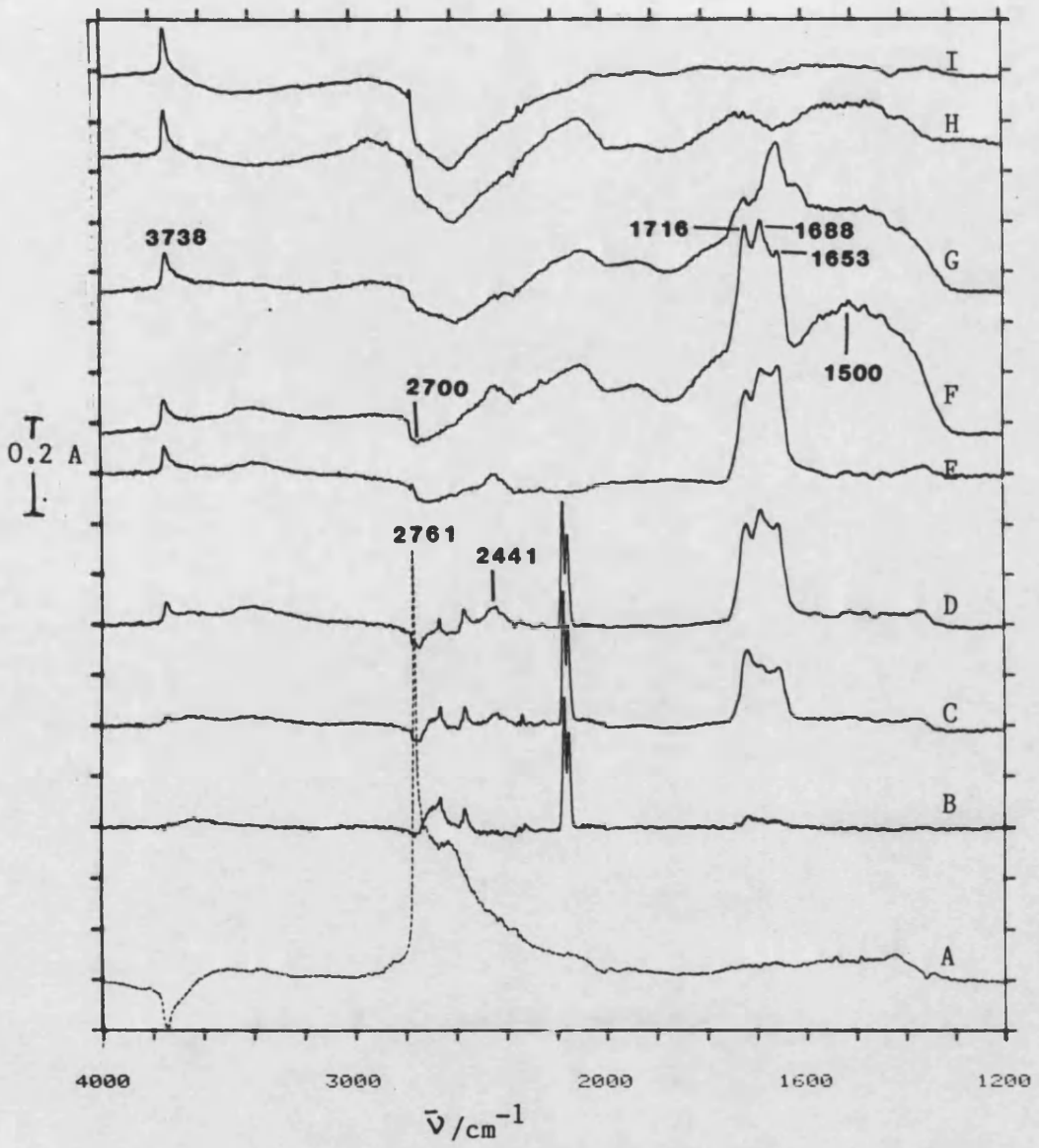

Fig. 4.23 I.r. Absorbance Difference Spectra of Cyanogen Interaction with Oxygenated-Deuterated CrO_3/SiO_2

A = Spectrum of oxygenated-deuterated CrO_3/SiO_2 minus spectrum of outgassed CrO_3/SiO_2

B = Difference spectrum after C_2N_2 challenge at 22 torr/5 min

C = Difference spectrum after C_2N_2 challenge at 22 torr/6 h

D = Difference spectrum after C_2N_2 challenge at 22 torr/14 h

E = As D after exposure to liquid nitrogen cold trap

F = As E after evacuation /291 K/15 min

G = As F after outgassing at 410 K/2 h

H = As G after outgassing at 560 K/2 h

I = As H after outgassing at 683 K/15 h

* Difference spectra from B onwards derived using Spectrum A as reference.

the appearance of the bands at 1716 and 1688 cm^{-1}, unmoved from their position over the H_2O-treated surface, confirms that no H or D atoms were associated with the sources of these absorptions. This was consistent with an earlier assignment of these bands to the C=O stretch of surface amides. After 16 h of C_2N_2 contact the amide bands at 1716 and 1688 cm^{-1} had increased in intensity suggesting that hydrolysis was a slow process. The band at 1653 cm^{-1} also intensified. This band was not observed in the spectrum of the previous experiment when H_2O was used in place of D_2O. One explanation for this feature is that it was due to a deuterated-amide species associated with either the silica or chromium surface. This suggestion is plausible since Desseyn et al (160) reported that the C=O stretch of $D_2NCOCOND_2$ was observed at 1640 cm^{-1}, some 20 cm^{-1} lower than in the case of $H_2NCOCONH_2$.

No spectral changes occurred when the gas phase was frozen into a cold trap but when the sample was evacuated at 291 K a broad trough developed around 2700 cm^{-1} (Fig. 4.23F) together with a broad band around 1500 cm^{-1}. The trough was due to removal of weakly held D_2O from the surface.

On outgassing to 410 K, the band at 1653 cm^{-1} became a prominent feature in the difference spectrum. The difference spectrum recorded after similar treatment using the oxygenated-hydroxylated disc (Fig. 4.21G) revealed a strong band at 1680 cm^{-1}. Since the

absorption was assigned to the carbonyl stretch of an amide group attached to a chromium site it is likely that the 1653 cm^{-1} band represents the equivalent deutero species similarly attached to a chromium site. All other spectral differences caused by outgassing upto 683 K were caused by changes in the degree of hydroxylation/ deuteration of the sample.

4.11 Infra-red Spectroscopic Studies of Cyanogen Interaction with Cr_2O_3/SiO_2

Some previous i.r. spectroscopic studies of the interaction of cyano-compounds with chromia and silica-supported chromia were reported in Secs. 1.6.3 and 1.6.4, respectively. The most relevant work was that of Surman (3) and Davies (4) who concluded that adsorbed HCN reacted to form surface amide species at room temperatures. At higher temperatures these species decomposed to CO_2 via surface formate and carboxylate species.

The results presented in the following pages supplement mass spectroscopic and gravimetric work described earlier (Sec. 4.4). The current work represents the first i.r. studies of C_2N_2 interaction with silica-supported chromia and the main objective was to investigate the decomposition mechanism of adsorbed C_2N_2 and to determine whether or not surface amide and/or diamide intermediates were formed.

4.11.1 Outgassed Cr_2O_3/SiO_2

A 100 mg sample of $Cr(NO_3)_3/SiO_2$ was compressed into a thin disc and placed into the i.r. cell which was connected to the vacuum frame. The sample was outgassed at 673 K/20 h. The Cr_2O_3/SiO_2 disc so formed was cooled to ambient temperature and an i.r. transmission spectrum was measured (Fig. 4.24 A). This spectrum was used as reference spectrum to derive absorbance difference spectra later in this experiment. Spectra recorded during and after C_2N_2 exposure of the sample are shown as % transmission spectra (Fig. 4.24) and as absorbance difference spectra (Fig. 4.25).

Exposure of the outgassed disc to C_2N_2 at 291 K caused the following changes to the i.r. spectrum:-

1) The intensity of the sharp O-H band at 3739 cm^{-1} rapidly decreased and remained at constant intensity during extended exposure to C_2N_2.
2) N-H stretching absorptions developed at 3454, 3362, 3311 and 3209 cm^{-1}. These features developed slowly at room temperature and were in similar positions to those reported over the outgassed CrO_3/SiO_2 surface (Sec. 4.10.1).
3) A strong band appeared at 1685 cm^{-1}. This band, assigned to amide species on the chromium ions (4), slowly intensified at room temperature.
4) A series of weak features appeared at 1607,1584, 1499,1428 and 1353 cm^{-1}. All these absorptions, with the exception of the one at 1428 cm^{-1}, intensified during extended exposure to C_2N_2.

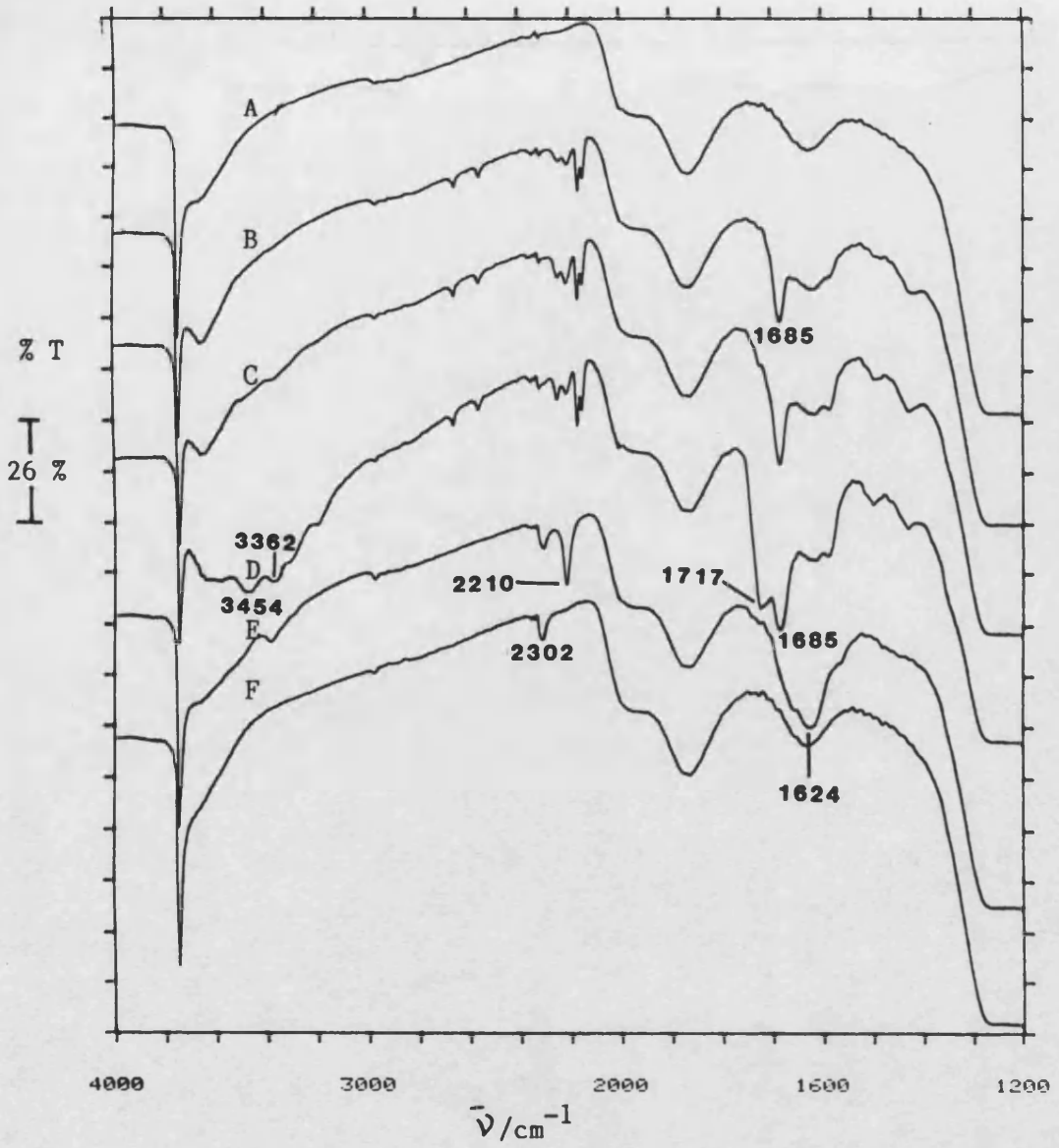

Fig. 4.24 I.r. Transmission Spectra of Cyanogen Interaction with Outgassed Cr_2O_3/SiO_2

A = Outgassed Cr_2O_3/SiO_2

B = Disc in A exposed to C_2N_2/291 K/15 min

C = " " " " /1.5 h

D = " " " " /21 h

E = Disc in D outgassed at 473 K/1.5 h

F = Disc in E outgassed at 673 K/21 h

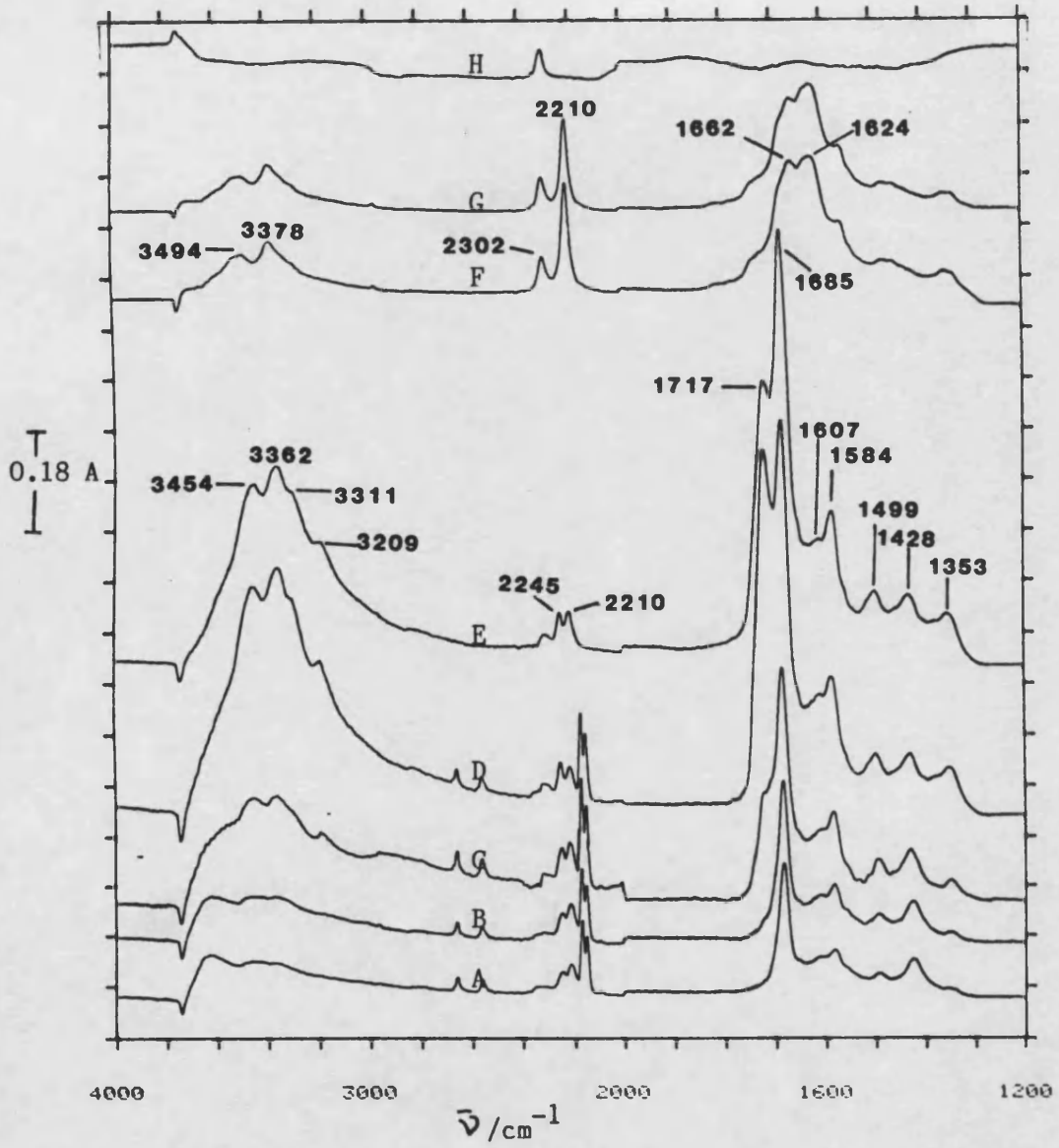

Fig. 4.25 I.r. Absorbance Difference Spectra of Cyanogen Interaction with Outgassed Cr_2O_3/SiO_2

A = Gas phase plus adsorbed species after exposure of outgassed Cr_2O_3/SiO_2 to C_2N_2 /291 K/15 min

B = As A but C_2N_2/291 K/40 min

C = " " " /3.5 h

D = " " " /21 h

E = Adsorbed species after outgassing at 291 K

F = " " " " " 473 K/2 h

G = " " " " " 473 K/2 h

H = " " " " " 673 K/21 h

* All difference spectra serived by subtracting spectrum of outgassed Cr_2O_3/SiO_2 from appropriate spectra.

5) A new band at 1717 cm^{-1} became visible after 3.5 h C_2N_2 contact, this was associated with amide formation on the silica surface. The slow growth of this band was in agreement with earlier studies of C_2N_2 interaction with hydroxylated silica (Fig. 4.4).

6) Two weak bands appeared at 2245 and 2210 cm^{-1} after 15 minutes C_2N_2 contact. Only the 2245 cm^{-1} band intensified during extended exposure.

The i.r. difference spectrum recorded through the disc after outgassing at 473 K revealed that major changes had occurred to the adsorbed layer. The strong N-H bands between 3500-3200 cm^{-1} were replaced by two small peaks at 3494 and 3378 cm^{-1}. The series of bands at 1717,1685,1607,1499 and 1428 cm^{-1} disappeared whilst the intensity of those at 1584 and 1353 cm^{-1} were weakened. Many of these changes were attributed to the removal of the surface-amide species which had formed at 291 K. Two new bands at 1662 and 1624 cm^{-1} appeared after heating to 473 K. By comparison with i.r. spectra recorded during the hydroxylation of silica (Sec. 4.8.2), the 1624 cm^{-1} band was ascribed to adsorbed H_2O on the silica surface.

Heating to 473 K also caused changes in the 2400-2000 cm^{-1} spectral region. These changes were:

1) development of a new band at 2302 cm^{-1},

2) strong growth of the 2210 cm^{-1} band due to the Cr-NCO species (Sec. 4.10.1),

3) loss of the absorption at 2245 cm^{-1}.

After outgassing at 673 K, the only spectral feature caused by adsorbed species was that at 2302 cm^{-1}. The thermal stability of the SiNCO species accounted for this observation.

4.11.2 Hydroxylated Cr_2O_3/SiO_2

A transmission spectrum of outgassed Cr_2O_3/SiO_2 is shown in Fig. 4.26A. This spectrum was used as a reference to derive absorbance difference spectra during this experiment. The effect of hydrolysis was clearly visible in Fig. 4.27A. The broad band around 3467 cm^{-1} and the weak one at 1615 cm^{-1} were due to adsorbed water (Sec. 4.8.1) whilst the negative peak at 3744 cm^{-1} was due to reduction in the number of isolated silanol groups.

I.r. spectra showing the interaction of C_2N_2 with hydroxylated Cr_2O_3/SiO_2 are shown as % transmission spectra (Fig. 4.26) and as absorbance difference spectra (Fig. 4.27). The following spectral changes were observed during room temperature C_2N_2 interaction:-

1) A sharp band due to N-H stretching slowly grew at 3385 cm^{-1}. After 15 h this feature was so intense that it masked the broad band at 3467 cm^{-1}, due to adsorbed moisture.
2) After 5 h C_2N_2 exposure a weak band appeared at 2248 cm^{-1}, no intensification occurred during extended exposure.

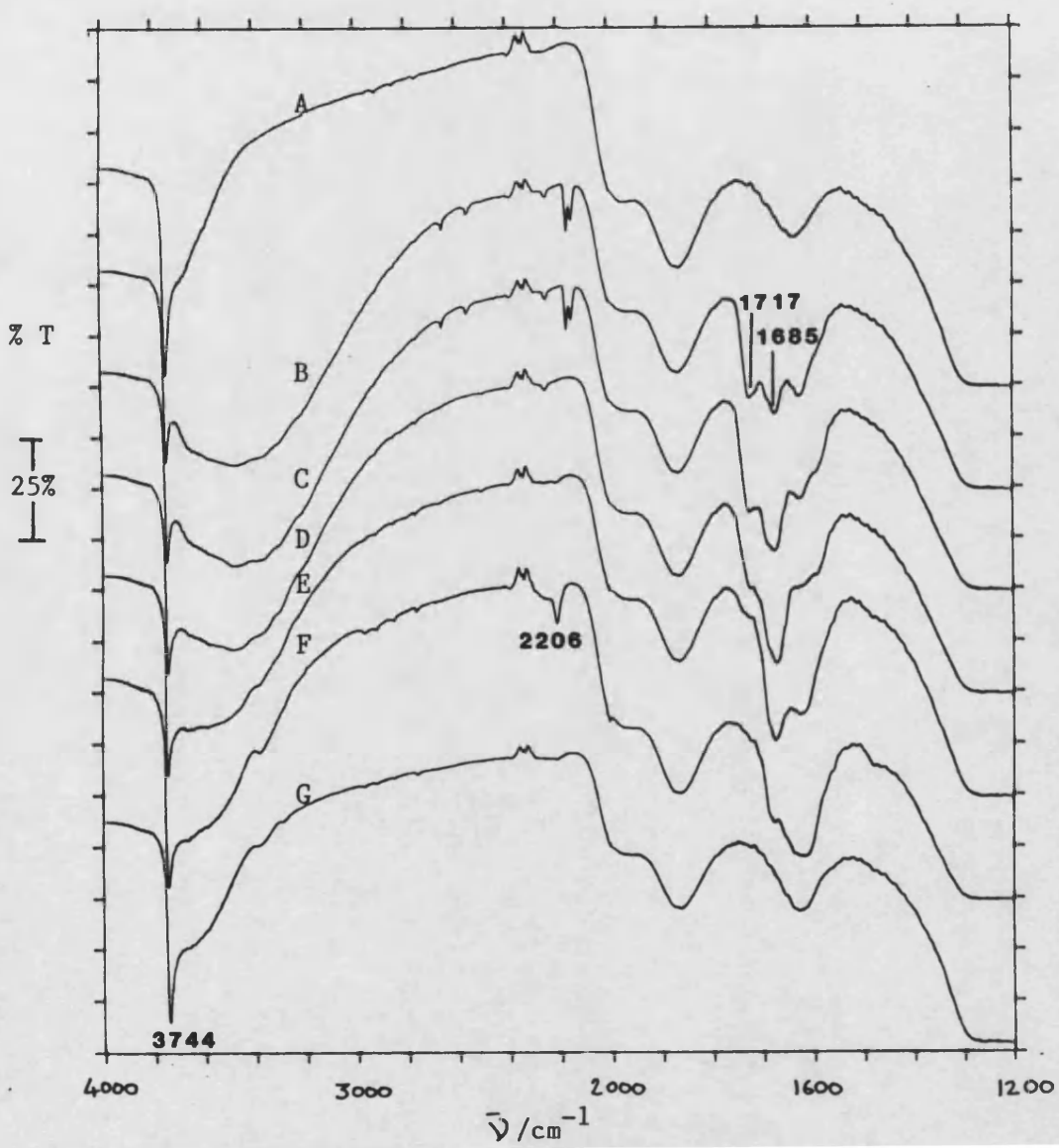

Fig. 4.26 I.r. Transmission Spectra of Cyanogen Challenge with Hydroxylated Cr_2O_3/SiO_2

A = Outgassed Cr_2O_3/SiO_2

B = Hydroxylated Cr_2O_3/SiO_2 after C_2N_2 challenge/298 K/5 h

C = " " " " " /15 h

D = As C, then evacuated at 298 K

E = As D, then outgassed at 411 K

F = As E, then outgassed at 485 K

G = As F, then outgassed at 590 K

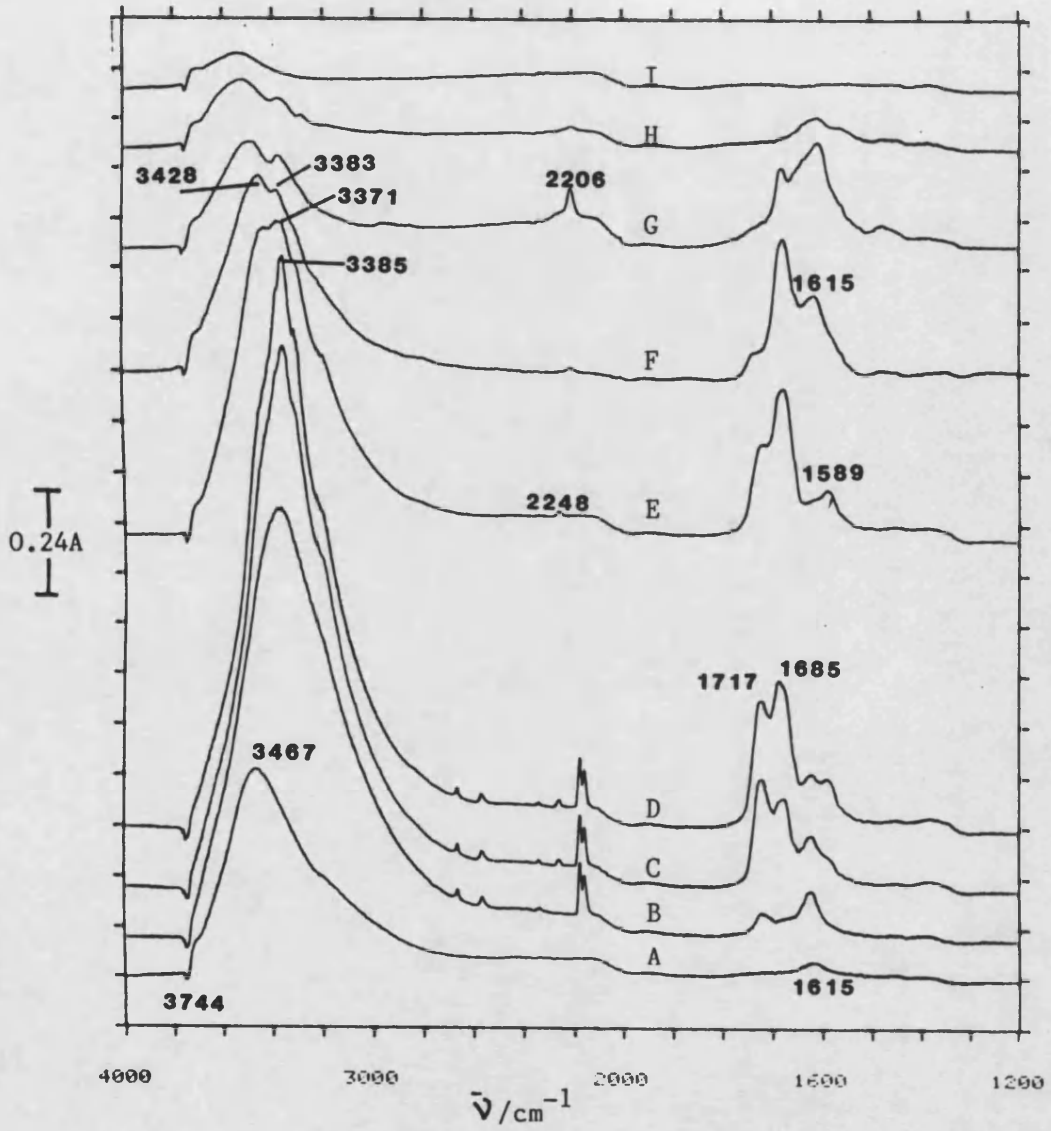

Fig. 4.27 I.r. Absorbance Difference Spectra of Cyanogen Interaction with Hydroxylated Cr_2O_3/SiO_2

A = Differences caused by hydroxylation of Cr_2O_3/SiO_2

B = Gas phase plus adsorbed species after exposure of hydroxylated Cr_2O_3/SiO_2 to C_2N_2/298 K/5 min

C = As B, except C_2N_2/298 K/5 h

D = " " /15 h

E = Adsorbed species resistant to condensation in a liquid nitrogen cold trap.

F = Adsorbed species after outgassing at 411 K/2 h

G = " " " " 485 K/2 h

H = " " " " 590 K/2 h

I = " " " " 630 K/21 h

3) A band rapidly developed at 1717 cm^{-1}, the intensity of which slowly increased. This absorption was due to the formation of a hydrolysis intermediate associated with the silica support (Sec. 4.8.1).

4) Bands at 1685 cm^{-1} (due to surface amide-like species on the chromium surface) and 1589 cm^{-1} developed slowly at room temperature.

5) The bands observed at 2210, 1499, 1428 and 1353 cm^{-1} in the case of C_2N_2 contact with outgassed Cr_2O_3/SiO_2 were not seen in this study.

After 15 h C_2N_2 exposure it was decided to check if gaseous products were released so a spectrum was recorded of the gaseous phase alone. This confirmed that only C_2N_2 was present. The i.r. cell was then exposed to a liquid nitrogen cold trap. An absorbance difference spectrum (Fig. 4.27E) showed that spectral intensity above 3000 cm^{-1} decreased and two maxima were resolved at 3428 and 3371 cm^{-1}. The intensity of the 1717 cm^{-1} due to silica amide-like species were also reduced.

When the sample was heated at 411 K, the 1717 cm^{-1} band was reduced to a weak feature and the ones at 2248 and 1587 cm^{-1} vanished whilst a small peak re-appeared at 1615 cm^{-1}. The band previously observed at 3385 cm^{-1} weakened and was now visible as a weak shoulder.

Raising the outgassing temperature to 485 K reduced the intensity of the O-H and N-H absorptions above 3000 cm^{-1}. The peak at 1685 cm^{-1} weakened whilst the one at 1717 cm^{-1} disappeared altogether. A new band appeared at

2206 cm^{-1}. This feature was removed when the disc was heated to 590 K. The band at 1685 cm^{-1} was also removed and the peak at 1608 cm^{-1} became weaker. By 630 K all features caused by C_2N_2 interaction were removed (Fig. 4.27I).

4.12 Infra-red Spectroscopic Studies of Cyanogen Interaction with $CuO-CrO_3/SiO_2$

Some i.r. spectroscopic studies of the interaction of cyano-compounds with mixed copper oxide-chromium oxide surfaces were reported earlier (Secs. 1.6.3 and 1.6.4). Davies (4) concluded that the adsorption and decomposition of HCN over these adsorbents mainly occurred by separate mechanisms on the individual metal oxide surfaces. Davies also presented evidence which showed that the conversion of adsorbed HCN on the mixed oxide system was not simply a combination of the reactions on the individual oxides.

The experiments reported in this section were carried out because mixed copper oxide-chromium oxide samples were known to be an active combination for the conversion of HCN to oxidation products. The results supplement the mass spectrometric and gravimetric work described earlier (Sec. 4.5). The current work represents the first i.r. studies of C_2N_2 interaction with the silica-supported copper oxide-chromium oxide system. The effect on the reactions of different sample pretreatments is also presented.

4.12.1 Outgassed $CuO-CrO_3/SiO_2$

A transmission spectrum of outgassed $CuO-CrO_3/SiO_2$ was recorded and used as a reference spectrum throughout this experiment (Fig. 4.28A). The results of C_2N_2 contact with this sample are shown as transmission spectra (Fig. 4.28) and as absorbance difference spectra (Fig. 4.29). The spectral region between 2400-2000 cm^{-1} in Fig. 4.29 was expanded and replotted in Fig. 4.30.

Spectra recorded during C_2N_2 exposure at ambient temperature revealed that reaction was rapid and two bands in the 'cyanide' region occurred within 10 minutes. By comparison with the i.r. studies involving outgassed CuO/SiO_2 and outgassed CrO_3/SiO_2 these bands, at 2203 and a weaker one at 2303 cm^{-1}, were explained by the formation of CuNCO and SiNCO species. The band due to SiNCO was noticeably weaker than on the CuO/SiO_2 surface. Initial C_2N_2 contact also caused a negative band to appear at 3736 cm^{-1} identical to that observed with CuO/SiO_2. This was due to consumption of isolated surface hydroxyl groups. A series of ripples which formed between 1700-1430 cm^{-1} were characteristic of the presence of oxidation and hydrolysis intermediates but they could not easily be related to the copper or chromium parts of the surface.

After 24 h C_2N_2 exposure the intensity of the CuNCO band had not significantly changed but the one due to SiNCO was much stronger than after initial exposure (compare spectra A,B and C in Fig. 4.29). A band also

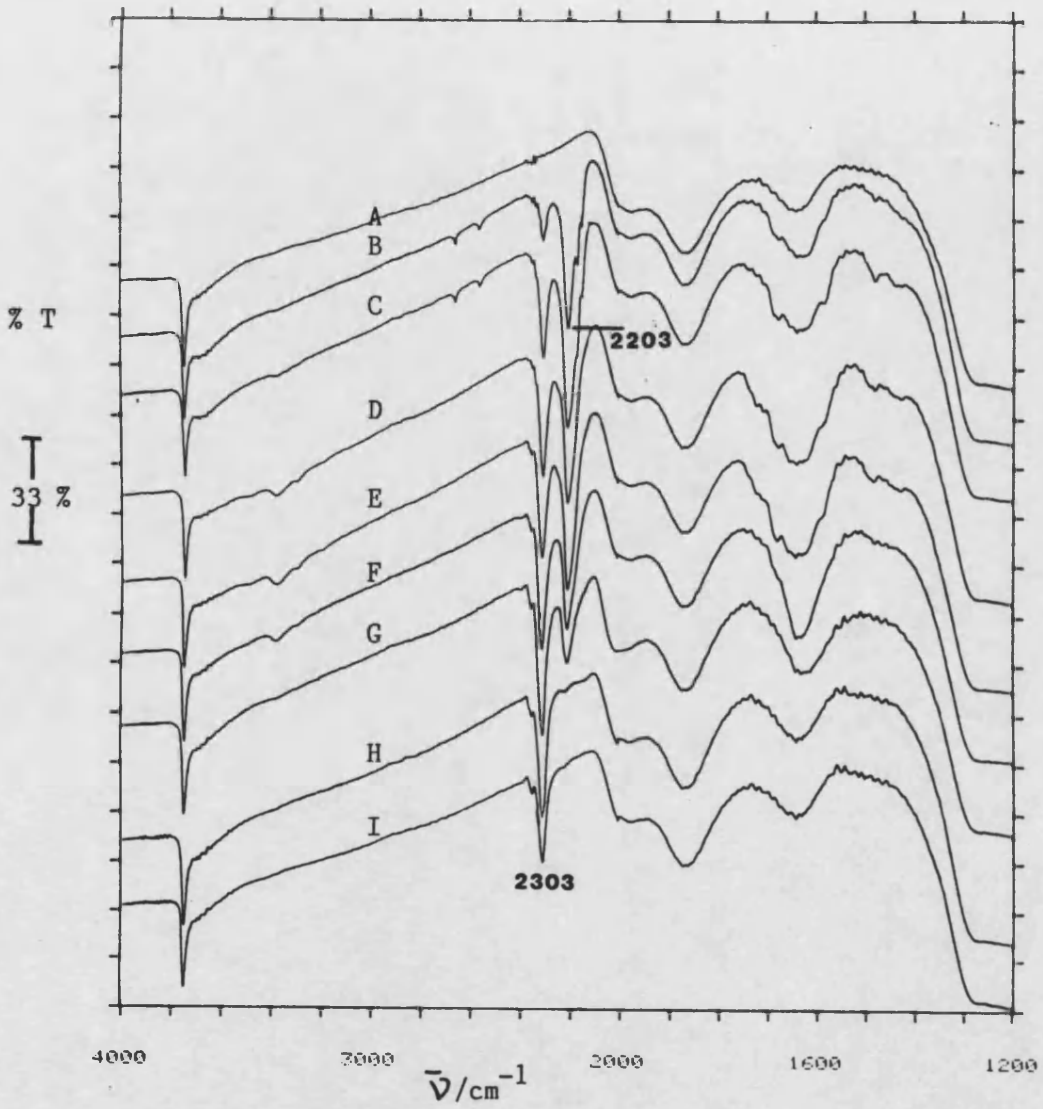

Fig. 4.28 I.r. Transmission Spectra of Cyanogen Challenge with Outgassed $CuO-CrO_3/SiO_2$

A = $CuO-CrO_3/SiO_2$ outgassed at $< 10^{-4}$ torr/688 K/15 h

B = Sample A exposed to C_2N_2 295 K/10 min

C = " " " /5 h

D = " " " /24 h, exposed to liquid nitrogen trap.

E = As D except sample evacuated at 295 K/2 h

F = Sample E outgassed at 439 K/2 h

G = Sample F outgassed at 528 K/2 h

H = Sample G outgassed at 593 K/2 h

I = Sample H outgassed at 688 K/2 h

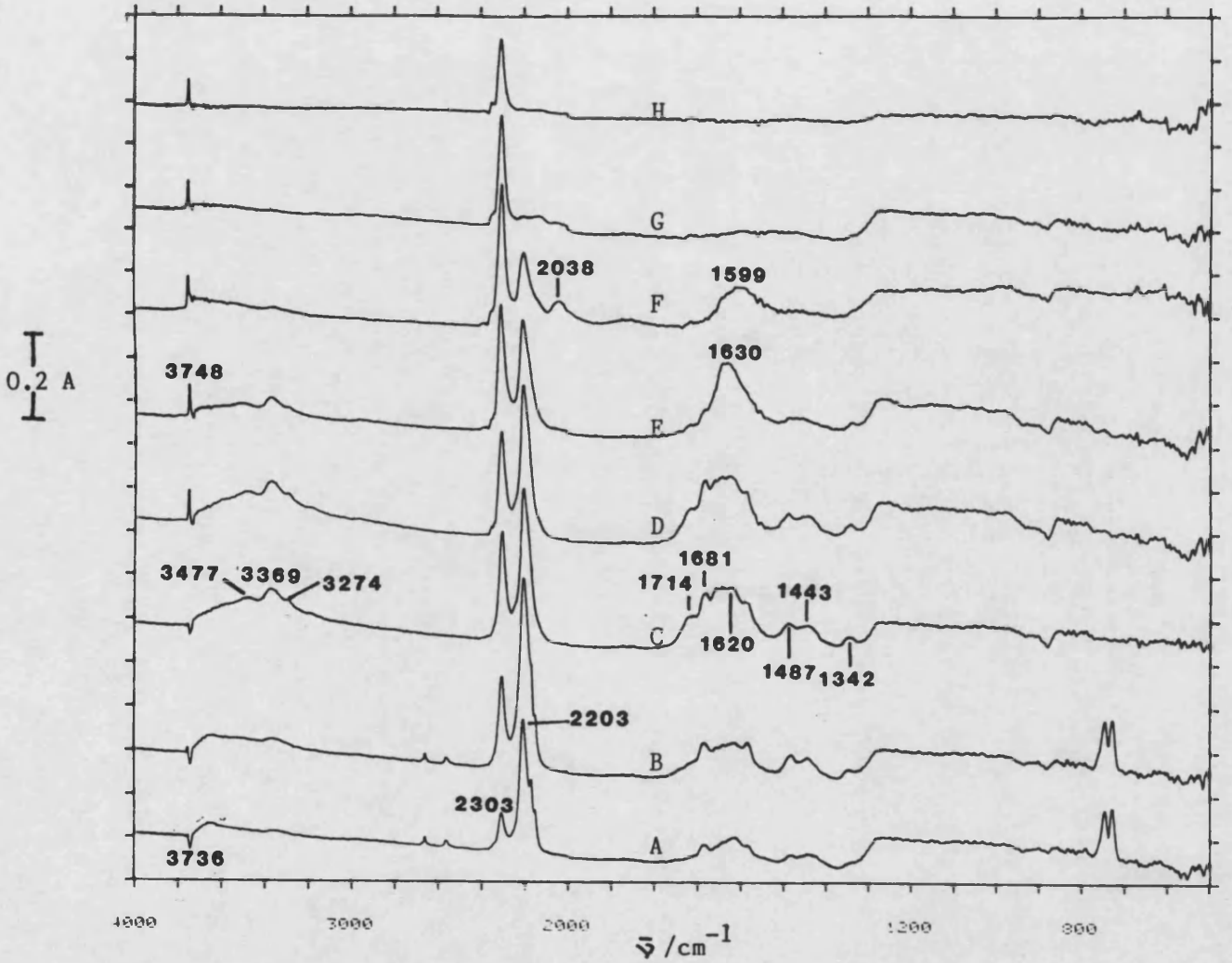

Fig. 4.29 I.r. Absorbance Difference Spectra of Cyanogen Interaction with Outgassed $CuO-CrO_3/SiO_2$

A = Adsorbed species plus gaseous phase after C_2N_2 challenge 295 K/10 min

B = Adsorbed species plus gaseous phase C_2N_2 challenge 295 K/5 h

C = Adsorbed species resistant to condensation after C_2N_2 challenge 295 K/24 h

D = Adsorbed species resistant to evacuation after C_2N_2 challenge 295 K/24 h

E = Adsorbed species after outgassing at 439 K/2 h

F = Adsorbed species after outgassing at 528 K/2 h

G = Adsorbed species after outgassing at 593 K/2 h

H = Adsorbed species after outgassing at 688 K/2 h

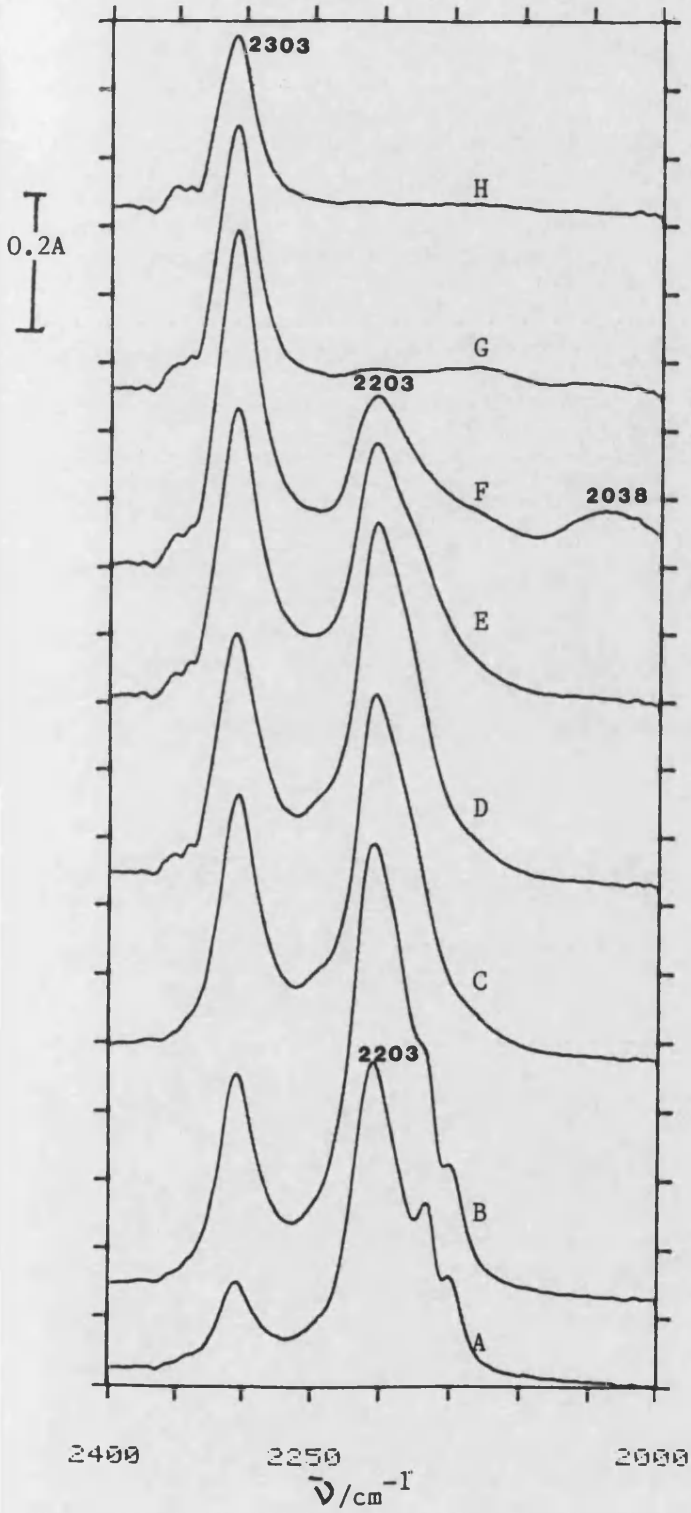

Fig. 4.30 I.r. Absorance Difference Spectra of C_2N_2 Interaction with Outgassed $CuO-Cr_2O_3/SiO_2$

A = Adsorbed species plus gaseous phase after C_2N_2 challenge 295 K/10 min

B = Adsorbed species plus gaseous phase after C_2N_2 challenge 295 K/5 h

C = Adsorbed species resistant to condensation after C_2N_2 challenge 295 K/24 h

D = Adsorbed species resistant to evacuation after C_2N_2 challenge 295 K/24 h

E = Adsorbed speceis after outgassing at 439 K/2 h

F = Adsorbed species after outgassing at 528 K/2 h

G = Adsorbed speceis after outgassing at 593 K/2 h

H = Adsorbed species after outgassing at 688 K/2 h

developed at 3369 cm^{-1} together with weak features at 3477 and 3294 cm^{-1}. These features were due to N-H stretching and closely resembled those seen in the case of the CuO/SiO_2 sample (Sec. 4.2.1). The intensity of the N-H stretching region was nowhere near as intense as that obtained with the CrO_3/SiO_2 surface (Sec. 4.3.1). A complex series of peaks and ripples was observed in the 1720-1340 cm^{-1} region with peaks at 1714, 1681, 1620, 1582, 1487, 1443 and 1345 cm^{-1}. The ones at 1714 and 1681 cm^{-1} were previously assigned to amide-like species on silica and chromia surfaces but these bands were much less intense than those seen over the outgassed CrO_3/SiO_2 surface. It was notable that whereas a band occurred at 2175 cm^{-1} when outgassed CuO/SiO_2 was exposed to C_2N_2 for 21 h, no such observation was made in the case of the mixed oxide. All of the features described thus far resisted outgassing at 295 K. Indeed the only change induced by pumping away the gaseous phase was restoration of spectral intensity at 3736 cm^{-1} and growth of a sharp one at 3748 cm^{-1} (Fig. 4.29D). This suggested that more than one type of isolated hydroxyl group was present on the surface.

When the outgassing temperature was raised to 439 K, the intensity of the CuNCO band decreased but it was still stronger than that observed on the equivalent chromium-free sample. (i.e. compare the intensity of the 2209 cm^{-1} band in Fig. 4.6D to that of the one at 2203 cm^{-1} in Fig. 4.30E).

Heating to 439 K removed many of the weak absorptions below 1720 cm^{-1} and the presence of a strong band became apparent at 1630 cm^{-1}.

On increasing the outgassing temperature to 528 K the bands below 2000 cm^{-1} were largely removed; Only a feature at 1599 cm^{-1} remained, and even this was removed at higher temperatures. By 578 K all traces of species containing i.r. active N-H and O-H vibrations were removed. The CuNCO absorption remained strong and a new peak appeared at 2638 cm^{-1}. This band was not reported in any of our studies so far described. The band due to CuNCO and the one at 2038 cm^{-1} were removed on heating to 593 K. Indeed no i.r. active adsorbed species were present above this temperature.

4.12.2 Oxygenated $CuO-CrO_3/SiO_2$

A $CuO-CrO_3/SiO_2$ disc was oxygenated at 688 K/12 h in oxygen (200 torr). A transmission i.r. spectrum of the yellow disc is shown in Fig. 4.31A. The oxygenated disc was exposed to C_2N_2 at 288 K for 23 h before condensing the gas phase and outgassing in stages upto 688 K. I.r. transmission spectra recorded during this experiment are shown in Fig. 4.31 and corresponding absorbance difference spectra, obtained using Fig. 4.31A as a reference, are replotted in Fig. 4.32.

After initial C_2N_2 exposure (288 K/5 minutes) the absorbance difference spectrum (Fig. 4.32A) showed that

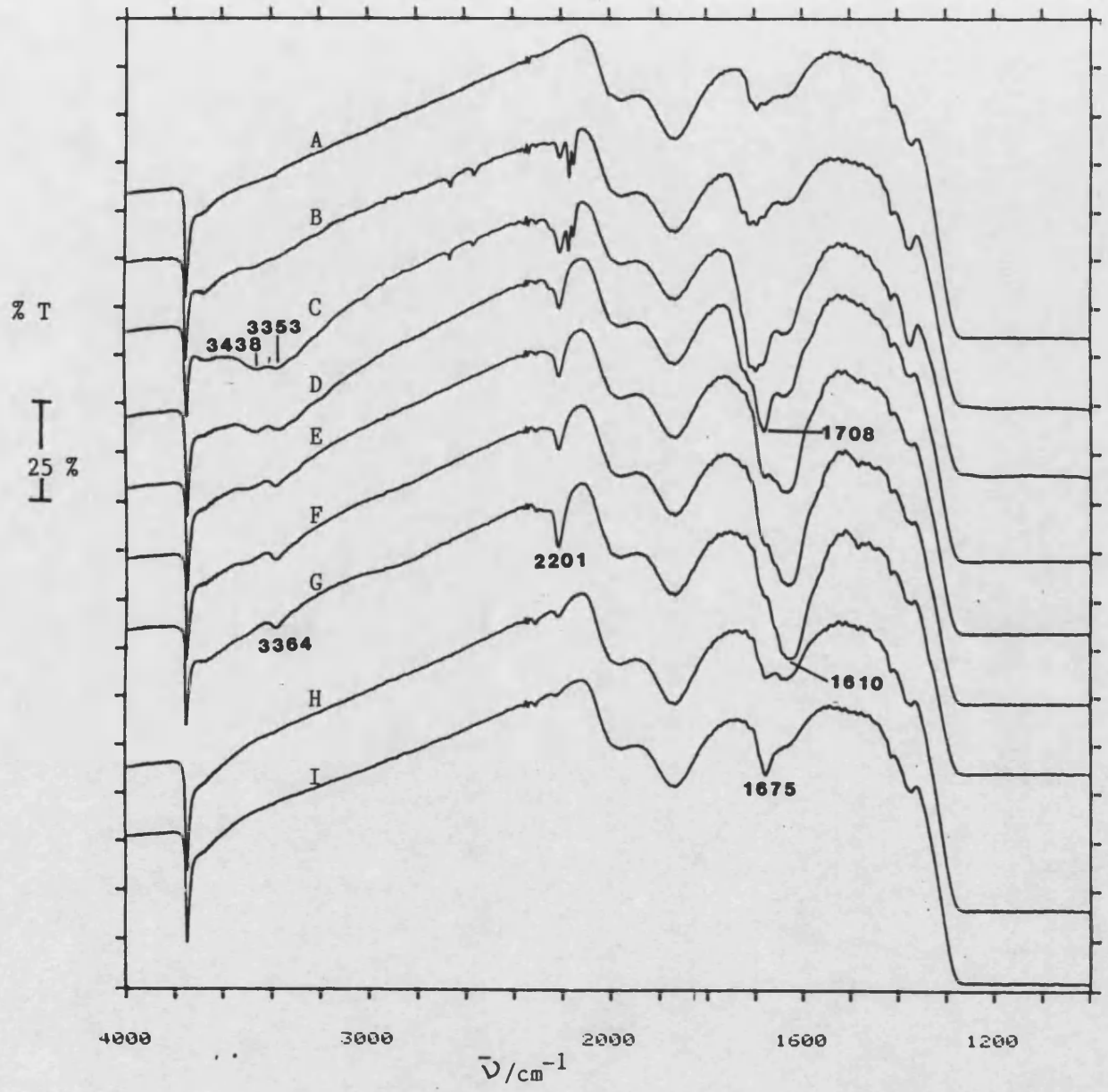

Fig. 4.31 I.r. Transmission Spectra of C_2N_2 Challenge with Oxygenated $CuO-CrO_3/SiO_2$

A = Oxygenated $CuO-CrO_3/SiO_2$

B = C_2N_2 challenge 288 K/5 min

C = " " " /23 h

D = Sample C evacuated at 288 K

E = Sample D evacuated at 396 K/2 h

F = " E " " 435 K/2 h

G = " F " " 504 K/2 h

H = " G " " 588 K/2 h

I = " H " " 688 K/3 h

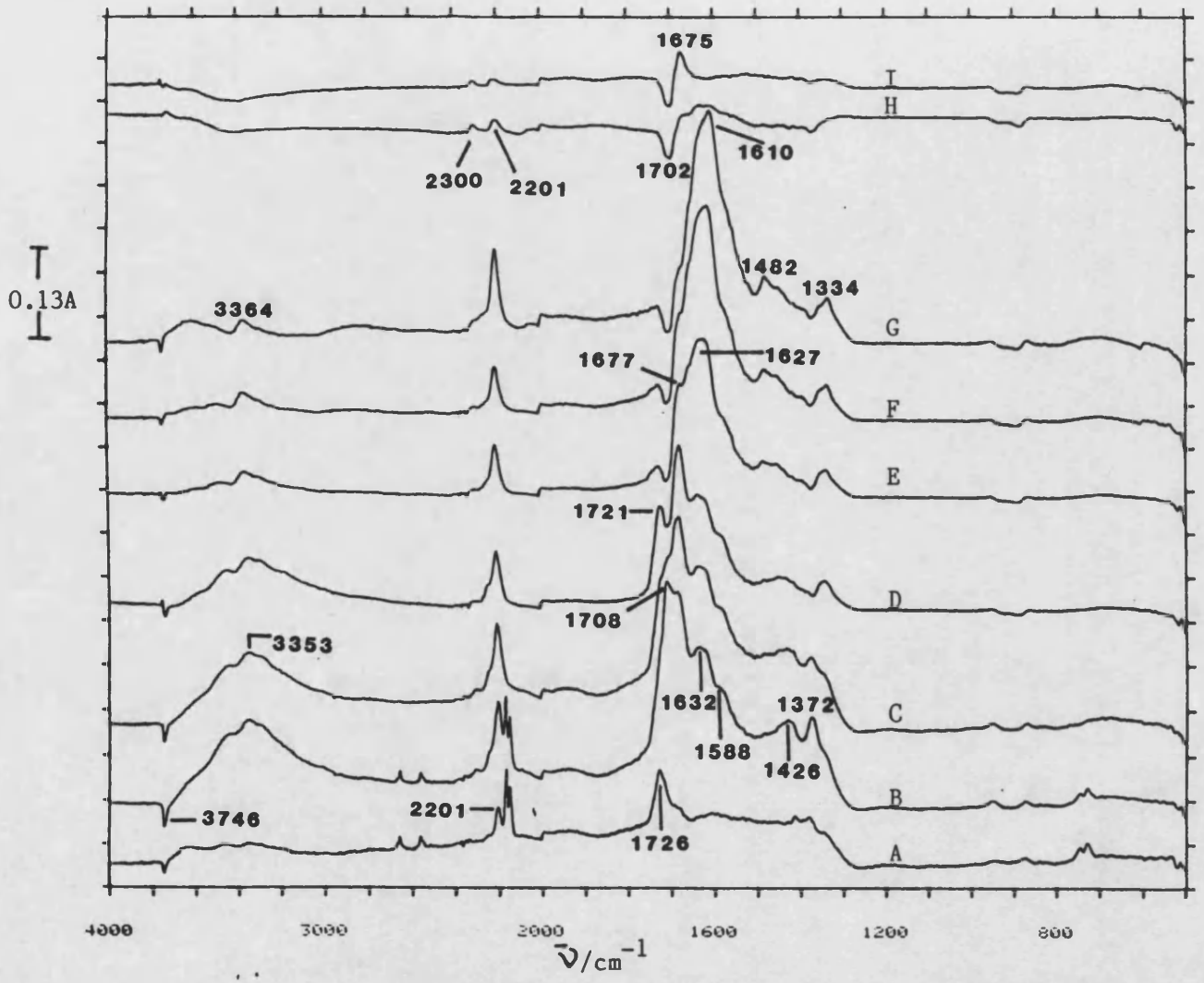

Fig. 4.32 I.r. Absorbance Difference Spectra of C_2N_2 Challenge with Oxygenated $CuO-CrO_3/SiO_2$

A = Adsorbed species plus gaseous phase after C_2N_2 288 K/5 min

B = Adsorbed species plus gaseous phase after C_2N_2 288 K/23 h

C = Adsorbed species in B which resisted condensation into cold trap

D = Irreversibly adsorbed species after evacuating at 288 K

E = Adsorbed species after outgassing at 396 K/2 h

F = As E but 435 K/2 h

G = " " " 504 K/2 h

H = " " " 588 K/2 h

I = " " " 688 K/3 h

reaction had occurred. The main spectral changes were as follows:-

1) A negative band was seen at 3746 cm^{-1} due to consumption of hydrogen-bonded isolated hydroxyl groups.

2) Two new bands appeared at 2201 and 1726 cm^{-1}. The 2201 cm^{-1} band was due to CuNCO whilst the one at 1726 cm^{-1} was tentatively assigned to a surface amide species.

3) An absorption edge was seen between 1380-1280 cm^{-1}.

Reaction at room temperature was monitored by recording i.r. spectra at a series of time intervals. Only that recorded after 23 h exposure is shown here (Fig. 4.31C) since the series of spectra merely showed that a gradual development of the features seen after 23 h occurred. After this time the spectral intensity was enhanced in two main regions of the spectrum, namely at 3500-3200 cm^{-1} and 1730-1300 cm^{-1}. The first area consisted of two N-H bands at 3438 and 3353 cm^{-1} superimposed on a broad O-H band. The second area contained a series of overlapping bands. These were deconvoluted using the data station and peaks were identified at 1708, 1678, 1632, 1588, 1426 and 1372 cm^{-1}. This region of the spectrum was much more intense than that observed in the case of outgassed $CuO-CrO_3/SiO_2$. The CuNCO band at 2201 cm^{-1} was also more intense after extended exposure to C_2N_2 but unlike the outgassed

Cu(II)-Cr(VI) sample no SiNCO species formed on this oxygenated sample.

The absorption at 1708 cm^{-1} was partially removed by exposing the disc to a liquid nitrogen trap and was totally removed by evacuating the i.r. cell. The disappearance of this band revealed a smaller one at 1721 cm^{-1} which was probably due to a surface amide species. The band between 3500-3200 cm^{-1} also diminished due to the removal of some weakly adsorbed moisture.

Outgassing at 396 K caused a strong band to occur at 1627 cm^{-1} (Fig. 4.32E). This feature intensified and shifted to lower wavenumbers at higher temperatures. By 504 K it was observed at 1610 cm^{-1} but on heating to 588 K it was removed. This band was in a similar position and exhibited similar thermal characteristics to ones observed on oxygenated CrO_3/SiO_2 and on outgassed $CuO\text{-}CrO_3/SiO_2$, however, it was much more intense than in either of those studies.

On heating to 588 K most bands due to adsorbed species were removed. Only two weak bands remained, at 2300 and 2201 cm^{-1}, due to SiNCO and CuNCO respectively.

Finally it was noteworthy that whereas three strong bands were observed at 2303, 2220 and 2145 cm^{-1} after outgassing C_2N_2 exposed CuO/SiO_2 at 688 K (Sec. 4.9.1) only a hint of bands were observed in the 2300-2100 cm^{-1} region after similar treatment of this oxygenated mixed oxide.

4.12.3 Hydroxylated $CuO-CrO_3/SiO_2$

A $CuO-CrO_3/SiO_2$ disc was outgassed and an i.r. spectrum was measured (Fig. 4.33A). The spectrum was used throughout this experiment as the reference spectrum to derive difference spectra. A transmission spectrum of the disc after hydroxylation is shown in Fig. 4.33B. The changes caused by hydroxylation, namely the decrease in intensity of the band at 3744 cm^{-1}, the broad absorption between 3700-3000 cm^{-1} and a peak at 1624 cm^{-1} plus weak features at 940 and 874 cm^{-1} (Fig. 4.34A) were all due to vibrations associated with silica and adsorbed moisture.

I.r. transmission spectra recorded during and after C_2N_2 contact with this hydroxylated disc are shown sequentially in Fig. 4.33. Corresponding absorbance difference spectra are shown in Fig. 4.34. Unlike other spectra reported in this thesis it was not possible to standardise the transmission spectra recorded during this experiment using the program described earlier (Sec. 3.2.2). This was due to the presence of strong spectral features around 3400-3150, 1700-1600 and at 1350 cm^{-1} in some spectra which caused data to be produced outside the limits of the data station (i.e. outside the range ±165% transmission). For this reason the % transmission spectra shown in Fig. 4.33 were replotted in the raw (un-standardised) form.

Initial contact of the hydroxylated disc with C_2N_2 at 293 K produced several bands in the N-H stretching region and at 2246, 1718, 1684, 1592, 1349 and 1337 cm^{-1}.

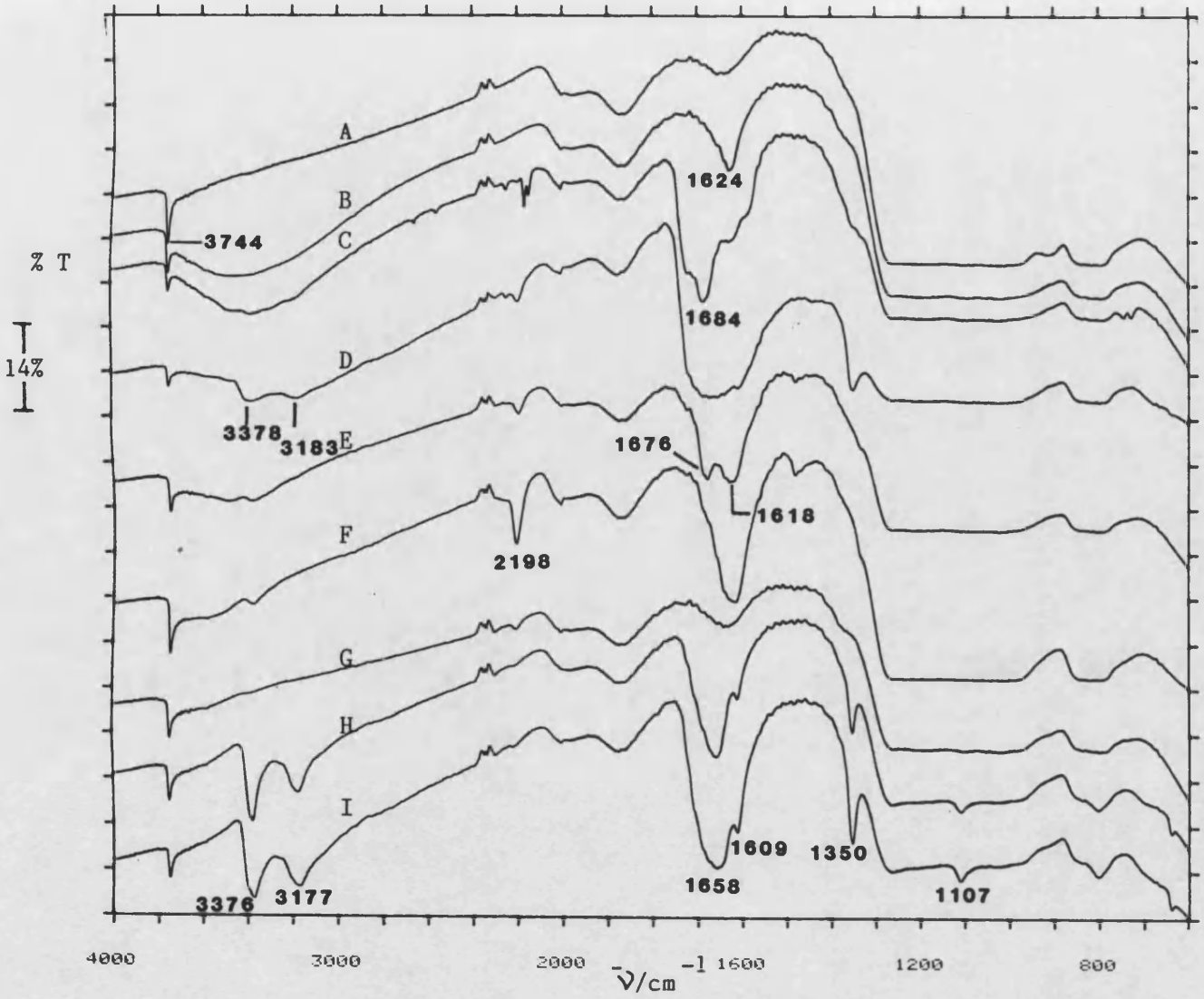

Fig. 4.33. I.r. Transmission Spectra of Cyanogen Interation with Hydroxylated $CuO-CrO_3/SiO_2$

A = Outgassed $CuO-CrO_3/SiO_2$

B = Hydroxylated $CuO-CrO_3/SiO_2$

C = Sample B exposed to C_2N_2/293 K/5 min

D = " " " /20 h then evacuated.

E = Sample D outgassed at 373 K/2 h

F = Sample F outgassed at 473 K/2 h

G = Sample F outgassed at 553 K/2.5 h

H = Sample G outgassed at 613 K/2 h

I = Sample H outgassed at 688 K/2 h

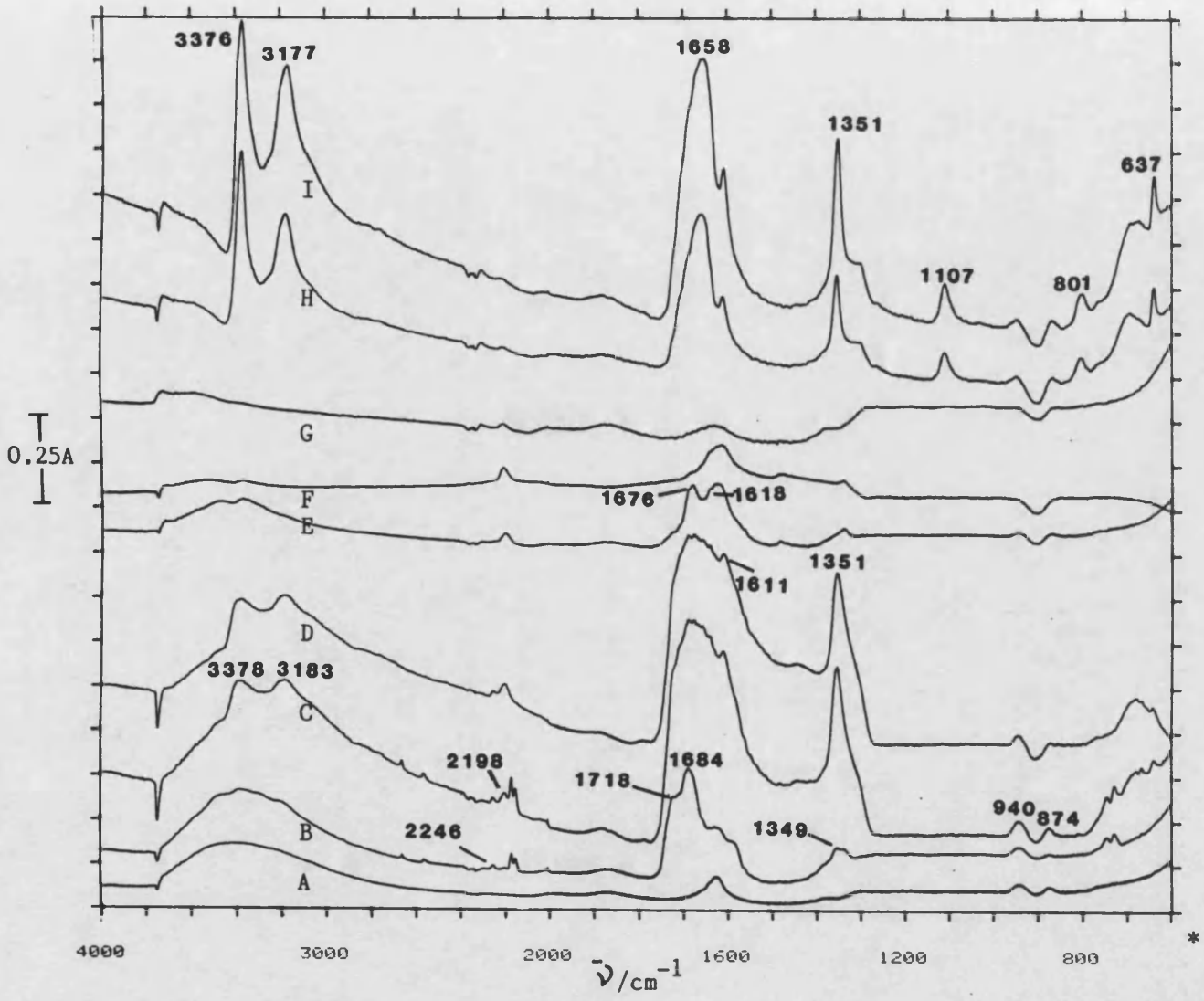

Fig. 4.34 I.r. Absorbance Difference Spectra of C_2N_2 Interaction with Hydroxylated $CuO-CrO_3/SiO_2$

A = Difference spectrum produced by hydroxylated of $CuO-CrO_3/SiO_2$

B = Adsorbed species plus gaseous phase after 5 min C_2N_2 challenge at 293 K.

C = As B except 5 h C_2N_2 challenge

D = Adsorbed species after C_2N_2/298 K /20 h (after evacuation of gaseous phase)

E = Adsorbed species after outgassing at 373 K/2 h

F = Adsorbed species after outgassing at 473 K/3 h

G = Adsorbed species after outgassing at 553 K/2.5 h

H = Adsorbed species after outgassing at 613 K/2 h

I = Adsorbed species after outgassing at 653 K/2 h

* All spectra derived by subtracting spectrum of outgassed $CuO-CrO_3/SiO_2$ from appropriate spectra.

Most of these features were identical in those observed when C_2N_2 was interacted with hydroxylated CuO/SiO_2. After 5 h C_2N_2 exposure the spectrum intensified and peaks were clearly visible at 3378, 3183, 2246, 2198, 1670, 1611 and 1351 cm^{-1} (Fig. 4.34C). These features were unaffected by extended C_2N_2 exposure and evacuation at 293 K. The transmission spectrum recorded through the disc after 20 h C_2N_2 contact (Fig. 4.35C) was compared with a spectrum of pure oxamide (BDH)(Fig. 4.35B). This confirmed that the bands at 3378, 3183, 1670, 1611 and 1351 cm^{-1} were due to oxamide. The sample was raised out of the i.r. beam and a spectrum was recorded through the cell windows. No oxamide bands were observed, showing that the observed bands ascribed to oxamide were due to the di-amide present on the surface of the hydroxylated disc. It was interesting to note that the bands observed in free oxamide at 1104 and 793 cm^{-1} (Table 4.21) were not observed here. After accounting for the oxamide bands in the absorbance difference spectrum (Fig. 4.34D) a band was observed at 2246 cm^{-1} and a broad feature at 1670 cm^{-1}. These features were explained by the presence of a partially hydroxylated C_2N_2 species. Another weak band at 2198 cm^{-1} was ascribed to CuNCO (see Sec. 4.22).

When the disc was outgassed at 373 K the oxamide bands disappeared and three weak features were revealed at 1676, 1618 and 1337 cm^{-1}. Heating to 473 K removed the one at 1676 cm^{-1}. The behaviour of the latter feature was similar to that observed in the case of the

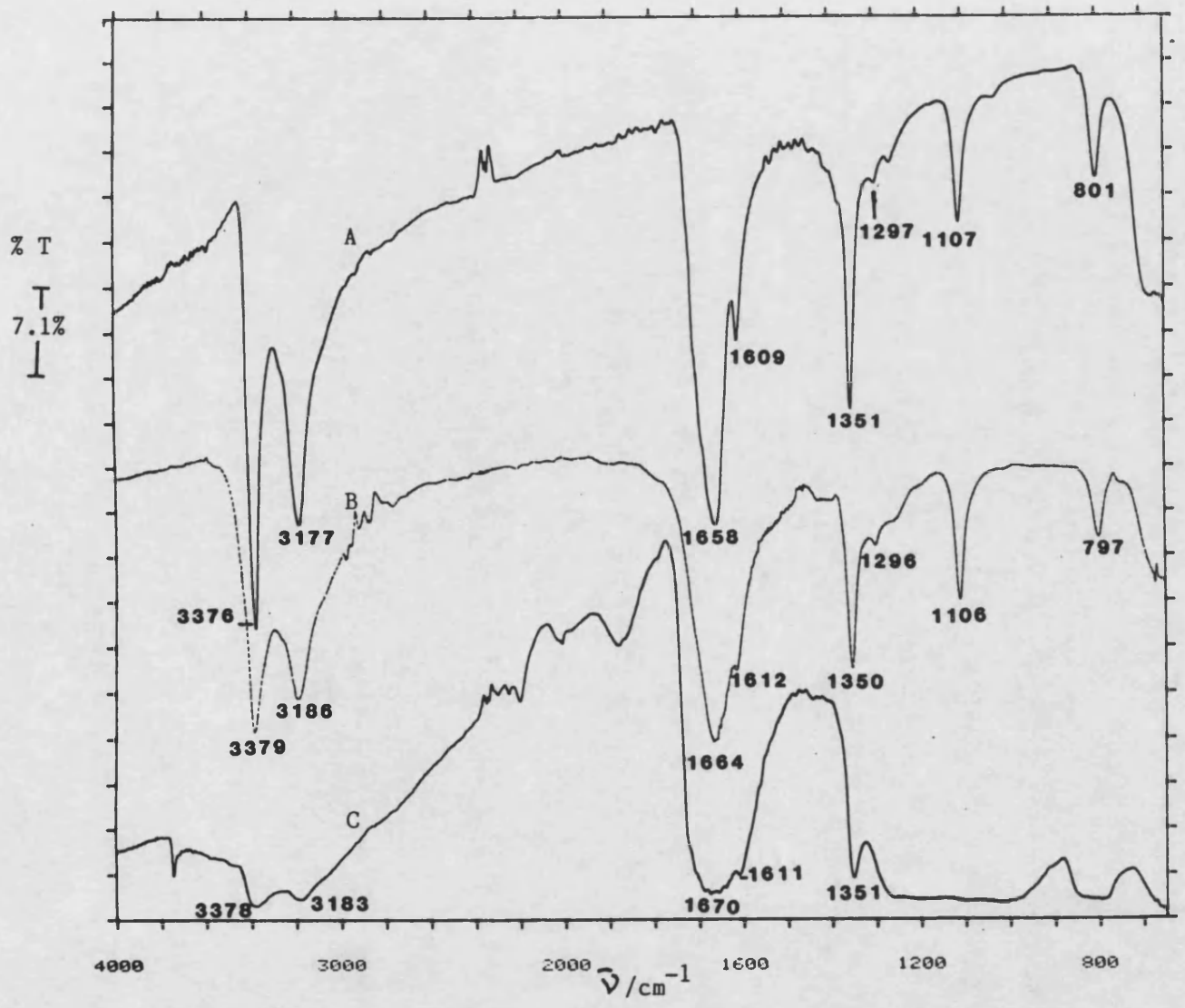

Fig. 4.35 Comparison of i.r. Transmission Spectrum of Oxamide with Key Spectra Rescorded after Cyanogen Challenge with Hydroxylated $CuO-CrO_3/SiO_2$

A = Spectrum of White sublimate deposited on the cell windows after outgassing C_2N_2-challenged 'HYDR' - $CuO-CrO_3/SiO_2$ at 613 K/2 h

B = Spectrum of Oxamide (BDH)

C = Spectrum of 'HYDR' - $CuO-CrO_3/SiO_2$ after C_2N_2/293 K/20 h followed by evacuation.

oxygenated Cu(II)-Cu(VI) disc (Sec. 4.12.2). On heating further, to 553 K, the 1618 cm^{-1} band due to adsorbed moisture was removed.

When the disc was outgassed to 613 K a white material sublimed onto the cell windows. The sample was raised out of the i.r. beam and a spectrum of the sublimate was recorded (Fig. 4.35A). Comparison of this spectrum to one of pure oxamide (Fig. 4.35B) confirmed that the sublimate was indeed oxamide. No other i.r. bands due to adsorbed species were observed when the spectrum of the sublimate was subtracted from the outgassed disc (Fig. 4.33H). Despite this observation more oxamide sublimed when the outgassing temperature was raised to 653 K (i.e. compare the spectral intensity of spectrum H to spectrum I in Fig. 4.34).

Air was then admitted into the i.r. cell and the oxamide which had sublimed onto the sodium chloride cell windows was removed using dichloromethane. The cell was re-connected to the vacuum frame, re-outgassed to 673 K/15 h, cooled to ambient temperature in vacuo and re-hydroxylated. C_2N_2 was dosed at 293 K for a period of 18 h before evacuating the cell. An i.r. spectrum recorded through the disc (Fig. 4.36D) again revealed that oxamide had formed on the surface of the sample. On outgassing this re-hydroxylated sample oxamide sublimed at 541 K a lower temperature than in the case of the first hydroxylation cycle.

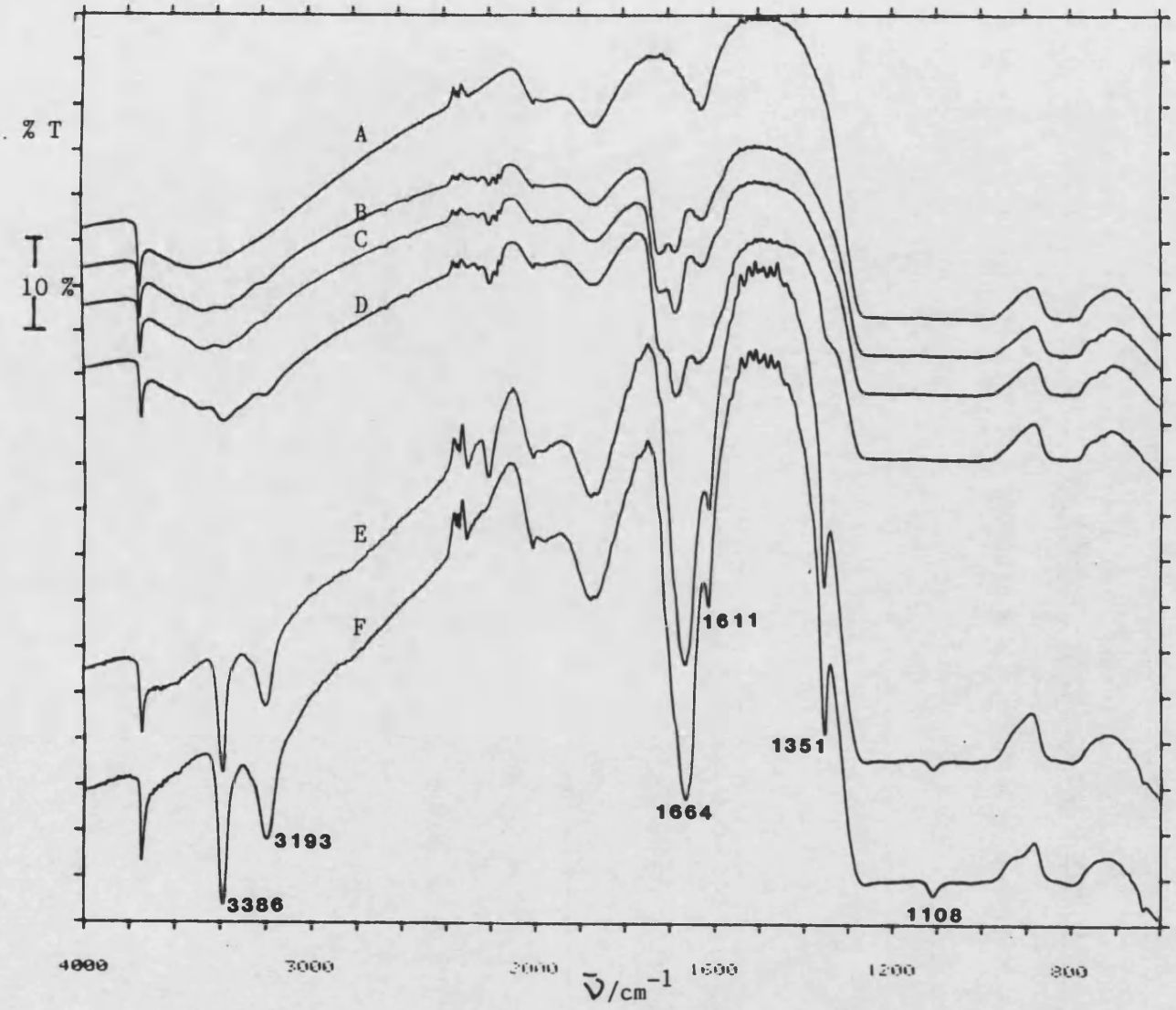

Fig. 4.36 I.r. Transmission Spectra of Cyanogen Interaction with re-Hydroxylated $CuO-CrO_3/SiO_2$

A = Re-hydroxylated $CuO-CrO_3/SiO_2$

B = Sample A exposed to C_2N_2/293 K/15 min

C = " " " /30 min

D = " " " /18 h

E = Sample D outgassed at 541 K/3 h

F = Sample E outgassed at 683 K/15 h

4.12.4 Oxygenated-Hydroxylated $CuO-CrO_3/SiO_2$

Transmission i.r. spectra relating to C_2N_2 exposure of oxygenated-hydroxylated $CuO-CrO_3/SiO_2$ are plotted in Fig. 4.37. Difference spectra, derived using the spectrum of the oxygenated sample as a reference, are presented in the absorbance mode in Fig. 4.38. The spectrum of the orange, hydroxylated disc revealed that the broad absorption centred at 3488 cm^{-1} and the band at 1620 cm^{-1} both present in the spectrum of the oxygenated specimen had intensified whereas the sharp band at 3741 cm^{-1} had weakened.

Contact of this sample with cyanogen for 15 minutes gave rise to new bands at 1721, 1684, 1585 and 1340 cm^{-1} whilst a shoulder appeared at 3369 cm^{-1} (Fig. 4.38B). After 3 h exposure to C_2N_2 the spectrum contained intense broad absorptions centred at 3377, 3184 and 1684 cm^{-1} with a small peak near 1343 cm^{-1}. These peaks were characteristic of oxamide. After 5 h these peaks became so intense that spectral resolution became impaired and standardisation became impossible, with the result that difference spectra would not be computed. This situation worsened until after 10 h exposure; the sample, now grey in colour, absorbed nearly all of the incident i.r. radiation. Evacuation at 293 K did not resolve this problem. Measurement of an i.r. spectrum through the cell windows after raising the disc out of the infra-red beam confirmed that the oxamide was not on the cell

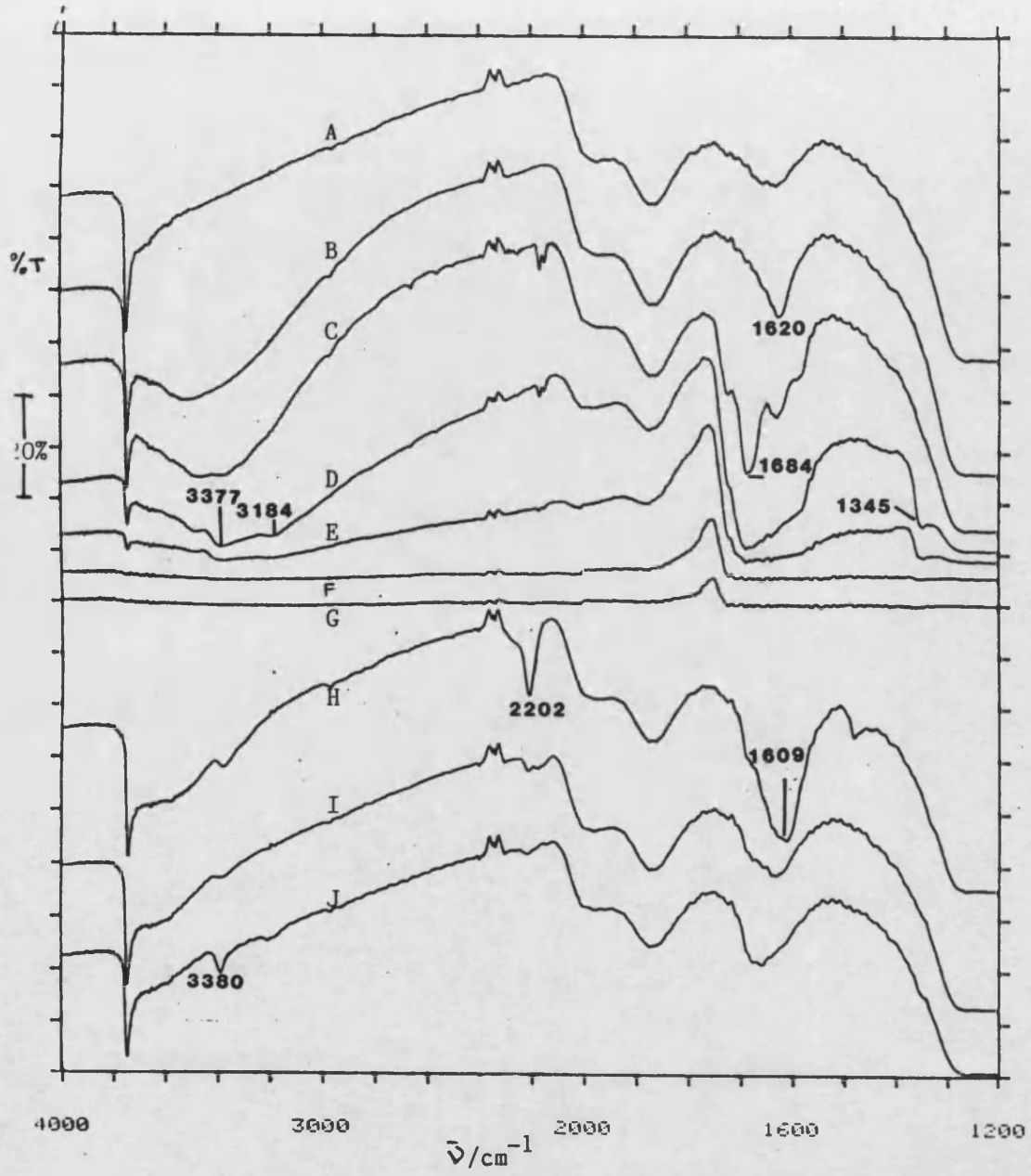

Fig. 4.37 I.r. Transmission Spectra of Cyanogen Interaction with Oxygenated Hydrogenated $CuO-CrO_3/SiO_2$

A. $CuO-CrO_3/SiO_2$ outgassed 673 K/5.5 h., then heated in oxygen (150 torr/12 h.)

B. Sample in A hydroxylated with water vapour.

C. Sample in B exposed to C_2N_2/20 torr/15 min./293 K.

D. Sample in B exposed to C_2N_2/3 h./293 K.

E. Sample in B exposed to C_2N_2/5 h./293 K.

F. Sample in B exposed to C_2N_2/10 h./293 K.

G. Sample in F evacuated at 293 K.

H. Sample in G outgassed at 459 K/2 h.

I. Sample in H outgassed at 553 K/4 h.

J. Sample in I outgassed at 673 K/2 h.

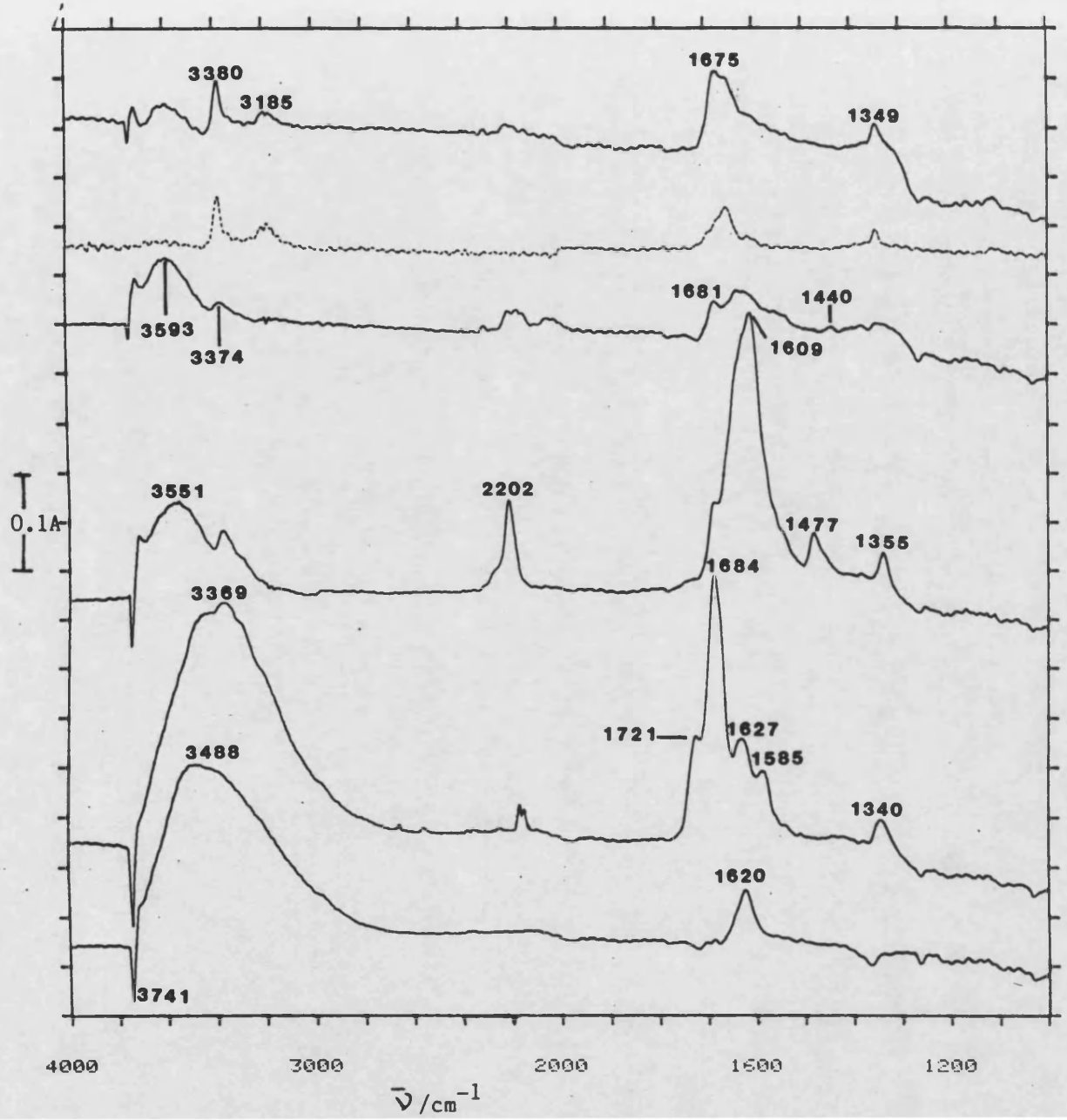

Fig. 4.38 I.r. Absorbance Difference Spectra of Cyanogen Interaction with Oxygenated-Hydroxylated $CuO-CrO_3/SiO_2$

A. Adsorbed water on oxygenated $CuO-CrO_3/SiO_2$

B. Adsorbed species and gaseous phase after C_2N_2challenge 293 K/15 min

C. Adsorbed species after C_2N_2 challenge/ 10 h. followed by outgassing at 459 K/2 h.

D Adsorbed species after outgassing at at 553 K/4 h.

E. Sublimate on cell windows after outgassing at 673 K/2 h.

F. Adsorbed species and sublimate after outgassing at 673 K/2 h.

windows, hence it was present on the surface of this specimen.

After outgassing at 459 K/2 h the strong bands due to surface oxamide disappeared and spectral resolution was regained; only a small amount of white sublimate was observed and the sample changed to a brown-green colour. The difference spectrum C (Fig. 4.38) contained i.r. bands at 3551, 3369, 2202, 1684, 1609 (very strong), 1477 and 1355 cm^{-1} and a negative peak at 3741 cm^{-1}. The 2202 cm^{-1} band was characteristic of the antisymmetric NCO vibration of CuNCO. The band at 1684 cm^{-1} was typical of an amide group associated with the chromium surface.

On increasing the outgassing temperature to 553 K the sample became black and many of the spectral features present at lower temperatures disappeared or became reduced in intensity. Finally, outgassing at 673 K resulted in the deposition of a white sublimate on the cell windows. A difference spectrum of the disc recorded through these stained windows (Fig. 4.38F) contained weak bands at 3380, 3185, 1675, 1664 and 1349 cm^{-1}. Comparison of these bands to those caused by the sublimed oxamide (Fig. 4.38E) revealed that only the 1676 cm^{-1} band was due to an adsorbed species. A similar band was seen when oxygenated $CuO-CrO_3/SiO_2$ was contacted with C_2N_2 and outgassed at 688 K.

4.13 Infra-red Spectroscopic Studies of Cyanogen Interaction with $CuO-Cr_2O_3/SiO_2$

A summary of the work presented by Surman (3) and Davies (4) relating to the interaction of HCN with the CuO/Cr_2O_3 surface was given in Sec. 1.6.3. Studies involving silica-supported $CuO-Cr_2O_3$ conducted by Davies (4) were described in a later section, 1.6.4. The work which follows extends these studies to investigate the interaction of C_2N_2 with the Cu(II)-Cr(III) oxide system.

The results presented in this section complement earlier studies of the Cu(II)-Cr(III) system using mass spectrometric and gravimetric techniques (Sec. 4.6). The effect of various pretreatments, namely outgassing and hydroxylation, was also investigated. The effect of oxygenation was not studied since this was expected to give similar results to oxygenated $CuO-CrO_3/SiO_2$ studied earlier.

4.13.1 Outgassed $CuO-Cr_2O_3/SiO_2$

I.r. spectroscopic results of the interaction of C_2N_2 with outgassed $CuO-Cr_2O_3/SiO_2$ are shown as percentage transmission spectra in Fig. 4.39 and as absorbance difference spectra in Fig. 4.40. Absorbance spectra, expanded in the 2400-2000 cm^{-1} region, are presented in Fig. 4.41. All difference spectra were derived using the spectrum of outgassed $CuO-Cr_2O_3/SiO_2$ (Fig. 4.39A) as a reference.

Examination of the spectra recorded after initial C_2N_2 exposure showed that strong bands rapidly formed at 2302 and 2202 cm^{-1} due to the formation of SiNCO and

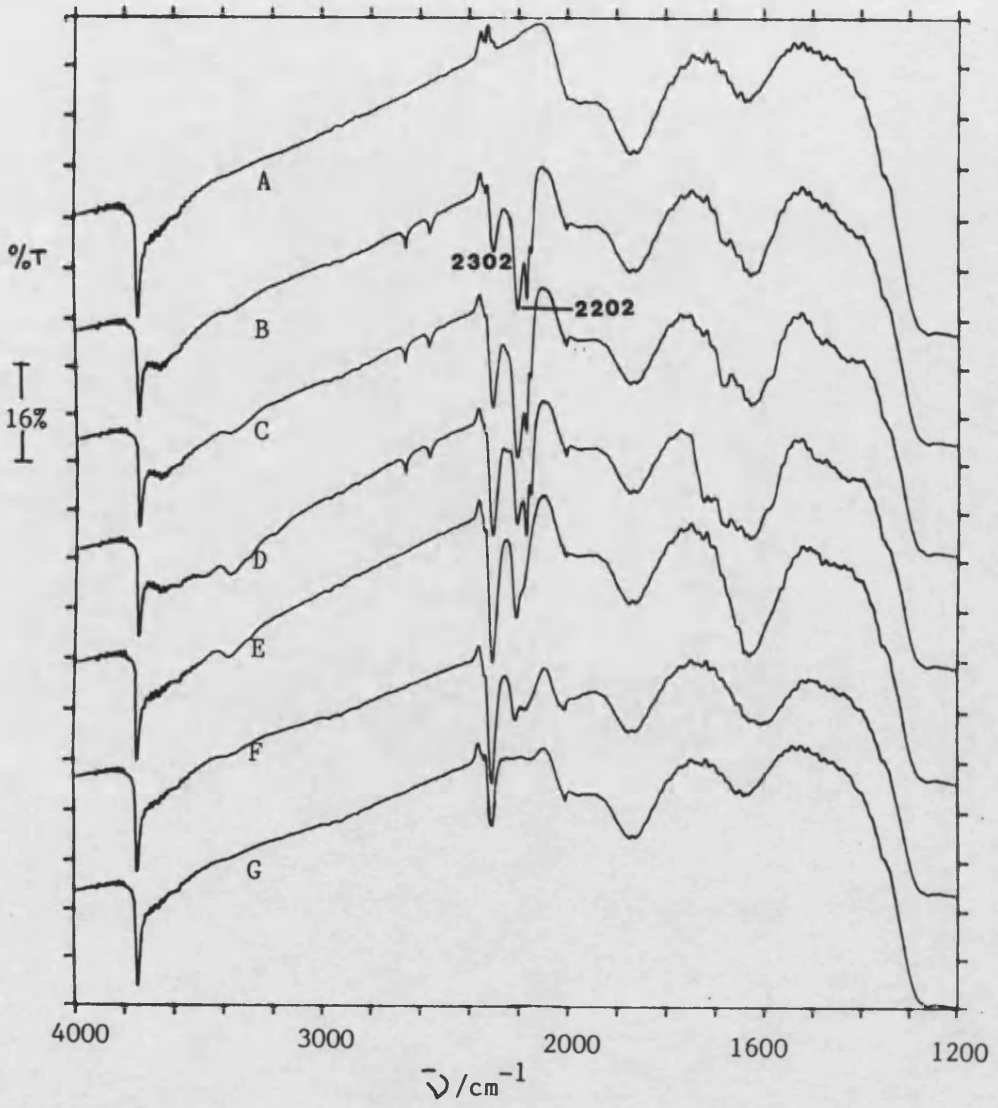

Fig. 4.39. I.r. Transmission spectra of Cyanogen Interaction with Outgassed $CuO-Cr_2O_3/SiO_2$

A = Outgassed $CuO-Cr_2O_3/SiO_2$

B = Sample A exposed to C_2N_2 20 torr/298 K/15 h

C = " " " " " /2.5 h

D = " " " " " /17.5 h

E = Sample D evacuated then outgassed at 440 K/2 h

F = Sample E outgassed at 572 K/2 h

G = Sample F outgassed at 668 K/10 h

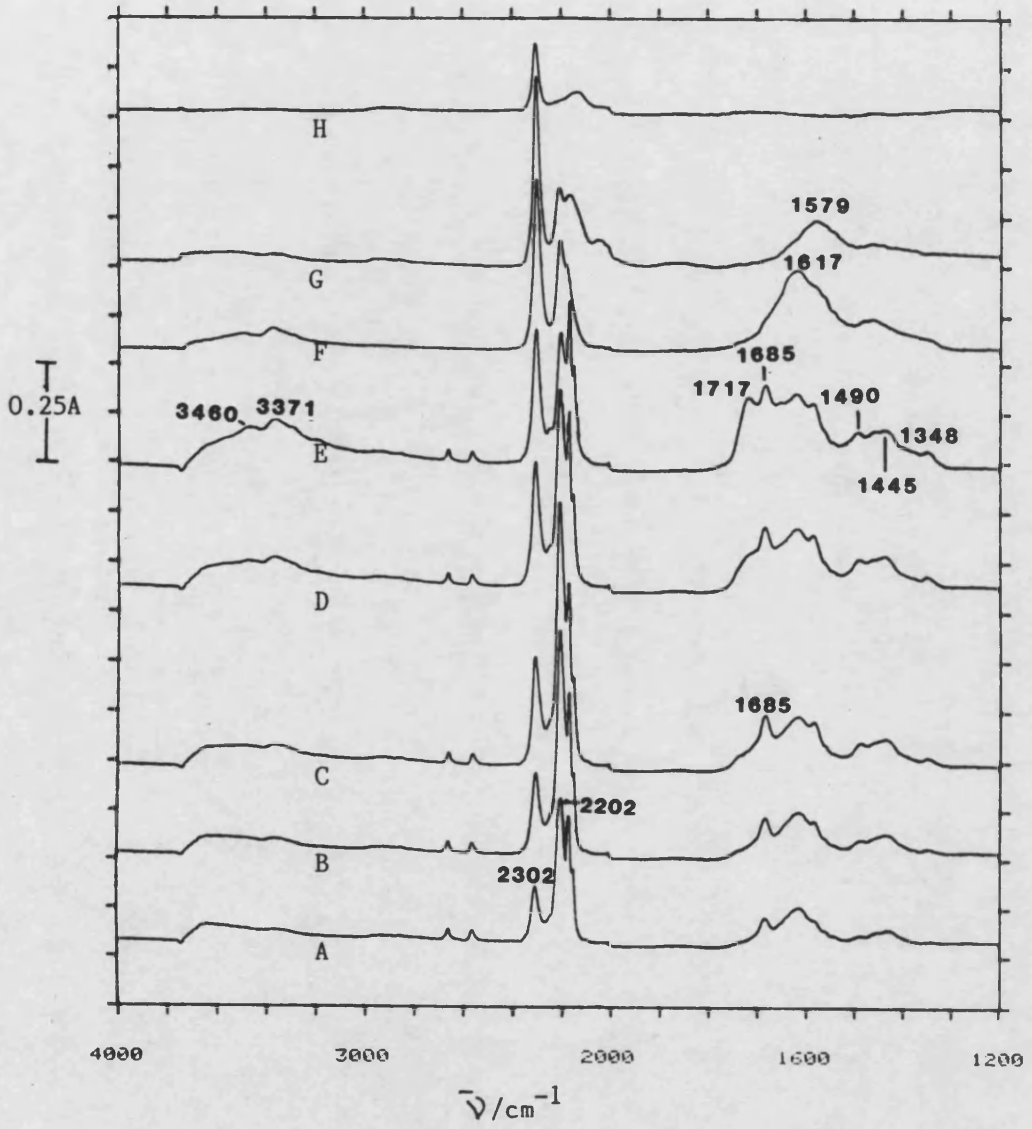

Fig. 4.40 I.r. Absorbance Difference spectra of Cyanogen Interaction with Outgassed $CuO-Cr_2O_3/SiO_2$

A = Adsorbed species plus gaseous phase after exposure of outgassed $CuO-Cr_2O_3/SiO_2$ to C_2N_2/298 K/15 min

B = As A except C_2N_2/298 K/1 h

C = " " /2.5 h

D = " " /7.5 h

E = " " /17.5 h

F = Adsorbed species after evacuating sample in E and outgassing to 440 K/2 h

G = as F then outgassed to 572 K/2 h

H = as G then outgassed to 668 K/10 h

* spectrum of outgassed $CuO-Cr_2O_3/SiO_2$ used as reference

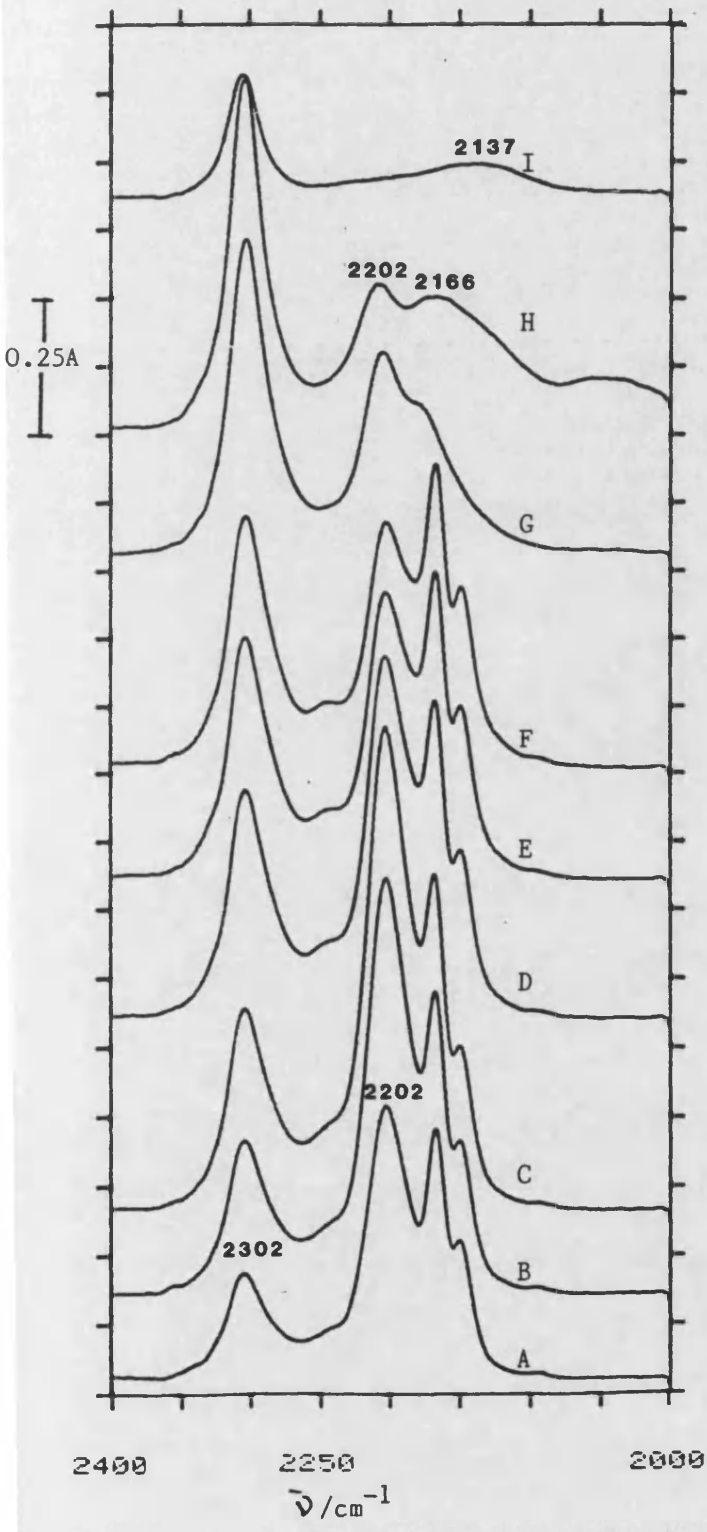

Fig. 4.41 I.r. Absorbance Difference Spectra of Cyanogen Interaction with Outgassed $CuO-Cr_2O_3/SiO_2$

A = Adsorbed species plus gaseous phase after exposure of outgassed $CuO-Cr_2O_3/SiO_2$ to C_2N_2/298 K/5 min

B = As A except C_2N_2/298 K/1 h

C = " " " /2.5 h

D = " " " /7.5 h

E = " " " /12.5 h

F = " " " /17.5 h

G = Adsorbed species after evacuating sample in E and outgassing to 440 K/2 h

H = as F then outgassed to 572 K/2 h

I = as G then outgassed to 668 K/10 h

CuNCO. A weak band also appeared at 1685 cm^{-1}; this was ascribed to the formation of an amide group associated with the chromia surface. A series of weak features between 1660 and 1400 cm^{-1} were also similar to those observed on the chromia surface.

Continued interaction between C_2N_2 and the surface was followed closely at ambient temperature, and revealed that a new band appeared at 1717 cm^{-1}. This was ascribed to amide associated with the silica surface. A series of weak features also appeared at 3460, 3371, 3301 and 3197 cm^{-1}. The spectral intensity below 1660 cm^{-1} gradually intensified during extended exposure at 298 K: this enabled peaks to be identified at 1654, 1617, 1585, 1490, 1467, 1445 and 1348 cm^{-1}. The formation of oxamide on the surface of the sample accounted for many of the bands present after 17.5 h (namely those at 3371, 3197, 1654, 1617 and 1348 cm^{-1}). The other bands were ascribed to species associated with the chromia since they were similar to those seen on the outgassed Cr_2O_3/SiO_2 surface.

The intensity of the SiNCO and CuNCO bands formed at room temperature were measured as a function of time. The results, presented in Fig. 4.42, clearly show that CuNCO formed rapidly at room temperature reaching maximum abundance after 2.5 h. The 2202 cm^{-1} band then faded at a rate equivalent to 0.03 A h^{-1} (absorbance units per hour). The SiNCO band at 2302 cm^{-1} also appeared rapidly

at first but after 2.5 h the rate of growth of the band slowed to a rate of approximately 0.7 A h^{-1}

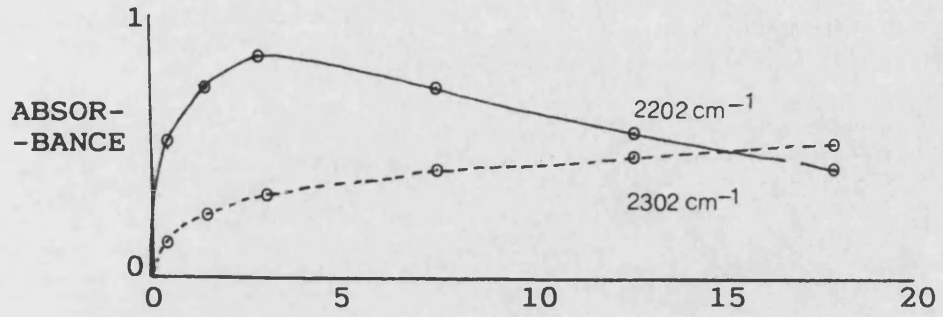

Fig. 4.42 The Intensity of i.r. bands due to CuNCO and SiNCO as a Function of Time

When the sample was outgassed at 440 K most of the bands due to surface oxamide disappeared, and only bands at 3371, 1617 and 1467 cm^{-1} remained. Outgassing at 440 K also enhanced the intensity of the SiNCO band at the expense of the one due to CuNCO. By 572 K the CuNCO band decreased still further and new bands were seen at 2166 and 1579 cm^{-1}. The only features which resisted outgassing at 688 K were the SiNCO band at 2302 cm^{-1} and a weak band feature centred at 2137 cm^{-1}.

4.13.2 Hydroxylated $CuO-Cr_2O_3/SiO_2$

The results of C_2N_2 interaction with hydroxylated $CuO-Cr_2O_3/SiO_2$ are shown as transmission spectra (Fig. 4.43), absorbance difference spectra (Fig. 4.44) and as

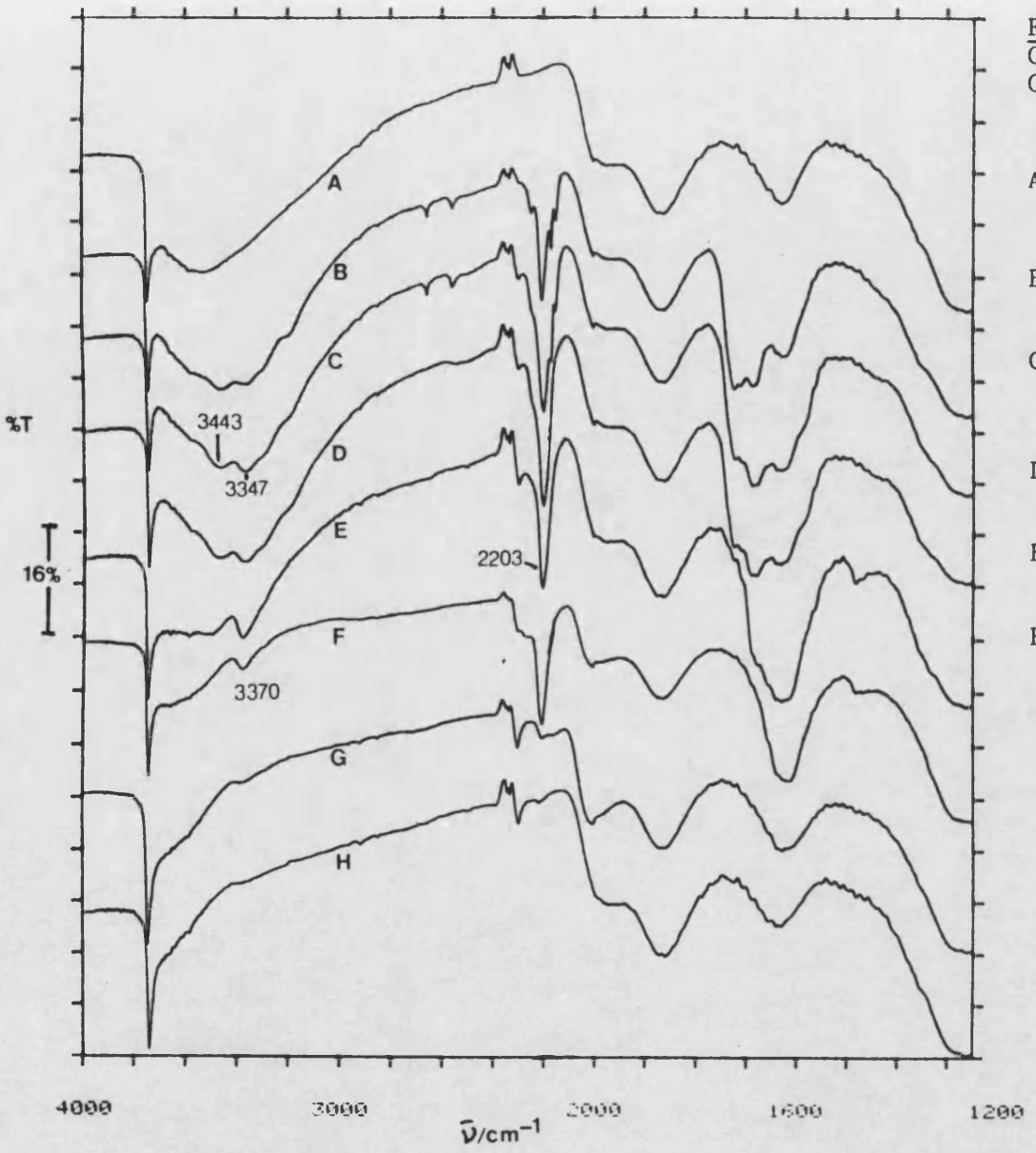

Fig. 4.43 I.r. Transmission Spectra of Cyanogen Interaction with Hydroxylated $CuO-Cr_2O_3/SiO_2$

A = Hydroxylated $CuO-Cr_2O_3/SiO_2$

B = Sample A exposed to C_2N_2/298 K/5 min

C = Sample A exposed to C_2N_2/298 K/24 h then evacuated.

D = Sample C outgassed at 403 K/2 h

E = Sample D outgassed at 563 K/2 h

F = Sample E outgassed at 713 K/4 h

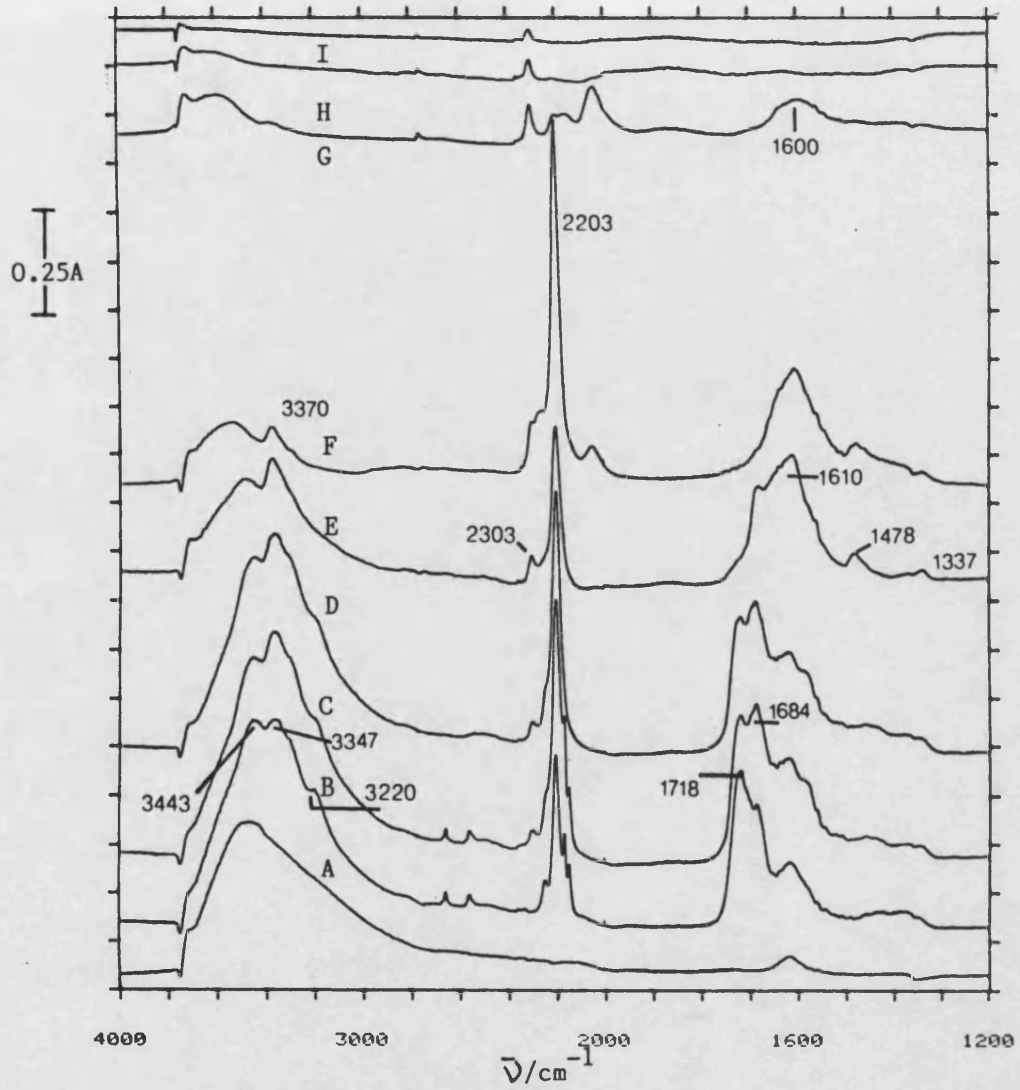

Fig. 4.44 I.r. Absorbance Difference Spectra of Cyanogen Interaction with Hydroxylated $CuO-Cr_2O_3/SiO_2$

A = Difference spectrum produced by hydroxylation of $CuO-Cr_2O_3/SiO_2$

B = Adsorbed species plus gaseous phase after C_2N_2 298 K/5 min

C = Adsorbed species plus gaseous phase after C_2N_2 298 K/24 h

D = Adsorbed species after C_2N_2/298 K/24 h after evacuating the i.r. cell

E = Adsorbed species after outgassing at 403 K/2 h

F = Adsorbed species after outgassing at 485 K/2 h

G = Adsorbed species after outgassing at 563 K/2 h

H = Adsorbed species after outgassing at 630 K/12 h

I = Adsorbed species after outgassing at 713 K/4 h

* All spectra dervied by subtracting a spectrum of outgassed $CuO-Cr_2O_3/SiO_2$ from appropriate spectrum.

expanded absorbance difference spectra in the 2400-1900 cm^{-1} region (Fig. 4.45).

Initial exposure of the hydroxylated sample to C_2N_2 at 298 K caused rapid reaction. Bands due to species associated with the copper oxide sites were identified by comparing the results obtained in this experiment to those reported earlier using hydroxylated CuO/SiO_2 (Sec. 4.9.2) and hydroxylated Cr_2O_3/SiO_2 (Sec. 4.11.2). Comparative studies showed that a band at 2203 cm^{-1} was assigned to surface CuNCO. This band was slightly more intense after 24 h and a weak one at 2303 cm^{-1} appeared. A weak feature at 2240 cm^{-1} was similar to that seen on hydroxylated CuO/SiO_2 (Sec. 4.9.2). The development of three bands at 3443, 3347 and 3200 cm^{-1} was characteristic of the NH moiety. The band at 3443 cm^{-1} was near that expected for O-H and N-H absorptions but its identity was confirmed as N-H using a spectral subtraction technique using the data station. Identification of bands due to species associated with the chromium part of the surface was not as simple since no unique bands appeared on the hydroxylated Cr_2O_3/SiO_2 surface (Sec. 4.11.2). However, the rate of growth of the band at 1684 cm^{-1} was more characteristic of amide formation on chromia rather than on copper sites. Evidence for amide formation on silica was provided by a strong band at 1718 cm^{-1}. Comparison of the appropriate peak heights after 5 minutes and 24 hours exposure (Figs. 4.44B and 4.44C) revealed that the build up of amide

Fig.4.45 I.r. Absorbance Difference Spectra (2400 - 1900 cm^{-1}) of C_2N_2 Challenge with Hydroxylated $CuO-Cr_2O_3/SiO_2$

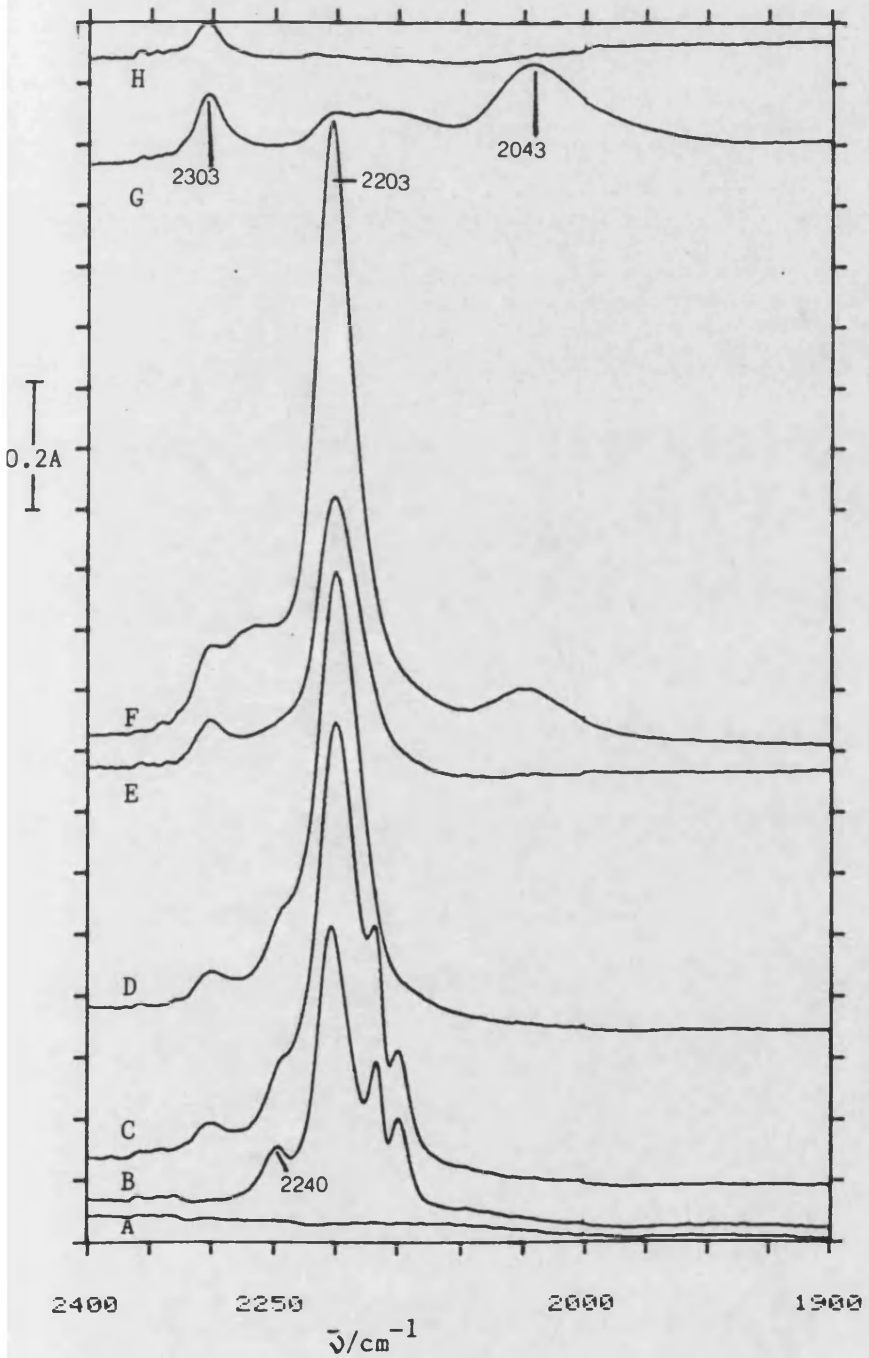

A = HYDR-$CuO-Cr_2O_3/SiO_2$

B = Adsorbed species plus gaseous phase after C_2N_2/298 K/5 min

C = as B except 24 h

D = as C then evacuated

E = Adsorbed species after outgassing at 403 K/2 h

F = as E then outgassed at 485 K/2 h

G = as F then outgassed at 563 K/2 h

H = as G then outgassed at 630 K/12 h

I = as H then outgassed at 713 K/4 h

* All spectra dervied by subtracting a spectrum of outgassed $CuO-Cr_2O_3/SiO_2$ from appropriate spectra.

species on the silica sites (1718 cm^{-1} band) occurred more quickly than on the metal oxide sites (1684 cm^{-1} band).

On outgassing at 403 K several spectral changes occurred (Fig. 4.44E):-

(a) spectral intensity above 3000 cm^{-1} was reduced.

(b) the 1718 cm^{-1} band due to amide on silica disappeared.

(c) a broad absorption centred at 1610 cm^{-1} developed together with two minor features at 1478 and 1337 cm^{-1}.

On heating to 485 K, the 1684 cm^{-1} band disappeared whilst the intensity of the CuNCO band doubled (Fig. 4.44F) and a new band was observed at 2043 cm^{-1} The intensity of this band was much stronger after outgassing at 563 K whereas the bands at 3370 cm^{-1} (N-H species), 2203 cm^{-1} (Cu-NCO), 1478 and 1337 cm^{-1} disappeared. Furthermore the intensity of the band at 1610 cm^{-1} was also reduced. Disappearance of the CuNCO band revealed a very weak, broad absorption centred at 2165 cm^{-1}. This feature was also observed in the case of the analogous outgassed surface.

By 630 K, the only species which resisted evacuation was SiNCO. No further changes occurred on heating to 713 K.

5. DISCUSSION

5.1 Surface Considerations of Silica-Supported Metal Oxides

In this section the reasons for supporting metal oxides on a high surface area support and for choosing low loadings of metal oxides are explained. The loading of the metal oxides has been related to the amount required to form a monolayer and to the number of surface silanol groups and silicon atoms present in the surface. The levels of loading are then discussed in terms of the nature and distribution of the metal oxides on the silica support.

The number of surface metal ions exposed in bulk metal oxides can be greatly enhanced by dispersing the oxide on a high surface area support. Furthermore, many catalytic studies have shown that the dispersion and loading of the active metal ions on the support can greatly influence catalyst reactivity (165). For these reasons and to enable i.r. spectroscopic experiments to be carried out, the copper and chromium oxides studied in this work were supported on a high surface area silica (Aerosil 300). To ensure that the metal oxides were well dispersed, the loading of each oxide was relatively low (1.5 wt % of each metal).

In order to relate the 1.5 wt % loading of Cu (as CuO) to that required to form a monolayer of CuO on the

silica surface, it is first necessary to calculate the amount of CuO required to form the monolayer.

The assumption was made that CuO forms a square lattice on the silica surface, as in the (100) face of the NaCl or MgO structure (Fig. 5.1).

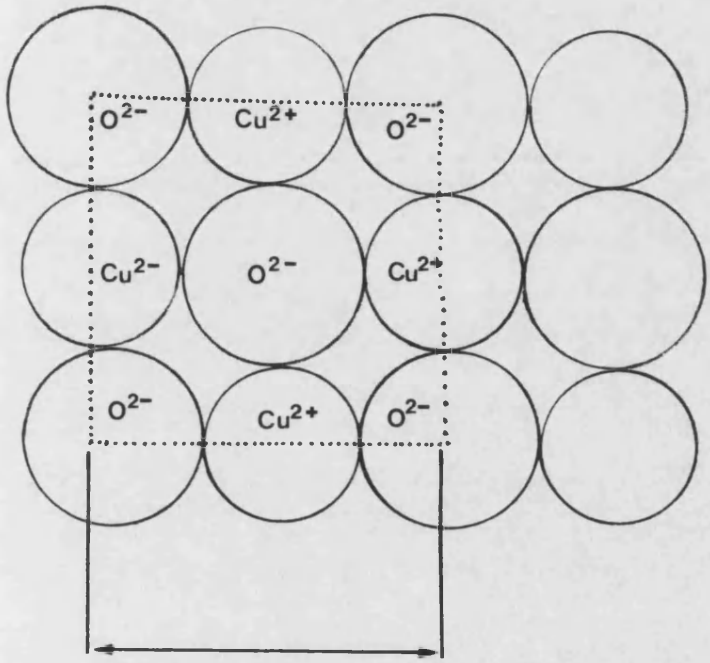

Ionic radii

$r_{Cu}2+ = 0.073$ nm

$r_{O}2- = 0.140$ nm

Fig. 5.1 Two Dimensional View of the CuO Lattice

The dotted square has an area of $(0.426 \times 10^{-9})^2$ m^2. The square contains the equivalent of $2Cu^{2+}$ and $2O^{2-}$ ions. Hence the area occupied by one $Cu^{2+}O^{2-}$ ion pair on the surface $= 0.5 \times (0.426 \times 10^{-9})^2 = 9.07 \times 10^{-20}$ m^2.

$\therefore$ Number of $Cu^{2+}O^{2-}$ ion pairs in a monolayer on 1 m^2 of surface is: $1/9.07x10^{-20} = 1.10x10^{19}$ $Cu^{2+}O^{2-}$ ion pairs. Thus a 'monolayer' of CuO on any surface contains $1.1x10^{19}$ ion pairs per m^2.

The weight of this monolayer is = $1.10x10^{19}x(63.5+16)/6.02x10^{23}$ g.....= 1.45 mg m^2.

Assuming that the ion pairs are well dispersed on the surface of the silica and not clumped 3-dimensionally then the wt.% of CuO required to form a monolayer on the silica surface, which has a specific surface area of 224 m^2 g^{-1}, is calculated as follows:-

Weight of the CuO monolayer is 224x1.45 mg.....=325 mg

Wt.% CuO for a full monolayer: =0.325x100/(0.325x1.000)

.....=24.5 wt.% CuO

Expressed as wt.% Cu for a monolayer this is equivalent to 19.6 wt % Cu.

It is clear that the loading of 1.5 wt.% Cu used in the current work equates to only 7.6% of a full monolayer.

To calculate the amount of CrO_3 required to form a monolayer a slightly different approach was taken since the structure of the chromium oxide monolayer was unknown. The calculation which follows was based on a method described by Bond and Bruckman (166). This method assumed that (i) the monolayer consisted of a two-dimensional array of CrO_3 'molecules' similar to a lamella of the three-dimensional crystal and (ii) a

single 'molecule' has a cubic structure. The calculation follows :-

Density of CrO_3.....2.7 g cm^{-3}

Molecular weight of CrO_3.....99.99

Molecules per cm^{-3} 2.7 x 6.02 x 10^{23}/99.99 = 1.63 x 10^{22}

Vol occupied by 1 molecule = 1/1.63x10^{22} =6.17x10^{-23} cm^3

Cross-sectional area of 1 CrO_3 'molecule' = 15.6x10^{-16} m^2

Number of CrO_3 'molecules' per m^2 of surface.....

.....= 6.4 X 10^{18} 'molecules'

Specific surface area of CrO_3/SiO_2 sample.....= 273 m^2 g^{-1}

For monolayer coverage 1 g CrO_3/SiO_2 contains.....

.....= 1.75 X 10^{21} molecules

1.75 X 10^{21} molecules weigh.....

.....1.75 X 10^{21} X 51.996/6.02 X 10^{23} = 0.15 g

Hence 0.15 g of Cr (as CrO_3) is required to form a monolayer on the silica sample. (ie 15 wt. % Cr)

The loading of 1.5 wt. % Cr used in the current work equates to approx 10% of a full monolayer.

The metal oxide loadings used in this work were chosen to be considerably lower than that required for monolayer coverage even in the mixed $CuO-Cr_xO_y/SiO_2$ samples. However, it does not follow that the metal ions were present as discrete entities in the form of an incomplete monolayer. This fact was demonstrated by Gil-Llambias et al (167) who studied the surface coverage of a δ-Al_2O_3 support with MoO_3. In this work it was shown that even at low loadings the molybdenum was not present

simply as an incomplete monolayer but that patches of multilayer MoO_3 also occurred.

It is interesting to relate the number of surface metal ions, N_m, to the number of surface silanol groups, N_{OH}, and to the number of surface silicon atoms, N_{Si}, present on the Aerosil sample after outgassing at 673 K. To do this it is first necessary to calculate the values of N_m, N_{OH} and N_{Si}.

Using CuO/SiO_2 as an example, N_m, in this case N_{Cu} was calculated as follows:-

Loading of Cu on the CuO/SiO_2 sample.....1.5 wt %
Specific surface area of CuO/SiO_2 outgassed at 673 K (measured by N_2 adsorption at 77 K).....224 $m^2\ g^{-1}$
Weight of Cu in 1 g of CuO/SiO_2.....0.015 g
Wt of Cu in 1 m^2 of surface (= 0.015/224)=6.69 X 10^{-5} g
Moles of Cu per m^2 of surface (= 6.69 X 10^{-5}/63.55).....
.....=1.05 X 10^{-6} mol.
Number of Cu ions per m^2 of surface:-.....
(= 1.05 X 10^{-6} X 6.023 X 10^{23}).....=6.32 X 10^{17} ions.

The number of copper and chromium ions per m^2 present on other samples used in this work were calculated using a similar method. These are shown in the third and fourth columns of Table 5.1. The total number of metal ions m^{-2} is shown in the fifth column of the table.

The value of N_{OH} for Aerosil outgassed at 673 K was taken as 4.5 ± 1.0 μmoles m^{-2} (equivalent to $27\pm6\times10^{17}$ silanol groups per square metre of surface). This value was obtained from data published by Okkerse (168). Although this value for N_{OH} was not determined using a silica sample identical to the one used in the current work, it was considered to be of sufficient accuracy since the surface structures and indeed the N_{OH} levels of a range of different silica samples, containing an array of structural characteristics, preparative routes and subsequent treatments give very similar results (168). The $N_m:N_{OH}$ ratios for the various adsorbents is shown in the penultimate column of Table 5.1.

The value for N_{Si} was taken from the work of Peri and Hensley (169). These workers reported that the surface density of silicon atoms in silica was 4.56 atoms/100 $Å^2$ (equivalent to 4.56×10^{18} atoms m^{-2}). It is interesting to relate the number of surface silicon atoms to the number of silanol groups on the outgassed sample, the ratio is $4.56 \times 10^{18}:2.7 \times 10^{17}$ (i.e. 1.67:1). The ratios of surface metal ions to surface silicon atoms ($N_m:N_{Si}$ for all samples used in the current work are shown in the far right-hand column of Table 5.1. These results are used throughout this discussion to compare and contrast the interaction of C_2N_2, H_2O and O_2 with copper oxide-chromium oxide surfaces.

Table 5.1 Surface Areas, Metal Oxide Loadings and N_m:N_{OH}, N_m=N_{Si} Ratios for Silica-Supported Copper Oxide-Chromium Oxide Samples

Sample *1	Specific Surface Area (m^2 g^{-1}) *2	Nm ($\times 10^{17}$ ions m^{-2}) copper	chromium	total	Ratios N_m:N_{OH}	N_m:N_{Si}
Aerosil	298	0.00	0.00	0.00	0.00:1	0.00:1
CuO/SiO_2	224	6.34	0.00	6.34	0.24:1	0.14:1
CrO_3/SiO_2	273	0.00	6.36	6.36	0.24:1	0.14:1
Cr_2O_3/SiO_2	227	0.00	7.65	7.65	0.28:1	0.17:1
$CuO\text{-}CrO_3/SiO_2$	193	7.36	9.00	16.36	0.61:1	0.37:1
$CuO\text{-}Cr_2O_3/SiO_2$	225	6.31	7.72	14.03	0.52:1	0.31:1

*1 All samples outgassed at 673 K/1 X 10^{-6} torr.

*2 Dtermined by N_2 adsorption at 77 K.

It is worth considering the distribution of metal ions in each of the silica-supported metal oxide samples used in this work in more detail. Davies (4) reported that in the case of samples containing Cu(II) ions, the amount of C_2N_2 produced could be used to estimate the number of surface cupric ions. Using this method Davies concluded that 90% of the copper present in a $CuO\text{-}Cr_2O_3/SiO_2$ sample (containing 4.6 wt % Cu) was exposed. Reduction studies of CuO/SiO_2 samples containing low

levels of copper (0.5 to 1.0 wt. %) suggested that unlike bulk CuO which reduced to Cu_2O on heating, silica-supported Cu(II) was stable (56). This result can be interpreted to mean that at low loadings, Cu(II) ions were stabilised by interaction with the surface and that cluster formation did not occur. CuO/SiO_2 samples containing high loadings of CuO (10-30 wt. %) were found to contain both CuO clusters and isolated Cu(II) ions (58) (Sec. 1.4). The low $N_{Cu}:N_{Si}$ and $N_{Cu}:N_{OH}$ ratios in this work suggests that CuO is likely to be highly dispersed.

The 1.5 wt.% loading of Cr in the CrO_3/SiO_2 sample equated to an $N_{Cr}:N_{OH}$ ratio of 0.24. At this loading, chromium is known to be fully dispersed on silica (16). However, there is more controversy in the literature as to whether Cr is present in the chromate or dichromate form. The most convincing studies were those of McDaniel (19) who favoured the chromate option (Sec. 1.3.1). He also calculated that saturation coverage occurred at about 4.3 wt.% Cr. At higher loadings excess Cr(VI) becomes unstable and decomposes at 673 K to Cr_2O_3. In the current work Cr(VI) is considered to be predominantly present as chromate, however, it is possible that a small amount of Cr was present as dichromate since chromium ions are known to be mobile during activation and some clustering is possible under these conditions.

Davies (4) studied HCN adsorption on Cr_2O_3/SiO_2 containing 5 wt.% Cr. Assuming a 1:1 ratio between

irreversibly adsorbed HCN and surface chromium ions, his results showed that only 30% of the total number of chromium ions were present on the surface. From this result Davies concluded that the chromia particles were at least partially aggregated. The 1.5 wt.% loading of Cr(III) in this work could give rise to both isolated and clustered chromia.

In the case of the Cu(II)-Cr(VI)/SiO_2 and Cu(II)-Cr(III)/SiO_2 samples used in this work the N_m:N_{OH} and N_m:N_{Si} ratios were all less than 1:1. This suggested that there were sufficient silanol and silica sites to enable the two oxides to exist separately. If this simplistic distribution of ions occurred then the reaction of C_2N_2 on the mixed oxide could simply be the sum of the reactions occurring on the individual oxide surfaces. In this thesis i.r. spectroscopic and microgravimetric results show that when C_2N_2 interacted with mixed oxide systems the results could not be wholly explained by reaction with individual Cu or Cr sites. Instead it is evident that some C_2N_2 molecules interact with both copper and chromium sites. This can be envisaged, if some copper ions are adjacent to chromium sites and visa-versa. This would occur if some parts of the surface contained a mixed phase of copper and chromium ions. The presence of such a layer is not unreasonable since copper and chromium ions were impregnated simultaneously (Sec. 2.7). Further support for the presence of a mixed layer is provided by the

existence of copper chromates and copper chromites (78-85). Copper and chromium ions can also be envisaged to be in close proximity if some ions are supported on the other metal oxide instead of on the silica.

5.2 Adsorption and Reaction of Cyanogen on Silica

The gravimetric and mass spectral results presented earlier (Sec. 4.1) showed that outgassed silica was not capable of converting C_2N_2. This result was in contrast to the work of several other groups of workers who reported that HCN was released and that surface silyl isocyanate was formed (112,113) (Sec. 1.6.3.2). These workers also reported that at high temperatures C_2N_2 reacted with SiO_2 to give surface silyl cyanide, silyl isocyanide and a polymer. The i.r. spectroscopic studies conducted in the current work suggested that C_2N_2 did not form these species presumably due to the lower silica outgassing temperature used in the current work. Instead adsorbed C_2N_2 interfered with silanol groups causing water molecules to form on the silica surface. Evidence for the reaction of adsorbed C_2N_2 was provided by the appearance of a band at 1720 cm^{-1} which formed at ambient temperature and resisted evacuation. This is best explained by the formation of a surface hydrolysis product containing the C=O moiety. Morrow and Cody (113) and others (112) did not observe this hydrolysis reaction presumably because they pre-outgassed silica at

1273 K whereas the silica was only outgassed to 673 K in the current work.

Spectral changes caused by hydroxylation of an outgassed silica disc are best seen in the difference spectrum (Fig. 4.4 spectrum A). The broad band around 3432 cm^{-1} is due to strongly H-bonded -OH groups of the adsorbed water molecules. The band at 1619 cm^{-1} is characteristic of the H_2O deformation mode of adsorbed water. The band at 920 cm^{-1} can also be assigned to adsorbed water. The band at 3740 cm^{-1} is due to -OH vibrations of isolated surface hydroxyls. This band decreased in intensity after the adsorption of water vapour, due to hydrogen bonding with adsorbed molecules. During cyanogen challenge a band appeared near 1720 cm^{-1} similar to the one observed with outgassed silica. This band shows that quite a strong interaction occurs between adsorbed cyanogen and the surface. The intensity of this band increased during extended exposure in cyanogen (Fig. 4.4, spectrum E). This suggests that the reaction leading to the unknown species is slow. The presence of weak ν(C≡N) bands at 2330, 2247 and 2091 indicates that at least one C≡N species exists. In addition, the fine structure observed at 3450-3200 cm^{-1} is typical of N-H vibrations. The best explanation of these features would appear to be that the formation of surface-stabilised hydrolysis species are involved, similar to those depicted below:

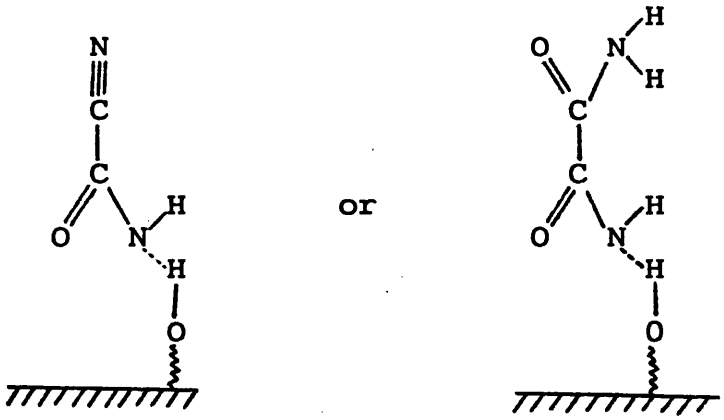

It is interesting that the i.r. spectrum of cyanoformamide contains bands near to those seen here (Table 5.2). Reduction of the bands near 3450, 1620 and 907 cm^{-1} during evacuation at room temperature is due to removal of the weakly held water molecules. The hydrolysis product was not removed, suggesting that it is either bonded irreversibly to the support or that it has deposited as a non-volatile compound. The hydrolysis product was removed by outgassing at 472 K but since no sublimate was observed it is assumed that it has decomposed, presumably by dehydroxylation. The fact that the surface species was unstable implies that it is only a partially-hydrolysed species akin to cyanoformamide. The appearance of peaks at 3713, 3550 and 907 cm^{-1} in the difference spectrum (Fig. 4.4, spectrum G) reveals that the silica surface still contained rather more -OH content than it did when pre-outgassed at 673 K.

The results for C_2N_2 adsorption at ambient temperature here are comparable to those reported by Davies (4) and Williams (2) who studied HCN adsorption. They only observed physical adsorption of HCN at 293 K

Table 5.2 Comparison of the i.r. Spectrum of the Adsorbed Species Present on Hydroxylated SiO_2 After Cyanogen Contact with that of Cyanoformamide

Band positions/cm^{-1}	
Adsorbed species on hydroxylated Silica	Cyanoformamide (170)
3450 - 3200 several bands	3410 vs 3260 vs
2330	-
2247	2249 w
2091	-
1720	1710 vs
1607 *1	1610 m
-	1346 m
-	1113 mw

*1 The 1607 cm^{-1} band was severely masked by the strong 1619 cm^{-1} band due to adsorbed moisture.

but they did observe reaction to yield SiNCO and SiCN on heating silica in HCN above 570 K.

5.3 Adsorption and Reaction of Cyanogen on CuO/SiO_2

In this section the gravimetric results relating to water and cyanogen uptake on CuO/SiO_2 surfaces are discussed. The reactions of adsorbed C_2N_2, at room

temperature (Sec. 5.3.1) and at elevated temperatures (Sec. 5.3.2), are then separately considered.

It is interesting to relate the uptake of H_2O (Table 5.3) to the underlying CuO/SiO_2 surface. For example the presence of 19.5 μg m^{-2} of irreversibly adsorbed H_2O molecules is equivalent to 6.5 x 10^{17} water molecules per m^2 of surface. This compares with 6.3 x 10^{17} copper ions per m^2; thus the ratio between copper ions and irreversibly adsorbed water molecules is 1:1.03. Neglecting the bare silica, this suggests that if all of the copper ions are exposed each $Cu^{2+}O^{2-}$ ion pair can have reacted with one water molecule to become fully hydroxylated as $OH^-Cu^{2+}OH^-$.

Table 5.3 The Uptake of Water Vapour and Cyanogen by CuO/SiO_2

	outgassed CuO/SiO_2	hydroxylated CuO/SiO_2	hydroxylated-hydrated CuO/SiO_2
Pre-adsorbed H_2O (μg m^{-2})	0.0	19.5	110.9
Irreversible C_2N_2 uptake at ambient temp. (μg m^{-2})	13.8	>48.1	>35.1

Comparison of the amount of water held by the hydroxylated-hydrated and hydroxylated surfaces given in

Table 5.3 shows that 91.4 μg of physically adsorbed water was present per m^2 of surface. The ratio between the number of copper ions and adsorbed water molecules is then 1:5.86. At this level of hydration exposed copper ions would very probably have their coordination spheres saturated.

The next comparison to make is that of the levels of uptake of cyanogen onto the outgassed, hydroxylated and hydroxylated-hydrated surfaces and to relate this to the coverage of copper ions by cyanogen molecules. The results in Table 5.3 show that the hydroxylated CuO/SiO_2 surface is more reactive towards cyanogen uptake than the outgassed surface and that the presence of physically adsorbed water suppresses this reactivity. The ratio between the number of copper ions in the outgassed CuO/SiO_2 surface and adsorbed cyanogen molecules is approximately 4:1. One interpretation of this is that on the outgassed surface C_2N_2 does not adsorb strongly on isolated $Cu^{2+}O^{2-}$ ion pairs, but requires, for instance, two such pairs (two copper ions) to be in proximity. On the hydroxylated surface, the number of C_2N_2 molecules adsorbed is of the same order of magnitude as the number of hydroxylated $HO^-Cu^{2+}OH^-$ sites (Table 5.3). This suggests that C_2N_2 now needs only one copper ion for adsorption, being held through the agency of the hydroxyl and singly bonded as  . Isolated $Cu^{2+}O^{2-}$ ion pairs (hydroxylated as $HO^-Cu^{2+}OH^-$) are then active centres for C_2N_2 adsorption and moreover the first step

towards hydrolysis is accomplished. The presence of physically adsorbed water molecules reduces the capacity of the surface to irreversibly adsorb C_2N_2 (Table 5.3). Presumably this is because excess water molecules shield the hydroxylated copper from direct interaction with cyanogen molecules and the resultant C_2N_2-water interactions are weaker than those with the ion pairs.

5.3.1 Reactions of Adsorbed C_2N_2 at Ambient Temperatures

Both outgassed and hydroxylated CuO/SiO_2 are active for hydrolysis of C_2N_2. A band which gradually developed at 1719 cm^{-1} also seen over hydroxylated silica, is due to the ν(C=O) stretch of a cyanoformamide-like species associated with silica sites (Table 5.2). After 2.5 h C_2N_2 exposure of the hydroxylated surface a second band appeared at 1687 cm^{-1} which was not seen over pure silica or outgassed CuO/SiO_2. The formation of a surface hydrolysis species by reaction with the hydroxyl groups associated with the copper sites is considered to account for this band.

Several species can be envisaged to explain the i.r. data. The most likely involves a cyanoformamide-like species similar to that described in the case of the silica-C_2N_2 reaction (Sec. 5.2). Species in which the C-C band is broken can also be envisaged (I) and (II) :-

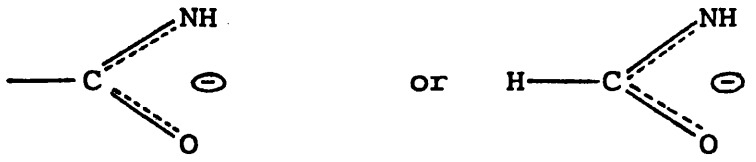

(I) (II)

This activity of hydroxylated $Cu^{2+}O^{2-}$ ion pairs is consistent with the enhanced uptake of C_2N_2 on the hydroxylated CuO/SiO_2 surface. A shoulder at 3383 cm^{-1}, characteristic of N-H stretching, supports the view that hydrolysis is occurring. After 6 h exposure the N-H absorptions seen at 3383 and 3199 cm^{-1} are characteristic of oxamide (Fig. 4.11). The slight shift from free oxamide bands at 3380, 3190 cm^{-1} is because the shoulders are superimposed on the broad -OH band above 3000 cm^{-1}. Since oxamide appears to form at room temperature it is unlikely that initial hydrolysis of C_2N_2 involved cleavage of the C-C bond, instead hydrolysis via the cyanoformamide-like species is more likely. Further enhancement of the 1687 cm^{-1}, and to a lesser extent the 1719 cm^{-1} band after 6 h exposure indicates that the hydrolysis reactions are slow. Indeed, the 1719 cm^{-1} band continued to grow for 17 hours. After this time, a new feature was observed near 2240 cm^{-1}. This was ascribed to the C≡N stretch of partially hydroxylated cyanogen. This latter band was lost on evacuation at 298 K suggesting that this intermediate is reversibly formed.

Another feature which developed during room temperature exposure of outgassed and hydroxylated

CuO/SiO_2 to cyanogen is a bond at 2302±2 cm^{-1}. This feature, not observed over hydroxylated silica, grew asymptotically (Fig. 4.8) reaching its maximum intensity after 21 h on the outgassed surface and after 2.5 h on the hydroxylated one. It resisted evacuation up to at least 674 K. This band is assigned to the anti-symmetric stretch of a silyl isocyanate, SiNCO. The band position is near to the value of 2284 cm^{-1} reported by Miller et al for $Si(NCO)_4$ (171). Miller also reported a peak at 1482 cm^{-1} ascribed to the symmetric stretch of the NCO moiety. A band at 1464 cm^{-1} seen in the current work is due to this vibration. The positions of the two bands plus the thermal stability of the SiNCO species is in good agreement with that seen by Ruttenberg and Low, who reported a band at 2310 cm^{-1} on reaction of cyanogen with silica at high temperature. Eley et al (117) also assigned a band at 2308 cm^{-1} to SiNCO following the reaction of ethyl isocyanate with silica at 573 K. Williams (2) also attributed a band at 2300 cm^{-1} to SiNCO when he adsorbed HCN onto CuO/SiO_2.

Since SiNCO formed at 298 K on CuO/SiO_2 in this work yet high temperatures are required to induce the reaction using pure silica it is clear that CuO assists the formation reaction. To account for this observation it is proposed that isocyanate first forms over the copper oxide sites and there spills over onto an adjacent silica site. The phenomenon of spillover of sorbed species is well documented. A recent review of the subject has been

written by Conner et al (172). In this article spillover was defined as the mobilisation of a sorbed species from one phase to another phase where it would not adsorb directly. In the current work spillover can be represented as shown if Fig. 5.2.

Fig. 5.2 Spillover of Adsorbed -NCO on CuO/SiO_2

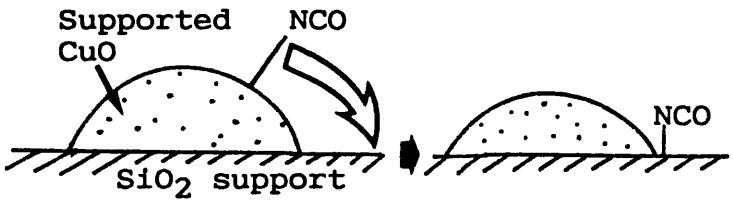

Spillover of the isocyanate moiety has received considerable attention due to its significance in automotive exhaust gas catalysis. The most widespread system studied involves NCO spillover on the Pt/SiO_2 surface (see for example the work of Bánsági et al (119). The current work represents the first time that -NCO spillover has been observed using supported CuO.

Spillover of NCO from copper sites would suggest that copper isocyanate is present as a precursor to SiNCO. Indeed CuNCO accounts for bands observed at 2209 cm^{-1} on outgassed CuO/SiO_2 and at 2203 cm^{-1} on the hydroxylated surface. Furthermore, a spectrum recorded after 5 minutes of C_2N_2 contact (Fig. 4.10 A) shows that a band due to CuNCO was already present even when the i.r. band due to SiNCO was barely visible. The rapid formation of CuNCO shows that spillover to form SiNCO is

the slow step in the reaction. The assignment of the isocyanate band of CuNCO was close to the value of 2200 cm^{-1} reported by London and Bell (64) after the reaction of NO and CO over CuO/SiO_2.

Another reaction of adsorbed cyanogen which occurred on outgassed CuO/SiO_2 was slow dissociation to yield surface CuCN (ν= 2175 cm^{-1}). Dissociative adsorption of HCN to yield CuCN followed by combination of CN groups to yield C_2N_2 was reported by Williams (2). Thus it is apparent that conversion of C_2N_2 to HCN in this work was a reversible process. In agreement with Williams (2) no i.r. bands due to adsorbed C_2N_2 were observed on outgassed CuO/SiO_2 even though C_2N_2 was desorbed on outgassing at elevated temperatures (Table 4.3). This could be explained by assuming that C_2N_2 adsorbs with its molecular axis parallel to the surface, in which position the stretching modes of C_2N_2 are polarised parallel to the surface. When adsorbed parallel to the surface, C_2N_2 is probably π-bonded. This can be depicted as :-

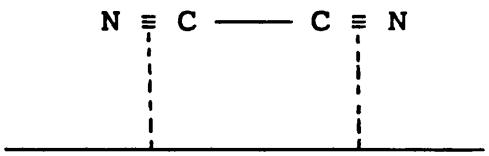

A similar configuration was proposed by Kordesch et al (100) when C_2N_2 was adsorbed on a Pd surface.

When C_2N_2 was adsorbed on hydroxylated CuO/SiO_2 the bands due to gaseous cyanogen, at 2165 and 2147 cm^{-1},

were shifted slightly to 2168 and 2151 cm^{-1}, the doublet also intensified (Fig. 4.10 spectra A and B). No such shift or intensification was seen over pure silica or outgassed CuO/SiO_2 surfaces. Weak molecular adsorption of cyanogen on the copper sites would account for the observed shifts. The adsorbed gas increases the amount of C_2N_2 in the i.r. beam, thus accounting for the observed band intensification. Further evidence for molecularly adsorbed cyanogen is provided by the fact that the bands at 2660, 2560, 2168 and 2150 cm^{-1}, characteristic of cyanogen, resisted evacuation at 298 K (Fig. 4.10 spectrum C).

The final points worthy of comment after room temperature adsorption were as follows:

-A small amount of oxidation to CO_2 occurred particularly on the outgassed surface (Table 4.3).

-The release of NH_3 at 291 K from both the outgassed and hydroxylated CuO/SiO_2 surfaces was in accord with observations made by Williams (2) in his study of HCN adsorption on silica-supported oxide copper. The proposal is that some nitrogen is retained as surface-hydrides even though the only source for hydrogen atoms on the outgassed surface is from the hydroxyl groups.

5.3.2 Reactions of Adsorbed C_2N_2 above Ambient Temperature

The reactions of adsorbed C_2N_2 are treated separately under the following sub-headings:

(a) reactions involving carbon-carbon triple bonds

(b) hydrolysis reactions

(c) isocyanate and other reactions

A summary of the desorbates recovered between ambient temperature and 693 K are shown in Table 5.4.

Table 5.4 Comparison of the Products Desorbed from Cyanogen-Contacted CuO/SiO_2 Surfaces

Product	Mass desorbed per m^2 of surface on outgassing from ambient temperature to 683±10 K ($\mu g\ m^{-2}$)		
	Outgassed CuO/SiO_2	Hydroxylated CuO/SiO_2	Hydroxylated-hydrated CuO/SiO_2
C_2N_2	9.06	0.29	1.20
HNCO	2.15	0.91	9.43
CO_2	0.31	0.38	2.81
HCN	1.24	0.30	3.31
NH_3	0.18	0.14	0.45
H_2O	1.19	3.12	19.61
CH_3NH_2	0.00	0.21	0.00
oxamide	0.00	78.60	<39.40
other organics	0.00	0.40	0.00

(a) Reactions involving carbon-carbon triple bonds

It was evident that the degree of hydroxylation affected the reactivity of the surface towards adsorbed

C_2N_2 above ambient temperature. The outgassed surface was relatively inactive for converting adsorbed C_2N_2. Approximately 65% of the gas was desorbed unchanged mainly below 433 K. This result suggested that C_2N_2 had only been weakly held. In contrast, only 1% of the irreversibly held C_2N_2 was desorbed unchanged from the hydroxylated surface even though some C_2N_2 molecularly adsorbed at 291 K. Approximately 3% of the irreversibly adsorbed C_2N_2 was desorbed from the hydroxylated-hydrated surface. Decomposition of adsorbed C_2N_2 to yield cyano-compounds was similar on both outgassed and hydroxylated surfaces. The chemistry associated with this reaction is best explained with reference to the hydroxylated surface. I.r. spectroscopy revealed that Cu(II)CN formed at 291 K and resisted outgassing upto 433K, however, on outgassing to 539 K and finally to 674 K, the Cu(II)CN gave way to species exhibiting a pair of bands at 2220 and 2150 cm^{-1}. The band at 2220 cm^{-1} is assigned to SiCN since its position is in good agreement with that reported to Morrow and Cody (113) who heated silica in cyanogen at 600 K. The 2150 cm^{-1} band is 10 cm^{-1} lower than one reported by Williams (2) following adsorption of HCN on CuO/SiO_2, but was in an identical position to one seen by Davies (4) who adsorbed HCN on $CuO-Cr_2O_3/SiO_2$. In both these studies, the 2150 cm^{-1} band was assigned to Cu(I)CN. The appearance of Cu(I)CN (2150 cm^{-1}) and of SiCN (2220 cm^{-1}) simultaneously as the 2125 cm^{-1} band disappeared suggests a link between these observations.

Furthermore, the 2175 cm^{-1} band itself developed at the same time as evidence for molecularly adsorbed cyanogen vanished. It is therefore proposed that the following sequence of events occurred. Firstly, the loss of molecularly adsorbed C_2N_2 occurs due to dissociation on the CuO surface as follows:

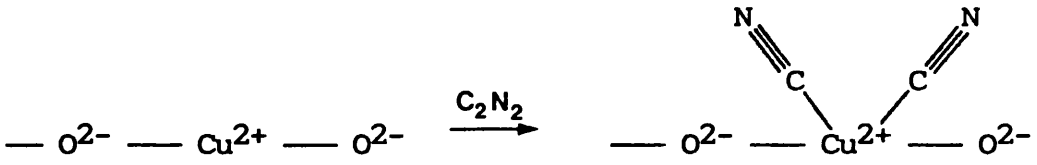

The dicyano-complex is thought to be responsible for the 2175 cm^{-1} band. On outgassing to 539 K this species breaks down to yield Cu(I)CN and SiCN, and these are the species giving rise to bands at 2150 and 2220 cm^{-1}. These species are then stable to outgassing upto 674 K.

(b) Hydrolysis reactions

The degree of hydrolysis greatly influenced the capacity of the surfaces to hydrolyse adsorbed C_2N_2. The outgassed surface was not very reactive. I.r. evidence (Sec. 4.9.1) showed that a surface hydrolysis intermediate, with a characteristic ν(C=O) band at 1718 cm^{-1}, was associated with silica sites. This species decomposed by 423 K. Evidence for an oxamide-like surface hydrolysis intermediate on the hydroxylated CuO/SiO_2 disappeared on outgassing to 423 K. However, by 539 K i.r. bands characteristic of oxamide were apparent at 3383, 3186, 1663, 1351 and 1106 cm^{-1} (Fig. 4.11). The

diamide was strongly held onto the surface and was not released until the temperature reached 674 K. Since oxamide was not released from cyanogen-contacted outgassed CuO/SiO_2 or from hydroxylated silica, it was apparent that the hydroxylated copper sites were active in the hydration of C_2N_2 to oxamide. Sublimation of oxamide from hydroxylated CuO/SiO_2 was confirmed during microgravimetric studies (Sec. 4.2.2). In this case however, sublimation occurred at a much lower temperature (~425 K). The discrepancy over the sublimation temperature was probably due to a variation in the level of hydroxylation of the two samples.

Oxamide formation was the predominant reaction on hydroxylated CuO/SiO_2. Indeed by 673 K, assuming that no carbon or nitrogen atoms remained on the surface, 78.6 μg m^{-2} of oxamide had formed. This was equivalent to converting 97% of irreversibly adsorbed C_2N_2 to the diamide. Evidence for other hydrolysis products was provided by the appearance of small peaks in the mass spectra of the desorbates collected above 291 K. Such products included formamide (H_2NCHO) and methanoic acid ($HC(=O)-OH$). It is also highly likely that oxamic acid ($H_2NC(=O)-CO_2H$) was produced but its presence could not be confirmed unambiguously.

Hydrolysis was also the major reaction of adsorbed C_2N_2 over the hydroxylated-hydrated surface. In this

case less than 66% of the irreversibly adsorbed C_2N_2 was converted to oxamide. The presence of formamide (m/z=45) and methanol (HCHO,m/z=30) was also inferred from mass spectral results. The enhanced release of HNCO and HCN over this surface could be explained by the simple stoichiometric reaction of C_2N_2 with water thus:-

$$C_2N_2 + H_2O \longrightarrow HCN + HNCO$$

(c) Isocyanate and other reactions

The CuNCO which formed at room temperature over outgassed CuO/SiO_2 became less abundant on outgassing upto 673 K. In addition, the position of the i.r. band ascribed to this species (2209 cm^{-1}) shifted at higher temperatures due to changes in the surface environment. The final position of the band, 2220 cm^{-1}, was identical to that already assigned to SiCN. Both assignments are however valid and correspond closely to reported literature values (3,112-113). The intensity of the SiNCO band (2303 cm^{-1}) remained constant on heating upto 673 K, suggesting that all silica-acceptor sites for -NCO spillover were covered by 293 K.

The CuNCO which formed on the hydroxylated surface was less stable than that on the outgassed surface; indeed, it was decomposed on heating to 423 K. This result is best explained in conjunction with the observations that the presence of physically adsorbed water tends to enhance the production of NH_3 (Table 5.4). It is proposed that water molecules interact with surface

CuNCO to form NH_3, The release of ammonia was also reported by Solymosi et al (173) when NCO groups associated with a copper surface were exposed to moisture.

Another possible decomposition route for adsorbed NCO involves reaction with the oxygen atoms of neighbouring CuO sites. This can be envisaged to lead to the desorption of CO_2, N_2* and C_2N_2 according to the following scheme:-

(i) $CuNCO+CuO \longrightarrow CuN+Cu-CO_2$

(ii) $Cu-CO_2 \longrightarrow Cu+CO_{2(g)}$

(iii) $CuNCO+Cu \longrightarrow CuO+CuNC$

(iv) $CuNC+CuNC \longrightarrow 2Cu+C_2N_2$

(v) $CuN+N-Cu \longrightarrow 2Cu+N_{2(g)}$

Similar reaction sequences proposed by Solymosi et al when HNCO was adsorbed on Cu(III) (68) and when HCN was adsorbed onto oxygenated Cu(III) (66). Recombination of CN groups to yield C_2N_2 explains the release of C_2N_2 at elevated temperatures measured in this work.

A more likely explanation for the production of CO_2 involved the intermediate formation of copper carboxylate. Indeed the appearance of a band at 1587 cm^{-1} at room temperature, notably over the hydroxylated-hydrated surface, was near to the literature value for copper carboxylate (61). Amerikov and Kasatkina observed a band at 1565 cm^{-1} during adsorption studies of CO_2 on

---

* It was not possible to quantify the amount of N_2 formed during this work since nitrogen was non-condensable under the conditions used.

copper oxide (62). The removal of this band on outgassing in the range 423-673 K coincided with the release of CO_2.

One other possible decomposition route of the NCO group to CO_2 is via an intermediate $-O_2CN$ species (104). Since no spectral evidence was found to support the presence of such a species, this route seems unlikely.

5.4 Adsorption and Reaction of Cyanogen on CrO_3/SiO_2

Gravimetric considerations relating to water and cyanogen uptake on CrO_3/SiO_2 surfaces are discussed in this section. The reactions of adsorbed C_2N_2 at room temperature and at elevated temperatures are then considered in sections 5.4.1 and 5.4.2 respectively.

A comparison between the uptake of water and cyanogen on CrO_3/SiO_2 surfaces is given in Table 5.5. The presence of 120.0 μg m^{-2} of irreversibly adsorbed water molecules is equivalent to 40.1 x 10^{17} water molecules per m^2 of surface. This compares with 6.4 x 10^{17} chromium ions per m^2 of surface (Table 5.1). Thus the ratio between Cr ions and irreversibly adsorbed water molecules is 1:6.3. At this level of hydroxylation all exposed chromium ions would be fully hydroxylated, as would a high proportion of the silica surface.

It is intersting to compare the levels of uptake of C_2N_2 onto the outgassed, oxygenated and hydroxylated surfaces and to relate this to the coverage of chromium ions by C_2N_2 molecules. The results in Table 5.5 show

Table 5.5 The Uptake of Water Vapour and Cyanogen by CrO_3/SiO_2

	Outgassed CrO_3/SiO_2	Oxygenated CrO_3/SiO_2	Hydroxylated CrO_3/SiO_2
Pre-adsorbed H_2O ($\mu g\ m^{-2}$)	0.0	0.0	120.0
Pre-adsorbed C_2N_2 ($\mu g\ m^{-2}$)	47.0	40.0	2.8

that the outgassed surface is more active towards C_2N_2 uptake than the oxygenated surface, which in turn is more active than the hydroxylated one. The ratio between the number of chromium ions in the outgassed CrO_3/SiO_2 surface and the number of adsorbed C_2N_2 molecules is 1.2:1 (i.e. 6.36×10^{17} Cr ions m^{-2}: 5.44×10^{17} adsorbed C_2N_2 molecules m^{-2}). If it is assumed that:

(i) every Cr ion in the sample is a surface ion and accessible to cyanogen;

(ii) there is irreversible adsorption of C_2N_2 only on Cr ions and not on the silica support;

(iii) one C_2N_2 molecule occupies one Cr ion, then then coverage of Cr ions by C_2N_2 is 85% This result is hypothetical since i.r. spectroscopic results (Sec. 4.10.1) show that some C_2N_2 molecules are converted to other species at room temperature. Each reaction product

molecule formed could be envisaged to cover more than one Cr site; alternatively, the dissociation of each irreversibly adsorbed C_2N_2 molecule could yield two or more adsorbed species, each occupying one Cr site.

The colour change from brown to yellow during the oxygenation treatment of CrO_3/SiO_2 has been observed by others (16,21,17,18). This phenomenon was attributed to the formation of a completely oxidised surface phase i.e. one consisting of chromium in the (VI) oxidation state only. Table 5.5 shows that this surface was less active towards C_2N_2 uptake than the outgassed sample. This is thought to be due to the reduced ability of the C_2N_2 molecule to enter the co-ordination sphere of chromium ions when they are fully co-ordinated by oxygen.

The dramatically reduced irreversible C_2N_2 uptake on the hydroxylated surface, which equates to a ratio between chromium ions and adsorbed C_2N_2 molecules of 1:0.05, is thought to be due to the shielding of active chromium ions by adsorbed water molecules.

5.4.1 Reactions of Adsorbed C_2N_2 at Ambient Temperature

In contrast to the discussion dealing with the CuO/SiO_2 surface, there was very little evidence for the presence of adsorbed species (or products) containing C-N multiple bonds when C_2N_2 was interacted with the CrO_3/SiO_2 surface at room temperature. This result was in agreement with the work of Davies (4) who adsorbed

C_2N_2 and HCN onto various CrO_3/SiO_2 surfaces. Indeed the only evidence for any adsorbed species containing C-N multiple bonds was a very weak i.r. band at 2207±1 cm^{-1} which is ascribed to CrNCO. This species formed slowly on the outgassed and hydroxylated surfaces but did not form on the oxygenated surface.

Another minor reaction which occurred at ambient temperature was the formation of a surface species containing the methyl moiety. The two bands at 2974 and 2905 cm^{-1} were characteristic of C-H vibrations of such a species. Bands due to antisymmetric and symmetric vibrations of the methyl group are expected in the 2980-2840 cm^{-1} region (Table 5.6). The main reactions which occurred on CrO_3/SiO_2 surfaces were hydrolysis and oxidation, and these are discussed separately in the following sub-sections.

Hydrolysis Reactions

Amide-like hydrolysis species developed slowly over both the chromium and silicon sites on the outgassed surface at 291 K. These species were characterised by i.r. bands at 1681 and 1715 cm^{-1}, respectively. Similar bands were observed with the oxygenated sample, except that in comparison with the outgassed surface the intensity of the Cr-amide band was diminished. This was probably because the oxygenation treatment reduced the hydroxyl content of the surface. This argument is enforced by the fact that i.r. bands at 3734 and 3609 cm^{-1}, due to isolated and H-bonded silanol groups, were

Table 5.6 I.r. Spectroscopic Stretching Frequencies (cm^{-1}) for the CH_3 Group Between 2980 and 2840 cm^{-1}

Current work	Borello et a (174-175)*1		Eley et al (30)*2	Assignment
	a	b		
2905	2855	2845	2890	Symm. vibration
2974	2959	2950	2960	Antisymm. vib.

*1 From studies of methanol adsorption on silica (a) = strongly adsorbed methanol, (b) = physically adsorbed methanol.

*2 From studies of ethylene adsorption on silica-supported chromium oxide.

diminished in comparison with the situation on the outgassed surface (Fig. 4.17 spectrum A). The Si-amide species (1681 cm^{-1}) was very unstable, its abundance decreasing when the sample was exposed to a cold finger and decreasing still further on evacuating at room temperature. As one would expect, hydrolysis was a more abundant reaction on the hydroxylated CrO_3/SiO_2 surface than on the outgassed surface. Comparison of the band positions seen here (3462, 3366, 3210, 2246, 1715, 1605 and 1364 cm^{-1}) with those seen on hydroxylated silica (Table 5.2), coupled with the fact that no band was seen

at 1681 cm^{-1}, confirms that the hydrolysis product here was a cyanoformamide-like species formed on the silica, not on the chromium surface. The positions of the bands above 3000 cm^{-1} (due to N-H vibrations) are shifted in comparison with cyanoformamide. This suggests that the molecule is bound to the surface via the N-H end of the molecule (Sec. 5.2). The Si-amide species formed on the hydroxylated surface was more resistant to evacuation than that formed on the outgassed surface. This stabilisation is clearly due to the increased level of H-bonding between the hydroxylation product and the hydroxylated surface. An investigation using D_2O, in place of H_2O, did not provide any additional information on the nature of the hydrolysis intermediate.

Oxidation Reactions

Outgassed CrO_3/SiO_2 was active for oxidation of C_2N_2 even at room temperature, although no products were returned to the gas phase until the sample temperature was raised (Sec. 5.4.2). The oxidation evidently involved formation of surface bidentate carbonate associated with the chromium sites (ν = 1560, 1340 cm^{-1})(Sec. 4.10.1).

Comparison of the i.r. spectroscopic results obtained when C_2N_2 was interacted with hydroxylated CrO_3/SiO_2 with the work of Zecchina et al (163) (Sec. 4.10.4) showed that strongly chemisorbed bicarbonate

(ν = 1620, 1432 and 1225 cm^{-1}) and carbonate (= 1580 and 1346 cm^{-1}) species were present in this work. Only the latter carbonate species was observed over oxygenated-hydroxylated CrO_3/SiO_2.

5.4.2 Reactions of Adsorbed C_2N_2 above Ambient Temperature.

The reactions of adsorbed C_2N_2 are described under the following sub-headings; (a) hydrolysis reactions (b) oxidation reactions and (c) isocyanate formation and other reactions. A summary of the desorbates collected after heating the sample from ambient temperature upto 693-733 K are shown in Table 5.7. In view of the special experimental limitations pertaining to these results (Sec. 4.3), only qualitative statements about relative amounts can be made in this case. However, several important conclusions emerge from these results.

(a) Hydrolysis Reactions.

The hydrolysis of HCN and of C_2N_2 to oxamide over CrO_3/SiO_2 surfaces has previously been reported by Davies (4). In the case of HCN the diamide was thought to form via the combination of two single amide groups. The hydrolysis of C_2N_2 to oxamide requires no such combination; it is considered to occur via a cyanoformamide-like species. The existence of this species was inferred from i.r. bands at 3375, 3210, 2246, 1715, 1605 and 1364 cm^{-1} (see Table 5.2). The fact that the C-C bond vibration was not observed in this work does

Table 5.7 Comparison of the Products Desorbed from Cyanogen-Contacted CrO_3/SiO_2 Surfaces

	Mass desorbed per m^2 of surface on outgassing between ambient temperature and 693-733 K		
Desorbate	Outgassed CrO_3/SiO_2 ($\mu g\ m^{-2}$)	Oxygenated CrO_3/SiO_2*1 (arbitrary units)	Hydroxylated CrO_3/SiO_2 (arbitrary units)
C_2N_2	7.1	10.5	31.1
HNCO	8.0	1.1	2.9
CO_2	2.3	20.9	83.2
HCN	3.9	1.5	3.6
NH_3	0.1	0.0	7.9
H_2O	3.0	30.3	230.4
oxamide	absent	present	present

*1 Sample heated in C_2N_2-O_2 atmosphere.

not contradict this argument, since this vibration occurs at 780 cm^{-1} in cyanoformamide (170), a region of thespectrum which contains very strong silica absorptions. On heating the cyanoformamide-like species in vacuo, two distinct behaviours can be envisaged, either hydrolysis to yield oxamide or decomposition to yield, for example C_2N_2, H_2O and HNCO and (by reaction with adsorbed H) $HCONH_2$. The reaction route was found to be dependent upon the surface pretreatment.

In the case of the C_2N_2-exposed outgassed CrO_3/SiO_2 surface, heating to 473 K caused the i.r. bands at 1715 and 1681 cm^{-1} (ascribed to hydrolysis species associated with the silica and chromium sites respectively) to disappear. Mass spectrometric studies showed that C_2N_2, HNCO and H_2O were desorbed thus decomposition had occurred. Some of the H_2O was retained on the surface giving rise to an i.r. band at 1622 cm^{-1}. This adsorbed water was desorbed by outgassing to 567 K.

When outgassed CrO_3/SiO_2 was heated in C_2N_2 upto 423 K the i.r. band at 1681 cm^{-1} characteristic of the chromium-cyanoformamide species intensified. This is thought to be due to the reaction of surface hydroxyl groups or water molecules with gaseous phase C_2N_2.

Decomposition of the cyanoformamide-like species occurred when oxygenated CrO_3/SiO_2 was heated to 423 K and oxamide was also formed. In the case of the hydroxylated CrO_3/SiO_2 sample, outgassing to 471 K reduced the i.r. spectral intensity of the partially hydrolysed intermediate and again oxamide sublimed; a similar result was obtained using the oxygenated-hydroxylated sample.

These results show that conversion of the partially hydroxylated surface species is dependent upon the availability of H_2O or -OH groups. In the absence of such groups, decomposition to C_2N_2, HNCO and H_2O occurs, whereas in the presence of such groups hydrolysis to

oxamide also occurs.

(b) Oxidation Reactions

I.r. spectroscopy showed that the bands characteristic of monodentate and bidentate/chromium carbonate species which formed at room temperature on the outgassed surface disappeared on outgassing to 473 K. Gravimetric studies showed that CO_2 was released on outgassing upto 567 K. Taken together these results show that some surface chromium carbonate is fully oxidised to yield CO_2 by 567 K. The degree of oxidation of C_2N_2 on the outgassed surface was minor in comparison to the extent of hydrolysis. The percentage of C_2N_2 converted to CO_2 is calculated using a carbon mass balance as follows:-

irreversibly adsorbed C_2N_2.....= 47.0 μg m^{-2}

carbon (as C_2N_2).....47 X 24/52 = 21.7 μg m^{-2}

CO_2 released above 298 K.....= 2.3 μg m^{-2}

carbon released as CO_2.....2.3 X 12/44 = 0.6 μg m^{-2}

Hence the % of C converted to CO_2...0.6 X 100/21.7 = 2.8%

Thus less than 3% of the irreversibly held C_2N_2 is oxidised to CO_2. The strong bands which appeared at 1614, 1572 and 1472 cm^{-1} when outgassed CrO_3/SiO_2 was heated in C_2N_2 to 673 K are attributed to oxidation species. These were removed by evacuation at 673 K.

When C_2N_2-exposed, oxygenated CrO_3/SiO_2 was outgassed at 473 K, a band appeared at 1625 cm^{-1}. This peak is between the positions reported for surface bicarbonate (1620 cm^{-1}) and carboxylate (1630 cm^{-1}) species (163). Other bands due to these species have been reported at 1440, 1430 and 1225 cm^{-1} by Zecchina et al (163). These features were not seen here presumably because they were of low intensity. The build-up of bidentate carbonate (1350 cm^{-1}) (163) was also observed in the current work. The proportion of irreversibly adsorbed C_2N_2 converted to CO_2 was much higher on the oxygenated surface than on the outgassed one (Table 5.7).

The m/z = 30 peak referred to in Table 4.8 is likely to be due to the release of small amounts of NO. This assignment, however, is uncertain since i.r. bands due to adsorbed NO on silica-supported CrO_3 surfaces are known to occur near 1875-1735 cm^{-1} (176) and no such bands were seen in this work.

In the case of the hydroxylated sample, outgassing at 471 K caused the surface bicarbonate (1432 and 1225 cm^{-1}) bands (163) to be replaced by a chromium monodentate carbonate species (1490 and 1365 cm^{-1}) (163). The i.r. bands due to this species disappeared on outgassing to 573 K. When these i.r. results are considered in conjunction with the microgravimetric and mass spectrometric results, especially the result that little CO_2 was desorbed upto 493 K whereas large quantities were released by 563 K (Table 4.9), it is

apparent that the bicarbonate species does not decompose directly to CO_2. Instead oxidation to CO_2 proceeds via chromium-carbonate species.

(c) Isocyanate Formation and other Reactions

When outgassed CrO_3/SiO_2 was heated in C_2N_2, CrNCO and SiNCO formed. These species were characterised by i.r. bands at 2206 and 2302 cm^{-1}. The i.r. band position at 2206 cm^{-1} corresponded closely to that observed by Solymosi and Raskó (41,45) who interacted NO and CO over unsupported chromia (ν = 2210 cm^{-1}). These workers suggested that chromium ions were in the +2 oxidation state. The close proximity of the i.r. band in the current work suggests that Cr(II) may well exist here. The appearance of an i.r. band at 2210 cm^{-1} when HNCO was adsorbed on chromia at 298 K supported the assignment of the band at 2206 cm^{-1} to CrNCO.

The intensity and rate of growth of the pair of bands at 2206, 2302 cm^{-1} on the outgassed CrO_3/SiO_2 surface suggest that, compared with the hydrolysis reactions, isocyanate formation was a minor reaction which occurred slowly. Indeed CrNCO formation was much less prominent than formation of the analogous species on the Cu(II) surface (Sec. 5.3). The release of ammonia above room temperature occurred as the intensity of the 2206 cm^{-1} band decreased. Thus it is assumed that -NCO reacted to form NH_3. Solymosi and Raskó (45) observed a similar feature and suggested that CrNCO

reaction with adsorbed water accounted for the release of NH_3.

When C_2N_2-exposed CrO_3/SiO_2 was evacuated to 733 K, hydrolysis and oxidation products decomposed and C_2N_2, HCN and HNCO were released. Dissociation of C_2N_2 followed by interaction of adsorbed CN groups with surface hydroxyl groups explains the release of HCN.

5.5 Adsorption and Reaction of Cyanogen on Cr_2O_3/SiO_2

In this section gravimetric results relating to water and cyanogen uptake on Cr_2O_3/SiO_2 surfaces are considered. The reactions of adsorbed C_2N_2, at room temperature (Sec. 5.5.1) and at elevated temperatures (Sec. 5.5.2) are then discussed.

It is interesting to compare the amounts of irreversibly held water on the hydroxylated and hydroxylated-hydrated Cr_2O_3/SiO_2 surfaces and to relate these figures to the number of surface chromium ions. The uptakes of H_2O and of C_2N_2 on Cr_2O_3/SiO_2 surfaces are shown in Table 5.8.

The irreversible uptake of water by the surface was 50.0 μg m^{-2}, equivalent to 16.7 x 10^{17} molecules of H_2O per square metre of surface. Thus there were 2.19 molecules of H_2O per surface chromium ion. The hydroxylated-hydrated sample contained 83.2 μg H_2O per m^2, equivalent to 27.8 x 10^{17} molecules of H_2O per square metre of surface. By comparison with the amount of H_2O adsorbed by the hydroxylated surface, the amount of

Table 5.8 Comparison of Water Vapour and Cyanogen Uptake by Cr_2O_3/SiO_2 Surfaces

	Outgassed Cr_2O_3/SiO_2	Hydroxylated Cr_2O_3/SiO_2	Hydroxylated-hydrated Cr_2O_3/SiO_2
Pre-adsorbed H_2O ($\mu g\ m^{-2}$)	0.0	50.0	83.2
Irreversible C_2N_2 uptake ($\mu g\ m^{-2}$)	28.8	>57.3	<14.9

physically adsorbed water is calculated to be 11.1 x 10^{17} molecules per square metre. The ratio of chromium ions to adsorbed water molecules on this sample was therefore 1:3.6.

The amount of cyanogen irreversibly adsorbed by the Cr_2O_3/SiO_2 surface was clearly influenced by the degree of surface hydroxylation. The outgassed surface irreversibly adsorbed 28.8 $\mu g\ m^{-2}$, equivalent to 3.34 X 10^{17} C_2N_2 molecules m^{-2}. The ratio between Cr sites and irreversibly adsorbed C_2N_2 molecules is 1:0.44. This level of uptake is much lower than the 82 $\mu g\ m^{-2}$ of HCN which irreversibly adsorbed onto 5% Cr_2O_3/SiO_2 reported by Davies (4). The hydroxylated surface irreversibly adsorbed twice as much C_2N_2 as the outgassed sample. The presence of physically adsorbed water reduced the capacity to retain C_2N_2 and the ratio of surface chromium

ions to irreversibly adsorbed C_2N_2 molecules is 1:0.23. The reduced uptake capacity of the hydroxylated-hydrated surface is probably due to shielding of the active chromium sites by adsorbed water molecules.

5.5.1 Reactions of Adsorbed C_2N_2 at Ambient Temperature

The key reaction which occurred when C_2N_2 was adsorbed onto Cr_2O_3/SiO_2 surfaces was hydrolysis. Other less pronounced reactions are discussed under a separate sub-heading.

Hydrolysis Reactions

Hydrolysis of C_2N_2 over outgassed Cr_2O_3/SiO_2 gave rise to two species. One was associated with the chromium sites, the other with the silica sites. The nature of the silica-hydrolysis intermediate, characterised by an i.r. band at 1717 cm^{-1}, was described earlier (Sec. 5.2). However, there is some doubt regarding the exact nature of the species formed on the Cr(III) sites, which was characterised by an i.r. band at 1685 cm^{-1}. Surman (3) who contacted HCN with unsupported chromia at room temperature, observed a surface amide species which resulted from interaction between HCN and surface hydroxyl groups. He proposed two possible structures, designated earlier as (I) and (II), respectively (Sec. 5.3.1). I.r. bands at 1600, 1440 and 1375 cm^{-1} were assigned to structure (I) whilst a band at 1685 cm^{-1} was attributed to structure (II). Similar species are possible here; however, hydrolysis products

also retaining the C-C bonds are equally likely. Evidence for the consumption of surface hydroxyl groups was evident from the weakening of the sharp band at 3740 cm^{-1} (compare difference spectra A to D in Fig. 4.25). Thus hydrolysis may be represented by the following scheme:

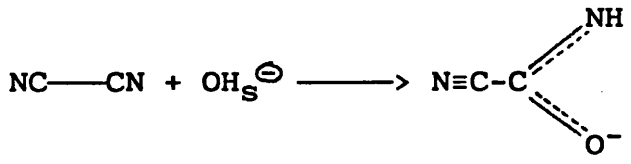

The position of the i.r. bands due to the hydrolysis species associated with the Cr(III) sites are identical (within experimental error) to those observed on the Cr(VI) surface. This suggested that the oxidation state of the chromium reaction sites made little difference to the bond strengths in the adsorbed hydrolysis species. Alternatively, it is possible that the Cr(VI) sites were reduced to Cr(III) prior to, or during, the hydrolysis reaction.

Comparison of the rate and extent of the hydrolysis reaction on the Cr(III) and Cr(VI) surfaces was investigated using i.r. spectroscopy. After initial C_2N_2 exposure the strength of the 1681 cm^{-1} band formed on CrO_3/SiO_2 (Fig. 4.13 spectrum A) was considerably weaker than the equivalent peak on the Cr(III) counterpart (Fig. 4.25 spectrum A). This showed that the reaction which yielded the surface hydrolysis intermediate was more rapid on the Cr(III) surface. After extended exposure

the ratio between the peak intensities near 1715 and 1681 cm^{-1} was roughly th same on the Cr(III) and Cr(VI) samples. This suggests that similar amounts of surface hydrolysis species were formed on these samples. This in turn suggests that similar numbers of active surface chromium ions are present on the two surfaces. Since the chromium ions in the $Cr(VI)/SiO_2$ sample are known to be fully dispersed (Sec. 5.1), the same is likely to be true of the chromium ions in the Cr(III) sample.

Comparison of the intensity of the i.r. band at 1685 cm^{-1} on outgassed and hydroxylated Cr_2O_3/SiO_2 with that on the outgassed surface suggested that irreversibly adsorbed moisture reduced the extent of conversion to the adsorbed hydrolysis products containing the 1685 cm^{-1} band. Mass spectroscopic studies showed that hydroxylated Cr(III) samples converted C_2N_2 to HNCO even at room temperature, whereas no such release occurred from the outgassed surface. HNCO was also released from the hydroxylated-hydrated surface despite the chromium ions being surrounded by adsorbed water molecules. These results suggest that the lower conversion to adsorbed hydrolysis species when moisture is present may be due to the fact that further hydrolysis to HNCO occurs.

Other Reactions

A series of bands at 2302, 2210, 1584, 1499 and 1428 cm^{-1} could not be ascribed to hydrolysis intermediates. The formation of a small amount of CrNCO accounts for

the weak band at 2210 cm^{-1} and an even weaker one at 2302 cm^{-1} was caused by spillover of NCO to form SiNCO.

The band at 1499 cm^{-1} is assigned to a surface $-NH_2$ group. Peri (177) ascribed a band at 1510 cm^{-1} to this group when NH_3 was adsorbed onto $-Al_2O_3$. Surman (3) also attributed a band at 1510 cm^{-1} to surface $-NH_2$ when he studied the adsorption of HCN on chromia. A possible mechanism for the formation of this species could be as follows:-

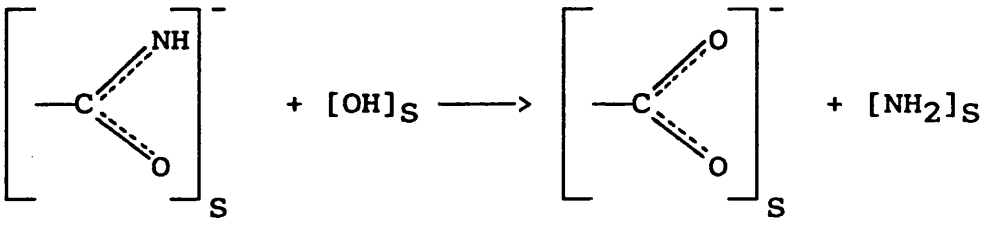

This reaction clearly results in the formation of surface carboxylate which is known to exhibit i.r. bands near 1630 and 1440 cm^{-1} (163). Such a species may be responsible for the very weak shoulder near 1630 cm^{-1} and the band at 1428 cm^{-1} (Fig. 4.25 spectrum E).

The band at 1584 cm^{-1} is typical of the $C\text{-}O^1$ stretching of a surface bidentate carbonate. The $C\text{-}O^2$ stretch is expected near 1340 cm^{-1} (163). The band at 1353 cm^{-1}, already assigned to a hydrolysis intermediate, may also receive a contribution from this vibration.

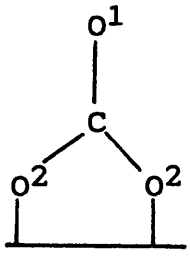

Although adsorbed oxidation intermediates were evident at room temperature, mass spectroscopic results confirmed that no decomposition products were released from outgassed Cr_2O_3/SiO_2 at room temperature. The presence of adsorbed moisture suppressed the formation of surface carboxylate and only a very small amount of bidentate carbonate (ν= 1589 cm^{-1}) was present on the hydroxylated surface. Indeed the amount of this species was so small that the weak 1340 cm^{-1} absorption was not visible. Despite weak evidence for oxidation on this surface some unstable intermediates did form since some CO_2 was desorbed even at 293 K.

In the case of the hydroxylated-hydrated surface both CO_2 and NH_3 were released. The formation of ammonia can be explained by the reaction of surface -NH_2 species with moisture as follows:-

$$[NH_2]_s + H_2O \longrightarrow NH_{3(g)} + [OH]_s$$

5.5.2 Reactions of Adsorbed C_2N_2 above Ambient Temperature

The reactions of adsorbed C_2N_2 are described under two sub-headings; (a) hydrolysis reactions, (b) other reactions. A summary of the desorbates collected after heating C_2N_2-exposed Cr_2O_3/SiO_2 samples from ambient temperature to 668-673 K is shown in Table 5.9.

Table 5.9 Comparison of the Products Desorbed from Cyanogen-Exposed Cr_2O_3/SiO_2

Desorbate	Mass desorbed on outgassing between ambient temperature and 668-673 K (μg m^{-2})		
	Outgassed Cr_2O_3/SiO_2	Hydroxylated Cr_2O_3/SiO_2	Hydroxylated-Hydrated Cr_2O_3/SiO_2
C_2N_2	14.3	13.7	2.3
HNCO	0.0	8.9	2.5
CO_2	9.1	12.5	9.6
HCN	3.4	3.9	0.4
NH_3	1.3	0.9	0.3
H_2O	0.5	32.2	29.6
oxamide	0.0	0.0	>8.6

(a) Hydrolysis Reactions

When C_2N_2-exposed, outgassed Cr_2O_3/SiO_2 was outgassed at 473 K, the strong i.r. bands ascribed to surface amide intermediates on the chromia and silica surfaces (Fig. 4.25 spectrum E) disappeared. However, no hydrolysis products were released. Instead, spectral evidence suggests that one decomposition route involved dehydroxylation. This explains the development of an i.r. band at 1624 cm^{-1} which is due to adsorbed moisture. The dehydroxylation process can be represented as follows:-

$$[NC-\overset{\overset{O}{\|}}{C}-NH_2]_s \longrightarrow C_2N_{2(g)} + [H_2O]_s$$

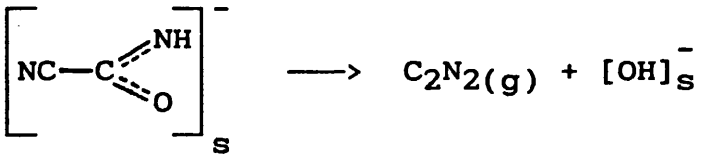

This reaction would account for the high percentage (~50%) of C_2N_2 which was desorbed unchanged from outgassed Cr_2O_3/SiO_2.

When C_2N_2-exposed hydroxylated Cr_2O_3/SiO_2 was outgassed, the desorption of the hydrolysis intermediates on the chromia and silica sites were distinguishable. The silica-amide species decomposed slightly by 411 K and totally by 485 K whereas the chromia-amide species was more resistant. The characteristic i.r. band at 1685 cm^{-1} weakened by 485 K and vanished by 590 K. In this case adsorbed moisture interacted with the decomposing amide and HNCO desorbed. Although sufficient moisture was present to completely hydrolyse all of the irreversibly adsorbed C_2N_2, only 10% of the carbon atoms were converted to hydrolysis products.

The hydroxylated-hydrated sample was active for converting C_2N_2 to oxamide, some of which was released by 403 K and more by 501 K. Oxamide formation was the dominant reaction of adsorbed C_2N_2; more than 33% of the irreversibly held carbon was converted to the diamide. Only a small amount of C_2N_2 was desorbed unchanged which confirmed that little dehydroxylation occurred during outgassing. It is pertinent to recall that the presence of physically adsorbed moisture lowered the C_2N_2 uptake on Cr_2O_3/SiO_2 samples. However, it appears that the

weakly held H_2O molecules are responsible for the oxamide formation.

The formation of chromium-amide species over Cr(III) surfaces was similar to that reported by Surman who adsorbed HCN on α-chromia (3). However, whereas Surman proposed that heating the amide yielded CO_2 via surface oxidation species, it is clear that dehydroxylation is also an important reaction.

Other Reactions

A key feature of the interaction of adsorbed cyanogen with outgassed and hydroxylated Cr_2O_3/SiO_2 is the high proportion of C_2N_2 released at elevated temperature. Although this phenomenon is largely explained by dehydroxylation of hydrolysis species, other precursors to desorbed C_2N_2 are likely. Unfortunately no i.r. spectral evidence for adsorbed C≡N-containing species was observed but this does not necessarily mean that such species were not present since CN can be held in on i.r. inactive form (3,67). Recombination of CN groups to yield C_2N_2 may occur at elevated temperatures. Evidence for adsorbed CN groups is provided by the release of HCN which can form by reaction of surface CN groups with adsorbed moisture.

This weak CrNCO band, 2210 cm^{-1}, produced on the outgassed Cr(III) surface intensified when the sample was heated from 291 to 473 K. The SiNCO which formed by spillover was stable upto at least 673 K. No isocyanate spillover reaction occurred on the hydroxylated surface

presumably because the NCO acceptor sites were blocked by adsorbed OH and H_2O groups. Based on the intensity of the i.r. band at 2206-2210 cm^{-1} the extent of CrNCO formation on the Cr(III) sample was similar to that observed on supported Cr(VI). However, isocyanate formation was much less prominent than on Cu(II) surfaces. The extent of spillover from chromium onto the silica sites was also less pronounced than on Cu(II) surfaces. Thus some form of hindrance mechanism is present with the Cr(III) (and Cr(VI)) samples. Solymosi and Raskó (41,45) reported that spillover on Cr_2O_3/SiO_2 was highly restricted when compared to Cr_2O_3/Al_2O_3. Indeed, spillover was as rapid on the alumina supported sample that the band due to CrNCO did not appear. CrNCO was unstable at 590 K.

Oxidation of C_2N_2 to CO_2 (and N_2) was enhanced above room temperature. The reaction presumably involved conversion of Cr(III) to Cr(II). The release of CO_2 from outgassed, hydroxylated and hydroxylated-hydrated surfaces between 411 and 473 K coincided well with the disappearance of i.r. bands ascribed to surface carboxylate (1428 cm^{-1}) and surface bidentate carbonate (1584 cm^{-1}) respectively. The hydroxylated surface was the most active for CO_2 formation, some 13% of irreversibly adsorbed carbon atoms (as C_2N_2) being desorbed as CO_2. The enhanced activity of the hydroxylated surface can be explained by reference to the work of Surman (3). He proposed that when HCN was

interacted with α-Cr_2O_3, CO_2 was formed via surface amides which decomposed to surface formates then to carboxylates. Since more amide is present on the hydroxylated surface it follows that higher conversion to CO_2 is likely.

Finally the release of NH_3 from the outgassed surface, notably above 504 K, is thought to be due to the interaction of surface $-NH_2$ species (1499 cm^{-1}) with co-ordinated moisture.

5.6. Adsorption and Reaction of Cyanogen on CuO-CrO_3/SiO_2

A summary of the gravimetric and mass spectrometric results relating to oxygen, water and cyanogen uptake onto CuO-CrO_3/SiO_2 surfaces are shown in Table 5.10.

The amount of oxygen irreversibly adsorbed on the oxygenated sample was 38.5 $\mu g\ m^{-2}$, equivalent to 7.25 $x10^{17}$ oxygen molecules per m^2 or 14.5 $x10^{17}$ oxygen atoms per m^2. Comparison of this value with the total number of copper and chromium ions (i.e. 16.36 $x10^{17}$, table 5.1) shows that on a simple basis each metal ion is associated with one adsorbed oxygen atom.

In the case of the hydroxylated CuO-CrO_3/SiO_2 sample, 154.0 $\mu g\ m^{-2}$ of adsorbed H_2O, roughly equivalent to 3 H_2O molecules for every copper and chromium ion, is present. Thus it is assumed that the co-ordination spheres of the metal ions are fully saturated. A comparison of the irreversible uptake of H_2O on the

Table 5.10 Comparison of Oxygen, Water and Cyanogen Uptake by $CuO-CrO_3/SiO_2$ Surfaces

	Outgassed $CuO-CrO_3/SiO_2$	Oxygenated $CuO-CrO_3/SiO_2$	Hydroxylated $CuO-CrO_3/SiO_2$	Oxygenated-Hydroxylated $CuO-CrO_3/SiO_2$
Pre-adsorbed oxygen ($\mu g\ m^{-2}$)	0.0	38.5	0.0	84.22*
Pre-adsorbed H_2O ($\mu g\ m^{-2}$)	0.0	0.0	154.0	~150.0
Irreversibly adsorbed C_2N_2 ($\mu g\ m^{-2}$)	35.5	32.0	115.0	>100.0

* This includes weakly adsorbed oxygen since in this case H_2O was adsorbed in the presence of residual gaseous oxygen.

CuO/SiO_2 and CrO_3/SiO_2 samples with that on the mixed oxide is presented in Table 5.11. This shows that the H_2O uptake on the mixed oxide is slightly more than the sum of the amounts held by the single oxide surfaces. When considered in conjunction with the fact that the oxygen coverage of Cu and Cr ions is near unity, it is concluded that most of the metal ions in the mixed oxide are exposed on the surface prior to dosing O_2 or H_2O.

It is relevant to compare the C_2N_2 uptake on the supported mixed oxide with that obtained on the supported

Table 5.11 Comparison of the Irreversible Uptake of H_2O on CuO/SiO_2, CrO_3/SiO_2 and $CuO-CrO_3/SiO_2$ Samples

	CuO/SiO_2	CrO_3/SiO_2	$CuO-CrO_3/SiO_2$
H_2O uptake $\mu g\ m^{-2}$	19.5	120.0	154.0

single oxides, Table 5.12. The results clearly show that C_2N_2 uptake on the mixed oxide is enhanced when adsorbed water is present, whereas on the individual oxides adsorbed H_2O suppresses C_2N_2 uptake. Furthermore, in the absence of moisture the uptake of C_2N_2 on the mixed oxide is lower than the sum of the values on the individual oxides. These results show that when copper and chromium are present together, the combined reactivity is not simply the sum of the values obtained over the individual oxide surfaces; instead the two metal ions exert a synergetic effect which may be due to C_2N_2 interacting with copper and chromium sites which occupy adjacent sites (Sec.5.1). This synergy is greatly affected by the presence of moisture.

5.6.1 Adsorption and Reaction of C_2N_2 at Ambient Temperature

In this section the reactions of C_2N_2 adsorbed on

Table 5.12 Comparison of Irreversible Cyanogen Uptake ($\mu g\ m^{-2}$ surface) on Silica-Supported Copper(II), Chromium(III) and Copper(II)-Chromium(III) Surfaces

	Pretreatment			
	Outgassing	Oxygenation	Hydroxylation	Hydroxylation-hydration
CuO/SiO_2	13.8	>48.1	>35.1	not quantifiable
CrO_3/SiO_2	47.0	40.0	2.8	not quantifiable
$CuO-CrO_3/SiO_2$	35.5	32.2	115.0	>100.0

$CuO-CrO_3/SiO_2$ are discussed and compared with the interaction of C_2N_2 on the single transition metal oxide systems. The discussion is divided into two broad areas (a) hydrolysis reactions and (b) other reactions.

(a) Hydrolysis Reactions

Hydrolysis of cyanogen adsorbed on Cu(II)-Cr(VI) surfaces is a key reaction as indeed it was over the individual oxide surfaces. Formation of hydroxylation products occurred on both the silica and metal oxide sites. This was demonstrated by the growth of i.r. bands near 1714 and 1681 cm^{-1}, respectively. It was not possible to distinguish between hydroxylation on the

copper and chromium sites using i.r. spectroscopy. However, comparison with adsorption studies over the individual oxides suggests that hydrolysis is more likely on the Cr sites.

Hydrolysis of C_2N_2 on the outgassed surface was slow and involved consumption of surface -OH groups. Judging by the intensity of the i.r. bands at 1714 and 1681 cm^{-1}, hydrolysis was less pronounced than on the individual oxides.

The spectral bands observed near 3438, 3353, 1708, 1632 and 1372 cm^{-1} which occurred when C_2N_2 was interacted with an oxygenated surface were similar to those reported for cyanoformamide (Table 5.2). Reduction in the intensity of these bands during evacuation suggested that this hydrolysis product was either reversibly formed or that it decomposed. The latter possibility is likely since some HNCO, HCN and H_2O was released to the gas phase during evacuation.

The presence of pre-adsorbed water enhanced the uptake of C_2N_2. This is explained by the reaction of C_2N_2 with the surface to form a partially hydroxylated intermediate. After 5 h, i.r. bands characteristic of oxamide were observed (Fig. 4.35B). With the exception of some N-H vibrations the spectrum was remarkably similar to that of free oxamide. The species producing these bands resisted evacuation, which is consistent with the fact that oxamide is a non-volatile molecule. Furthermore since oxamide also formed on hydroxylated

CuO/SiO_2 but not on hydroxylated CrO_3/SiO_2, formation of the diamide was associated with the copper sites. A small amount of HNCO was formed on the hydroxylated surface due to decomposition/hydroxylation of adsorbed C_2N_2. The oxygenated-hydroxylated surface was less active than the hydroxylated surface towards converting C_2N_2 to HNCO and instead more surface oxamide was formed at 293 K. Indeed, the oxygenated-hydroxylated surface was such a powerful hydrolysing surface that the large amount of surface oxamide formed absorbed most of the incident i.r. radiation. This high level of hydrolysis explains why Davies (4) only recovered small amounts of C_2N_2 from HCN-exposed $CuO-CrO_3/SiO_2$ samples. Davies also reported that less C_2N_2 was recovered from the mixed oxide than from CuO/SiO_2 which suggests that the mixed oxide is more capable of converting adsorbed C_2N_2.

(b) Other Reactions

When C_2N_2 reacted with outgassed Cu(II)-Cr(VI) at room temperature, formation of isocyanate was the most prominent reaction measured using i.r. spectroscopy. NCO was formed rapidly on the copper sites (ν=2203 cm^{-1}) and slowly on the silica sites (ν=2203 cm^{-1}). This suggested that, as in the case of CuO/SiO_2 (Sec. 5.3.1), spillover from the copper sites to the silica sites is the slow step in the reaction. The formation of isocyanate was dramatically influenced by pre-adsorbed oxygen or moisture. No SiNCO formed on the oxygenated

surface. No isocyanate bands were seen on either the metal or silica sites on the hydroxylated or oxygenated-hydroxylated surfaces. This is in contrast with studies over hydroxylated CuO/SiO_2. The lack of NCO formation is ascribed to the fact that adsorbed C_2N_2 is preferentially hydroxylated by the influence of the active chromium sites. It should be remembered that the intense spectrum due to adsorbed oxamide on the 'oxy-hydr' surface may have masked NCO bands.

The enhanced activity of the metal oxide sites on the mixed oxide sample was also evidenced by the fact that no i.r. bands due to adsorbed C_2N_2 were observed on the hydroxylated mixed oxide, whereas bands at 2168 and 2151 cm^{-1} were observed with hydroxylated CuO/SiO_2. Furthermore, the CuCN band at 2175 cm^{-1} observed on the outgassed CuO/SiO_2 surface was not seen on the outgassed mixed oxide and only a trace of HCN was released at room temperature. These results confirm that species containing the C≡N moiety on the hydroxylated mixed oxide were either i.r. inactive, or more likely they were rapidly hydrolysed or oxidised.

Oxidation of C_2N_2 was evident even at room temperature. I.r. spectroscopic evidence for strongly chemisorbed chromium bicarbonate (ν = 1620 and 1443 cm^{-1}) (163) and chromium bidentate carbonate or copper carboxylate (ν = 1582 and 1345 cm^{-1}) (163) was seen on the outgassed and oxygenated surfaces (Sec. 4.10.4). The i.r. bands due to these oxidation intermediates were more

intense than on the CrO_3/SiO_2 surface which suggests that the mixed oxide was more strongly oxidising than the single oxide. An alternative explanation for several of the i.r. bands ascribed to oxidation intermediates is that an amide species, similar to that reported by Krietenbrink and Knozinger (110), occurred. They assigned bands at 1600, 1440 and 1375 cm^{-1} to surface amide when HCN was adsorbed on δ-Al_2O_3.

5.6.2 Adsorption and Reaction of C_2N_2 above Ambient Temperature

A summary of the desorbates collected after heating C_2N_2-exposed CuO-CrO_3/SiO_2 samples from ambient temperature to 673 K is shown in Table 5.13.

(a) Hydrolysis Reactions

The hydrolysis intermediates formed at room temperature either decomposed or sublimed as oxamide at elevated temperatures. The reaction mechanism was dependent upon the surface pretreatment. For example, the hydrolysis intermediates formed on the outgassed surface decomposed by 439 K yielding HNCO, HCN, C_2N_2 and H_2O. Davies (4) did not observe HNCO when he interacted an outgassed CuO-CrO_3/SiO_2 sample with HCN. Thus it is likely that HNCO formed by decomposition of a hydrolysis product of C_2N_2. The cyanoformamide-like hydrolysis product formed at room temperature on the oxygenated surface also decomposed on heating to 435 K and the

Table 5.13 Comparison of the Products Desorbed from Cyanogen-Exposed $CuO-CrO_3/SiO_2$ Surfaces

Desorbate	Mass desorbed per m^2 of surface on outgassing between ambient temperature and 673 K ($\mu g\ m^{-2}$)			
	Outgassed $CuO-CrO_3/SiO_2$	Oxygenated $CuO-CrO_3/SiO_2$	Hydroxylated $CuO-CrO_3/SiO_2$	Oxygenated-Hydroxylated $CuO-CrO_3/SiO_2$
C_2N_2	9.5	15.5	8.2	0.9
HNCO	4.4	9.7	25.2	9.3
CO_2	4.2	11.3	21.7	107.5
HCN	1.7	1.7	13.3	0.5
NH_3	0.0	0.2	0.7	1.1
H_2O	0.2	5.2	30.5	66.4
organics	1.2	1.1	0.0	0.0
CH_4	0.0	0.4	0.0	0.0
oxamide	0.0	0.0	~265.0	trace

characteristic i.r. band at 1678 cm^{-1} shifted to 1627 and then to 1610 cm^{-1}. This change can be explained by conversion of the cyanoformamide-like species to one similar to Structure I in sec. 5.3.1. This species has been proposed when HCN adsorbed on δ-Al_2O_3 and i.r. bands near 1600, 1440 and 1375 cm^{-1} have been ascribed to it (110). Similar bands were reported by Surman when HCN was adsorbed on chromia (3). The bands observed in the current work at 1610, 1482 and 1334 cm^{-1} are close to those reported by these workers. Surman proposed that the amide decomposed via a surface formate to CO_2 (3). Davies (4) suggested that decomposition of surface amide

on $CuO-Cr_2O_3/SiO_2$ occurred via surface carbonate and surface NH_x species. No i.r. spectroscopic evidence to support either view was seen here although the release of CO_2, especially above 543 K, did occur (Table 4.14).

The i.r. bands characteristic of surface oxamide formed at room temperature on the hydroxylated surface vanished on outgassing to 373 K. Nevertheless, oxamide sublimed when the sample was outgassed between 553 and 613 K. It is clear that oxamide either became i.r. inactive or that it decomposed to an i.r. inactive species which re-formed and sublimed at higher temperatures. Oxamide also sublimed from hydroxylated CrO_3/SiO_2 and from hydroxylated CuO/SiO_2 surfaces; thus it is likely that the di-amide formed on both Cu and Cr sites. However, the amount of oxamide produced, ca 265 $\mu g\ m^{-2}$, was much higher than the sum of that produced on the individual oxide surfaces. Thus some co-operative effect between the oxides to enhance hydrolysis was evident. The formation of oxamide from a re-cycled sample shows that if it were not for surface oxamide blocking the active surface hydrolysis sites, then the conversion of C_2N_2 to oxamide in the presence of moisture would be a continual reaction.

The intense i.r. bands characteristic of adsorbed oxamide which formed at room temperature on the oxygenated-hydroxylated sample also disappeared on heating to 459 K. However, unlike the hydroxylated surface, only a small amount of oxamide sublimed. It is

evident that adsorbed oxygen was capable of cleaving the C-C bond of the diamide to yield an amide intermediate similar to that formed on the oxygenated surface. Mass spectrometric data suggested that this amide species decomposed to yield CO_2.

(b) Other Reactions

Although isocyanate formation was identified as a key reaction at room temperature, spillover of the -NCO moiety from the metal ions to the silica sites was hindered. On heating the C_2N_2-exposed mixed oxide the spillover reaction was enhanced and the i.r. bands due to SiNCO grew at the expense of CuNCO. No NCO spillover was seen on the oxygenated surface until the outgassing temperature reached 588 K. By this temperature mass spectrometric results showed that oxygen was desorbed. This may have re-exposed silica-acceptor sites permitting NCO spillover.

The decomposition of surface NCO has already been described (Sec. 5.3.2). However, the study over the outgassed mixed oxide surface showed that decomposition of CuNCO is probably linked with an intermediate species characterised by an i.r. band at 2038 cm^{-1}. The identity of the species giving rise to this band remains uncertain; however copper isocyanide, CuNC, is expected to contain vibrations in this region. Indeed, Morrow and Cody (113) observed a band at 2100 cm^{-1} due to SiNC. A more probable explanation for the 2038 cm^{-1} band is due

to the vibration of a cyanide moiety, bridged across one copper and one chromium site.

Oxidation of adsorbed C_2N_2 was evident on all pretreated Cu(II)-Cr(VI) surfaces (Table 5.13). The high degree of C_2N_2 oxidation to CO_2 which occurred on the oxygenated-hydroxylated surface, coupled with the fact that intense i.r. bands due to surface oxamide were observed after room temperature C_2N_2 exposure yet little oxamide was released at elevated temperatures confirms that CO_2 is released by decomposition of surface hydrolysis species. This hypothesis is supported by the observation that no i.r. bands due to any other oxidation were seen on either the hydroxylated or oxygenated-hydroxylated surfaces. Furthermore, comparison of the amount of CO_2 released from hydroxylated CuO/SiO_2 and hydroxylated CrO_3/SiO_2 surfaces confirms that oxidation was associated with the chromium sites.

In the absence of moisture, oxidation occurred via surface carbonate and bicarbonate-like species (Sec. 5.6.1). I.r. spectroscopic evidence showed that these intermediates decomposed by 439 K to a species containing a band at 1630 cm^{-1} similar to that seen on outgassed and oxygenated CrO_3/SiO_2. This feature is assigned to surface bicarbonate or carboxylate (Sec. 4.12.1). The 1630 cm^{-1} band disappeared by 528 K which coincided with the release of CO_2.

Unlike the reactions described over CuO/SiO_2, no surface species containing the C≡N bond were seen on the

Cu-Cr oxide. This is due to the enhanced oxidising/ hydrolysing power of the mixed oxide. However, small amounts of CH_3CN, CH_3NH_2 and CH_4 were detected. These species are characteristic of reaction over copper sites (Sec. 4.2).

5.7 Adsorption and Reaction of Cyanogen on CuO-Cr_2O_3/SiO_2

It is first appropriate to consider the uptake of water prior to cyanogen contact. A summary is given in Table 5.14

Table 5.14 Comparison of Water Vapour Uptake by CuO-Cr_2O_3/SiO_2

	CuO-Cr_2O_3/SiO_2 Pretreatment		
	Outgassed	Hydroxylated	Hydroxylated-hydrated
pre-adsorbed H_2O ($\mu g\ m^{-2}$)	0.0	28.3	92.6

The amount of water irreversibly held by the mixed oxide sample was 28.3 $\mu g\ m^{-2}$, equivalent to 9.47×10^{17} molecules m^{-2}. This was significantly lower than on the Cr_2O_3/SiO_2 surface but is higher than on the CuO/SiO_2 counterpart. It is surprising that when the number of surface metal sites capable of irreversibly adsorbing H_2O

increases, the number of water molecules held actually decreases.

Cyanogen uptake on the $CuO-Cr_2O_3/SiO_2$ surface was considerably higher than on the single oxide surface (Table 5.15). Indeed, uptake of C_2N_2 on the outgassed and on the hydroxylated-hydrated $CuO-Cr_2O_3/SiO_2$ surfaces exceeded the sum of the amounts adsorbed on the individual oxides. If the Cu and Cr ions had acted independently the irreversibly C_2N_2 uptake would have been approximately 35.1 + 14.9 = 50 μg m^{-2} surface. The actual figure of 441 μg m^{-2} shows that the surface is almost on order of magnitude more reactive towards C_2N_2 uptake than if the Cu and Cr ions acted independently.

Table 5.15 Comparison of Irreversible Cyanogen Uptake (μg m^{-2} surface) on Silica-Supported Copper(II) and Chromium(III) Surfaces

	Pretreatment		
Adsorbent	Outgassed	Hydroxylated	Hydroxylated-hydrated
CuO/SiO_2	13.8	>48.1	>35.1
Cr_2O_3/SiO_2	28.8	>57.3	<14.9
$CuO-Cr_2O_3/SiO_2$	52.9	>100.6	>440.9

5.7.1 Adsorption and Reaction of C_2N_2 at Ambient Temperature

(a) Hydrolysis Reactions

The formation of surface-amide was evident on the mixed oxide. However, using i.r. spectroscopy, it was not possible to distinguish between amide on the copper and on the chromium sites. Despite this, comparison with the individual oxide surfaces showed that the band at 1685 cm^{-1} was most probably due to amide on the chromia sites. Amide also formed on the silica sites (1717 cm^{-1}). The intensities of the amide bands were weaker on the mixed oxide than on the outgassed Cr_2O_3/SiO_2 surface. This is explained due to the reduced availability of surface hydroxyl groups. Despite this, i.r. spectroscopic evidence for surface-oxamide formation was apparent.

Hydrolysis over the silica sites was facilitated when adsorbed moisture was present but unlike similar studies with hydroxylated CuO/SiO_2 and $CuO\text{-}CrO_3/SiO_2$ no oxamide bands were observed.

(b) Other Reactions

Isocyanate formation was the predominant reaction on the outgassed mixed oxide. Comparison with studies over the individual oxide surfaces confirmed that CuNCO (2203 cm^{-1}) and SiNCO (2303 cm^{-1}) fully explained the observed spectra and that no CrNCO formed. The results showed that CuNCO formed rapidly at room temperature but the band intensity at 2203 cm^{-1} declined during extended

exposure. This is explained by the following sequence of events. Initially, a high proportion of copper sites were exposed. These reacted rapidly with C_2N_2 to produce CuNCO. The isocyanate slowly spilled over onto the silica sites accounting for the slow growth of the 2303 cm^{-1} band. Spillover re-exposed the copper surface; however, reaction with more C_2N_2 to re-form Cu-NCO did not occur despite the availability of cyanogen. Instead it is evident that either the copper sites became inactive for CuNCO formation, or that the copper sites became covered with surface-amide species. I.r. spectral evidence for the slow intensification of surface amide bands supports the latter mechanism.

The presence of chromia in the mixed oxide did influence the -NCO spillover process, especially on the hydroxylated surface. This was clear since whereas spillover onto silica sites occurred on the hydroxylated chromium-free surface, the reaction was severely hindered on the hydroxylated mixed oxide. As a consequence of this restricted spillover, the CuNCO band remained strong. At first sight this a surprising result since there were many silica NCO-acceptor sites not covered by metal oxide (i.e. $N_m:N_{Si}$ ratio = 0.31:1, Table 5.1). Furthermore, SiNCO also formed on the outgassed mixed oxide. Taken together these results show that when moisture is present together with Cr_2O_3, a surface-hydroxylation mechanism occurs which blocks the silica

sites. It is possible that H_2O co-ordinated to the chromium ions is responsible for this effect.

The low capacity of the outgassed mixed oxide for converting C_2N_2 to decomposition products at room temperature is consistent with the findings of Davies (4). He noticed that when HCN was interacted with outgassed $CuO-Cr_2O_3/SiO_2$ only C_2N_2 was released.

One significant difference between the reactivity of CuO in the mixed oxide to that of the CuO/SiO_2 system was that whereas CuCN (2175 cm^{-1}) and irreversibly adsorbed C_2N_2 was seen over the single oxide surface at room temperature no such bands were seen over the mixed oxide at this temperature. Interaction of surface cyanide species associated with the copper sites with adsorbed H_2O co-ordinated to the chromia would explain this observation.

Only weak spectral evidence for oxidation of C_2N_2 over the mixed oxide was seen. I.r. bands at 1585, 1490, 1467, and 1445 cm^{-1} are ascribed to a mixture of copper and chromium oxidation species.

To summarise, it is clear that C_2N_2 interacts with both the Cu(II) and Cr(III) ions in the surface. This is in good agreement with the findings of Davies (4) who studied HCN interaction with a Cu(II)-Cr(III) system. However, some interaction between the oxides modified the combined reactivity towards C_2N_2.

5.7.2 Adsorption and Reaction of C_2N_2 above Ambient Temperature

A summary of the desorbates collected after heating C_2N_2-contacted $CuO-Cr_2O_3/SiO_2$ samples from ambient temperature to 685±13 K is shown in Table 5.16.

(a) Hydrolysis Reactions

The amide and diamide species which formed at ambient temperature on outgassed $CuO-Cr_2O_3/SiO_2$ surfaces decomposed at elevated temperatures. The i.r. band due to silica amide disappeared at a lower temperature than the one due to metal amide(s). This showed that the latter species was more stable. The simultaneous development of a band at 1617 cm^{-1}, ascribed to surface moisture, suggests that decomposition of surface amide occurred by dehydroxylation. In the case of the hydroxylated sample the release of oxamide and formamide was inferred from mass spectroscopic results. The hydroxylated-hydrated sample was very active for hydrolysis and 48% of carbon atoms irreversibly adsorbed as C_2N_2 were converted to oxamide. Since a much smaller proportion of the C_2N_2 was converted to the diamide on the hydrated surface, it is clear that reversibly adsorbed moisture was active for oxamide formation.

(b) Other Reactions

The reaction of adsorbed isocyanate species at elevated temperatures was dependent on the surface pretreatment. On the outgassed surface spillover onto the silica sites was enhanced by 440 K, and the

Table 5.16 Comparison of Products Desorbed from Cyanogen-Contacted $CuO-Cr_2O_3/SiO_2$ Surfaces

Product	Mass desorbed per m^2 on outgassing from ambient temperature to 685±13 K ($\mu g\ m^{-2}$)		
	Outgassed $CuO-Cr_2O_3/SiO_2$	Hydroxylated $CuO-Cr_2O_3/SiO_2$	Hydroxylated-hydrated $CuO-Cr_2O_3/SiO_2$
C_2N_2	8.9	5.6	3.4
HNCO	1.2	12.0	31.9
CO_2	9.5	19.0	29.3
HCN	4.8	9.8	4.8
NH_3	0.2	0.7	6.9
H_2O	1.1	15.1	29.7
Oxamide	0.0	trace	357.0

corresponding i.r. band due to CuNCO weakened. However, when the C_2N_2-exposed, hydroxylated surface was heated, the intensity of the CuNCO band doubled. Since no irreversibly adsorbed C-N moieties were seen in the i.r. spectrum of the sample after outgassing at 403 K, it is concluded that the source of carbon and nitrogen atoms involved in forming the additional NCO must have originated from an i.r. inactive species. The release of NH_3 from both the hydroxylated and hydroxylated-hydrated surfaces was probably due to reaction of moisture with the isocyanate. Raskó and Solymosi (178) suggested that NH_3 formed by this route may well account for the

presence of this gas in automobile exhaust catalyst studies.

A significant difference between the single oxide and mixed oxide surfaces was that with the former, i.r. spectra showed that surface cyanide groups were associated with individual metal ions. However, when C_2N_2-contacted hydroxylated $CuO-Cr_2O_3/SiO_2$ was outgassed at 485 K a band unique to the mixed oxide surface appeared at 2043 cm^{-1}. This band intensified on heating to 563 K. The adsorption is ascribed to a cyano species bridged across one copper and one chromium ion; the metal ions presumably occupy adjacent sites (Sec. 5.1). A similar species was observed when HCN was adsorbed onto chromium-supported copper oxide (Sec. 1.6.4.2). Furthermore, a dicyano-Cu(II) species is proposed to account for the band at 2166 cm^{-1} observed when C_2N_2-contacted outgassed $CuO-Cr_2O_3/SiO_2$ was outgassed to 572 K. The latter species was also seen on the CuO/SiO_2 surface. The dicyano species decomposed by 668 K to yield Cu(I)CN. This was characterised by a band at 2137 cm^{-1} near to one at 2150 observed on C_2N_2-exposed CuO/SiO_2.

Oxidation of C_2N_2 to CO_2 (and N_2) was a relatively minor reaction on the mixed oxide in comparison to isocyanate and hydrolysis reactions. However, in comparison to the individual oxide surfaces conversion to CO_2 was enhanced especially when pre-adsorbed water was present. Thus, whereas only a weak band at 1579 cm^{-1}

ascribed to copper carboxylate was seen on the outgassed surface, bands at 1478 and 1337 cm^{-1} ascribed to monodentate carbonate were seen on the hydroxylated surface. These bands were near those at 1490 and 1365 cm^{-1} reported by other workers (3, 163). The enhanced conversion of C_2N_2 to CO_2 in the presence of adsorbed H_2O suggests that oxidation may occur via surface amide.

Finally, evidence confirming the synergistic effect of copper and chromium on the conversion of adsorbed C_2N_2 was provided by the reduced amount of C_2N_2 which was desorbed unchanged. For example, in the case of the hydroxylated-hydrated surface, despite a high irreversible uptake of cyanogen, less than 1% of the irreversibly held carbon was desorbed as C_2N_2. This compares with 3% and 15% over the hydroxylated-hydrated CuO/SiO_2 and Cr_2O_3/SiO_2 surfaces respectively.

To summarise, reaction on the mixed oxide is seen to occur mainly via NCO species on the copper sites and via amide species on the chromium sites. A similar conclusion was reached by Davies using HCN (4). Some interplay between the copper and chromium ions was also evident which modified the uptake and conversion characteristics of the surface towards C_2N_2.

6. CONCLUSION

Hydroxylated silica was active for C_2N_2 uptake and partial hydrolysis occurred to form a cyanoformamide-like intermediate. This species decomposed by 472 K and C_2N_2 and H_2O were the only gaseous products. It was concluded that silica was a relatively inert support for spectroscopic studies.

CuO/SiO_2, CrO_3/SiO_2, Cr_2O_3/SiO_2, $CuO\text{-}CrO_3/SiO_2$ and $CuO\text{-}Cr_2O_3/SiO_2$ surfaces were all active for C_2N_2 uptake and conversion.

Hydrolysis was a major reaction when C_2N_2 was interacted with CuO/SiO_2. Surface-bound oxamide formed at ambient temperature via a cyanoformamide-like intermediate. The capacity of the surface to hydrolyse C_2N_2 was enhanced when pre-adsorbed water was present, and in this case 97% of carbon atoms irreversibly adsorbed as C_2N_2 was released as oxamide on outgassing to 540 K.

Copper isocyanate was formed rapidly when outgassed or hydroxylated CuO/SiO_2 was exposed to C_2N_2. During extended exposure the NCO group spilled-over onto silica sites adjacent to the copper ones giving rise to SiNCO. This species resisted evacuation at 673 K but CuNCO decomposed mainly to SiNCO, CO_2 and presumably N_2.

Whereas C_2N_2 dissociated at room temperature on outgassed CuO/SiO_2, evidence for molecularly adsorbed C_2N_2 was seen over the hydroxylated surface. At elevated

temperatures, this dissociated to a dicyano-copper(II) complex which decomposed to Cu(I)CN and SiCN above 539 K. Oxidation of adsorbed C_2N_2 to CO_2 also occurred at elevated temperatures. This was only a minor reaction and it proceeded via a copper carboxylate intermediate.

The amount of C_2N_2 irreversibly adsorbed on CrO_3/SiO_2 and on Cr_2O_3/SiO_2 was determined by the surface pretreatment. The active sites on the Cr(VI) surface were blocked by adsorbed moisture and by adsorbed oxygen molecules whereas irreversibly adsorbed moisture enhanced the capacity of the surface to adsorb C_2N_2.

Oxidation of adsorbed C_2N_2 was the main reaction on the Cr(VI) surface. Chromium bicarbonate and bidentate carbonate formed at room temperature, but at elevated temperatures, especially in the presence of pre-adsorbed oxygen, these species decomposed and CO_2 desorbed. A similar reaction occurred to a lesser extent on the Cr(III) surface.

Hydrolysis was a major reaction on both Cr(VI) and Cr(III) surfaces. Surface amide, including cyanoformamide-like species formed on the chromium and silica sites at room temperature on most pretreated surfaces. The subsequent reaction of these species was determined by the extent of surface hydroxylation. In the presence of pre-adsorbed moisture, further hydrolysis to oxamide occurred and some oxamide was released as a sublimate. In the absence of moisture, dehydroxylation and decomposition to yield C_2N_2, HNCO, HCN and H_2O took

place. Some amide decomposed via a surface formate and carboxylate species to yield CO_2.

CrNCO formation was only a minor reaction in comparison to analogous studies over copper surfaces. Furthermore, spillover to yield SiNCO was a more restricted process and in some cases spillover only occurred when the sample was heated above ambient temperature. In certain circumstances, NH_3 was released. This is explained by decomposition of amide via surface NH_2 species and/or by reaction of CrNCO with adsorbed moisture.

The metal oxide loading used for C_2N_2 adsorption and reaction studies over mixed copper oxide-chromium oxide systems was chosen such that there were sufficient silica sites to allow the oxides to exist independently of one another, i.e. the loading was well below that required to form a monolayer of the metal oxides on the silica surface. The irreversible uptake of C_2N_2 on the mixed oxide surfaces was enhanced as compared with the amounts held by the individual oxide surfaces. The presence of adsorbed moisture enhanced the affinity of the surface towards C_2N_2 uptake. Indeed, when the $CuO-Cr_2O_3/SiO_2$ surface contained physically adsorbed water molecules, the C_2N_2 uptake was an order of magnitude greater than the sum of the amounts adsorbed on the individual oxides.

The combined copper and chromium oxides effected both hydrolysis and oxidation of cyanogen. Amide formation occurred on both the chromium and silica sites

at room temperature, but whereas only partial hydrolysis occurred on the outgassed and oxygenated Cu(II)-Cr(VI) surfaces, hydrolysis was more extensive when adsorbed moisture was present and oxamide was formed. At elevated temperatures some oxamide and formamide were released from hydroxylated mixed oxide surfaces. Decomposition of hydrolysis intermediates also occurred via carbonate, formate and surface NH_x species which at still higher temperatures released CO_2.

Isocyanate was formed from adsorbed cyanogen particularly on the copper sites, but spillover onto the silica sites was restricted especially when Cr(VI) or moisture was present. NCO formation and spillover was enhanced at elevated temperatures especially over the Cu(II)-Cr(III) surfaces. In addition to the aforementioned decomposition mechanisms of surface isocyanate, copper isocyanide is also considered as a decomposition intermediate.

The Cu(II)-Cr(VI) surface was also capable of oxidising C_2N_2 to CO_2. This reaction occurred on Cr(VI) sites yielding chromium bicarbonate and carboxylate intermediates at room temperature. More CO_2 was released from the mixed oxides than the sum of the amounts released from the individual oxides.

A dicyano-copper(II) species formed at elevated temperatures on the Cu(II)-Cr(III) surface. This decomposed by a similar route to an analogous species formed over the CuO/SiO_2 surface. Furthermore, a bridged

cyano-species, unique to the mixed oxide surfaces, was characterised by an i.r. band between 2043 and 2038 cm^{-1}.

It is clear that reaction over the mixed Cu-Cr oxide surfaces involved both reaction on the pure copper oxide and chromium oxide sites but some interaction between the oxides modified both the uptake and overall reactivity of the mixed-oxide surfaces towards C_2N_2. This can be explained by considering that an intimately mixed layer of copper and chromium ions is present in the supported system. Alternatively microparticles of CuO and Cr_xO_y may be in contact, mutually supporting each other on the silica surface. Reaction on the mixed oxides occurred mainly via isocyanate intermediates on copper oxide sites and via amide on the chromium sites.

REFERENCES

1. J.G. Mellor; Ph.D. Thesis, Bristol, (1968).

2. T.H. Williams; Ph.D. Thesis, Bath, (1975).

3. D.J. Surman; Ph.D. Thesis, Bath, (1981).

4. G.H. Davies; Ph.D. Thesis, Bath, (1985).

5. D. Dollimore, P. Spooner and A. Turner; Surf. Technol., 4, 121, (1976).

6. J.M. Bridges, D.S. MacIver and H.H. Tobin; Actes 2nd Int. Catal., 2161 (1960), Pub. Technip Press, Paris, (1961).

7. Th.J. Osinga, B.G. Linsen and W.P. Van Beek; J. Catal., 7, 277, (1967).

8. J. Pritchard and T. Catterick; Experimental Methods in Catalytic Research, 3, 281, (1976).

9. E. Borello, A Zecchina, C. Morterra and J. Ghiotti; J. Phys. Chem., 73, 1286, (1969).

10. A. Zecchina, C. Morterra, G. Ghiotti and E. Borello; J. Phys. Chem., 73, 1292, (1969).

11. A. Zecchina, G. Ghiotti, C. Morterra and E. Borello; J. Phys. Chem., 73, 1295, (1969).

12. A. Zecchina, E. Guglielminotti, S. Coluccia and E. Borello; J. Chem. Soc. (A), 2196, (1969).

13. J.P. Hogan and R.L. Banks; B.E.530.617 (24-1-1955) and U.S.2.825.721 (to Phillips Petroleum Company).

14. K.K. Kearby, in "Catalyisis" (P.H. Emmett, ed.), Vol.3, p.453. Reinhold, New York, (1955).

15. R. Merryfield, M. McDaniel and G. Parks; J. Catal., 77, 348, (1982).

16. A. Zecchina, E. Garrone, G. Ghiotti, C. Morterra and E. Borelle; J. Phys. Chem., 79, 966, (1975).

17. C. Groeneveld, P.P.M.M. Wittgen, A.M. van Kersbergen, P.L.M. Mestrom, C.E. Nuijten and G.C.A. Schuit; J. Catal., 59, 153, (1979).

18. J.P. Hogan; J. Polym. Sci., A-1-8, 2637, (1970).

19. M.P. McDaniel; J. Catal., 67, 71, (1981).

20. M.P. McDaniel; J. Catal., 76, 29, (1982).

21. B. Fubini, G. Ghiotti, L. Stradella, E. Garrone and C. Morterra; J. Catal, 66, 200, (1980).

22. M.P. McDaniel; J. Catal., 76, 37, (1982).

23. A. Cimino, B.A. De Angelis, A. Luchetti and G. Minelli; J.Catal., 45, 316, (1976).

24. B. Rebenstorf and R. Larsson; J. Mol. Catal., 11, 247, (1981).

25. M.P. McDaniel; J. Catal., 76, 17, (1982).

26. H.L. Krauss; Proc. 5th Intern. Cong. Catalysis, (J.W. Hightower, ed.) p.207, Amsterdam, (1973).

27. B. Parlitz, W. Hanke, R. Fricke, M. Richter, U. Roost and G. Öhlmann; J. Catal., 94, 24, (1985).

28. P.P.M.M. Wittgen, C. Groeneveld, P.J.C.J.M. Zwaans, H.J.B. Morganstern, A.H. van Heughten, C.J.M. van Heumen and G.C.A. Schuit; J. Catal., 77, 360, (1982).

29. P.P.M.M. Wittgen, C. Groenveld, J.H.G.J. Janssens, M.L.J.A. Wetzels and G.C.A. Schiut; J. Catal., 59, 168, (1979).

30. D.D. Eley, C.H. Rochester and M.S. Scurrell; Proc. Roy. Soc. A329, 361, (1972).

31. D.D. Eley, C.H. Rochester and M.S. Scurrell; J. Catal., 29, 20, (1973).

32. L.K. Przhevalskaya, V.A. Shvets and V.B. Kazansky; J. Catal, 39, 363, (1975).

33. M. Shelef; J. Catal., 15, 289, (1969).

34. D.D. Beck and J.H. Lunsford; J. Catal., 68, 121, (1981).

35. C.P. Poole and D.S. McIvor, Adv. Catal., 17, 223, (1966).

36. C. Groeneveld, P.P.M.M. Wittgen, H.P.M. Swinnen, A. Wernsen and G.C.A. Schuit; J. Catal., 83, 346, (1983).

37. J.H. Anderson; J. Catal., 28, 76, (1973).

38. E.L. Kugler, R.J. Kokes and G.W. Gryder; J. Catal., 36, 142, (1975).

39. E.L. Kugler and G.W. Gryder; J. Catal., 36, 152, (1975).

40. A. Zecchina, E. Garrone, C. Morterra and S. Coluccia; J. Phys. Chem., 79, 978, (1975).

41. J. Raskó and F. Solymosi; J. Chem. Soc. Farad. Trans. 1, 76, 2383, (1980).

42. J. Raskó and F. Solymosi; Acad. Chim. Acad. Sci. Hung. Tomus; 95(4), 389, (1977).

43. J. Raskó and F. Solymosi; J. Mol. Catal., 3, 305, (1978).

44. M.L. Unland; J. Catal., 31, 459, (1973).

45. F. Solymosi and J. Raskó; J. Catal., 65, 235, (1980).

46. H.L. Krauss and H. Stach; Inorg. Nucl. Chem. Letters; 4, 393, (1968).

47. H.L. Krauss and H. Stach; Z. Anorg. Allg. Chem., 366, 280, (1969).

48. C. Groeneveld, P.P.M.M. Wittgen, J.P.M. Lavrijsen and G.C.A. Schuit; J. Catal., 82, 77, (1983).

49. D.L. Myers and J.H. Lunsford; J. Catal., 92, 260, (1985).

50. D.L. Myers and J.H. Lunsford; J. Catal., 99, 140, (1986).

51. M.B. Welch and M.P. McDaniel; J. Catal., 82, 110, (1983).

52. H.J. Lugo and J.H. Lunsford; J. Catal., 91, 155, (1985).

53. G. Ghiotti, E. Garrone, G. Della Gatta, B. Fubini and E. Giamello; J.Catal., 80, 249, (1983).

54. D.D. Eley, C.H. Rochester and M.S, Scurrell; J. Chem. Soc. Farad. Trans. 1, 69, 660, (1973).

55. M.P. McDaniel and M.B. Welch; J. Catal., 82, 98, (1983).

56. N. Takezawa, H. Kobayashi, Y. Kamegai and M. Shimokawabe; Appl. Catal., 3, 381, (1982).

57. M. Amara, M. Bettahar, L. Gengembre and D. Olivier; Appl. Catal., 35, 153, (1987).

58. K.P. de Jong, J.W. Geus and J. Joziasse; J. Catal., 65, 437, (1980).

59. R. Deen, P.I.Th. Scheltus and G. de Vries; J. Catal., 41, 218, (1976).

60. P. Ehrburger, J.M. Henlin and J. Lahaye, J. Catal., 100, 429, (1986).

61. J.W. London and A.T. Bell; J. Catal., 31, 32, (1973).

62. V.G. Amerikov and L.A. Kasatkina; Kinet. Katal., 12, 165, (1971).

63. F.S. Stone; Adv. Catal., 13, 1, (1962).

64. J.W. London and A.T. Bell; J. Catal., 31, 96, (1973).

65. P.G. Harrison and E.W. Thornton; J. Chem. Soc. Farad. Trans. 1, 74, 2604, (1978).

66. F. Solymosi and A. Berko; Surf. Sci., 122, 275, (1982).

67. F. Solymosi and J. Kiss; Surf. Sci., 108, 368, (1981).

68. F. Solymosi and J. Kiss; Surf. Sci., 104, 181, (1981).

69. F. Solymosi and J. Kiss; Vide, Couches Minces 201 (Suppl., Proc. Int. Conf. Solid Surf., 4th, VI), 213, (1980).

70. C. Lory; J. Phys. Chem., 37, 685, (1933).

71. W.L. Morgan and R.J. Farrauto; J. Catal., 31, 140, (1973).

72. R.P. Gura and G.E. Yuzefovich; Kinet. Katal., 14, 12, (1976).

73. W. Hertl and R.J. Farrauto; J. Catal., 29, 352, (1973).

74. R. Conner, K. Folkers and H. Adkins; J. Amer. Chem. Soc., 53, 1091, (1931).

75. S.P. Tonner, M.S. Wainwright, T.M. Trimm and N.W. Cant; Appl. Catal., 11, 93, (1984).

76. A. Iimura, Y. Inoue and I. Yasumori; Bull. Chem. Soc. Jpn., 56, 2203, (1983).

77. F.M. Capece, V.D.I. Castro, C. Furlani, G. Mattogno, C. Fragale, M. Gargano and M. Rossi; J. Electron. Spectrosc. Relat. Phenom., 27, 119, (1982).

78. H. Charcosset, P. Turlier and Y. Trambouze; Compt. Rend., 254, 2990, (1962).

79. H. Charcosset, P. Turlier and Y. Trambouze; J. Chim. Phys., 61, 1249, (1964).

80. L. Walter-Levy and M. Goreaud; Bull. Soc. Chim. Fr., 3, 836, (1973).

81. W.M. Keely and W.B. Mathes; J. Chem. Eng. Data, 11, 582, (1966).

82. J.R. Monnier, M.J. Hanrahan and G. Apai; J. Catal., 92, 119, (1985).

83. P. Courty, D. Durand, E. Freund and A. Sugier; J. Mol. Catal., 17, 241, (1982).

84. V.I. Sharkina, G.I. Salomatin and E.A. Boevskaya; Kinet. Katal., 19, 1598, (1978).

85. I.A. Kanteeva, I.A. Leont'eva and B.P. Sereda; Zh. Prikl. Khim. (Leningrad), 49, 1874, (1976).

86. N. Rubene and A.A. Davydov; Teor. Eksp. Khim., 12, 391, (1976).

87. B.R. Alves and A.J. Clark; Ministry of Defence, Chemical Defence Establishment, Porton Down, (1983).

88. J.R. Anderson and N.J. Clark; J. Catal., 6, 20, (1966).

89. J.R. Anderson and N.J. Clark; Proc. 3rd Int Congr. Catal., 2, 1048, 1964, Pub. North Holland, (1965).

90. G. Fabbri and P. Baraldi; Atti. Soc. Natur. Mat. Modena., 103, 241, (1972).

91. F.P. Netzer; Surf. Sci., 52, 709, (1975).

92. F.P. Netzer; Surf. Sci., 61, 343, (1976).

93. R.A. Wille, F.P. Netzer and J.A.D. Matthew; Surf. Sci., 68, 259, (1977).

94. M.E. Bridge, R.A. Marbrow and R.M. Lambert; Surf. Sci., 57, 415, (1976).

95. F.P. Netzer and R.A. Wille; Surf. Sci., 74, 547, (1978).

96. M.E. Bridge and R.M. Lambert; Surf. Sci., 63, 315, (1977).

97. J.C. Hemminger, E.L. Muetterties and G.A. Somorjai; J. Am. Chem. Soc., 101, 62, (1979).

98. K. Besenthal, G. Chiarello, M.E. Kordesch and H. Conrad; Surf. Sci., 178, 667, (1986).

99. M.E. Kordesch, W. Stenzel and H. Conrad; Surf. Sci., 175, L687, (1986).

100. M.E. Kordesch, W. Stenzel and H. Conrad; Surf. Sci., 186, 601, (1987).

101. M.E. Kordesch, W. Stenzel and H. Conrad; J. Electron. Spectrosc. Rel. Phenom. 39, 89, (1986).

102. K.G. Lloyd, J.C. Hemminger; Surf. Sci., 179, L6, (1987).

103. N.J. Gudde and R.M. Lambert; Surf. Sci., 124, 372, (1983).

104. D.A. Outka, S.W. Jorgensen, C.M. Friend and R.J. Madix; J. Mol. Catal., 21, 375, (1983).

105. R.J. Gorte, L.D. Schmidt and B.A. Sexton; J. Catal. 67, 387, (1981).

106. F.S. Stone and T.H. Williams; Stud. Surf. Sci. Catal., 7, (Pt. B. New Horiz. Catal.), 1394, (1981).

107. M.J.D. Low and P. Ramamurthy; J. Res. Inst. Catal. Hokkaido Univ., 16, 535, (1968).

108. G. Kortum and H. Delfs; Spectrochim. Acta., 20, 405, (1964).

109. H. Knözinger, H. Krietenbrink, H.D. Muller and W. Schulz; Proc. 6th Int. Congr. Catal. 1976, Pub. Chem. Soc., (1977).

110. H. Krietenbrink and H. Knözinger; Z. Phys. Chem. (Frankfurt), 102, 43, (1976).

111. F. Koubowetz, J. Latzel anf H. Noller; J. Coll. Inter. Sci., 74, 322, (1980).

112. F.E. Ruttenberg and J.D. Low; J. Am. Cer. Soc., 56, 241, (1973).

113. B.A. Morrow and I.A. Cody; J. Chem. Soc. Farad. Trans. 1, 71, 1021, (1975).

114. B.A. Morrow and I.A. Cody; J. Phys. Chem., 80, 1995, (1976).

115. G.A. Blomfield and L.H. Little; Canad. J. Chem., 51, 1771, (1973).

116. J.C. Petit and H. James; Thermochimica Acta, 35, 111, (1980).

117. D.D. Eley, G.M. Kiwanuka and C.H. Rochester; J. Chem. Soc. Farad. Trans. 1, 69, 2062, (1973).

118. F. Solymosi and T. Bánsági; J. Phys. Chem., 83(4), 552, (1979).

119. T. Bánsági, J. Rasko and F. Solymosi in "Spillover of Adsorbed Species, Proceedings Int. Symp., Lyon Villeurbane, 1983" (G.M. Pajonk, S.J. Teichner and J.E. Germain, eds.), (Elsevier, Amsterdam 1983), p.109.

120. W. Mueller-Litz and H. Hobert; Z. Phys. Chem. (Leipzig), 236, 84, (1967).

121. H. Dunken and H. Hobert; Z. Chem., 4, 275, (1964).

122. W. Reimenschneider, Chemtech, 6, 658, (1976).

123. B. Corain; Coord. Chem. Rev., 47, 165, (1982).

124. M. Bressan, G. Favero, B. Corain and A. Turco; Inorg. Nucl. Chem. Lett., 7, 203, (1971).

125. M.T. Beck, V. Gaspar and J. Ling; Inorg. Chim. Acta, 33, L177, (1979).

126. S.K. Tobia and M.F. El Shahat; J. Chem. Soc. A, 2444, (1968).

127. G.M. Tom and H. Taube; J. Am. Chem. Soc., 97, 5310, (1975).

128. E. Ciganek, W.J. Linn and O.W. Webster in "The Chemistry of the Cyano Group" (Z. Rappoport, ed.), (Interscience, London 1970).

129. B. Corain, M. Basato and G. Favero; J. Chem. Soc., Dalton. Trans., 2081, (1977).

130. C.A. Tolman and E.J. Lukosius; Inorg. Chem., 16, 940, (1977).

131. M. Morán and M. Gayoso; Z. Naturforsch, 38B, 177 (1983).

132. R.P. Welcher, M.E. Castellion and V.P. Wystrach; J. Am. Chem. Soc., 81, 2541, (1959).

133. T.A. Scott and E.L. Wagner; J. Chem. Phys., 30, 465, (1959).

134. H.O. Desseyn, W. van Reil, L. van Haverbeke and A. Goeminne; Trans. Met. Chem., 5, 88, (1980).

135. P. Armendarez and K. Nakamoto; Inorg. Chem., 5, 796, (1966).

136. A. Cornu and R. Massot; Compilation of Mass Spectral Data, Heyden, (1966).

137. A. Henglein, G. Jacobs and G.A. Muccini; Z. Naturforsch, 184, 98, (1963).

138. M. Inoué and M. Cottin; Advan. Mass Spectrom., 3, 339, (1966).

139. D.P. Stevenson; J. Chem. Phys., 18, 1347, (1950).

140. D.J. Bogan and C.W. Hand; J. Phys. Chem., 75, 1532, (1972).

141. C.J. Rowland, J.H.D. Eland and C.J. Danby; Chem. Commun., 1535, (1968).

142. F. Compernolle; Org. Mass Spectrom., 10, 289, (1975).

143. S.R. Smith and A.B. Jonassen; J. Inorg. Nucl. Chem., 29, 860, (1967).

144. J.C. Petit, J.C. Boettner and H. James; J. Calorim. Anal. Therm., 11, 3-17-1, (1980).

145. G.D. Craine and H.W. Thompson; Trans. Farad. Soc., 49, 1273, (1953).

146. A.G. Maki; J. Chem. Phys., 43, 3193, (1965).

147. A. Picard; Spectrochim. Acta., 30A, 691, (1974).

148. D.J. Belson and A.N. Strachan; Chem. Soc. Rev., 11, 41, (1982).

149. B.P. Winnewisser and M. Winnewisser; J. Mol. Spectrosc., 29, 505, (1969).

150. C. Reid and G. Herzberg; Disc. Faraday Soc., 9, 92, (1950).

151. H.W. Morgan and J.R. Lawson; Columbus Spectrosc. Symp., private communication, (1961).

152. J.H. Benyon; Mass Spectrometry and its Applications to Organic Chemistry, Elsevier, Amsterdam, (1960).

153. R.W. Kiser; Introduction to Mass Spectrometry and its Applications, Prentice Hall Inc., Englewood Cliffs, N.J., (1965).

154. F.W. Melpolder and R.A. Brown; Treatise on Analytical Chemistry, (I.M. Kolthoff and P.J. Elving, eds.), 4, 2047, Interscience, New York, (1963).

155. B.J. Millard; Quantitative Mass Spectrometry, Heyden, Philadelphia, (1977).

156. D.A. Skoog and D.M. West; Principles of Instrumental Analysis, 2nd Edition, Saunders College, Philadelphia, (1980).

157. H.A. Benesi and A.C. Jones; J. Phys. Chem., 63, 179, (1959).

158. L.H. Little and M.V. Mathieu; Actes Intern. Congr. Catalyse, 2e, Paris, 1, 771, (1961).

159. J.B. Peri; J. Phys. Chem., 70, 2937, (1966).

160. H.O. Desseyn, B.J. van der Veken and M.A. Herman; Spectrochimica Acta, 33A, 633, (1977).

161. A.A. Davydov, Y.M. Shchekochikhin and N.P. Keier; Kinet. Katal., 10, 1103, (1969).

162. L.H. Little and C.H. Amberg; Can. J. Chem., 40, 1997, (1962).

163. A. Zecchina, S. Coluccia, E. Guglielminotti and G. Ghiotti; J. Phys. Chem., 75, 2790, (1971).

164. F. Boccuzzi, S. Coluccia, G. Ghiotti, C. Morterra and A. Zecchina; J. Phys. Chem., 82, 1298, (1978).

165. R. Spitz, A. Revillon and A. Guyot; J. Catal., 35, 335, (and 345), (1974).

166. G.C. Bond and K. Bruckman; Farad. Disc. Chem. Soc., 72, 235, (1981).

167. F.J. Gil Llambiás, A.M. Escudey-Castro, A. López Agudo and J.L. Garciá-Fierro; J. Catal., 90, 323, (1984).

168. C. Okkerse, Physical and Chemical Aspects of Adsorbents and Catalysts, Chapter 5, (B.J. Linsen, ed.), Acad. Press, New York, (1970).

169. J.B. Peri and A.L. Hensley; J. Phys. Chem., 72, 2926, (1968).

170. H.O. Desseyn, F.K. Vansant and B.J. van der Veken; Spectrochimica Acta, 31A, 625, (1975).

171. F.A. Miller and G.A. Carlson; Spectrochimica Acta, 17, 977, (1961).

172. W.C. Conner, G.M. Pajonk and S.J. Teichner; Advan. in Catalysis, 34, 1, (1986).

173. F. Solymosi, J. Kiss and J. Sarkany; Proc. 7th Intern. Vacuum Cong. and 3rd. Intern. Conf. on Solid Surfaces, (R. Dobrozemsky, ed.). p.207, Vienna, (1977).

174. E. Borello, A. Zecchina and C. Morterra; J. Phys. Chem., 71, 2938, (1967).

175. E. Borello, A. Zecchina and C. Morterra; J.Phys. Chem., 71, 2945, (1967).

176. M.C. Kung and H.H. Kung; Catal. Rev. Sci. Eng., 27(3), 425, (1985).

177. J.B. Peri; J. Phys. Chem., 69, 231, (1965).

178. J. Raskó and F. Solymosi; Magy. Kem. Foly., 84(10), 476, (1978).

APPENDIX I

Solid State Mass Spectra

m/z	% Abundance		
	oxamide	cyanuric acid	white sublimate*
27	2.3	2.0	2.5
28	27.1	7.0	7.5
29	3.3	9.0	4.3
36	0.0	2.0	0.0
41	1.0	6.0	5.8
42	1.8	8.0	2.5
43	8.8	82.0	18.8
44	100.0	84.0	100.0
45	65.5	2.0	52.1
55	0.0	4.0	0.0
56	0.0	0.0	1.2
57	0.0	4.0	0.0
60	38.0	2.0	26.9
69	0.0	6.0	0.0
70	0.0	20.0	0.0
86	0.0	22.0	0.0
88	35.2	0.0	32.9
89	1.7	0.0	0.0
100	0.0	0.0	0.5
107	0.0	0.0	0.6
129	0.0	100.0	0.0
130	0.0	4.0	0.0

* White sublimate released after C_2N_2 contact with hydroxylated $CuO\text{-}CrO_3/SiO_2$ (Sec. 4.5.3)

APPENDIX II

Listing of the computer program 'DELAY.OY' for automatic recording of infra-red spectra using the Perkin Elmer 983 Spectrometer when interfaced to the Perkin Elmer 3600 Data Station (see section 2.4.4)

Computer Program 'DELAY.OY'

```
SET WAIT OFF
CALC V1=1
CALC V2=0
&L1 *
DO PAUSE 20
CALC V2=V2+1
CALC V3=V1-V2
&IF V3 L2 L2 L1
&L2 *
AVRAGE X 3 4000 180
SAVE X SPECTRUM 1
CALC V1=10
CALC V2=0
&L3 *
DO PAUSE 1680
CALC V2=V2+1
CALC V3=V1-V2
&IF V3 L4 L4 L3
&L4 *
AVRAGE X 3 4000 180
```

```
SAVE X SPECTRUM 2
CALC V1=10
CALC V2=0
&L5 *
DO PAUSE 1680
CALC V2=V2+1
CALC V3=V1-V2
&IF V3 L6 L6 L5
&L6 *
AVRAGE X 3 4000 180
SAVE X SPECTRUM 3
CALC V1=10
CALC V2=0
&L7 *
DO PAUSE 1680
CALC V2=V2+1
CALC V3=V1-V2
&IF V3 L8 L8 L7
&L8 *
AVRAGE X 3 4000 180
SAVE X SPECTRUM 4
SET WAIT ON.
```

APPENDIX III

Listing of Mass Spectra Analysis Program 'MS1' cited in Sec. 3.1.3

```
READY.

 2 DIM A(200),AA(200),B(200),P(200),F(200)
 3 DIM J(200),N(200),O(200),Q(200)
 5 PRINT"□"
 10 INPUT "REFERENCE NUMBER";R$:PRINT
 20 INPUT "TEMPERATURE";T:PRINT
 30 A9=0:P9=0:F9=0
 31 J=0
 35 PRINT"□"
 40 FOR I=12 TO 60 STEP 0.5
 41 IF I-INT(I)=0 GOTO 55
 42 IF I=13.5 GOTO 55
 43 IF I=21.5 GOTO 55
 53 GOTO 120
 55 REM
 60 PRINT"MASS NUMBER";I;
 70 INPUT"BACKGROUND";B(I):PRINT
 90 INPUT"AND RESPONSE";AA(I):PRINT
 100 A(I)=AA(I)-B(I)
 105 IF A(I)=<0 GOTO 120
 110 A9=A9+A(I)
 114 J=J+1
 115 N(J)=AA(I):O(J)=B(I):Q(J)=A(I)
 116 J(J)=I
 120 NEXT I
 121 J1=J
 130 PRINT:INPUT"PRESSURE FACTOR";X
 140 FOR J=1 TO J1
 150 P(J)=Q(J)/A9*100
 160 F(J)=P(J)*X
 165 P9=P9+P(J):F9=F9+F(J)
 166 NEXT J
 168 PRINT"□"
 170 OPEN1,4:CMD1
 172 PRINT"MASS SPEC. REF NO.";R$;" RUN AT";T;"K"
 175 PRINT:PRINT
 180 PRINT#1,"MASS NO   RESP    B.G.    P.CORR    MASS NO    %AGE    CORR.%AGE"
 181 PRINT#1,"
 182 OPEN2,4,1:OPEN3,4,2
 183 PRINT#3,"  99.9    9999.9  999.9    9999.9     99.9      99.99   9999.99"
 260 FOR J=1 TO J1
 272 IF P(J)<0.01 THEN P(J)=0.01
 273 IF F(J)<0.01 THEN F(J)=0.01
 280 PRINT#2,J(J);N(J);O(J);Q(J);J(J);P(J);F(J)
 290 NEXT J
 295 PRINT#3:CLOSE3:PRINT#2:CLOSE2
 297 PRINT#1:PRINT#1:PRINT#1,"TOTAL INTENSITY=";A9
 298 PRINT#1:PRINT#1,"PRESSURE FACTOR=";X:PRINT#1:PRINT#1
 300 PRINT#1:PRINT#1,"TOTAL %AGE =";P9;"TOTAL CORR. %AGE =";F9
 302 PRINT#1:PRINT#1,"NUMBER OF LINES ANALYSED =";J1
 305 PRINT#1:PRINT#1:PRINT#1
 306 PRINT#1:CLOSE1
 310 INPUT "DO YOU WANT ANOTHER CALCULATION";A$
 320 IF A$="YES" GOTO 5
 330 END
 1000 DATA
 1005 DATA
 1010 DATA
 1015 DATA
 1020 DATA
 1025 DATA
 1030 DATA
```

APPENDIX IV

Listing of Mass Spectral Analysis Program 'MS ANALYSIS' cited in Sec 3.1.3

READY.

```
100 REM MASS SPEC FINAL VERSION
110 PRINT
120 PRINT
130 PRINT
140 PRINT
150 PRINT
160 PRINT
170 PRINT
180 PRINT
190 PRINT
200 PRINT
210 PRINT
220 PRINT "MASS SPEC ANALYSIS PROGRAM"
230 PRINT
240 PRINT
250 PRINT
260 PRINT
270 PRINT
280 PRINT
290 PRINT
300 PRINT
310 PRINT
320 PRINT
330 PRINT
340 PRINT
350 PRINT
360 FOR I=1TO400:NEXTI
370 PRINT "THIS PROGAM ACCEPTS DATA"
380 PRINT
390 PRINT "IN THE FORM OF LINE LENGTHS"
400 PRINT
410 PRINT "FOR SPECIFIC M/E VALUES AND"
420 PRINT
430 PRINT "PROVIDES A QUANTITATIVE ANALYSIS"
440 PRINT
450 PRINT "OF THE COMPOUNDS PRESENT THE"
460 PRINT
470 PRINT "DATA IS ENTERED FIRST BY TYPING"
480 PRINT
490 PRINT "RESPONSES AFTER EACH M/E PROMPTER"
500 PRINT
510 PRINT
520 FOR I=1TO400:NEXT I
530 REM INPUT OF RAW DATA AND DIMENSIONING
540 DIM F(12),G(18),H(12),I(12),J(12)
550 DIM K(12),L(12),M(12),N(12),O(12),P(100),R(100)
560 DIM A(100),B(100),Z(50)
570 PRINT:INPUT"PRESSURE FACTOR";X
580 A=0
585 B=0
590 FOR J=12TO60 STEP 0.5
592 IF J-INT(J)=0 GOTO 600
593 IF J=13.5 GOTO 600
594 IF J=21.5 GOTO 600
595 GOTO 630
600 REM
605 PRINT"MASS NUMBER";J;
610 INPUT"RESPONSE";A(J):PRINT
620 A=A+1
625 B=B+A(J)
628 P(A)=J:R(A)=A(J)
630 NEXT J
```

```
635 A1=A
790 REM END OF RAW DATA INPUT
792 INPUT"REFERENCE NUMBER";R$:PRINT
794 INPUT"TEMPERATURE";T:PRINT
800 F(1)=A(52)
810 F(2)=F(1)*0.029
820 A(52)=0
830 A(38)=A(38)-F(2)
840 F(3)=F(1)*0.18
850 A(28)=A(28)-F(3)
860 F(4)=F(1)*.03
870 A(53)=A(53)-F(4)
880 F(5)=F(1)*0.146
890 A(26)=A(26)-F(5)
900 F(6)=A(24)
910 A(24)=A(24)-F(6)
911 F(7)=F(1)*0.01
912 A(14)=A(14)-F(7)
913 F(8)=F(1)*0.047
914 A(12)=A(12)-F(8)
920 F(10)=F(1)+F(2)+F(3)+F(4)+F(5)+F(6)+F(7)+F(8)
930 REM ABOVE FOR C2N2
940 FOR I=1 TO 60
950 IF A(I)<=0 THEN A(I)=0
960 NEXT I
970 G(1)=A(43)
980 G(2)=G(1)*0.015
990 A(43)=0
995 A(44)=A(44)-G(2)
1000 G(3)=G(1)*0.543
1005 A(42)=A(42)-G(3)
1010 G(4)=G(1)*0.033
1015 A(30)=A(30)-G(4)
1020 G(5)=G(1)*0.179
1025 A(29)=A(29)-G(5)
1030 G(6)=G(1)*0.172
1035 A(28)=A(28)-G(6)
1040 G(7)=G(1)*0.148
1045 A(27)=A(27)-G(7)
1050 G(8)=G(1)*0.087
1055 A(26)=A(26)-G(8)
1060 G(9)=G(1)*0.013
1065 A(21.5)=A(21.5)-G(9)
1070 G(10)=G(1)*0.021
1075 A(18)=A(18)-G(10)
1080 G(11)=G(1)*0.017
1085 A(17)=A(17)-G(11)
1090 G(12)=G(1)*0.022
1095 A(16)=A(16)-G(12)
1100 G(13)=G(1)*0.083
1105 A(15)=A(15)-G(13)
1110 G(14)=G(1)*0.048
1115 A(14)=A(14)-G(14)
1120 G(15)=G(1)*0.023
1125 A(13)=A(13)-G(15)
1130 G(16)=G(1)*0.032
1135 A(12)=A(12)-G(16)
1140 A(12)=A(12)-G(9)
1150 M(1)=G(1)+G(2)+G(3)+G(4)+G(5)+G(6)+G(7)+G(8)+G(9)+G(10)+G(11)
1152 M(2)=G(12)+G(13)+G(14)+G(15)+G(16)
1155 G(17)=M(1)+M(2)
1160 REM ABOVE FOR  HNCO
1170 FOR I=1 TO 60 STEP .5
1180 IF A(I)<=0 THEN A(I)=0
1190 NEXT I
1200 H(1)=A(44)
1210 H(2)=H(1)*0.057
1215 A(44)=0
```

```
2020 Q(3)=H(10)*100/B
2030 Q(4)=I(10)*100/B
2040 Q(5)=J(10)*100/B
2050 Q(6)=K(10)*100/B
2060 Q(7)=L(10)*100/B
2110 OPEN 1,4:CMD1
2120 PRINT
2130 PRINT"▒▒▒
```

APPENDIX V

A Listing of the Infra-Red Standardisation Program 'STD.OY' cited in Sec 3.2.2

```
SET WAIT OFF
* ENTER THE FIRST FILID OF THE SAMPLE GROUP (A1) AND
*(TOTAL NUMBER-1) OF SPECTRA TO BE STANDARDIZED (A2)
&ENTER A1,A2
* &A1,A2
DO PAUSE
DO SCLEAR
CALC V8=&A2
CALC V9=0
&L1 *
RETRVE X &A1
&ERROR L1
COPY X X 4000 500
TAAT X
RETRVE Y CELL
TAAT Y
SUB X,Y,Z
COPY Z X
TAAT X
SUB X 100
MULT X -1
CALC V1=99.8/X(1200)
MULT X &V1
SUB X 100
MULT X -1
CALC V13=X(1200)-10
SUB X &V13
TAAT X
CALC V2=X(1869)-X(1968)
ABEX X 1
CALC V3=X(4000)
TAAT X
CNTENT DELETE &A1
SAVE X &A1
&L2 *
&INCR A1
&L3 *
RETRVE X &A1
&ERROR L3
COPY X X 4000 500
TAAT X
RETRVE Y CELL
TAAT Y
SUB X,Y,Z
COPY Z X
TAAT X
```

```
SUB X 100
MULT X -1
CALC V1=99.8/X(1200)
MULT X &V1
SUB X 100
MULT X -1
CALC V14=X(1200)-10
SUB X &V14
TAAT X
CALC V4=X(1869)-X(1968)
CALC V5=V2/V4
ABEX X &V5
CALC V6=X(4000)
CALC V7=V3-V6
ADD X &V7
TAAT X
CNTENT DELETE &A1
SAVE X &A1
CALC V9=V9+1
CALC V10=V8-V9
&IF V10 L4 L4 L2
&L4 *
SET WAIT ON
DO PAUSE
* ENTER THE FIRST FILID OF THE SAMPLE GROUI (A3) AND
*(TOTAL NUMBER-1) OF SPECTRA TO BE STANDARDIZED
&ENTER A3,A4
DO PAUSE
CALC V8=&A4+1
&L5 *
RETRVE X &A3
CALC V11=X(4000)
CALC V12=X(1200)
&INCR A3
CALC V8=V8-1
&IF,V8,L6,L6,L5
&L6 *
```

APPENDIX VI

Mass spectra of selected organic compounds as cited in 'Eight Peak Index of Mass Spectra' 2nd. Ed., Vol. 1, Publ. M.S.D.C. (Reading), 1974.

m/z	Formamide	Formaldehyde	Methyl Cyanide	Methyl amine	Ethyl amine	1-2-diamino-ethane
	% Abundance					
45	100				51	
44	27				100	4
43	12				14	5
42	2		4		19	6
41			100			
40			54			
39			21			
38			14			
31	1	2		56		
30		86		100	13	100
29	28	100		16		4
28	10	31	4	88	68	
27	12		3	16		5
26				2		
18				1	16	13
17						4
16		2				
15					20	
14	4	10				
12	3					